

May 1996



**Idaho
National
Engineering
Laboratory**

**TECHNICAL EVALUATION REPORT
WESTINGHOUSE CODE
QUALIFICATION DOCUMENT FOR
BEST ESTIMATE LOSS OF COOLANT
ACCIDENT ANALYSIS, WCAP-12945-P**

**C. P. Fineman
C. L. Atwood
D. S. Lucas
L. W. Ward**

 **Lockheed**
Idaho Technologies Company

INEL-95/0608

TECHNICAL EVALUATION REPORT
WESTINGHOUSE CODE QUALIFICATION DOCUMENT
FOR
BEST ESTIMATE LOSS OF COOLANT ACCIDENT ANALYSIS
WCAP-12945-P

C. P. Fineman
C. L. Atwood
D. S. Lucas
L. W. Ward

Published May 1996

Idaho National Engineering Laboratory
Nuclear Regulatory Support Programs Department
Lockheed Idaho Technologies Company
Idaho Falls, Idaho 83415

Prepared for the
U.S. Nuclear Regulatory Commission
Washington D.C. 20555
Under DOE Contract No. DE-AC07-94ID13223
JCN L1696, Task Order 7, TAC No. M81712

ABSTRACT

The Idaho National Engineering Laboratory (INEL) reviewed the five volume topical report Code Qualification Document for Best Estimate Loss of Coolant Accident Analysis, WCAP-12945-P. The review evaluated Westinghouse's realistic methodology for large-break loss-of-coolant accident (LBLOCA) analysis to determine the performance of emergency core cooling systems (ECCS) following a LBLOCA. The methodology will be applied to Westinghouse three- and four-loop pressurized water reactors (PWRs) with cold leg injection. Because of the realistic approach to determining the performance of the ECCS, the INEL evaluated conformance of the methodology described in WCAP-12945-P to Nuclear Regulatory Commission requirements in 10 CFR 50.46; guidance in Regulatory Guide 1.157 (RG 1.157); and the Code Scaling, Applicability, and Uncertainty (CSAU) methodology. Based on the INEL review of the information provided by Westinghouse in WCAP-12945-P, responses to NRC questions, and special submittals, the INEL recommends the Westinghouse realistic methodology be approved subject to certain suggested restrictions. This recommended approval is for LBLOCA analyses in Westinghouse three- and four-loop plants with cold leg ECC injection.

CONTENTS

ABSTRACT	iii
LIST OF FIGURES	ix
LIST OF TABLES	ix
SUMMARY	xi
PREFACE	xiii
ACKNOWLEDGEMENTS	xv
1. INTRODUCTION	1
2. WESTINGHOUSE METHODOLOGY AND CSAU COMPARISON	4
2.1 Element 1 - Requirements and Capabilities	4
2.1.1 Step 1. Specify the Scenario	4
2.1.2 Step 2. Select the Nuclear Power Plant	4
2.1.3 Step 3. Identify and Rank Phenomena	5
2.1.4 Step 4. Select a Frozen Code	6
2.1.5 Step 5. Provide Code Documentation	6
2.1.6 Step 6. Determine Code Applicability	7
2.2 Element 2 - Assessment and Ranging of Parameters	8
2.2.1 Step 7. Establish an Assessment Matrix	8
2.2.2 Step 8. Define Nuclear Power Plant Nodalization	9
2.2.3 Step 9. Determine Code and Experiment Accuracy	10
2.2.4 Step 10. Determine the Effect of Scale	11
2.3 Element 3 - Sensitivity and Uncertainty Analyses	12
2.3.1 Step 11. Determine the Effect of Reactor Input Parameters and State	12
2.3.2 Step 12. Perform PWR Sensitivity Calculations	13
2.3.3 Step 13. Combine Biases and Uncertainties	14
2.3.4 Step 14. Determine Total Uncertainty	14
2.4 Summary of INEL Review	16
3. PIRT EVALUATION (CSAU STEP 3)	17
4. CODE ASSESSMENT (CSAU STEP 7)	21
4.1 Separate Effects Tests	21
4.2 Integral Effects Tests	22
4.3 Other Assessments	23

5.	PLANT NODALIZATION (CSAU STEP 8)	25
6.	CODE/EXPERIMENT ACCURACY (CSAU STEP 9)	27
	6.1 Westinghouse Realistic LBLOCA Methodology Roadmap	28
	6.2 Models - Global Effects	35
	6.3 Plant Conditions - Global Effects	36
	6.4 Local Effects Models/Parameters	38
	6.5 WCOBPA/TRAC Experiment Based Uncertainty	39
	6.6 Other Parameters/Factors Considered by Westinghouse	40
	6.7 INEL Review of Uncertainty Propagation	41
7.	EFFECTS OF SCALE (CSAU STEP 10)	43
8.	REACTOR INPUT PARAMETERS/STATE (CSAU STEP 11).....	45
	8.1 Westinghouse's Methodology - CQD Sections 21/22	45
	8.2 INEL Review of CQD Sections 21/22	49
9.	ADDITIONAL METHOD DESCRIPTION AND REVIEW	51
	9.1 LBLOCA Method Description/Review - Code Description	51
	9.2 LBLOCA Method Description/Review - Uncertainty Distributions and Assumptions	57
	9.3 LBLOCA Method Description/Review - Split Breaks	67
	9.4 LBLOCA Method Description/Review - Westinghouse HOTSPOT model	68
	9.5 Summary of INEL Review	69
10.	COMPARISON WITH REGULATORY GUIDE 1.157	71
	10.1 Summary of Westinghouse Methodology/RG 1.157 Comparison ...	71
	10.2 WCOBRA/TRAC Range of Conditions/Applicability	72
11.	WESTINGHOUSE EVALUATION OF COMPENSATING ERRORS	76
	11.1 Post-CHF Heat Transfer Evaluations	77
	11.1.1 ORNL Film Boiling Tests	77
	11.1.2 INEL Film Boiling Tests	77
	11.1.3 FLECHT-SEASET Test Analysis	78
	11.1.4 G-1 Blowdown Tests	80
	11.1.5 INEL Review	80

11.2	ECC Bypass/Condensation	81
11.3	Blowdown/Post-Blowdown Thermal-Hydraulics/Entrainment	82
	11.3.1 LOFT Analyses - Tests L2-3 and L2-5	83
	11.3.2 SCTF Test 619 Analysis	86
	11.3.3 CCTF Test 62 Analysis	88
11.4	Westinghouse Conclusions from the Compensating Error Report	91
11.5	Summary of INEL Review	92
12.	OTHER TECHNICAL ISSUES	97
	12.1 WCOBRA/TRAC CCFL Modeling Assessment	97
	12.2 Modeling the Effects of Accumulator Nitrogen	99
	12.3 Evaluation of Rewet Temperature	101
13.	COMPLIANCE WITH 10 CFR 50.46 REQUIREMENTS	104
14.	CONCLUSIONS	110
15.	REFERENCES	114

APPENDICES

A.	WESTINGHOUSE WCOBRA/TRAC MODEL DESCRIPTION AND REVIEW	A-1
	A.1 Conservation Equations - CQD Section 2	A-3
	A.1.1 Model Description	A-3
	A.1.2 INEL Review of CQD Section 2	A-4
	A.2 Flow Regimes and Interfacial Area - CQD Section 3	A-7
	A.2.1 Model Description	A-7
	A.2.2 INEL Review of CQD Section 3	A-9
	A.3 Momentum Transfer Models - CQD Section 4	A-10
	A.3.1 Model Description	A-10
	A.3.2 INEL Review of CQD Section 4	A-13
	A.4 Critical Flow Models - CQD Section 4-8	A-18
	A.4.1 Model Description	A-18
	A.4.2 INEL Review of Critical Flow - Section 4-8	A-18

A.5	Interfacial Heat and Mass Transfer Models - CQD Section 5 ..	A-19
A.5.1	Model Description	A-19
A.5.2	INEL Review of CQD Section 5	A-20
A.6	Wall Heat Transfer Models - CQD Section 6	A-27
A.6.1	Model Description	A-27
A.6.2	INEL Review of CQD Section 6	A-28
A.7	Models for Heated and Unheated Structures - CQD Section 7 ..	A-38
A.7.1	Model Description	A-38
A.7.2	INEL Review of CQD Section 7	A-40
A.8	Reactor Kinetics and Decay Heat Models - CQD Section 8	A-41
A.8.1	Model Description	A-41
A.8.2	INEL Review of CQD Section 8	A-41
A.9	One-Dimensional Component Models - CQD Section 9	A-42
A.9.1	Model Description	A-42
A.9.2	INEL Review of CQD Section 9	A-43
B.	INEL REVIEW OF WESTINGHOUSE <u>W</u> COBRA/TRAC ASSESSMENT	B-1
B.1	<u>W</u> COBRA/TRAC Separate Effects Assessment	B-3
B.1.1	ORNL THTF Blowdown Tests	B-6
B.1.2	G-1 Blowdown Tests	B-7
B.1.3	G-2 Blowdown Tests	B-7
B.1.4	G-2 Refill Tests	B-7
B.1.5	Separate Effects Reflood Tests	B-8
B.2	<u>W</u> COBRA/TRAC Integral/Large Scale Assessment	B-9
B.2.1	LOFT Assessment	B-10
B.2.2	CCTF Assessment	B-12
B.2.3	SCTF Assessment	B-13
B.2.4	UPTF Assessment	B-14
B.3	Other <u>W</u> COBRA/TRAC Assessments	B-16
B.3.1	Westinghouse/EPRI 1/3rd-Scale Steam/Water Mixing Tests	B-16
B.3.2	Creare 1/15th and 1/5th Scale ECC Bypass Tests	B-17
B.3.3	NRU Reactor Assessments	B-18
B.4	Summary of INEL Review	B-19
B.4.1	Separate Effects Tests	B-19
B.4.2	Integral Effects Tests	B-21
B.4.3	Other Assessments	B-22

C.	COMPARISON OF WESTINGHOUSE REALISTIC LBLOCA METHODOLOGY TO REGULATORY GUIDE 1.157	C-1
D.	EVALUATION OF THE <u>W</u> COBRA/TRAC DISPERSED FLOW FILM BOILING HEAT TRANSFER MODEL	D-1
	D.1 Reflood Behavior	D-3
	D.2 <u>W</u> COBRA/TRAC Dispersed Flow Film Boiling Model	D-4
	D.2.1 Wall-to-Vapor Heat Transfer	D-7
	D.2.2 Radiation to Drops and Vapor	D-8
	D.2.3 Droplet-Wall Contact Heat Transfer	D-8
	D.2.4 Interfacial Heat Transfer	D-10
	D.3 Omission of a Rod-to-Rod Radiation Model	D-11
	D.4 INEL Conclusions	D-13

FIGURES

1.	Breakdown of Westinghouse's Uncertainty Parameters	29
2.	Flowchart of Uncertainty Determination Procedure	30

TABLES

11.1	Tests Used in Westinghouse's Compensating Error Analysis	76
B.1-1	Westinghouse <u>W</u> COBRA/TRAC Separate Effects Assessment Matrix	B-4
B.2-1	Westinghouse <u>W</u> COBRA/TRAC Integral/Large Scale Assessment Matrix	B-11
C-1	Comparison of Regulatory Guide 1.157 and Westinghouse's LBLOCA Realistic Model	C-4

SUMMARY

This report documents the review of the Westinghouse realistic methodology for analyzing the performance of emergency core cooling systems (ECCS) following a large-break loss-of-coolant accident (LBLOCA). The method will be used to analyze Westinghouse three- and four-loop pressurized water reactors (PWRs) with cold leg injection.

The Westinghouse realistic LBLOCA methodology uses the WCOBRA/TRAC computer program to perform realistic LBLOCA licensing analyses. WCOBRA/TRAC is Westinghouse's version of the Nuclear Regulatory Commission (NRC) developed COBRA/TRAC code. Westinghouse uses this program to perform integral analyses of the system thermal-hydraulic and hot rod response from blowdown through reflood. In addition, the methodology determines and applies the calculational uncertainty to the calculated peak cladding temperature. The methodology is used to show compliance with the acceptance criteria of 10 CFR 50.46 using methods that conform to NRC guidance in Regulatory Guide 1.157 (RG 1.157). Westinghouse submitted the methodology to the Office of Nuclear Reactor Regulation for approval. The Office of Nuclear Reactor Regulation requested assistance from the Idaho National Engineering Laboratory (INEL) in reviewing the methodology.

The INEL reviewed the methodology using the information provided by Westinghouse in the five volume topical report, Westinghouse Code Qualification Document for Best Estimate Loss of Coolant Accident Analysis, WCAP-12945-P, in Westinghouse's responses to NRC questions, and other special Westinghouse submittals. Based on this review, the INEL recommends the Westinghouse realistic methodology be approved subject to certain suggested restrictions. This recommended approval is for LBLOCA analyses in Westinghouse three- and four-loop plants with cold leg ECC injection.

PREFACE

This report was prepared for the U.S. Nuclear Regulatory Commission, Office of Nuclear Reactor Regulation, by Lockheed Idaho Technologies Company, Nuclear Regulatory Support Programs Department.

ACKNOWLEDGEMENTS

The authors wish to acknowledge the help of G. Berna and D. Hagrman for their assistance in the review of WCAP-12945-P, Code Qualification Document (CQD) for Best Estimate LOCA Analyses, Section 7, and J. L. Judd for his help in reviewing CQD Section 8.

TECHNICAL EVALUATION REPORT
WESTINGHOUSE CODE QUALIFICATION DOCUMENT
FOR
BEST ESTIMATE LOSS OF COOLANT ACCIDENT ANALYSIS
WCAP-12945-P

1. INTRODUCTION

In 1988, the Nuclear Regulatory Commission (NRC) revised 10 CFR 50.46²¹⁶ to allow the use of realistic/best estimate (BE) computer models in calculating emergency core cooling system (ECCS) performance. The approach allowed realistic computer models to be used to calculate a nuclear power plant's response to a large-break loss-of-coolant accident (LBLOCA) provided the uncertainty in the calculated results was determined. The uncertainty was to be added to the calculated results, including the peak cladding temperature (PCT), when comparing the ECCS performance to the requirements of 10 CFR 50.46. Westinghouse submitted to the NRC a realistic methodology for performing LBLOCA analysis of Westinghouse three- and four-loop pressurized water reactors (PWRs) with cold leg injection.¹ In the following discussion, Reference 1 is referred to as the CQD. The methodology is based on the WCOBRA/TRAC code that Westinghouse developed from the NRC's COBRA/TRAC² computer program.

The realistic LBLOCA models are designed to show conformance of the ECCS to 10 CFR 50.46 requirements. Westinghouse submitted the methodology to the NRC for review and acceptance as a method to analyze LBLOCAs in a manner that conforms to NRC requirements in 10 CFR 50.46; guidance contained in Regulatory Guide (RG 1.157);²¹⁷ the Code Scaling, Applicability, and Uncertainty (CSAU) methodology;⁶¹ and other pertinent NRC documents.

The Office of Nuclear Reactor Regulation (NRR) is responsible for the evaluation and review of computer codes and their proposed applications. The Office of Nuclear Reactor Regulation requested the Idaho National Engineering Laboratory (INEL) to provide assistance in the review of the Westinghouse methodology. Specifically, the request for assistance included evaluating the method for compliance with the guidance contained in RG 1.157, and how the

method would be used to meet the requirements and acceptance criteria of 10 CFR 50.46.

Related to the above reviews, NRR also requested INEL review and evaluate Westinghouse's responses to NRC questions regarding their realistic LBLOCA modeling applications. The NRC questions were transmitted to Westinghouse in References 3 to 6. Westinghouse's responses to those questions are contained in References 7 to 53, 190, 203, 205, 206, 214, and 215. Westinghouse also made several special submittals to the NRC on their realistic LBLOCA methodology. These submittals are contained in References 54 to 60 and 213. At the Staff's request, INEL reviewed the information provided by Westinghouse in the special submittals.

This technical evaluation report documents the results of INEL's review of the Westinghouse realistic LBLOCA methodology for licensing analyses of Westinghouse three- and four-loop PWRs with cold leg injection. Section 2 discusses a comparison of the Westinghouse methodology to the CSAU methodology, and Section 3 discusses Westinghouse's phenomena identification and ranking table (PIRT). Sections 4 and 5 discuss Westinghouse's methodology regarding code assessment and plant nodalizations. Section 6 gives an overview of the Westinghouse methodology (methodology roadmap), the details on Westinghouse's assessment of code/experiment accuracy, and discusses the methods used to analyze propagation of uncertainty. Section 7 discusses the effects of scale, and Section 8 discusses how Westinghouse accounts for the effects of reactor input and state. Section 9 describes several other aspects of Westinghouse's methodology (WCOBRA/TRAC code description, uncertainty distribution review, handling of split breaks, and the HOTSPOT (Reference 31) model). Section 10 discusses how the method meets the guidance of RG 1.1.57 and addresses range of applicability. Compensating error analyses are discussed in Section 11. Reviews of the WCOBRA/TRAC countercurrent flow limitation (CCFL), accumulator nitrogen, and minimum film boiling temperature models are found in Section 12. Section 13 summarizes how the Westinghouse method complies with 10 CFR 50.46. Section 14 provides a summary of the review status, and the references are listed in Section 15. Appendix A contains the details of the WCOBRA/TRAC code review, Appendix B contains the details of the INEL review of the WCOBRA/TRAC code assessment, Appendix C

compares the Westinghouse methodology to RG 1.157, and Appendix D summarizes the INEL review of the Westinghouse dispersed flow film boiling model.

10 CFR 50.46 requires that it be shown that the ECCS criteria set forth in the regulation are not exceeded with a high level of probability. Based on the recommendation in RG 1.157, the INEL review used a 95% probability level as the basis for a high level of probability.

2. WESTINGHOUSE METHODOLOGY AND CSAU COMPARISON

In Reference 54, Westinghouse submitted a comparison of its realistic LBLOCA methodology based on WCOBRA/TRAC to the CSAU methodology (Reference 61). This section summarizes that comparison and, where appropriate, references the sections in this report that describe the Westinghouse methodology and the INEL review in more detail. The information is presented by following the three elements and 14 steps in the CSAU methodology.

2.1 Element 1 - Requirements and Capabilities

This element consists of the first 6 steps of the CSAU methodology. These steps are intended to determine the scenario modeling requirements and compare them to computer code capabilities to determine the applicability of the computer code to the particular scenario. Element 1 is also used to identify potential limitations.

2.1.1 Step 1. Specify the Scenario

The capabilities of a computer code are scenario dependent. For example, the requirements to properly calculate a LBLOCA are different from a small-break LOCA. This is because the dominant phenomena and processes are different. Therefore, the first step in the CSAU methodology is to specify the scenario being considered.

The CSAU and Westinghouse realistic methodologies selected the LBLOCA. In identifying the specific scenario being considered, Westinghouse fulfilled CSAU Step 1.

2.1.2 Step 2. Select the Nuclear Power Plant

The response of a particular PWR plant to a LBLOCA will vary from plant to plant. Therefore, the type of plant or plants being considered must be identified.

For CSAU, a Westinghouse four-loop PWR with 17x17 fuel bundles was selected. Westinghouse selected three- and four-loop Westinghouse plants with cold leg ECC injection. Fuel bundle types included 15x15 and 17x17.

By specifying the type of plants considered, Westinghouse fulfilled CSAU Step 2.

2.1.3 Step 3. Identify and Rank Phenomena

Not all phenomena are equally important in calculating a plant's response to a LBLOCA. Therefore, the phenomena must be identified and ranked relative to their importance on the primary safety criteria for a LBLOCA. For the LBLOCA, the primary safety criterion is the PCT. Phenomena important to each phase of the LBLOCA are identified and ranked separately. By identifying and ranking phenomena in a PIRT, the list of phenomena needing to be considered in the analysis is simplified and reduced to a manageable size.

In CSAU, expert opinion and user experience formed the basis for the PIRT developed during the review.¹⁰⁴

Westinghouse developed the code modeling requirements by analyzing the important phenomena and processes needed to achieve an accurate estimate of PCT. These included fluid flow, heat transfer, structural considerations, and mass and energy sources and sinks. See CQD Section 1-6. Westinghouse also developed a PIRT similar to that in the CSAU methodology. Each phase of a LBLOCA was considered separately. INEL review of the Westinghouse PIRT is discussed in Section 3 of this report.

Westinghouse developed a PIRT similar to that developed in the CSAU study (References 61 and 104). As discussed in Section 3 of this report, the important phenomena were identified and ranked. This was done for each phase of a LBLOCA. Therefore, Westinghouse fulfilled CSAU Step 3.

2.1.4 Step 4. Select a Frozen Code

Selecting a frozen code is important because it ensures that changes to the code after an evaluation is completed do not impact the conclusions of the study. Also, it ensures changes occur in an auditable and traceable manner.

CSAU used TRAC-PF1 MOD1, Version 14.3.¹⁰⁰

Westinghouse selected WCOBRA/TRAC, MOD7, which was later modified by improving the reflood entrainment model. The modified code, WCOBRA/TRAC, MOD7A, was used to recalculate all reflood tests that had a PCT used in the code bias and uncertainty assessment. Only blowdown tests not affected by the entrainment model change were not reanalyzed with WCOBRA/TRAC, MOD7A. Westinghouse made additional modifications (in the form of added capabilities needed for the uncertainty propagation methodology and error corrections) to WCOBRA/TRAC, MOD7A, to produce WCOBRA/TRAC, MOD7A.Rev.1. These modifications were described in Reference 58, Appendix A. Westinghouse stated that the effects of the error corrections on the experiment simulations were considered to be negligible. INEL review of the Reference 58 information led to the same conclusion because only some error corrections would apply to the assessments used to calculate the code bias and uncertainty. Also, Westinghouse stated the effects of the error corrections that could affect the experiment simulations that impact the code bias were insignificant, no effect, or the original calculations were still valid. INEL review concluded that only error corrections were made. Therefore, INEL agreed with Westinghouse that no reanalysis was needed for WCOBRA/TRAC, MOD7A.Rev.1.

Because Westinghouse selected a frozen code and recalculated all analyses that were impacted by the MOD7 to MOD7A changes and reanalysis was not needed for the MOD7A.Rev.1 changes, it has met the intent of CSAU Step 4.

2.1.5 Step 5. Provide Code Documentation

This step provides documentation that is consistent with the frozen code version. Adequate documentation allows the codes applicability to the specific scenario and plants to be evaluated. CSAU recommends the

documentation include a user manual, user guide, developmental assessment reports, and a models and correlations quality evaluation report.

TRAC code documentation available to the CSAU methodology included a code users manual and code description, a models and correlations document, and developmental code assessment reports.

Westinghouse documented its realistic LBLOCA methodology in the five volume CQD. The CQD included a description of the WCOBRA/TRAC models and correlations, a series of code assessments, description of applying the methodology to a PWR, and the uncertainty evaluation. Westinghouse's CQD formed the basis for the INEL review of the Westinghouse methodology. Significant documentation was also generated during the review of as a result of Westinghouse's responses to NRC questions. INEL review of the code models and correlations is found in Section 9.1 and Appendix A of this report, the code assessment review is found in Section 4 and Appendix B of this report, plant models and applications in Sections 5 and 8 of this report, and the uncertainty evaluation in Section 6 and 9.2 of this report.

Adequate documentation was one of the issues that arose during the review. To address documentation problems, Westinghouse developed a plan, documented in a letter on September 18, 1995,²⁰⁴ to address the NRC concerns raised during the review.

Except for the user manual and user guide, documentation equivalent to that outlined in CSAU Step 5 was provided by Westinghouse. The user manual and guide were not included in the scope of the INEL review.

2.1.6 Step 6. Determine Code Applicability

The applicability of a computer code is determined by evaluating the conservation equations, closure relationships, code numerics, and structure and nodalization relative to the important phenomena identified by the PIRT in Step 3. This step identifies the code's applicability and helps to identify areas needing modification or needing to be considered in the uncertainty evaluation.

To determine code applicability, CSAU used the PIRT to identify important phenomena and evaluated the capabilities of the chosen code, TRAC-PF1, to calculate those phenomena. CSAU concluded the TRAC-PF1 code was applicable to LBLOCA analyses.

Westinghouse performed a similar evaluation but described the LOCA transient in terms of physical processes: fluid flow, structural heat transfer, and structural distortion. The capabilities of WCOBRA/TRAC to predict the phenomena associated with the above processes was assessed, and Westinghouse concluded the code was applicable to LBLOCA analyses. During the review process, Westinghouse developed a PIRT for three- and four-loop plants with cold leg injection. INEL review of the CQD and the PIRT found nothing to contradict Westinghouse's conclusion in this area.

Therefore, Westinghouse met the intent of CSAU Step 6.

2.2 Element 2: Assessment and Ranging of Parameters

In Element 2, Steps 7 to 10 are used to determine the effects of the important parameters over the specified ranges. The effects to consider include those associated with code accuracy, effects of scale, and parameter ranges for the uncertainty evaluation.

2.2.1 Step 7. Establish an Assessment Matrix

In this step, the data set used to determine the code uncertainty based on comparisons to test data is established. The PIRT table is used to help determine the assessment matrix, which should include both separate effects and integral tests. The assessment matrix is used to provide a data base for evaluating: (a) the code accuracy to calculate phenomena important to the scenario, (b) the code's capability to scale-up phenomena to the full-size plant, and (c) the influence of nodalization on the calculation.

The CSAU study reviewed prior TRAC-PF1 assessments to confirm they examined the dominant phenomena identified in the PIRT. Tests used in the CSAU study included the Upper Plenum Test Facility (UPTF) for ECC bypass; Marviken for break flow; Loss-of-Fluid Test Facility (LOFT) for scaling and

nodalization; Slab Core Test Facility (SCTF) and Cylindrical Core Test Facility (CCTF) for scaling, heat transfer, and steam binding; INEL film boiling tests for heat transfer; two-phase pump data; and rewet data.

The Westinghouse methodology included assessment of WCOBRA/TRAC against approximately 100 separate effects and integral tests. In Reference 54, Westinghouse compared the WCOBRA/TRAC assessment against the highly ranked phenomena in the Westinghouse PIRT. INEL review of the Westinghouse comparison found that all important phenomena identified in the PIRT were covered in the assessment tests. The INEL reviewed the results of the assessment studies, and the results of that review are discussed in Section 4 and Appendix B of this report. Also, the range of the tests was found to adequately cover the range of the conditions expected in Westinghouse three- and four-loop PWRs with cold leg injection (see Section 10.2 of this report) for the important parameters defined in the RG and Westinghouse's PIRT.

Therefore, Westinghouse established an assessment matrix consistent with CSAU Step 7.

2.2.2 Step 8. Define Nuclear Power Plant Nodalization

The nodalization studies discussed in this step are intended to define a PWR nodalization that is sufficient to provide needed detail yet economical to run full-scale PWR analyses.

CSAU used previous studies with developmental versions of TRAC-PF1 to define the noding detail for the PWR. The basic rule was to use the same number of nodes as in the LOFT code assessment work. The core model did not include a separate channel to represent the hot assembly.

Westinghouse established the PWR noding in the vessel based on system geometry (location of guide tubes, support columns, and flow mixers) and the LBLOCA processes discussed in Step 3. To meet RG 1.157 recommendations, a hot assembly is represented as a separate channel; engineering judgement and PWR calculations were used to determine the hot assembly location in the core. To allow use of the assessment calculations in determining the code uncertainty, the PWR nodalization was applied to experiment simulations to ensure nodes of

similar axial length. INEL review of the experiment and PWR nodalizations is discussed in Section 5 of this report.

Therefore, INEL concluded that Westinghouse developed three- and four-loop plant nodalizations consistent with CSAU Step 8.

2.2.3 Step 9. Determine Code and Experiment Accuracy

This step discusses two approaches to determining the code accuracy. First, there is the direct comparisons to experimental data. Second, there is the use of the experimental data to determine parameter ranges for use in PWR sensitivity studies.

In CSAU, this step consisted of two parts, ranging of parameters for the uncertainty evaluation and code and experiment accuracy. In the first part, models were assessed and ranged by comparing code predictions to data and use of scatter plots. The code bias was estimated and applied as a multiplier on a calculated result or as an additive term to correct the tendency of the model to overpredict or underpredict the data. The scatter about the bias line was used to develop the model uncertainty. In most cases, a uniform distribution was assumed due to lack of data. In the second part, code calculations of PCT were compared to experimental data for separate and integral effects tests.

In Westinghouse's methodology, several thermal-hydraulic models were ranged for the uncertainty evaluation including, critical flow, fuel rod parameters, heat transfer, minimum film boiling temperature (T_{MIN}), pump/nozzle resistance, and condensation. Other models were confirmed to not be important or were conservatively biased. Further information on the INEL review of this area is given in Section 6 of this report on the uncertainty propagation. In the second part, Westinghouse performed the extensive code assessment discussed above and used it to determine an experiment based code bias and uncertainty. INEL review of the experiment based bias and uncertainty is discussed in Section 6.5 of this report.

Westinghouse included both types of approaches in its determination of the code and experiment accuracy; however, there are some differences such as

the comparison of the model and code based uncertainties discussed in Sections 6.1 and 6.5 of this report. The Westinghouse methodology is considered to be consistent the intent of CSAU Step 9.

2.2.4 Step 10. Determine the Effect of Scale

Step 10 recognizes that not all of the code assessment work will be performed on tests completed at full-scale test facilities. This step assesses the effects of the scale differences on the code uncertainty estimate.

In the CSAU study, it was concluded that power-to-volume scaled test facilities adequately simulate the PWR response except in the areas of the downcomer (ECC bypass) and upper plenum entrainment. Sensitivity studies were performed for the PWR to determine the effects of scale based on the parameter ranges developed. For upper plenum entrainment, TRAC-PF1 calculations with the entrainment models altered were run to determine the bias for the effect of steam binding on PCT. In the case of ECC bypass, full-scale UPTF data were used to develop a bias applied to the calculated PCT. CSAU also identified critical flow and pump two-phase performance as needing additional review because of the lack of full-scale data and included variations in these models in the run matrix used to develop the PCT response surface.

Westinghouse concluded that the CSAU conclusions on the applicability of power-to-volume scaled facilities also applied to its methodology. Thus, Westinghouse evaluated the effects of ECC bypass and upper plenum entrainment. However, full-scale UPTF test data was now available in these areas. To evaluate the effects of ECC bypass, UPTF Test 6 was assessed, and Westinghouse determined that WCOBRA/TRAC overpredicted ECC bypass resulting in a conservative (negative) PCT bias (see response to Volume 4, question 2, Reference 21). At the present time, Westinghouse does not use the negative bias it calculated. For upper plenum entrainment, UPTF Test 29B was evaluated, and again Westinghouse found a conservative (negative) bias in its WCOBRA/TRAC calculations (see response to Volume 3, question 10, Reference 41). In this case, Westinghouse also does not apply the negative bias. Regarding critical flow, Westinghouse accounts for this directly in the uncertainty analysis with the effect determined by PWR sensitivity

calculations. For pump two-phase performance, Westinghouse evaluations (see CQD Section 16-3 and CQD Appendix C) showed that single-phase pump performance is more important and included this parameter directly in the uncertainty evaluation. The variations for critical flow and single-phase pump performance are discussed in Section 6 of this report on propagation of uncertainty.

Based on the above, INEL concluded the Westinghouse has met the intent of CSAU Step 10 and that conservative biases for ECC bypass and upper plenum entrainment were not used by Westinghouse to adjust the final calculated PCT.

2.3 Sensitivity and Uncertainty Analysis

In this element, the effects of individual contributors to the total uncertainty are determined and combined to provide a statement on the total uncertainty of the analysis.

2.3.1 Step 11. Determine the Effect of Reactor Input Parameters and State

Uncertainty in the operating state of the PWR at the time of the accident results in uncertainty in the calculated PCT. This step assesses the effects of the plant initial conditions on the accident results.

The CSAU study evaluated the peaking factor and fuel stored energy to define an operating point. Plant inputs were based on the assumption of base load operation.

Westinghouse considered the effects of a wide range of parameters on the calculated PCT and both plant initial conditions and boundary conditions were considered. Westinghouse determined the impact of:

1. Plant physical configuration: steam generator tube plugging, hot assembly location, and pressurizer location relative to the break.
2. Power distributions and operating history: load following maneuvers with their impact on peaking factors and power shapes

and uncertainties related to the time in the cycle at which the accident occurs.

3. Initial fluid conditions: reactor pressure, reactor T_{avg} , accumulator temperature, and accumulator pressure.
4. Boundary conditions: break location, type, and size; containment pressure; pumped safety injection (SI) flow and temperature; and offsite power availability.

The above items are discussed in more detail in Section 8 of this report.

The Westinghouse methodology accounts for the effects of the uncertainty in the initial plant operating conditions on the overall analysis. Therefore, the Westinghouse methodology is consistent with CSAU Step 11.

2.3.2 Step 12. Perform PWR Sensitivity Calculations.

This step provides information on the effects of the plant input conditions and code model uncertainties on the code output (primarily PCT). This is done by performing code sensitivity calculations with the input varied to determine the effects on the calculated results.

For CSAU, a thermal-hydraulic run matrix that varied break flow, pump two-phase head degradation, T_{MIN} , core entrainment, and combinations of break flow and pump two-phase head degradation was developed. Local effects were calculated using the TRAC supplemental rod option. This allows different rods to be modeled, but the rods do not feedback into the thermal-hydraulic analysis. The CSAU study used these rods to determine the effect of peaking factor, fuel conductivity, gap heat transfer coefficient (HTC), forced convection HTC, and combinations of gap HTC and fuel conductivity and gap HTC and forced convection HTC.

The Westinghouse thermal-hydraulic run matrix looks at the effects of break flow, broken loop vessel nozzle loss coefficient, and condensation multiplier. Another run matrix looks at the effects of power distributions. Also, the effects of initial conditions are determined through WCOBRA/TRAC

calculations. Local effects of hot rod peaking factor, gap HTC, fuel density, fuel conductivity, cladding burst temperature, cladding burst strain, metal-water reaction, convection HTC, and various cross products of these parameters are accounted for through HOTSPOT simulations. These simulations use the HOTSPOT code with break flow/condensation run matrix and power distribution run matrix results as boundary conditions. These are discussed in more detail in Sections 6 and 9.4 of this report.

Westinghouse performs the sensitivity calculations discussed above to determine the effects of code input and models on the WCOBRA/TRAC calculated PCT. In this way, the Westinghouse methodology is consistent with CSAU Step 12.

2.3.3 Step 13. Combine Biases and Uncertainties

In this step, the uncertainties associated with the various parts of the methodology (for example, code limitations, scale effects, and initial operating conditions) are combined. One approach is to use a Monte Carlo simulation to determine the PCT distribution.

In CSAU, the results of Step 12 were used to determine response surfaces for the blowdown and reflood PCTs using seven variables. The 95th percentile PCT was assessed through Monte Carlo simulation.

Westinghouse also developed response surfaces from the results of the analyses in Step 12. In addition, Westinghouse included the initial and boundary condition uncertainty. The 95th percentile PCT was developed through Monte Carlo simulation. This is discussed in Section 6 of this report.

Westinghouse combines the various components of uncertainty. In doing so, the methodology is consistent with CSAU Step 13.

2.3.4 Step 14. Determine Total Uncertainty

In this step, a final statement of total uncertainty given as a probability for the limiting value of the primary safety criteria is made for the code. Based on RG 1.157, this review used the 95th percentile as the

basis for compliance with the high probability requirement of 10 CFR 50.46. Biases may be applied to account for uncertainty contributors that could not be quantified or because it was not economical to quantify the effect of uncertainty contributors.

The CSAU study estimated the 95th percentile PCT with a Monte Carlo simulation using the response surface developed in Step 13 and randomly sampling the assumed distributions for the seven parameters. A number of biases were then applied based on the results of studies performed during the CSAU development.

The Westinghouse methodology also uses a Monte Carlo simulation to determine the 95th percentile PCT. In this way, the Westinghouse methodology is consistent with the CSAU approach in Step 14. The power distribution response surface calculates the effect on PCT of the randomly sampled power distribution variables. The initial condition bias and uncertainty is sampled and applied to the PCT equation. The model response surface developed in Step 13 is used to calculate a bias and uncertainty associated with those parameters using randomly sampled variables. The uncertainty from the model response surface is used as discussed in Sections 6.1 and 6.5 of this report. In the Monte Carlo analysis, the results of the various uncertainties are combined by superposition. To correct for inaccuracies in the superposition approach, Westinghouse performs WCOBRA/TRAC runs with off-normal conditions to provide a validation data set for the superposition assumption. The results of these WCOBRA/TRAC runs are compared to the results of the superposition approach. This comparison is used to develop a correction to the superposition approach that is applied during the Monte Carlo analysis. The superposition correction and the use of the uncertainty in the superposition correction are discussed in more detail in Sections 6.1 and 9.2 of this report. No biases are applied after the PCT is calculated, although several negative biases were estimated (see Section 6 of this report on the propagation of uncertainty).

Based on the above, the INEL concluded Westinghouse uses a methodology consistent with CSAU Step 14.

2.4 Summary of INEL Review

This CSAU comparison summary shows the Westinghouse methodology closely follows the CSAU methodology, and that Westinghouse accounted for the 14 steps of the CSAU methodology. Specific similarities include using a PIRT to identify important phenomena, ranging parameters and sensitivity studies to determine code uncertainty propagation, and use of Monte Carlo simulations and response surfaces to determine the 95th percentile PCT. Some differences are noted, however, because of Westinghouse's need to address the concerns of operating plants, the justification of operating plant limits, the different codes involved, and additional full-scale data available now. Overall, the INEL concluded that, based on the discussion above, the Westinghouse methodology is consistent with the CSAU methodology.

3. PIRT EVALUATIONS (CSAU STEP 3)

As noted in Section 2.1.3 of this report, a PIRT is important in identifying the important phenomena that control a specific accident scenario and ranking them for their relative importance. In this way, the important phenomena can be identified and accounted for in the uncertainty analysis. It also provides a means of reducing the phenomena needing to be considered to a manageable number. Westinghouse provided the WCOBRA/TRAC PIRT in References 37 and 54. INEL review of the PIRT is discussed below.

Westinghouse's PIRT discussion included the company's own ranking of phenomena and a comparison to that done by the experts panel during the CSAU review (Reference 104). Comparison of the two PIRTs found them very similar. In general, there was good agreement between the two PIRTs, and only occasionally was a phenomenon ranked differently by more than two. Based on Reference 104, the INEL considered a ranking difference of three or more an indication of a significant difference of opinion between the PIRTs. The areas where the ranking differed by three or more are discussed below.

According to the CSAU expert PIRT, the fuel rod gap conductance should be highly ranked during reflood, but it was not ranked by Westinghouse. Westinghouse stated this is because the cladding heat flux to the fluid is low during reflood. This implies the dominant resistance to heat flow during reflood is at the cladding/fluid interface, and gap conductance during reflood is sufficient to keep the fuel pellets and the cladding thermally coupled for heat transfer. Based on this, the INEL agrees with Westinghouse's not ranking gap conductance in its PIRT for reflood. The INEL also notes Westinghouse includes the gap conductance uncertainty in its uncertainty propagation methodology.

The ranking for core three-dimensional flow also differed. However, during reflood, the fluid radial profile is not significant based on SCTF and CCTF test results (see References 105 and 106). Therefore, the different (lower) ranking by Westinghouse appears to be justified based on test data. Also, the INEL notes the Westinghouse WCOBRA/TRAC core nodalization accounts for the core radial power profile that would drive three-dimensional flow effects.

Westinghouse stated that it differed from the CSAU study in the reflood ranking for core void generation/distribution. This was because it chose to emphasize core entrainment/deentrainment during reflood, which was not ranked by the CSAU experts for reflood, rather than core void generation/distribution. Westinghouse chose this approach because core entrainment/deentrainment will determine the amount of liquid at the PCT location, and it understood reflood to be a lower flow, more uniform process relative to void generation/distribution during blowdown (where Westinghouse highly ranked core void generation/distribution). The INEL also notes that Westinghouse's ranging of the overall HTC in the uncertainty distribution accounts for calculated versus measured differences in local fluid conditions that would address both core void generation/distribution and entrainment/deentrainment. Based on this, the INEL considers this PIRT difference adequately justified.

Upper plenum entrainment/deentrainment was another phenomenon that was ranked differently; it was ranked lower in the Westinghouse PIRT relative to the CSAU PIRT. Westinghouse noted this was because the importance of entrainment/deentrainment was included in its PIRT under the steam generator steam binding phenomenon. The Westinghouse ranking for steam binding was 7 versus a CSAU ranking of 9 (as noted above, INEL does not consider this ranking difference significant because they are within 2 of each other). INEL considers the Westinghouse ranking of upper plenum entrainment/deentrainment appropriate. This is because, even though it is lower than the CSAU ranking, the WCOBRA/TRAC review looked specifically at mass storage in the upper plenum. Comparisons to full-scale UPTF upper plenum tests showed WCOBRA/TRAC calculated lower upper plenum mass storage relative to the test data. This implies more mass entrained into the loops and greater steam binding. Greater steam binding is conservative, and Westinghouse does not take credit for the conservatism in its uncertainty analysis.

A similar justification was given for Westinghouse not ranking hot leg entrainment/deentrainment. WCOBRA/TRAC PWR calculations show very little liquid storage in the hot legs, and any liquid swept into the hot legs is entrained into the steam generators. NUREG/IA-0127, Reference 105, noted that UPTF and CCTF results showed little hot leg mass storage, but that SCTF results did show hot leg mass storage. This difference was attributed to the

differences in hot leg cross section between SCTF and UPTF. Based on the test data, the lower ranking by Westinghouse appears justified.

Pump two-phase performance during blowdown was ranked lower by Westinghouse because of the pump sensitivity studies performed in the CQD. The basis for and the approach used to account for the uncertainty in pump performance is discussed in Section 3.1.2 of Reference 58. Based on this information, the INEL found the pump two-phase performance ranking appropriate.

The ranking by Westinghouse for non-condensable gases in the cold leg during reflood differed also. The basis for this ranking of the accumulator nitrogen cover gas is the Westinghouse results presented in response to Volume 1, question 134, Reference 37. The INEL notes the Westinghouse models for determining the effect of nitrogen entering the primary system after the accumulators empty was given an in-depth review by Westinghouse and the INEL. The same response discussed the effects of dissolved nitrogen coming out of solution in the primary system, and Westinghouse showed that effect was negligible. The details of the INEL review are discussed in Section 12.2 of this report.

The Westinghouse PIRT did not rank loop oscillations during reflood while it was ranked a 9 in the CSAU study. Westinghouse noted it did not rank this phenomenon because the phenomena that drive loop oscillations such as ECC condensation and downcomer boiling were already addressed separately in the PIRT. INEL reviewed the Westinghouse PIRT and found the important phenomena for loop oscillations were ranked separately and appropriately (based on Westinghouse justification and/or comparison to the CSAU PIRT) in the Westinghouse PIRT. Therefore, the Westinghouse approach to loop oscillations is considered adequately justified.

The Westinghouse PIRT brought out several phenomena not previously ranked by the CSAU experts. These include the importance of the hot assembly (HA) location relative to upper plenum/upper head structures during blowdown; blowdown core flow reversal/stagnation, loop flow split/resistances, pump resistance, and break flow and their effect on blowdown PCT; uncertainty of

the single-phase pump performance; reflood core/downcomer level oscillations; and entrainment/deentrainment in the core during reflood.

In conclusion, the INEL found good agreement between the Westinghouse and CSAU expert PIRTs. Where a phenomenon ranking differed by three or more, the INEL found adequate justification by Westinghouse and/or the WCOBRA/TRAC model used to represent the phenomenon was included in the review scope. Based on this, the INEL concluded the Westinghouse PIRT for Westinghouse three- and four-loop plants with cold leg injection is adequate.

4. CODE ASSESSMENT (CSAU STEP 7)

This section summarizes the INEL review of the extensive code assessment work Westinghouse performed on WCOBRA/TRAC. This assessment is required by Part a of 10 CFR 50.46, RG 1.157, and CSAU, and Westinghouse uses the results in determining an experiment based uncertainty for WCOBRA/TRAC. In Reference 54, Westinghouse compared the highly ranked phenomena in its PIRT to the assessment test matrix. INEL review of the comparison found all the highly ranked phenomena were covered by the test matrix.

The details of the assessment work and the INEL review are contained in Appendix B of this report. The review of the separate effects experiments is summarized first followed by the integral experiments and other assessments.

4.1 Separate Effects Tests

Based on the INEL's review of the separate effects tests discussed in Section B.1 of this report, the following conclusions were reached:

1. Based on a review of the CQD and Westinghouse's response to Volume 2, question 2, Reference 39, the INEL concluded the assessment of blowdown heat transfer covered the appropriate range of conditions. Assessment of reflood heat transfer also covered the appropriate range of conditions.
2. WCOBRA/TRAC did a reasonable job of calculating the Oak Ridge National Laboratory (ORNL) Thermal-Hydraulic Test Facility (THTF) tests simulated.
3. Based on the comparisons of calculated and measured results shown in the CQD, INEL concluded WCOBRA/TRAC adequately calculated the G-1 and G-2 blowdown tests^{77,78} and the G-2 refill¹⁰⁸ tests.
4. WCOBRA/TRAC, MOD7A, had difficulty calculating turnaround time, cooldown rate, and quench time accurately relative to the forced reflood test data. The response to Volume 2, question 63, Reference 47, identified the fact that WCOBRA/TRAC tended to

overpredict entrainment and underpredict heat transfer to the vapor just above the quench front as the dominate reasons for these calculated results. For PCT, Westinghouse addressed these effects by determining heat transfer multipliers based on comparisons to test data that are applied in the uncertainty evaluation. Westinghouse addressed these issues for oxidation through the methodology discussed in Section 13 of this report. As discussed in that section, the oxidation methodology adequately accounts for the oxidation uncertainty resulting from the above issues by applying a time shift to the oxidation calculations. Westinghouse, in Reference 206, Attachment 6, addressed the effect of underpredicting the turnaround time on PCT. Westinghouse noted that the effect of turnaround time is covered in the methodology through the break flow/condensation run matrix. For the case of North Anna (VRA) given in Reference 206, Westinghouse found reflood turnaround time varied in the run matrix results from 69 to 114.5 s and 156 to 249 s for the first and second reflood peaks, respectively. Westinghouse also showed that WCOBRA/TRAC tended to overpredict quench time and turnaround time for the gravity reflood tests, which are the tests most representative of the PWR. Based on the turnaround time variation calculated in the break flow/condensation run matrix and the conservative estimates of quench time and turnaround time for the gravity reflood tests, INEL concluded that Westinghouse adequately addressed the effects of turnaround time on PCT. Therefore, the separate effects reflood test comparisons are considered adequate based on:

- (a) the INEL review of the comparisons provided and
- (b) Westinghouse's methodology adequately addressing uncertainty due to heat transfer, turnaround time, cooldown rate, and quench time on PCT and oxidation.

4.2 Integral Effects Tests

Based on the INEL's review of the integral effects tests discussed in Section B.2 of this report, the following conclusions were reached:

1. Although break flow mispredictions caused the WCOBRA/TRAC calculated PCTs for LOFT to be lower than the data, the INEL notes the WCOBRA/TRAC uncertainty evaluation directly accounts for the effect of break flow uncertainty on the calculated PCT. Therefore, the Westinghouse LOFT assessments are considered adequate. Also, the detailed analysis of LOFT Tests L2-3 and L2-5 in Section 11 of this report on compensating errors supports the adequacy of the WCOBRA/TRAC LOFT assessments.
2. Based on the conservative predictions, the CCTF assessments are considered adequate. Also, the assessment of CCTF Test 62 in Section 11 of this report supports the adequacy of the CCTF analyses.
3. Based on the conservative results, Westinghouse's SCTF assessments are considered adequate. Also, the detailed analysis on SCTF Test 619 in Section 11 of this report on compensating errors supports the adequacy of the SCTF analyses.
4. Based on the comparisons provided by Westinghouse, WCOBRA/TRAC does an adequate job of simulating the UPTF tests.

4.3 Other Assessments

Based on the INEL's review of the other assessments discussed in Section B.3 of this report, the following conclusions were reached:

1. Based on the Westinghouse comparisons, WCOBRA/TRAC does an adequate job of simulating the Westinghouse/Electric Power Research Institute (EPRI) 1/3rd-scale steam/water mixing tests and the Creare scaled ECC bypass tests.
2. Based on the National Research Universal Reactor (NRU) comparisons, INEL considers the NRU tests adequately calculated by WCOBRA/TRAC. PCTs were reasonably calculated as were the burst parameters. Based on the NRU results, there is some uncertainty in the transient rod internal pressure (RIP) calculation that will

affect the burst temperature criterion in WCOBRA/TRAC analyses. However, in Volume 4, question 40, Reference 53, Westinghouse showed the effect of the RIP uncertainty on the burst temperature criterion was small and well within the burst temperature uncertainty accounted for with the local effects models in HOTSPOT. Therefore, for local effects, the Westinghouse methodology accounts for the uncertainty in transient RIP. Westinghouse also calculates HA rod burst in the full WCOBRA/TRAC analyses called for in its methodology. If WCOBRA/TRAC calculates a HA rod reflood PCT greater than 1600°F but not rod burst, Westinghouse in Reference 214, List II, Item 2, committed to increasing the initial RIP in the WCOBRA/TRAC HA rod until burst is calculated and choosing the more limiting of the burst and non-burst cases. This will adequately account for transient RIP uncertainties and their effect on rod burst in the full WCOBRA/TRAC runs.

Based on the above results, the INEL concluded WCOBRA/TRAC is adequate to provide realistic analyses of three- and four-loop PWR LBLOCAs.

5. PLANT MODALIZATION (CSAU STEP 8)

Westinghouse's methodology addressed the PWR nodalization issue consistent with the guidance of RG 1.157, Section 3.5, and CSAU Step 8. Westinghouse's PWR nodalization was used as the basis for the nodalizations developed for the separate effects and integral assessment analyses. The main reason for this approach was Westinghouse's desire to apply the code bias and uncertainty developed from the assessment studies to the PWR calculations. Although there are geometric differences between PWRs, Westinghouse's methodology is flexible enough to accommodate differences in design and still maintain consistency with the assessment nodalization. If a consistent nodalization methodology is used for the assessment and PWR calculations, then Westinghouse concluded, and the INEL agrees, that geometric differences/nodalization will not add to the code bias and uncertainty.

In CQD Section 20-1-2, Westinghouse discussed how the nodalizations for three different plants could accommodate geometric design differences while maintaining consistency with the assessment cases. Westinghouse discussed core axial and radial nodalization, upper plenum nodalization, and loop nodalization. The Westinghouse comparison, presented in the form of tables and text, showed how the Westinghouse methodology provided consistent nodalizations between the tests and plants.

In CQD Sections 20-2 to 20-5, Westinghouse discussed the WCOBRA/TRAC nodalizations for two four-loop plants [Indian Point 2 (IP2) and Sequoyah (SQN)], and a three-loop plant (VRA). The reader is referred to those sections of the CQD for the nodalization details. However, it is important to note here one factor considered by Westinghouse. In the plant modeling, Westinghouse included explicit modeling of the HA in the location that leads to the least flow during blowdown. The intent is to limit the blowdown cooling of the HA and bound the effect on the PCT.

Based on the consistency between the PWR and assessment nodalizations, the INEL considers the PWR nodalizations adequate for realistic LBLOCA analyses. Also, review of the plant nodalizations found Westinghouse considered important information such as upper plenum structures in determining the types of core channels and the location of the HA, low power

assemblies on the core periphery, number of loops, and loop components in determining the nodalization. In particular, the INEL considers placing the HA in the location with the least blowdown flow an appropriate bounding assumption for the analyses.

6. CODE/EXPERIMENT ACCURACY (CSAU STEP 9)

The need to determine the code and experiment accuracy is discussed in RG 1.157, Section 4, and CSAU Step 9. Westinghouse described its method of uncertainty evaluation in References 58, 205, 206, 213, and 214. Westinghouse's approach and the INEL review are discussed below.

In evaluating uncertainty, Westinghouse identified initial plant conditions and model effects as the important factors to consider. The plant conditions were further subdivided into initial conditions and core power distributions. In addition, a model or plant condition may be global or local in its effect. A parameter has a global effect if it can affect the entire thermal and hydraulic transient. It has a local effect if it only affects the local conditions at the PCT location.

To determine the important items to consider in the uncertainty propagation, Westinghouse evaluated items ranked 7, 8, or 9 in the Westinghouse PIRT. See Reference 190, response to revised methodology report question 3. INEL review of the Westinghouse LBLOCA PIRT is discussed in Section 3 of this report, but here it is sufficient to note that items ranked 7, 8, or 9 are those having the greatest influence on the analysis of a LBLOCA, and INEL considers addressing those items as most important. Items ranked lower will have a smaller effect on the analysis, and, therefore, they are less important to the uncertainty propagation. Westinghouse's evaluation found the highly ranked items were addressed in a number of ways including: ranged directly in the uncertainty analysis, modeled directly or bounded in WCOBRA/TRAC analyses, covered in the variation of items ranged directly, or calculated with a conservative bias in WCOBRA/TRAC analyses.

In Reference 58, Westinghouse discussed the following parameters in more detail to clarify how they were included in the propagation of uncertainty analysis: critical flow; pump single-/two-phase performance (broken loop relative resistance); fuel rod conditions such as power distributions, stored energy, decay heat, cladding burst, cladding reaction, and gap conductance; core heat transfer and T_{MIN} ; ECC bypass; entrainment and steam binding; accumulator nitrogen (pressurization effect); and condensation. These parameters were discussed because of their potential importance to the

PCT calculation or the fact that Westinghouse used ranging of these parameters to cover other highly ranked phenomena.

For the parameters listed above, Westinghouse grouped them according to whether they have a global effect (that is, they can affect the entire thermal and hydraulic transient), a local effect (they only affect the local conditions at the PCT location), or both. This grouping of parameters is discussed in Section 4.1 of Reference 58 and illustrated in Figure 1 on the next page. As will be discussed later, ECC bypass and entrainment/steam binding do not need to be considered in the uncertainty analysis because the code conservatively calculates these phenomena.

The following discussion clarifies how Westinghouse evaluated each item above. A overview or roadmap of the Westinghouse methodology is given first, and it is followed by more detailed discussions on the models and the plant conditions. Then, the impact of local effects on models and plant conditions will be discussed.

6.1 Westinghouse Realistic LBLOCA Methodology Roadmap

This section gives a brief overview or roadmap of Westinghouse's realistic LBLOCA methodology. References to those sections in this report that describe and summarize the INEL review of the methodology are given.

The Westinghouse realistic LBLOCA methodology consists of several parts. To determine the 95th percentile PCT, Westinghouse uses the WCOBRA/TRAC code and then performs an uncertainty analysis. The WCOBRA/TRAC base code is described briefly in Section 9.1 of this report and in more detail in Appendix A of this report. Then there is the analysis to determine the 95th percentile PCT. This analysis is discussed in Sections 6.2 and following of this report. Westinghouse's use of WCOBRA/TRAC is described first followed by the 95th percentile PCT determination. Figure 2 summarizes the steps.

The WCOBRA/TRAC program is used in several ways. First, it is used to analyze a plant's response to changes in initial conditions through one-at-a-time sensitivity studies. The effect on PCT is measured by the PCT change (Δ PCT) as a result of the initial condition change. These sensitivity

29

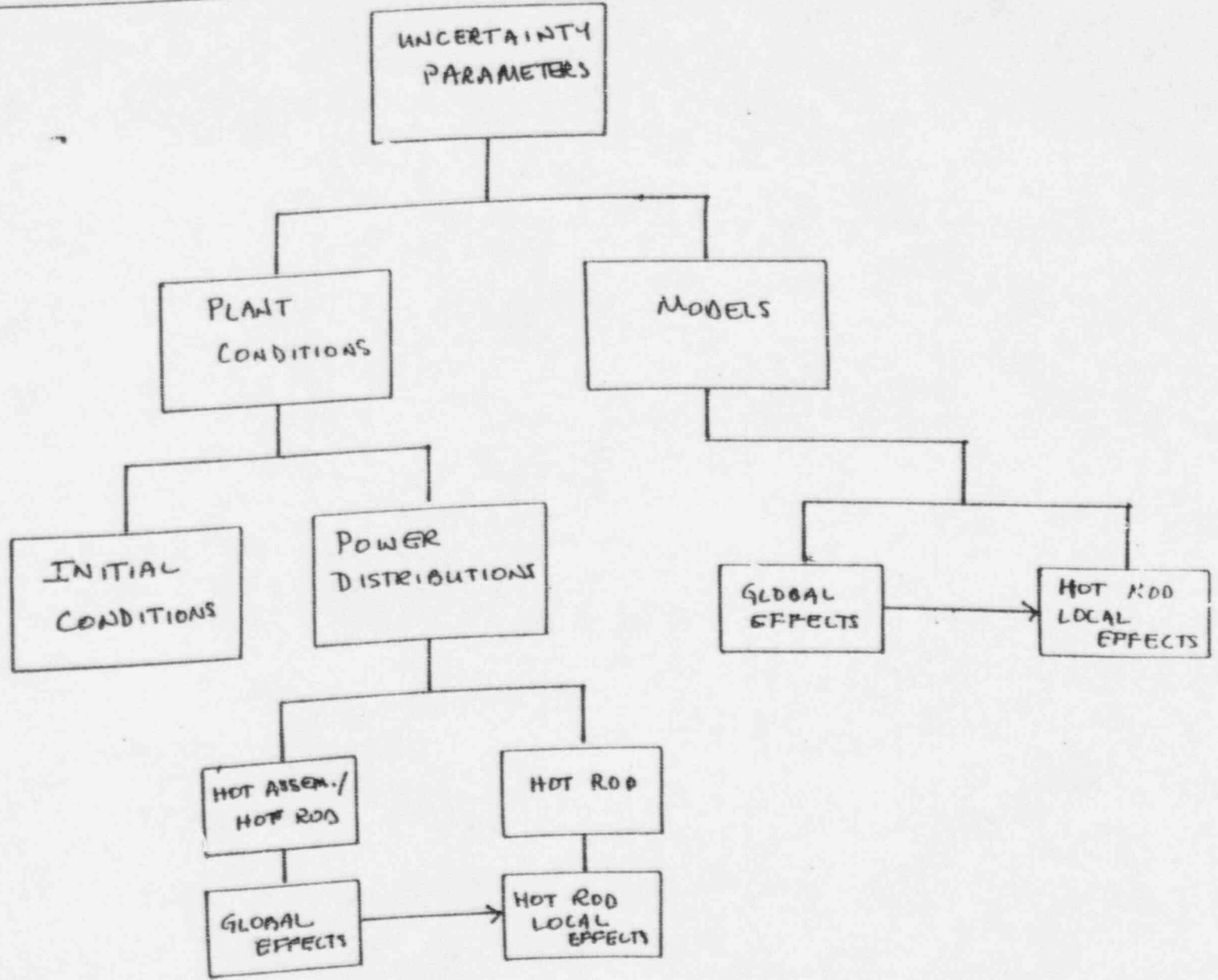
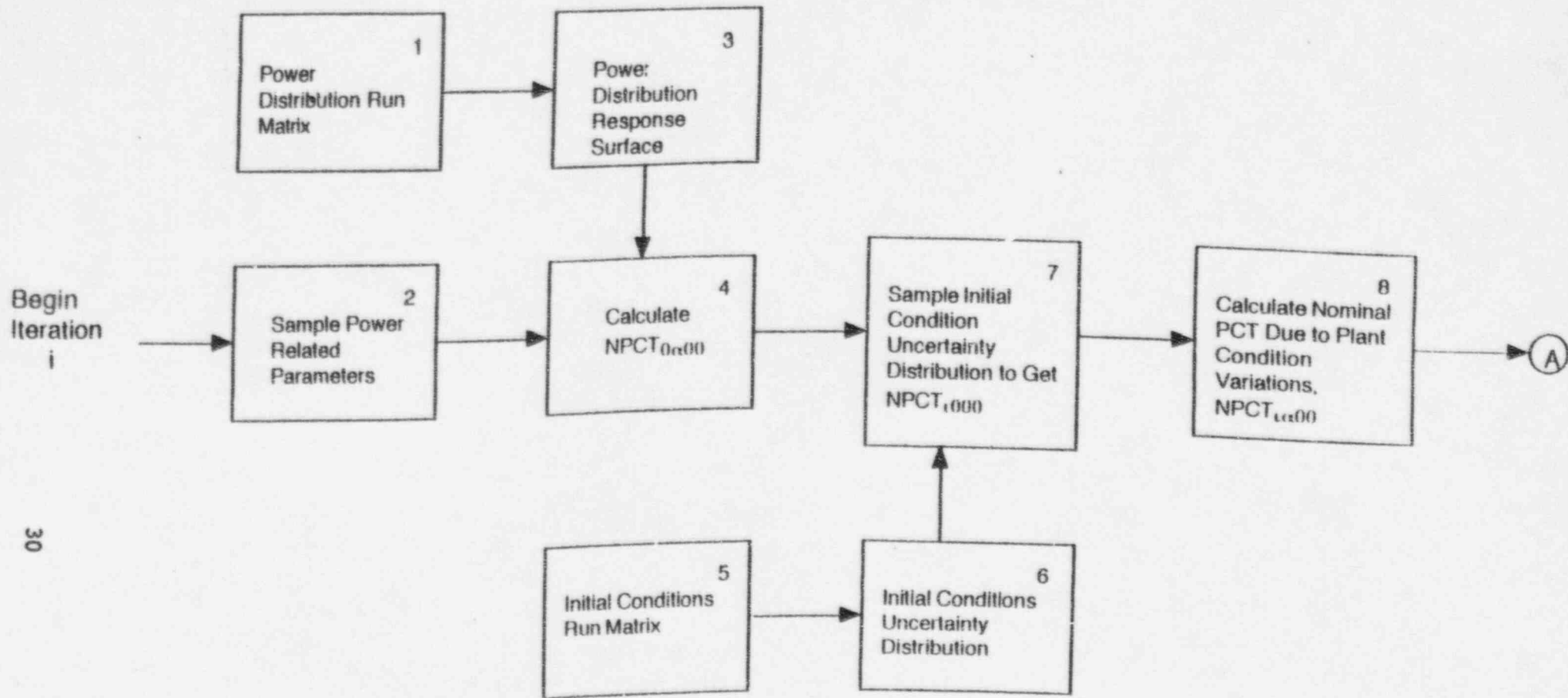


FIGURE 1 BREAKDOWN OF WESTINGHOUSE'S UNCERTAINTY PARAMETERS



30

FIGURE 2. FLOWCHART OF UNCERTAINTY DETERMINATION PROCEDURE

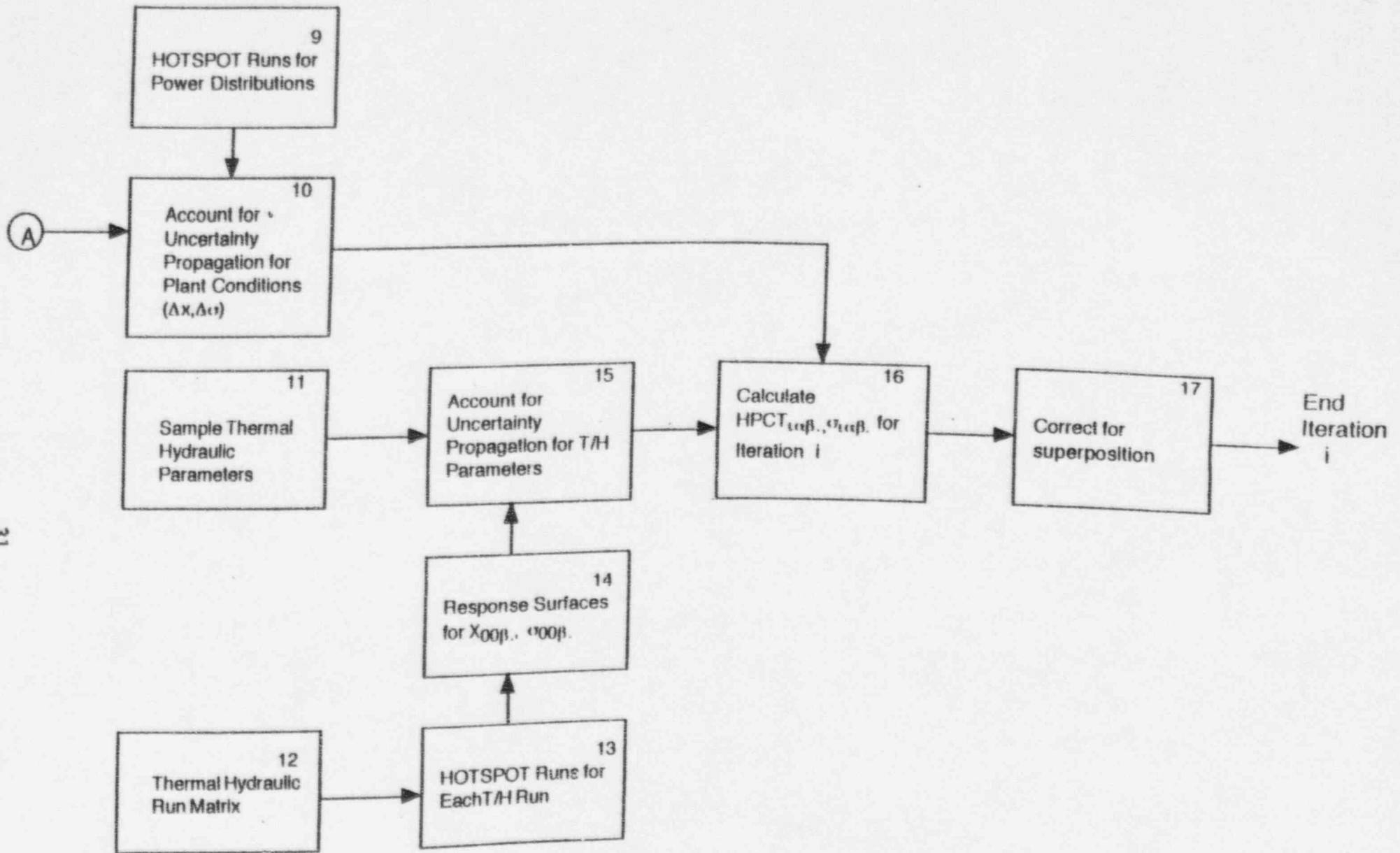


FIGURE 2. FLOWCHART OF UNCERTAINTY DETERMINATION PROCEDURE - (cont.)

studies are discussed in Section 8 of this report. The sensitivity studies are used to develop the initial conditions bias and uncertainty discussed below. Because the development of a 95th percentile PCT includes investigating many different combinations of variables, Westinghouse realized it would not be possible to analyze all of them directly using WCOBRA/TRAC. Therefore, Westinghouse uses WCOBRA/TRAC analyses to provide the Δ PCT information needed to develop response surfaces that it then uses to account for power shape effects and code model uncertainties in the uncertainty analysis. The response surfaces are also discussed in Sections 6.2 and following of this report.

Westinghouse's uncertainty analysis is divided into several parts. First, code models and initial plant condition parameters are ranged to determine their uncertainties and the effects of those uncertainties on PWR calculations (call this Part A). Part A is subdivided into global plant conditions (initial conditions and power distributions), global models (code models whose uncertainty is accounted for directly), and local effects at the PCT hot spot. This division is illustrated in Figure 1.

The initial conditions uncertainty distribution (bias and standard deviation) is based on the WCOBRA/TRAC sensitivity studies discussed above. Westinghouse does the studies on a plant specific basis and develops the initial conditions uncertainty distribution as discussed in its response to Volume 5, question 34, Reference 51. Response surfaces based on WCOBRA/TRAC runs are developed to account for power distribution effects and code model uncertainties. The power distribution effects are correlated based on several variables that affect the power distribution (see Section 4.1.1 of Reference 58). The code model effects are correlated based on several variables that affect the plant overall thermal-hydraulic response (see Section 4.1.2 of Reference 58). The model global response surface and the model local response surface (discussed next) are combined as discussed in Section 4.2.3 of Reference 58. To ensure the accuracy of the response surfaces, Westinghouse set the run matrixes to bound the expected sampling range so that accurate results would be obtained where most of the sampling would occur but without excessive extrapolation of the response surfaces outside the run matrix range.

The next subpart of Part A of the uncertainty evaluation is to account for local or hot spot uncertainties. Westinghouse uses the HOTSPOT model, discussed in Section 9.4 of this report, to perform the local uncertainty evaluation. The parameters affecting the local uncertainty are described in Section 4.1.3 of Reference 58. For selected WCOBRA/TRAC runs from the power distribution run matrix and the model run matrix, Westinghouse performs a direct Monte Carlo analysis using the HOTSPOT model to determine the spread of the PCT distribution due to local uncertainties. For the power distribution cases, Westinghouse methodology uses the HOTSPOT results for the selected runs to account for uncertainty propagation due to plant conditions. For the models, the PCT distributions due to local uncertainties for the selected runs in the thermal-hydraulic run matrix are fit to two response surfaces, one for the biases of the distributions and one for the standard deviations of the distributions that are obtained from the HOTSPOT runs. The response surface variables are the models varied in the run matrix. Westinghouse combines the model global and local effects as discussed in Section 4.2.3 of Reference 58.

In the Monte Carlo analysis, the results of the various uncertainties are combined by superposition. To correct for inaccuracies in the superposition approach, Westinghouse, in the final subpart of Part A, performs WCOBRA/TRAC runs with off-normal conditions to provide a validation data set for the superposition assumption. The results of these WCOBRA/TRAC runs are compared to the results of the superposition approach. This comparison is used to develop a correction to the superposition approach that is applied during the Monte Carlo analysis. This is discussed in more detail in Section 9.2 of this report.

For all parameters included in the uncertainty evaluation, Westinghouse has developed and justified the uncertainty distribution used. These are discussed in Section 9.2 of this report.

The second part of the uncertainty evaluation (Part B) is the code uncertainty based on comparisons between the code calculated PCT and the measured PCT in all the applicable assessment cases plus a nodalization uncertainty (combined using square root sum of the squares, uncertainty B1). Also, an uncertainty based on experimental data scatter is calculated (uncertainty B2). The uncertainty B1 is used to establish a lower bound on

the uncertainty determined from the superposition correction obtained in Part A. The uncertainty B2 is used to establish a lower bound on the uncertainty determined from the global models/local uncertainty obtained in Part A. That is, in the Monte Carlo analysis described below, the superposition correction is compared to uncertainty B1, and the global model/local uncertainty is compared to uncertainty B2. In both cases, the larger value is used.

Westinghouse now has the information needed to perform a Monte Carlo simulation to determine the 95th percentile PCT (that is, the PCT greater than that expected to occur in 95% of possible LBLOCAs). The general steps of a single Monte Carlo iteration are described next, and the steps are illustrated in Figure 2, which was taken from the January 1996 Westinghouse presentation to the Advisory Committee on Reactor Safeguards (ACRS) Subcommittee on Thermal-Hydraulics. First, power distribution parameters are sampled. These are used in the power distribution response surface to calculate the change in nominal PCT (ΔPCT) due to power distribution changes. Second, the initial conditions uncertainty distribution is sampled to get the ΔPCT due to initial conditions. The ΔPCT s from steps 1 and 2 are added to the reference PCT to get the PCT due to plant condition variations (PCT_{PC1}). Next, PCT_{PC1} is used to determine the ΔPCT due to plant conditions and local effects. This is added to PCT_{PC1} to give a PCT due to plant conditions and local conditions (PCT_{PC2}). Now, Westinghouse samples the model parameter distributions and uses them in the response surfaces for model bias and uncertainty to get the ΔPCT due to model uncertainties. The uncertainty value is compared to the B2 uncertainty (discussed above), and the larger value is selected. The resulting distribution is sampled to get the model uncertainty ΔPCT . This is added to PCT_{PC2} to get the preliminary hot spot PCT for the Monte Carlo iteration, $PCT_{HS1,i}$. Westinghouse then compares the B1 uncertainty (discussed above) to the superposition correction, and the larger uncertainty value is selected. The resulting distribution is sampled and added to $PCT_{HS1,i}$ to get the final hot spot PCT for the Monte Carlo iteration, $PCT_{HS2,i}$.

To determine the 95th percentile PCT, the above process is repeated many times. For each iteration, i , the calculated $PCT_{HS2,i}$ is binned. The PCTs in each bin are counted starting from the highest PCT and when 5% of the PCTs are counted, the 95th percentile PCT is determined.

6.2 Models - Global Effects

For critical flow, Westinghouse evaluated the bias and uncertainty based on WCOBRA/TRAC comparisons to Marviken test data. Based on those comparisons, the break flow uncertainty distribution was determined. As discussed in Reference 58, a cumulative distribution function (CDF) based on the Marviken test data comparisons is used to describe the uncertainty distribution.

Broken loop relative resistance is accounted for through the broken loop pump resistance and the broken cold leg nozzle K. This broken loop resistance ratio is the relative resistance from the core to the break through the vessel downcomer and the broken cold leg nozzle and the core to the break through the hot leg, steam generator, and pump. The basis for and the approach used to account for the uncertainty in the broken loop relative resistance is discussed in Section 3.1.2 of Reference 58. Also, as the result of sensitivity studies, Westinghouse found that the broken loop flow path relative resistance was more important than pump two-phase head variations. The resistance ratio was found to be dominated by the broken loop pump resistance in one path and the vessel nozzle loss coefficient in the other path. A Westinghouse analysis discussed in CQD Section 26-4 found the appropriate way to vary the resistance ratio in the uncertainty analysis. This approach is supported by the study in Section 5.1.5 of Reference 58.

Estimates of condensation efficiency in UPTF tests showed a wide variation depending on the approach taken (see Figure 3.1.7-1, Reference 58). Westinghouse compared WCOBRA/TRAC results to the UPTF data and found they agreed with the higher of the two estimates. However, because of the wide data variation, Westinghouse concluded the condensation rate should be ranged in the WCOBRA/TRAC uncertainty analysis. Therefore, the uncertainty range given in Reference 205, Attachment 2 (based on the WCOBRA/TRAC variation relative to the variation in the two UPTF estimates) was used.

The uncertainties in break flow, broken loop resistance ratio, and condensation are accounted for in Westinghouse's uncertainty methodology. The following process is used. The uncertainty distributions for each parameter are determined. Then, thermal-hydraulic sensitivity studies are performed where each parameter is varied (singly and in combination with the other two

parameters) over a range that adequately bounds the expected range of model variation. The ranges used for the sensitivity studies for each parameter are:

1. Break flow: 100% of the data in the break flow uncertainty distribution.
2. Break flow resistance ratio: The uncertainty in this parameter is ranged as discussed in CQD Section 26-4 and Sections 3.1.2 and 4.4.2.1 of Reference 58.
3. Condensation: For the run matrix, the maximum and minimum multipliers are based on test data (see Figure 3.1.7-1 of Reference 58). Although the sampled range in the uncertainty evaluation is larger, the run matrix covers almost 77% of the sampled range. The INEL considers this adequate because the extrapolation is small.

Westinghouse calls this the break flow/condensation run matrix, and it is shown in Table 4.4.2-1 of Reference 58. The results of this run matrix are used as input to the HOTSPOT code to determine the local HR uncertainty as discussed in Sections 6.4 and 9.4 of this report. The global model and HOTSPOT effects are then used to develop a response surface for the Monte Carlo analysis.

6.3 Plant Conditions - Global Effects

Westinghouse accounted for the uncertainty in the initial plant conditions. As mentioned above, this includes power distributions and initial conditions. The uncertainty in plant initial conditions is accounted for by developing the initial condition bias and uncertainty from plant sensitivity studies (discussed in Section 8 of this report). This distribution is sampled directly and applied during the Monte Carlo calculation.

The power distribution uncertainty is more complicated. It is due to uncertainties in peaking factors and power shapes, and Westinghouse accounts for both sources in its uncertainty evaluation. The peaking factors include

two sources of uncertainty: calculational uncertainties (what affects the calculation of peaking factor from plant data and modeling assumptions) and operational uncertainties (transient operation is allowed by the Technical Specifications). Power shapes are an operational effect due to transient plant operation. Each of these uncertainties is discussed below.

The peaking factor calculational uncertainties include those that affect the HA and the HR as part of the HA (HA/HR calculational uncertainties). See CQD Table 21-2-2 where there are the same entries in both the HA and HR columns for total peaking factor (F_Q) and radial power distribution ($F_{\Delta H}$). Westinghouse considers these uncertainties global in nature. The HA/HR calculational uncertainty is included in the global analyses because the HA power distribution could affect core/HA thermal-hydraulics, which will affect the HR PCT. Some peaking factor calculational uncertainties only affect the HR (HR calculational uncertainties; see CQD Table 21-2-2 where there are F_Q and $F_{\Delta H}$ entries for the HR only), and Westinghouse considers them local. The global effects are accounted for through the HA in WCOBRA/TRAC analyses and are discussed below. The local effects are accounted for through the HR hot spot as discussed in the next section.

Westinghouse found the following contributors to HA/HR average power rod power distribution uncertainty: F_Q and axial power distribution, $F_{\Delta H}$, initial core power level, decay heat, and gamma redistribution. These include all parameters that affect the HA power distribution. The F_Q and $F_{\Delta H}$ uncertainties considered here are the HA/HR calculational uncertainties. Also, a number of variables are combined to reduce the number of variables included in the uncertainty evaluation (see Section 3.1.3.2 of Reference 58). For justification of this approach, see Westinghouse's response to Volume 5, question 7, Reference 38.

Because transient operation is allowed by the Technical Specifications, Westinghouse accounts for the variation in F_Q and axial power distribution allowed in plant operation. The F_Q uncertainty is accounted for as discussed in Section 3.1.3.1 and page 32 of Reference 58.

To determine the effect of the F_Q variations on PCT, Westinghouse performs WCOBRA/TRAC analyses with F_Q variations that bound the F_Q range mentioned above plus the HA/HR calculational uncertainty. Westinghouse must also account for variations in axial power shape allowed by the Technical Specifications, and it does so by including bounding variations in axial power distributions in the WCOBRA/TRAC analyses discussed for F_Q . Finally, transient affects and time-in-life changes for $F_{\Delta H}$ are included in the WCOBRA/TRAC analyses by using a cycle bounding value in the WCOBRA/TRAC runs. This power distribution run matrix (see Table 4.4.1-1, in Reference 58), is used to develop a response surface that is used in the Monte Carlo analysis.

The effects of power distribution uncertainty is accounted for in the Monte Carlo simulation by a response surface approach using the response surface discussed above. The Monte Carlo analysis randomly samples the distributions and the associated uncertainties for the variables included in the response surface equation. For example, the F_Q distribution and the associated uncertainty distribution are sampled. Then, the response surface is used to calculate the effect on PCT.

6.4 Local Effect Models/Parameters

Having established the global uncertainties for models and plant conditions, Westinghouse addressed the effects of local uncertainties on the global results.

Westinghouse considered the local effects of uncertainties associated with the HR. The factors considered include those that affect local power and fuel rod models: HR calculational uncertainty; hot rod pellet diameter, enrichment, and rod bow uncertainties; fuel density and conductivity; gap HTC; rod internal pressure; cladding burst temperature and strain; metal-water reaction; and fuel relocation. As a reminder, the HR calculational uncertainties considered here are the uncertainties associated with only the HR (see CQD Table 21-2-2 where there are F_Q and $F_{\Delta H}$ entries for the HR only). For each parameter listed above, Westinghouse developed the uncertainty range and distribution (see Tables 3.1.3-1 and 3.1.4-1, Reference 58).

These sources of HR local uncertainty are evaluated using the HOTSPOT model. This model (see Section 9.4 of this report) is a stand alone calculation of local effects at the PCT locations (blowdown, first reflood, and second reflood) and the burst node location (see page 165, Reference 58). The HOTSPOT model is run many times in a direct Monte Carlo simulation. Boundary conditions input to the HOTSPOT model are taken from the WCOBRA/TRAC runs in the power distribution run matrix and the break flow/condensation run matrix. For each HOTSPOT run, Westinghouse develops a bias and distribution that describes the effect of the local uncertainties on the PCT. In this way, local effects are combined with global effects for models and plant conditions. For the WCOBRA/TRAC runs taken from the break flow/condensation run matrix, two response surfaces are fit to the distributions developed with HOTSPOT for the individual runs, one to the biases and one to the uncertainties. For the WCOBRA/TRAC runs taken from the power distribution run matrix, a table based on calculated PCT is used to determine the local bias and uncertainty. This table and the response surfaces are used in the Monte Carlo simulation to account for local uncertainty propagation.

6.5 WCOBRA/TRAC Experiment Based Uncertainty

In the original Westinghouse methodology presented in the CQD, the WCOBRA/TRAC uncertainty was largely based on comparisons between WCOBRA/TRAC results and test data (see CQD Section 19). This consisted of the code uncertainty based on comparisons to experimental results, a nodalization uncertainty, and a data scatter uncertainty. In the revised methodology discussed above, Westinghouse also estimates a code uncertainty based on ranging of model parameters. Westinghouse's revised methodology retains the experiment based uncertainty but divides it differently (see Reference 205, Attachment 2). First, the code uncertainty based on comparisons to experimental results plus the nodalization uncertainty is compared to the uncertainty in the superposition approach. Westinghouse notes these two represent the uncertainty in the bias or the ability of the code to calculate the average PCT. Second, the data scatter uncertainty is compared to the model based uncertainty. Westinghouse notes these two represent the uncertainty relative to local effects. In both cases, the larger of the two uncertainties is used in the Monte Carlo calculation of the 95th percentile PCT.

During the course of the review, Westinghouse identified and committed to correct several errors that affect the calculation of the WCOBRA/TRAC experiment based uncertainty. These are discussed in Westinghouse's responses to Volume 4, question 3, Reference 45, question 72, Reference 38, and question 73, Reference 21. In Reference 205, Attachment 2, Westinghouse recalculated the experiment based uncertainty to include the corrections discussed in the above responses.

6.6 Other Parameters/Factors Considered by Westinghouse

Westinghouse's list of important parameters considered a number of items not discussed directly in the previous sections. These include ECC bypass, entrainment/steam binding, and accumulator nitrogen. Westinghouse's disposition of these items is discussed below.

Westinghouse evaluated ECC bypass and found a negative bias could be applied to WCOBRA/TRAC analyses because of delayed and reduced ECC penetration relative to full-scale UPTF tests⁶⁴ (see Volume 4, question 2, Reference 21). However, the bias is not applied at this time resulting in conservative PCT calculations. Given that a conservative bias is ignored, INEL concluded Westinghouse's approach for ECC bypass uncertainty is adequate.

Steam binding effects are due to entrainment from the upper plenum and hot leg into the steam generators. Westinghouse evaluations of SCTF,⁶⁵⁻⁶⁹ CCTF,⁷⁰⁻⁷⁴ and full-scale UPTF⁷⁵ tests showed entrainment from the core to the upper plenum (SCTF/CCTF) and from the upper plenum to the hot leg (CCTF/SCTF/UPTF) was overpredicted. This indicates WCOBRA/TRAC calculations will overestimate the effect of steam binding and a conservative bias already exists in the calculations. As with ECC bypass, Westinghouse does not apply this negative bias. Given that a conservative bias is ignored, INEL concluded Westinghouse's approach for entrainment/steam binding uncertainty is adequate.

Westinghouse evaluated the effects of non-condensibles coming out of solution and the injection of the accumulator nitrogen into the primary system in its response to Volume 1, question 134, Reference 37. Regarding non-condensibles coming out of solution, the Westinghouse analysis showed the effect would be negligible. For the accumulator nitrogen, Westinghouse showed

that the uncertainty in the overall condensation rate due to the interfacial area and HTC was much larger than the potential effect of non-condensibles on condensation. Also, Westinghouse analyzed the Achilles test with nitrogen injection (International Standard Problem No. 25),⁷⁶ and the WCOBRA/TRAC results showed good agreement with the test data (see Volume 3, question 36, Reference 42). Based on these factors, Westinghouse concluded a bias for non-condensibles was not needed. Section 12.2 of this report discusses Westinghouse's accumulator nitrogen modeling. See Section 12.2 of this report.

6.7 INEL Review of Uncertainty Propagation

As the above description shows, Westinghouse's uncertainty methodology is very complex. Therefore, it was given a careful review to assess its adequacy.

The INEL reviewed the list of important parameters identified by Westinghouse in Reference 58. The highly ranked phenomena from the Westinghouse PIRT were considered and found to be ranged directly in the uncertainty analysis, modeled directly in WCOBRA/TRAC analyses, bounded in WCOBRA/TRAC analyses, covered in the variation of items ranged directly, or calculated with a conservative bias in WCOBRA/TRAC analyses.

At the heart of the uncertainty methodology is the assumed uncertainty distributions. The INEL reviewed Westinghouse's justification for each parameter range and the associated uncertainty distribution (see Reference 58) in Section 9.2 of this report. That review found Westinghouse's justification for the distributions adequate based on Westinghouse's submittals.

The INEL reviewed Westinghouse's approach to uncertainty propagation and found it adequate because WCOBRA/TRAC and HOTSPOT calculations cover the LBLOCA through reflood. This allows the effects of uncertainty in parameters and combinations of parameters to be calculated through the entire accident. The INEL also found run matrix development and response surface generation adequate. For the run matrix development, Westinghouse appropriately covered the expected sampling range, and, for response surface generation, Westinghouse's methodology appropriately prevents overfitting. Westinghouse

considered the important parameters from the PIRT and covered them as discussed above. In Reference 205, Attachment 2, Westinghouse modified the uncertainty methodology to account for inaccuracies in the separability assumptions made in the propagation of uncertainties (this is discussed in Section 9.2 of this report). Also, as noted above, all of the parameter ranges and uncertainty distributions were adequately justified.

7. EFFECTS OF SCALE (CSAU STEP 10)

The effects of scale on the calculated results need to be evaluated to ensure the code models can appropriately calculate full-scale PWR behavior given that most of the code assessment matrix is based on smaller-scale test facilities. This is discussed in RG 1.157, Sections 4.1 and 4.2, and CSAU Step 10. Westinghouse evaluated the effects of scale on the WCOBRA/TRAC code in Reference 58.

Westinghouse's evaluation built on the scaling work done during the CSAU study, Reference 61. The CSAU study concluded that power-to-volume scaled test facilities adequately represented full-scale plants except in the areas of ECC bypass and steam binding (core/upper plenum entrainment). CSAU also identified critical flow and pump two-phase performance as needing additional review because of the lack of full-scale data and included variations in these models in the run matrix used to develop the PCT response surface.

Westinghouse noted it concurred with the CSAU results regarding power-to-volume scaled facilities. Westinghouse also evaluated the effects of scale for different test facilities on the predicted versus measured PCT difference. The results shown in Reference 58 indicated there was data scatter but no apparent trend as a function of facility scale.

To address the other two issues identified during the CSAU study, ECC bypass and steam binding, Westinghouse compared WCOBRA/TRAC results in these areas to test facilities at various scales. In particular, Westinghouse used the full-scale UPTF test data to address these issues. At the time of the CSAU study, UPTF test data was just becoming available to use in computer code assessment of ECC bypass and steam binding predictions. For ECC bypass, Westinghouse used 1/5th-scale Creare data¹⁰⁷ and full-scale UPTF data to evaluate WCOBRA/TRAC's scalability for this phenomenon. Comparison showed that WCOBRA/TRAC has a conservative bias regarding the prediction of ECC bypass as the facility scale approached full-scale. That is, the code overpredicted the amount of fluid bypassing the vessel and going out the break.

Regarding steam binding, Westinghouse used SCTF, CCTF, and UPTF data to evaluate the code's ability to predict entrainment from the vessel to the steam generator as a function of scale. Again, the code showed a conservative trend with scale by underpredicting the amount of mass stored in the upper plenum as facility scale increased. This implies greater steam binding will be calculated by the code (with the corresponding reduction in core flooding rates and higher PCTs) relative to the steam binding observed in the experiments.

Regarding critical flow, Westinghouse accounts for this directly in the uncertainty analysis with the effect determined by PWR sensitivity calculations. For pump two-phase performance, Westinghouse evaluations (see CQD Section 16-3 and CQD Appendix C) showed that single-phase pump performance is more important and included this parameter directly in the uncertainty evaluation. The variations for critical flow and single-phase pump performance are discussed in Section 6 of this report on propagation of uncertainty.

The INEL reviewed Westinghouse's submittal. Regarding the effects of scale for different facilities on the predicted versus measured PCT difference, the INEL notes there is a pattern due to facility/test series and this a strong effect. This strong effect is the tendency for WCOBRA/TRAC results in some facilities/test series to consistently overpredict PCT, and WCOBRA/TRAC results in other facilities/test series to consistently underpredict PCT (see Figures 3.3-1 to 3.3-7). However, no additional pattern due to scale is obvious due to the lack of several facilities at a given scale. The figures provided by Westinghouse support the conservative trends discussed for ECC bypass and steam binding. Including critical flow and pump modeling in the uncertainty evaluation also adequately addresses questions in these areas. Based on the above, INEL considers Westinghouse to have adequately addressed issues relating to scaling.

8. REACTOR INPUT PARAMETERS/STATE (CSAU STEP 11)

Both RG 1.157, Section 3.1, and CSAU Step 11 discuss the need to identify the effects of the reactor input and initial/boundary conditions on the calculated PCT. Westinghouse addressed this issue in CQD Sections 21/22.

8.1 Westinghouse's Methodology - CQD Sections 21/22

CQD Section 21 described a large number of items that Westinghouse concluded needed to be considered with respect to their effect on the WCOBRA/TRAC calculated PCT. Included in the items to be considered were the plant physical configuration, plant initial operating conditions, accident boundary conditions, and WCOBRA/TRAC models needing further analysis due to lack of prototypical assessment or the need to consider the effects of different transient time scales in the tests and a PWR.

The plant physical configuration included the plant physical dimensions (the effects of thermal expansion), flow resistance (especially out the broken cold leg nozzle), pressurizer location, hot assembly location and type, and steam generator tube plugging.

The plant initial operating conditions included core power parameters. The core parameters considered by Westinghouse included total core power, peak linear heat rate (PLHR), HA peak heat rate, HR average power, HA average power, axial power distribution, low power region relative power, HA burnup, reactor power history, moderator temperature coefficient (MTC), and full power boron concentration. Westinghouse discussed in detail its modeling approach to the above parameters in Section 21-2-1 of the CQD, and the reader is referred there for additional information.

The other part of the plant initial operating conditions considered by Westinghouse included the reactor primary fluid conditions. Those included core average temperature; pressurizer pressure and level; loop flow rate; upper head temperature; and accumulator water temperature, pressure, water volume, line resistance, and boron concentration.

The reactor accident boundary conditions also impact the calculated PCT, and Westinghouse concluded that break location, type, and size (discharge coefficient (C_D)); availability of offsite power; SI flow, temperature, and delay; containment pressure; assumed single failure; and control rod drop time needed to be addressed by plant sensitivity studies.

The final area included models not adequately assessed, models that were simplified or lacking basic knowledge, and phenomena that may have more important effects on a PWR LBLOCA than a scaled experiment. Based on this, Westinghouse concluded that models for break flow, pumps, accumulator nitrogen, condensation, entrainment, ECC bypass, core heat transfer, and fuel rods needed additional review and possible inclusion in PWR sensitivity studies.

CQD Section 21 discussed the basis for how each parameter/model was determined and the input selected as the starting point for the plant sensitivity calculations. The options considered included using a nominal value, a BE value, or setting a parameter/model at a maximum/minimum value based on its possible effect on PCT. CQD Table 21-4-2 summarizes Westinghouse's conclusions regarding the base case values for the sensitivity studies. During the sensitivity studies, Westinghouse noted the parameters/models would be varied, often one at a time, to gain insight into their importance on determining PCT. The sensitivity studies would then be used to quantify uncertainty. In particular, the studies are used to account for a wide variety of plant initial/boundary conditions via the initial condition bias and uncertainty (see CQD Section 26-5).

Section 22 of the CQD documented Westinghouse's efforts with regards to sensitivity studies. Westinghouse selected three plants, Indian Point 2, Sequoyah, and North Anna, to demonstrate the sensitivity studies included in the realistic LBLOCA methodology. Westinghouse completed a large number of sensitivity studies for each plant; for example, 17 studies were completed for the Sequoyah plant. The results of the sensitivity studies are summarized in CQD Table 23-1.

Westinghouse also used the sensitivity studies in CQD Section 22 to determine how to treat each parameter in the uncertainty evaluation (see Section 4.3.1, Reference 58). Three categories were proposed:

1. Nominal - The nominal value of a parameter is used when the variation in it is tightly controlled or the sensitivity of the transient results to parameter variation is negligible.
2. Bounded - A conservative value of the parameter is used when the value of the parameter varies as a function of operating history or when the value of the parameter is indeterminate. A parameter may also be bounded if the sensitivity of the transient results to parameter variations is small or when the effort to develop and justify a detailed uncertainty treatment was judged to exceed the benefits.
3. Explicitly treated - In this case, a parameter is modeled with a BE value and parameter variation is directly treated in the uncertainty methodology discussed in Section 6 of this report.

In addition to the above studies, Westinghouse used sensitivity studies to evaluate the effects of time step control (CQD Section 22-5), break spectrum (CQD Section 22-6), and fuel rod burnup (CQD Section 22-7) on calculated PCT for the same three plants. These studies are discussed below.

The time step studies evaluated the effect of changing the time step controls for assessment studies and the PWR plant calculations. For the test assessments, the maximum difference in calculated PCT due to time step changes over all the cases analyzed was approximately 40°F. In these time step studies, the maximum allowed time step was varied by a factor of 2 to 500 (see CQD Section 19-1-2).

For the plant model time step studies in the CQD, Westinghouse also varied the maximum allowed time step but only by a maximum factor of 10. With the plant calculations, Westinghouse noted the PCT results were most sensitive to time step changes when the core flow reversed from upflow to downflow during blowdown and at the end of bypass due to the large condensation rates

calculated. To verify the PWR analysis time step scheme discussed in CQD Section 22-5-4, Westinghouse reanalyzed time step effects in its response to Volume 4, question 50, Reference 40. In this study, the effect of time step size in the blowdown, refill, and reflood portions of a LBLOCA was assessed and conservative time step sizes chosen. This study resulted in Westinghouse proposing new time step control parameters for PWR analyses.

Westinghouse discussed the break spectrum analyses for the three plants in CQD Section 22-6. The discharge coefficient was varied from 0.8 to 1.2 based on the WCOBRA/TRAC comparisons to Marviken test data.⁶³ In CQD Section 16-4, Westinghouse concluded that the WCOBRA/TRAC predicted break flow generally fell within a band of ± 20 percent of the measured data, and Westinghouse noted that much of the uncertainty comes from the transition from subcooled to saturated conditions. A more detailed comparison in CQD Appendix B (Volume 5) found that WCOBRA/TRAC tended to underpredict the measured break flow and the standard deviation of the average discharge coefficient was 20 percent. As Westinghouse indicated in their response to Volume 3, question 41, Reference 20, this indicates the ± 20 percent bands only capture approximately 70 percent of the data. It should be noted, however, that the results in CQD Section 22-6 are only illustrative. The effect of critical flow on PCT is included in the models response surface used in the uncertainty evaluation, and Westinghouse samples the full range of discharge coefficients developed from the Marviken test comparisons in the Monte Carlo simulation to determine the 95th percentile PCT.

In CQD Section 22-6, both split and double-ended guillotine breaks were analyzed. The break area for the split breaks included those equal to twice the cold leg area unless the maximum PCT occurred at a lower range of break areas. To account for the uncertainty in the break type, the determination of the 95th percentile PCT includes separate Monte Carlo simulations for the guillotine breaks and the limiting split break from the break spectrum study. The break spectrum results are summarized in CQD Table 22-6-2.

Fuel rod burnup studies were presented in Section 22-7 of the CQD. In these studies, Westinghouse varied the assumed fuel rod burnup by varying the initial fuel temperature and RIP to simulate rods at beginning-, middle-, and end-of-life (BOL, MOL, and EOL). Realistic combinations of initial fuel

temperature and RIP were used so that RIP was lowest when the fuel temperature was highest at BOL, and RIP was highest when fuel temperature was lowest at EOL. Westinghouse also analyzed two other cases. One simulated BOL conditions for Westinghouse Integral Fuel Burnable Absorber (IFBA) rods, and one simulated rods with MOL RIPs but not the reduction in fuel temperature associated with MOL conditions. These studies confirmed BOL conditions resulted in the limiting PCT for cases representing realistic conditions. For SQN, the case simulating BOL conditions for IFBA rods was higher than the case with non-IFBA rods because of differences in calculated rod burst behavior.

8.2 INEL Review of CQD Sections 21/22

INEL review of CQD Section 21 found that Westinghouse provided an exhaustive list of important LBLOCA parameters to be considered in the plant sensitivity studies. The INEL review did not identify any parameters to add to Westinghouse's list.

The INEL reviewed the sensitivity studies in CQD Section 22 and found that Westinghouse did perform one-at-a-time sensitivity studies. Westinghouse provided discussion and plots to support the conclusions regarding the effect of the parameter or model variation on the calculated PCT. In some cases, INEL review of that information resulted in a number of questions (see Volume 4, questions 45 to 61, Reference 4). Many questions asked Westinghouse to clarify reasons for the calculated differences before or after the calculated PCT occurred. Westinghouse adequately responded to all INEL questions.

The INEL reviewed the new time step parameters discussed above. They resulted in small variability or conservative variability in the PWR PCT, and the mass and energy error were small. Therefore, the INEL agrees with Westinghouse that the new parameters provide better time step control.

The uncertainty in break flow is appropriately accounted for in the uncertainty analysis, and Westinghouse's study on rod burnup showed that BOL is the limiting time-in-life.

Based on the review summarized above, the INEL concluded that Westinghouse adequately explained the sensitivity study results. Also, the sensitivity studies provide an adequate basis for determining initial condition uncertainties and for determining how to account for a particular parameter in the overall uncertainty analysis. This is because the studies show which parameters are important to PCT calculations and the effect of the parameter change on the calculated PCT.

9. ADDITIONAL METHOD DESCRIPTION AND REVIEW

This section describes those parts of Westinghouse's realistic LBLOCA methodology that are important but do not fall directly into the steps of the CSAU methodology. First, a summary of the WCOBRA/TRAC code is given. This is followed by a detailed discussion of the uncertainty distribution review; Westinghouse's handling of split breaks and the HOTSPOT model are also discussed. INEL conclusions are provided at the end of each subsection and summarized in Section 9.5 of this report.

9.1 LBLOCA Method Description/Review - Code Description

The following is a brief discussion of the WCOBRA/TRAC modeling approach and the INEL review of the code models. A more detailed description of the code models and a summary of the INEL review of the models is found in Appendix A of this report. During the course of the review, Westinghouse modified the WCOBRA/TRAC code. The code version documented in the CQD was WCOBRA/TRAC, MOD7. Two subsequent code versions were later produced. The first revision focused on improving the entrainment model and produced WCOBRA/TRAC, MOD7A. Appendix A of Reference 58 discussed the changes made to produce WCOBRA/TRAC, MOD7A.Rev.1 by adding additional modeling capability needed for the uncertainty propagation and correcting code errors. WCOBRA/TRAC, MOD7A.Rev.1, is the version documented in this review. Based on INEL review of the changes and Westinghouse discussion of their effects in Appendix A of Reference 58, INEL agrees with Westinghouse's conclusion that the effects of the changes on the experiment simulations are minimal. INEL review concluded that only error corrections were made. Therefore, reanalysis with MOD7A.Rev.1 does not appear to be warranted, and the MOD7A experiment simulations apply to MOD7A.Rev.1.

As discussed in Section 1 of this report, the Westinghouse realistic LBLOCA methodology is based on the WCOBRA/TRAC computer program. WCOBRA/TRAC is Westinghouse's modified version of the NRC's COBRA/TRAC program developed by the combining the COBRA-TF code (the best documentation of COBRA-TF as it was implemented in COBRA/TRAC is the COBRA/TRAC manual, Reference 2) to calculate the vessel LBLOCA response and the TRAC/PD2 code⁶² to calculate the loop response. The program includes the capability to model three-dimensional

flow behavior in the reactor vessel and all the major components in the primary system.

WCOBRA/TRAC uses a two-fluid, three-field representation of flow in the reactor vessel. The three fields are vapor, continuous liquid, and entrained liquid. Each field uses a three-dimensional set of continuity, momentum, and energy equations with one exception. The continuous and entrained liquid fields use the same energy equation; therefore, the two fields are assumed to be at the same temperature. In the vessel, each phase uses a separate set of conservation equations and constitutive relations. The effect of one phase on another is accounted for by the interaction terms appearing in the governing equations.

Outside the vessel, a one-dimensional representation of primary system components is used. Components such as pipes, pumps, valves, steam generators, and the pressurizer can be represented with models in WCOBRA/TRAC. The one-dimensional components use a two-phase, five equation, drift-flux model. Two equations are used to represent conservation of mass (mixture and steam mass), two equations are used for conservation of energy (mixture and steam energy), and a single equation is used to represent the conservation of momentum. Closure of the field equations requires specifying the interphase relative velocity, fluid properties, interphase mass and heat transfer, and other constitutive relationships.

INEL review of the WCOBRA/TRAC code models found them adequate to provide a realistic analysis of LBLOCA results. This conclusion is based on the INEL's review of information Westinghouse provided in the CQD, Volume 1, and in their responses to approximately 240 questions. The details supporting this conclusion are found in Appendix A of this report.

9.2 LBLOCA Method Description/Review - Uncertainty Distributions and Assumptions

INEL reviewed all of the uncertainty distributions assumed by Westinghouse in its uncertainty evaluation. Westinghouse's basis for the various distributions assumed is found in Reference 58, CQD Table 21-2-2, CQD

Section 26-5, and other supporting information, References 55, 56, 190, 205, 206, 214, and 31.

INEL review of the assumed uncertainty distributions found adequate justification for the following parameters based on Westinghouse responses:

1. F_Q : Nominal and Transient Values, Computational Uncertainty, Core Power Uncertainty, Decay Heat Uncertainty, and Gamma Energy.
2. $F_{\Delta H}$: Nominal and Transient Values, Computational Uncertainty, Core Power Uncertainty, Decay Heat Uncertainty, and Gamma Energy.
3. Axial Power Distributions: Transient PBOT/PMID (bottom and middle third axial power fractions).
4. Initial Conditions: Reactor Coolant System (RCS) Temperature, RCS Pressure, Accumulator Line K, Accumulator Temperature, Accumulator Pressure, SI Temperature, and Peripheral Assembly Power.
5. Code Models: Break Flow, Broken Loop Cold Leg Nozzle K, Condensation Multiplier, and Broken Loop Pump Resistance.
6. Other Parameters: Local Peaking, Fuel Conductivity (Pre-Burst and After Burst), Cladding Burst Strain/Average Strain, HTC, T_{MIN} , Fuel Density (Packing Fraction/After Burst), Gap Conductance, Rod Internal Pressure, Cladding Burst Temperature, Zirc-Water Reaction, and ZIRLO-Water Reaction.

In general, Westinghouse determined the uncertainty distributions by comparisons to applicable data. See Reference 58, for the details. For example, the break flow uncertainty was determined by comparisons to Marviken data. Another example is the bias and uncertainty for the HTCs. In this case, Westinghouse evaluated the results of WCOBRA/TRAC calculations relative to test data. See Appendix B of Reference 58. For each phase of a LBLOCA (blowdown heatup, blowdown cooling, refill, and reflood) the WCOBRA/TRAC overall HTC (heat flux divided by $T_{wall} - T_{sat}$) was determined and compared to the data overall HTC. The HTC multiplier for the particular period evaluated becomes the ratio of the data HTC divided by the WCOBRA/TRAC HTC. For most cases, this was done by comparing each valid thermocouple to the corresponding WCOBRA/TRAC result. The uncertainty in the multiplier is determined by scatter plots. That is, the range of the multiplier scatter determines the multiplier uncertainty for the period.

In addition to reviewing the uncertainty distributions, INEL also reviewed the simplifying assumptions Westinghouse made in order to make the uncertainty evaluation manageable. The assumptions reviewed were discussed in CQD Section 26-5 and Reference 58, Sections 3.1.2, 3.1.3, and 4.2. INEL review found the following assumptions adequately justified:

1. Combining IC Uncertainties: See CQD Section 26-5.
2. Break Type Selection: Westinghouse considers each break type separately.
3. Approach for R_p : Reference 58, Section 5.1.5.
4. Combining uncertainties in Peaking Factors, F_Q and $F_{\Delta H}$: See Reference 58, Section 3.1.3.

Westinghouse addressed the adequacy of the following assumptions by adding a validation step to the methodology (see Reference 205, Attachment 2): Separability of Initial Conditions and Power Distributions, Local Effects Separable for Plant Conditions and Global Models, Separability of Plant conditions and Global models, and Local Effects on power distribution runs represented by table look-up. This validation step uses additional WCOBRA/TRAC-HOTSPOT calculations that are compared to the results of Westinghouse's superposition methodology. The differences are curve fit and used to correct the Monte Carlo superposition results.

The basis for the above findings is summarized below. The Revised Methodology Report (RMR) refers to Reference 58.

DISTRIBUTION ASSUMPTIONS

F_Q , Axial Peaking Factor

Nominal Value: This is justified in Sections 3.1.3.1 and 4.4.1.1 and page 32 of the RMR. The uncertainty range is given in Section 3.1.3.1 of the RMR. This range is conservative and, therefore, adequate. The conservatism is illustrated in the figure on page 39 of the RMR, for a plant with a Technical Specification F_Q limit of 2.4.

Calculation Uncertainty: This is based on NRC-approved evaluations. See Footnote 2 of RMR Table 3.1.3-1 and Reference 1 of CQD Table 21-2-2.

F_{AHT} Radial Peaking Factor

Nominal Value: Use of the maximum calculated value, as done here, is conservative, and, therefore, adequate.

Calculational Uncertainty: This is based on NRC-approved evaluations. See Reference 1 of CQD Table 21-2-2.

Quantities Related to Both Peaking Factors

Core Power Uncertainty: This is based on NRC-approved evaluations; see Footnote 2 of RMR Table 3.1.3-1.

Decay Heat Uncertainty: The uncertainty given in Table 3.1.3-1 of the RMR results in a higher integrated decay heat power uncertainty than that obtained from the ANSI/ANS-5.1-1979 standard.⁸³ Westinghouse described this in Footnote 4 of Table 3.1.3-1 of the RMR and showed it in RMR Figure 3.1.3-6. Therefore, this is conservative.

Gamma Energy: The gamma redistribution uncertainty in Table 3.1.3-1 of the RMR is justified in Footnote 5 of the table.

PBOT/PMID (axial power shape parameters)

Use of limits that bound the data is adequate (Figures 3.1.3-3 and 3.1.3-4 of the RMR). This corresponds to uniform distributions for PBOT and PMID. According to Reference 190, the Reload Safety Analysis Checklist (RSAC) contains procedures to assure that the limits actually used will be adjusted as necessary to bound the data for each plant analysis. This is appropriate for the plant specific applications.

Initial Conditions

RCS Temperature: As explained in the Westinghouse response to comments, Reference 56, uncertainty in RCS temperature is not identified in plant Technical Specifications but is used in calculation of reactor trip setpoints. The uncertainty given in Reference 56 and used here is typical of such calculations. This small value does not warrant more detailed treatment.

RCS Pressure: The argument is the same as for RCS temperature, except the uncertainty is based on the pressure measurement uncertainty given in Reference 56.

Accumulator Temperature: Plant operating data, as discussed in Reference 214, Attachment 7, is used to determine the nominal value and the uncertainty range. Westinghouse's analysis of the data for an example plant, discussed in Reference 214, resulted in a slightly conservative distribution. In addition, Westinghouse indicated the intent of the procedure was to skew the distribution to be slightly conservative. Because Westinghouse performs this type of analysis using plant operating data (based on Reference 214) and/or plant Technical Specifications, this analysis must be performed for each plant.

Accumulator Pressure: The limits assumed by Westinghouse are given in the Reference 55 information on uncertainty distributions. In reality, the plant operators normally control the pressure to remain near the midpoint of the two limits. The assumed uniform distribution, therefore, puts more probability at the ends of the range than occurs in practice. This is somewhat conservative.

Accumulator Line Resistance: Westinghouse has two approaches to estimating the nominal accumulator line resistance as discussed in Reference 205, Attachments 1 and 1a. For plants with measured data, Westinghouse uses the measured line resistance. Based on the information in Reference 205, Westinghouse justified that the measurement uncertainty used is conservative relative to the actual measurement uncertainty.

For plants without measured data, Crane Co. Technical Paper No. 410¹⁹³ is used to calculate the accumulator line resistance. A comparison of this calculated result to test data in Reference 205 shows that Westinghouse's approach is conservative. This is adequate.

Safety Injection Temperature: Plant operating data, as discussed in Reference 214, Attachment 7, is used to determine the nominal value and the uncertainty range. Westinghouse's analysis of the data for an example plant, discussed in Reference 214, resulted in a conservative distribution. In addition, Westinghouse indicated the intent of the procedure was to skew the distribution to be slightly conservative. Because Westinghouse performs this type of analysis using plant operating data (based on Reference 214) and/or plant Technical Specifications, this analysis must be performed for each plant.

Peripheral Assembly Power: In Reference 214, List III, Item 6, Westinghouse noted that the distribution and mean of this variable are difficult to confirm on a cycle-to-cycle basis. Therefore, it will be bounded in the WCOBRA/TRAC calculations using plant specific sensitivity studies, and it will no longer be included in the initial condition uncertainty. Bounding the uncertainty based on plant specific studies is considered adequate.

Model Uncertainty

CD, Break Flow Multiplier: This uses the empirical distribution from Marviken data, and is, therefore, adequate. Figure 3.1.1-9 of the RMR shows the empirical distribution. This is modified slightly (and correctly) in Westinghouse's response to question 2a, Reference 190.

Broken CL Nozzle Resistance, K_N : The approach of the Westinghouse RMR, p. 21, estimates the mean and standard deviation from the five available data points. The range assigned this variable is discussed on the same page of the RMR. The distribution assigned this variable and Westinghouse's approach in using it in the uncertainty evaluation are discussed and justified in Attachment 6 of Reference 214 and Westinghouse's response to Volume 5, question 24, Reference 39.

Broken Loop Pump Resistance, K_p : On pp. 19-20 of the RMR, K_p is found as a multiple of the Westinghouse correlating parameter. This derivation is correct. CQD Figure C-2 shows the Westinghouse correlating parameter plotted against $(\text{speed}/\text{rated speed})/(Q/Q_r)$, the inverse of normalized flow. In WCOBRA/TRAC, the broken loop pump resistance is calculated using the correlation from the version of CQD Figure C-2 that corresponds to that pump. Therefore, scatter around the correlation is relevant. Figure C-2 shows the data range around the correlation, for a fixed value of normalized flow, and this range is typical of all the pumps. This data range corresponds to the K_p range given on RMR page 20 for a fixed value of normalized flow. The calculation of standard deviation and relative standard deviation are correct.

X_{COND} , Condensation Multiplier: This is based on pp. 70-72 of the RMR and revised on pages 6 and 19 of Attachment 2, Reference 205. The WCOBRA/TRAC calculation is sometimes slightly below the calculated value using Method 1, and the MPR report¹⁹⁴ that evaluated Methods 1 and 2 is not completely definite that the methods bound the true value.

Westinghouse supplied information (Reference 214, Attachment 2) to support the bounding nature of Methods 1 and 2. To address the fact that the WCOBRA/TRAC runs are sometimes slightly below the Method 1 results, Westinghouse used the condensation multiplier range based on page 19 of Attachment 2, Reference 205. INEL also notes that without reason for strongly preferring one of the MPR methods over the other, a uniform distribution is reasonable. Based on this review, justification of this item is considered adequate.

Local Condition Uncertainty

Local Peaking: Figure F-11 in Reference 3 of CQD Table 21-2-2 is based on observed rod bows, and the calculated corresponding increase in power. The figure has curves that show the total power increase that results from the rods with bow magnitudes less than or equal to a certain value. The curves in the figure rise more steeply on the left than on the right. This shows that the many rods with smaller bow contribute more than the fewer rods with larger bow. Therefore, a few

rods are not the dominant contributors to power increase. Therefore, by the Central Limit Theorem, the power increase is approximately normally distributed. The dominate contributor to local peaking is rod bow (Table 21-2-2 of the CQD). Therefore, because rod bow is normally distributed, the local peaking is normally distributed. The standard deviation used for rod bow is based on the maximum allowable at the end of life, which is appropriate.

Fuel Conductivity, Pre-burst: This is justified by Footnote 7 of Table 3.1.3-1 of the RMR, and Figure 2 (p. 37) of Reference 31.

Fuel Conductivity, After Burst: Batchelor and O'Brien¹⁸⁸ developed a correlation relating (effective conductivity)/(gas conductivity) to (solid conductivity)/(gas conductivity). This correlation was developed for granular material, but does not include particle size. Westinghouse reviewed the model against the data of Deissler and Boegli¹⁸⁹ who investigated the conductivity of three solids in four gases. Porosity of the gas/solid mixtures ranged from 0.30 to 0.5. When applied to UO₂ in steam, with conductivities appropriate for the anticipated temperatures, the effective conductivity given in Attachment 6 of Reference 206 results. The assumed range, also given in Reference 206, is consistent with the most scattered portion of Figure 8, Reference 189.

Fuel Density (Packing Fraction), After Burst: The uncertainty is given in Table 3.1.3-1 of the RMR. The justification is briefly summarized in Footnote 9 of the table, and it is given in more detail in Table 4 of the presentation on fuel density in Reference 56.

Gap Conductance: This is based on fuel temperature uncertainty from PAD3.4,⁷⁹ an approved code, as discussed in Footnote 10 of Table 3.1.3-1 of the RMR. The HOTSPOT calculations agree closely with the PAD3.4 calculations, as shown in "Figure 19, p. 54" in the presentation material on HGAP, in Reference 55.

Rod Internal Pressure: This is based on RIP uncertainty from PAD3.4 calculations, an approved code. See Table 3.1.3-1 of the RMR and

Footnote 11. The calculated uncertainties from PAD calculations as a function of PLHR were less than the uncertainty applied in the Westinghouse analysis, which is conservative and adequate.

Cladding Burst Temperature: The uncertainty is given in RMR Table 3.1.3-1, and justification is summarized in Footnote 12 of the table. In more detail, a correlation of Powers and Meyer (Reference 138) is used in WCOBRA/TRAC to calculate the cladding burst temperature based on engineering hoop stress and heatup rate (see CQD Eqn. 7-66). Figure 3 in Reference 138 shows experimental burst temperature plotted against engineering hoop stress. Based on Reference 138, the data from TREAT tests are outliers and are ignored. The remaining data show a scatter representative of the Westinghouse proposed uncertainty for the two burst temperatures INEL reviewed. The data scatter the INEL determined is for the distance to the data maximum and minimum, for a fixed value of engineering hoop stress. When data from a single heatup rate are plotted, the scatter should be less; this is true for the one data subset plotted in the report (see Figure 2, Reference 138). This justifies use of a uniform distribution with the range about the nominal given in RMR Table 3.1.3-1.

Cladding Burst Strain and Average Strain: The uncertainties on maximum burst strain are justified in Footnote 13 of Table 3.1.3-1 of the RMR, and Figures 6 and 7 of Reference 31. An upper bound is plotted in Figure 14 of Reference 31, relating the maximum burst strain to the average burst strain. Use of an upper bound is conservative. The average is obtained from the maximum in this way because little data exist on the average burst strain (Reference 214, Attachment 11). The average burst strain is used by the HOTSPOT model. Because validation of the internal workings of the HOTSPOT model is not in the uncertainty distribution review, this transformation is discussed in the HOTSPOT model review (see Section 9.4 of this report).

Zirc-Water and ZIRLO-Water Reactions: The justification is in Footnote 14 of Table 3.1.3-1 of the RMR (pp. 34-36). For Zircaloy, the method is described in Reference 214, Attachment 8. Westinghouse used the data and approach of Cathcart-Pawel (Reference 84), and it analyzed

the data as discussed in the reference. For ZIRLO, data from WCAP-12610-P-A, Reference 127, are used as documented in Reference 56. A consistent approach was used in the data analysis for Zircaloy and ZIRLO, and the approach used by Westinghouse is conservative.

Heat Transfer Coefficient: INEL review of the HTC uncertainty distributions found them adequately justified based on the information in Reference 58 and revised in Reference 206, Attachments 3 and 6, and Reference 213. The INEL notes that Westinghouse provided additional information in Reference 206 to support the uncertainty applied during the blowdown heatup period (Attachment 6) and the reflood period (Attachment 3). Reference 213 provided information on the blowdown cooling period. For all phases of the LBLOCA except blowdown heatup, Westinghouse uses empirical distributions (see RMR pages 437-438).

The development of the blowdown cooling HTC distribution proved to be difficult because of the size of some of the multipliers originally calculated based on the WCOBRA/TRAC comparisons to data. The information provided by Westinghouse in Reference 213 adequately addressed this issue. The reference gave appropriate reasons for the data used and the approach taken (including the approach needed to address biases in the heat transfer correlations themselves and the calculated boundary conditions) to derive the final blowdown cooling multipliers.

The data for the HTC distributions involve many experiments, which were scrutinized for their applicability. The resulting distributions are, therefore, considered appropriate. In addition, certain points were deleted solely because of their magnitudes, not because of how they were produced. This included one point during reflood and several during blowdown cooling. Normally, this would be a questionable practice. However, the effect of the deletions in this case is to make the distributions slightly more conservative. Therefore, INEL finds the deletions acceptable.

To account for rod-to-rod radiation effects in the data used to develop the heat transfer multipliers, Westinghouse uses a multiplier provided

in Reference 214, Attachment 4, and as discussed in Appendix D of this report.

T_{MIN} : Westinghouse originally proposed a T_{MIN} distribution in Appendix B, Reference 58, for use in HOTSPOT calculations. Based on Reference 213, however, Westinghouse eliminated the T_{MIN} distribution during blowdown for HOTSPOT calculations and replaced it with the correlation identified in the reference. This correlation provides a lower bound to T_{MIN} data during blowdown. Because use of a lower bound is conservative, INEL finds this approach adequate. Also, the uncertainty in reflood T_{MIN} is captured in the reflood HTC uncertainty methodology, which the INEL considers adequate. For more information, see Section 12.3 of this report.

Other Distribution Assumptions

Combining Initial Condition Uncertainties: The use of a normal distribution is adequate, possibly slightly conservative as discussed below. This conclusion is based on inspection of Tables 26-5-1 through 26-5-3 of the CQD. In each case, no one uncertainty parameter contributes an overwhelming portion of the variance. If one parameter dominated all the others, the Central Limit Theorem could not be invoked, so each table must be inspected. For the cases where one parameter may dominate, Westinghouse's approach is discussed below.

The normal assumption is somewhat conservative for the following reason. Typically, two parameters contribute about 80% of the uncertainty. Therefore, the sum roughly resembles the sum of two uniform random variables. Such a sum has a finite range, unlike the normal, which has an infinite range. Using the normal distribution with the matching variance allows larger values than can actually occur, which is conservative.

As part of the methodology, Westinghouse agreed in Attachment 5, Reference 214, to verify the normality assumption. If any element contributes over the percentage of the uncertainty identified in Reference 214, Westinghouse uses the approach outlined in Reference 214,

to further analyze the initial condition uncertainty and modify the uncertainty distribution. Based on the information in the reference, INEL concluded Westinghouse will appropriately modify the uncertainty distribution to account for the dominance of the one element.

Break Type Selection: Westinghouse considers each break type separately.

UNCERTAINTY PROPAGATION ASSUMPTIONS

Augmentation of Variables

Nozzle Resistance, K_N : K_N , pump resistance, K_p , and other minor quantities all enter into the resistance ratio R_B . Treatment of these variables is discussed on page 22 of the RMR. This treatment is justified based on WCOBRA/TRAC runs, presented in Section 5.1.5 of the RMR, and is supported by engineering understanding. Based on this information, INEL considers Westinghouse's approach conservative.

The calculation of the standard deviation of R_B , using the components in Tables 3.1.2-4 and 3.1.2-5 of the RMR, is also correct. The assumption of normality is based on the Central Limit Theorem (page 26-36 of the CQD) and confirmed by simulation (Fig. 26-31 of the CQD). The CQD figure was based on the assumed distribution for each random element (given in Section 3.2.1 of the RMR), and slightly different variances than given in the RMR. In the CQD, the K_N and K_p contributions to the variance of R_B cause the resulting distribution in Figure 26-31 to be somewhere between a triangular and a normal distribution. The revised variances of the RMR cause the two contributions to be different, but the distribution is still somewhere between a triangular and a normal. A normal distribution and a triangular distribution with the same mean and standard deviation have almost the same 95th percentiles, but the normal distribution has a wider range. Therefore, the normal approximation is good, though slightly conservative.

Peaking Factors, F_Q and F_{AH} : PCT is proportional to a product of the peaking factor times some other quantities. Because PCT depends on

these terms in such a simple way, uncertainty in any one of the terms could be used as a surrogate for uncertainty in all the terms. The peaking factors are used, although any other term could be also be used.

Form of Response Surface/Superposition Model, Including Separability of Effects

The response surface model uses a number of assumptions, but many of them do not have to be checked, because performance of the model is quantified during the validation portion of the method. In the validation portion, the results of the superposition method are compared with WCOBRA/TRAC/HOTSPOT results. This comparison is used to determine a correction to the superposition method. If the model used bad assumptions, so that it performs poorly, this is accounted for during the validation step.

A number of assumptions were supported using plant specific data; therefore, in Reference 214, Attachment 5, and Reference 215, Attachments 1 and 2, Westinghouse agreed to verify the following assumptions on a plant specific basis:

1. Validation data points are normally distributed, with constant variance, around a straight line: The normality must be checked for each phase of the accident for each plant. If the variance from the scatter around the line is not used, because it is relatively small compared to $\sigma_{WC/T}^2 + \sigma_3^2$, where WCOBRA/TRAC uncertainty based on experiments = $\sigma_{WC/T}$ and the nodalization uncertainty = σ_3 , then it is enough to show that the normal distribution involving $\sigma_{WC/T}^2 + \sigma_3^2$ conservatively bounds the scatter of the validation points around the straight line.
2. HOTSPOT PCTs are normally distributed: This must be checked at each point where the HOTSPOT PCT is varied in a Monte Carlo sample: the points used to build the response surface for the HOTSPOT standard deviation (σ_{conf}) and the validation points. It is adequate to find that a normal distribution is conservative. If the normal distribution is not conservative, Westinghouse on

page 2 of Attachment 5, Reference 214, proposed an procedure for increasing the normal standard deviation to make the normal distribution conservative. This approach is considered adequate if the standard deviation needs only a small increase. As discussed in Attachment 2, Reference 215, if a large increase is required, Westinghouse makes an additional comparison between the adjusted normal distribution and the empirical distribution to ensure the adjusted normal distribution appropriately represents or is conservative relative to the empirical distribution.

3. Response surface for σ_{adj} is accurate or conservative: This should be checked by comparing the response surface estimate with the Monte Carlo standard deviation at each validation point. The response surface method should not severely underestimate any standard deviation. For IP2, the value given in Reference 205, Attachment 2, had to be added to the response surface. For other plants, a different adjustment may be necessary as discussed in Reference 215, Attachment 1. In the reference, Westinghouse formalized the process to determine the error in the response surface for σ_{adj} on a plant specific basis. The approach used is analogous to the correction factor applied to the superposition PCT. Given the similarity of the two approaches and the INEL finding the approach adequate for the superposition PCT, the INEL concluded the approach is also adequate for the correction of the response surface estimate of σ_{adj} .

In addition, Westinghouse provided normality checks on the following items in Reference 214, Attachment 5:

The distributions corresponding to WCOBRA/TRAC uncertainty based on experiments ($\sigma_{\text{WC/T}}$), nodalization uncertainty (σ_3), and the uncertainty due to experimental data scatter (σ_{2p}): In Attachment 5, Reference 214, Westinghouse showed that, at the elevation used to calculate $\sigma_{\text{WC/T}}$, the differences between the mean of the experimental data and the corresponding WCOBRA/TRAC runs are consistent with a normal distribution. Similarly, the deviations (that is, the terms that are squared and summed) contributing to σ_3 are consistent with a normal

distribution. Even though they were not produced by a random process but by systematic variation of nodalization, etc., the resulting ΔPCT values appear to be distributed normally. Finally as discussed in Reference 214, the deviations that contribute to σ_{2p} are not normally distributed, but a normal distribution is conservative at the upper end of the distribution (note: a modification to the σ_{2p} calculation is discussed below and normality rechecked by the INEL). Therefore, none of the distributions presents any obstacle to the planned use of normal distributions in the Monte Carlo simulations. Also, Westinghouse in Reference 214, List III, Item 2, agreed to verify the continued adequacy of the normal distributions for $\sigma_{WC/T}$ and σ_{2p} if the code is modified or the assessment data base changes.

In Reference 214, Attachment 5, Westinghouse recalculated σ_{2p} . The variance between rods (thermocouples) and the average cladding temperature was calculated for various experiments. Three LOFT experiments were discarded for engineering reasons. This affects the calculation because two of the LOFT experiments had variances that were much larger than any other experiment. The remaining experiments were ordered by descending variance. The largest variances were pooled, with additional experimental variances added until Bartlett's test (a standard statistical test for equality of variances) found the variances were significantly different at the 5% significance level. In all, 15 out of 25 of the non-LOFT experiments with the largest variances were combined in this way. The resulting standard deviation, the square root of the pooled variance, was given in the reference. The recalculated value is slightly less than the previous value (also given in the reference) that was based on pooling all the data without considering whether the data were similar enough to be pooled. Because it is larger, the previous value will be retained for the analysis. The INEL considers the entire process justified and correct.

The final issue is whether the distribution is normal. For each experiment, the INEL calculated the deviations of the rod temperatures from their average. When these deviations are pooled, for the experiments used for the pooled variance, the resulting data set appears normally distributed. In particular, the Shapiro-Wilk test of normality

can reject normality only at a significance level of 0.31, not at the 0.05 level. Therefore, use of a normal distribution is justified.

9.3 LBLOCA Method Description/Review - Split Breaks

RG 1.157 indicates that split breaks should be considered in the break spectrum analysis used to determine the 95th percentile PCT. Westinghouse discussed its handling of this recommendation in Section 4.4.3 of Reference 58. Westinghouse addresses this issue by running a split break spectrum and determining the limiting break. Then, Westinghouse accounts for local uncertainty effects using the results from the limiting split break.

Westinghouse stated that because the limiting split break is used, model global uncertainties did not need to be considered for the split breaks. This was because use of the limiting break implies a lower PCT would result if conditions changed, and Westinghouse provided sensitivity studies to show that the limiting PCT did not change significantly with global model variations.

Westinghouse accounts for plant condition uncertainties on the limiting split break using the initial conditions uncertainty and power distribution response surface developed for the double-ended guillotine (DEG) break. In Section 4.4.3, Westinghouse noted this assumption was based on the similarity of the split break to one of the DEG breaks. INEL clarified this in a discussion with Westinghouse. Westinghouse pointed out the following items in Reference 58. First, the limiting split break (page 240, Reference 58) has similar event timing relative to one of the DEG breaks (see page 293). This implies a similar system thermal-hydraulic response for the two break types. Second, the limiting split break and the corresponding DEG break both have higher PCTs than the base case DEG break. This implies a similar system response to break flow changes. Third, Westinghouse demonstrated in Section 5.3.1 of Reference 58, that superposition of power distribution and break flow effects adequately represented the WCOBRA/TRAC calculated results. Therefore, given the above items, Westinghouse concluded that the DEG initial conditions uncertainty distribution and the power distribution response surface could be applied to the limiting split break.

The INEL reviewed the information in Reference 58 pointed out by Westinghouse. The information was found to support the conclusions reached by Westinghouse regarding the model global effects. The figures referenced by Westinghouse and the discussion in Section 5.1.3 of Reference 58 also support the extension of the DEG initial conditions uncertainty distribution and the power distribution response surface to the limiting split break for the reasons presented by Westinghouse. Therefore, the INEL concluded Westinghouse's approach to split breaks is adequate.

9.4 LBLOCA Method Description/Review - Westinghouse HOTSPOT Model

Westinghouse developed a model to evaluate the effects of the uncertainties associated with local parameters on the calculated PCT called the HOTSPOT model (see Reference 31). It models a portion of a fuel rod at the PCT or burst location including fuel, gap, and cladding. Input values include pellet and cladding geometry, linear heat rate, initial gap pressure, and initial gap conductance. Fuel rod models are the same as those in WCOBRA/TRAC except as noted in Reference 31 and discussed below. Boundary conditions are based on the vapor and liquid HTC's, vapor and liquid temperatures, and fluid pressure calculated by WCOBRA/TRAC at a specified location in the HA. After the HOTSPOT model reaches steadystate conditions, transient boundary conditions are applied. If the burst temperature is exceeded, burst is calculated, fuel relocation is assumed to occur with an increase in linear power, and inside metal-water reaction commences.

The HOTSPOT model is a simple physical model that allows the effects of uncertainties to be calculated directly by running the model many times with parameter values that vary randomly according to specified distributions. The parameter uncertainties considered are linear power, fuel density after cladding burst, fuel conductivity prior to and after burst, metal-water reaction rate, gap pressure, gap conductance, burst temperature, and burst strain. The INEL review of the uncertainty distributions for the above parameters is discussed in Section 9.2 of this report.

One area that the HOTSPOT model differs from the fuel rod models in WCOBRA/TRAC is the modeling of fuel relocation following burst. To get the volume inside the burst cladding for fuel relocation, Westinghouse converts

the maximum cladding strain to an average cladding strain based on data taken at Westinghouse. This data is shown in Figure 14 of Reference 31. As noted in Section 9.2 of this report, Westinghouse uses an upper bound line for the conversion which will result in conservative estimates of burst cladding volume increase for fuel relocation. The average cladding strain is used to estimate the cladding volume increase. The cladding volume increase is used to estimate the fuel relocation allowed as discussed in Reference 31. Finally, the linear heat rate is increased based on the fuel relocation (also as discussed in Reference 31).

INEL review of the fuel relocation methods used by Westinghouse found them adequate for realistic LBLOCA. INEL agreed with Westinghouse's derivations for cladding volume increase and linear power increase due to fuel relocation. However, INEL did note that Figure 15 of Reference 31 was based on peak volume increase not average volume increase as in the Westinghouse methodology. Review of the original reference,²⁰² found that it was not completely clear as to the meaning of the figure. Further INEL review, however, found that the effect of using the peak cladding volume increase rather than the average cladding volume increase was to increase the fuel relocation by 10 to 20%. The INEL does not consider this worth pursuing because: (a) the difference is small, (b) there is wide scatter in the data used to derive Westinghouse's fuel relocation equation (see Figure 15 of Reference 31), and (c) there is wide scatter in the peak cladding strain data (for example, see CQD Figures 7-18 and 7-20).¹⁹¹

Other HOTSPOT models are based on those in WCOBRA/TRAC.

Based on the INEL review of the fuel relocation models and because the HOTSPOT model uses other fuel rod models based on WCOBRA/TRAC, INEL concluded it is adequate for realistic LBLOCA analysis.

9.5 Summary of INEL Review

This section summarizes the results of the review of the Westinghouse realistic LBLOCA methodology. The following conclusions were reached:

1. INEL review of the WCOBRA/TRAC code models found them adequate to provide a realistic analysis of LBLOCA results. This conclusion is based on the INEL's review of information Westinghouse provided in the CQD, Volume 1, and in their responses to approximately 240 questions. The details supporting this conclusion are found in Appendix A of this report.
2. Uncertainty distributions/assumptions - Based on information from Westinghouse, Westinghouse has adequately justified the uncertainty distributions used. Westinghouse quantifies the effects of the assumptions made for its superposition method by performing validation runs to account for the differences between the superposition assumptions and full WCOBRA/TRAC/HOTSPOT runs. INEL review of this method considers it adequate to address questions on the superposition approach. This is because if bad assumptions are made, then this validation accounts for them.
3. Split breaks - The INEL reviewed the information provided by Westinghouse. The information was found to support the conclusions reached by Westinghouse regarding the model global effects and split breaks. The figures referenced by Westinghouse and the discussion in Section 5.1.3 of Reference 58 also support the extension of the DEG initial conditions uncertainty distribution and the power distribution response surface to the limiting split break for the reasons presented by Westinghouse. Therefore, the INEL concluded Westinghouse's approach to split breaks is adequate.
4. HOTSPOT - Based on the INEL review of the fuel relocation models and because the HOTSPOT model uses fuel rod models based on WCOBRA/TRAC, HOTSPOT is adequate for realistic LBLOCA analysis.

10. COMPARISON WITH REGULATORY GUIDE 1.157

The recommended features of a realistic LBLOCA analysis are described in RG 1.157. Comparison of the Westinghouse methodology with RG 1.157 is discussed in detail in Appendix C of this report, but that review is summarized in Section 10.1 of this report. In addition, RG 1.157 discussed determining the range of applicability for a number of different models. Compliance with the RG recommendations in this area is discussed in Section 10.2 of this report.

10.1 Summary of Westinghouse Methodology/RG 1.157 Comparison

In general, INEL found that Westinghouse's methodology met the RG guidance in Section 3, Best-Estimate Code Features, and Section 4, Estimation of Overall Computational Uncertainty. For example, Westinghouse uses a point kinetics model to analyze fission heat as allowed by RG Section 3.2.2, and the fission product decay heat model is based on the 1979 ANSI/ANS standard (Reference 83) allowed by RG Section 3.2.4.

Where Westinghouse took an alternative approach to that outlined in the RG, INEL review found that Westinghouse provided adequate justification for the approach presented. For example, Westinghouse uses the Cathcart-Pawel model⁸⁴ to calculate the Zirc-water reaction at temperatures above 1500°F. In the RG, Section 3.2.5, the Cathcart-Pawel model is recommended but only for temperatures greater than 1900°F. As discussed in Appendix C, Westinghouse notes the Cathcart-Pawel model overpredicts the reaction rate at temperatures below 1900°F; therefore, it is conservative to use it at the lower temperatures. Such conservatism is allowed by the RG (see RG Section 1.0).

RG 1.157, Section 4.5, notes the CSAU methodology was used to evaluate the overall calculational uncertainty in PCT predictions for NRC developed BE computer programs. In Section 2 of this report, INEL review found the Westinghouse methodology was consistent with the intent of CSAU.

Based on information provided by Westinghouse, Westinghouse has met the RG guidance or provided adequate justification for its alternate approach.

10.2 WCOBRA/TRAC Range of Conditions/Applicability

RG 1.157 identified the following models as needing the range of applicability justified: critical flow, ECC bypass, frictional pressure drop, critical heat flux, transition and film boiling heat transfer, single-phase vapor heat transfer, and level swell. Also, Westinghouse's PIRT identified the following models as important: critical flow, pump, accumulator nitrogen, condensation, entrainment, ECC bypass, core heat transfer (including T_{MIN}), and fuel rod. In Volume 1, question 3a, Reference 50, Westinghouse discussed the basis for the range of applicability in these models relative to the WCOBRA/TRAC assessment it performed. INEL review of that response found:

1. The WCOBRA/TRAC critical flow assessment covered the appropriate PWR range of conditions for pressure, subcooling, void fraction, and length/diameter (L/D). See Table 1, Volume 1, question 3a.
2. The ECC bypass assessment covered almost the full PWR range for geometry, downcomer circumference, ECC location, ECC temperature, ECC flow, and system steam flow. Where the assessment ranges did not fully cover the PWR range, the INEL considers the assessed range close enough to be representative of the PWR range. See Table 4, Volume 1, question 3a.
3. The WCOBRA/TRAC frictional pressure drop model assessment covered the right range of conditions for mass flow, void fraction, and pressure if the break is not considered. If the break is considered, the main components of uncertainty are the vessel nozzle loss and the broken loop pump. The uncertainty in both of these components was estimated by Westinghouse and directly included in the code uncertainty assessment. See Table 5, Volume 1, question 3a.
4. The code applies the Biasi correlation⁸⁵ above $30 \text{ g/cm}^2\text{-s}$ with linear interpolation to a modified Zuber correlation⁸⁶ at flows below $30 \text{ g/cm}^2\text{-s}$ (see CQD Eqn. 6-68). Collier⁸⁷ gives the lower bound of the Biasi correlation data base as $10 \text{ g/cm}^2\text{-s}$ which indicates WCOBRA/TRAC uses the Biasi correlation within the data

base flow range except for part of the interpolation regime (between 10 and 0 g/cm²-s) until the Zuber correlation is used alone at zero flow. The modified Zuber correlation is only applied at low flows as conditions approach pool boiling (less than 30 g/cm²-s) due to the interpolation, and it is used alone at zero flow. The extension of Biasi and Zuber in the interpolation regime is considered appropriate to allow for a smooth transition between the Biasi and Zuber correlations. The other data base ranges for diameter, length, flow, quality, and pressure for the Biasi correlation given in Collier indicate the Biasi correlation covers the range of conditions expected in a PWR.

5. For the post-critical heat flux (post-CHF) regimes of transition boiling and film boiling heat transfer, Westinghouse provided adequate information that the WCOBRA/TRAC assessment covered the appropriate range of conditions in its responses to:
 1. Volume 2, question 2, Reference 39, and CQD Tables 11-1 to 11-3 for blowdown.
 2. Volume 1, question 152, Reference 37, and CQD Tables 12-1 to 12-3 for reflood.
6. For single-phase vapor heat transfer, Volume 1, question 152, Reference 37, and Reference 205, Attachment 5, provided data to show the assessment of WCOBRA/TRAC covered the PWR range.
7. RG 1.157, Section 3.12.2.1, discussed the phenomenon of level swell and stated the range of applicability of the level swell model should be determined. Westinghouse noted in response to Volume 5, question 49, Reference 44, that level swell is more important for small-break LOCAs while the phenomena of importance to LBLOCAs are entrainment and carryover. Tables 5-1 and 5-2 in NUREG-1230⁸⁸ were referenced to support this distinction. Therefore, Westinghouse's discussion on the range of applicability focused on entrainment/carryover rather than level swell. The INEL agrees with this distinction as it is consistent with our

understanding of the important LBLOCA phenomena, and it is consistent with the Westinghouse PIRT. The entrainment considered by Westinghouse was entrainment in the core and upper plenum. Reflood assessments for the core and upper plenum were carried out in UPTF, CCTF, SCTF, and FLECHT⁸⁹⁻⁹² facilities. Various core radial and axial power distributions and various bundle geometries (15x15 and 17x17) were simulated in these facilities. Information was provided in Table 3 of Volume 1, question 3a. The INEL also reviewed CQD Tables 12-1-1, 12-1-2, 12-1-3, and 14-2-2. Based on this review, the appropriate range of conditions was covered in the entrainment model assessment.

8. The WCOBRA/TRAC pump model is an empirical model based on pump data. The two-phase data used to develop the pump model cover the range expected in a PWR. Westinghouse based this on a comparison of CQD Figures 16-3-5 and C-1 (C-1 is for a four-loop plant). Additional information for a three-loop plant was presented in Reference 56. The two-phase test data in Figure 16-3-5 (the asterisks in the figure) range from 0.5 to 2.75. In Figure C-1, except for one point, the calculated two-phase pump operation is well within the data range on which the two-phase model was based. For the three-loop plant data presented in Reference 56, two points (representing 1 s of pump operation) were outside the two-phase pump data range. The pump model was assessed against four LOFT tests, two with the pumps on and two with the pumps coasting down. This covers the range of pump operation expected in a PWR. Although a small number of tests was used, Westinghouse stated it is sufficient because it covers expected operating conditions, and Westinghouse's analysis shows the single-phase pump head model is the most important. See CQD Section 16-3, CQD Appendix C, and the material from Reference 56. The INEL notes the uncertainty in this model is accounted for in the WCOBRA/TRAC uncertainty analysis.
9. Westinghouse discussed the accumulator nitrogen model, and the INEL review of this model is found in Section 12.2 of this report.

10. Except for the minimum ECC temperature expected in a PWR, the condensation model was assessed against the appropriate range of conditions. See Table 2, Volume 1, question 3a. The INEL considers this adequate because no new phenomena would be introduced in cases where a lower ECC temperature was used to assess WCOBRA/TRAC.
11. For the other core heat transfer models, Westinghouse provided adequate information that the WCOBRA/TRAC assessment covered the appropriate range of conditions in its responses to Volume 1, question 152, Reference 37, (see also CQD Tables 12-1 to 12-3) for reflood and Volume 2, question 2, Reference 39, (see also CQD Tables 11-1 to 11-3) for blowdown. Because T_{MIN} is the temperature at the boundary between film boiling and transition boiling, the INEL notes the range of conditions for T_{MIN} is covered because the appropriate conditions for transition and film boiling are covered. Also, T_{MIN} is included directly in the uncertainty calculations.
12. The fuel rod model in WCOBRA/TRAC was assessed against NRU and LOFT experiments both of which use nuclear fuel rods. While these assessments cover a wide range of conditions, the assessments performed will not cover all fuel rod parameter ranges. To account for this, Westinghouse varies fuel rod models such as fuel relocation, gap conductance, burst temperature, and burst strain directly in the uncertainty analysis through its HOTSPOT model. The HOTSPOT model is reviewed in Section 9.4 of this report.

This shows the WCOBRA/TRAC assessment covered the appropriate range of conditions for the important models, or the methodology directly accounts for the uncertainty.

11. WESTINGHOUSE EVALUATION OF COMPENSATING ERRORS

Compensating errors are defined as those errors that when combined provide good but misleading results. For example, PCT could be calculated well but only because the heat transfer model overpredicted the local HTC compensating for a low core flow rate.

In Reference 59, Westinghouse provided its evaluation of compensating errors in the WCOBRA/TRAC code (this report will be referred to as the CER). Additional information on compensating errors was presented by Westinghouse at the January 1996 meeting between Westinghouse and the Thermal-Hydraulic Subcommittee of the ACRS, the February 1996 meeting with the full ACRS committee, and in References 213 and 214, Attachment 1. Unless noted otherwise, all figures referenced in this section are from Reference 59.

Westinghouse evaluated both separate effects and integral tests to determine the presence of compensating errors in the following areas: post-CHF heat transfer, ECC bypass/condensation, and blowdown and post-blowdown thermal-hydraulics/entrainment. Table 11.1 lists the tests used to evaluate each area.

Phenomena Evaluated	Tests Used for Evaluation
Post-CHF Heat Transfer	ORNL high pressure film boiling tests ⁹³⁻⁹⁴ INEL single tube film boiling tests ⁹⁵ FLECHT-SEASET forced flooding tests G-1 blowdown tests
ECC bypass/condensation	Stratified condensation tests ⁹⁶ Steam/water mixing tests ⁹⁷ UPTF ECC bypass tests
Blowdown/Post-Blowdown Thermal-Hydraulics/Entrainment	LOFT Test L2-3 ⁹⁸ LOFT Test L2-5 ⁹⁹ SCTF forced flooding Test 619 CTF gravity reflood Test 62

11.1 Post-CHF Heat Transfer Evaluations

Westinghouse evaluated two ORNL high pressure film boiling tests, INEL film boiling tests, and three FLECHT-SEASET tests for evidence of compensating errors. The ORNL tests are discussed first followed by the INEL tests and the FLECHT-SEASET tests.

11.1.1 ORNL Film Boiling Tests

Westinghouse evaluated two ORNL high pressure film boiling tests, 3.03.6AR and 3.08.6C, for evidence of compensating errors. For these tests, WCOBRA/TRAC tended to give PCT comparisons that were good to slightly low (see CQD Figure 11-2-22). In the CER, Westinghouse compared the calculated vapor superheat to an estimate of the superheat in the tests (vapor superheat was not measured directly in these tests). Because the superheats in the tests were estimated, Westinghouse noted that this quantity may have considerable uncertainty in the reported value. Therefore, the most important conclusion that can be reached from these tests is that WCOBRA/TRAC correctly predicts the presence of superheated steam in the tests. Comparison of the calculated and estimated values shows that WCOBRA/TRAC tended to predict vapor superheat that was good to slightly low consistent with the PCT comparisons. Based on this, Westinghouse concluded, and the INEL agrees, that this comparison supports a lack of significant compensating errors in these test analyses. Significant compensating errors would exist if no vapor superheat or high vapor superheat was calculated, but PCT predictions were good.

11.1.2 INEL Film Boiling Tests

Westinghouse also evaluated INEL film boiling tests for evidence of compensating errors. Figure 4 of the CER shows that relative to the TRAC-PF1 code¹⁰⁰ evaluated in the CSAU study, Reference 61, WCOBRA/TRAC does not have the severe overprediction of HTC observed in the CSAU work. Westinghouse discussed its understanding of the reason for this difference on page 7 of the CER. To evaluate the HTC/void fraction relationship, Westinghouse plotted the relative difference in calculated HTC and measured HTC versus void fraction (see Figure 5). This figure shows the code does have a bias towards overprediction of HTC as the vapor fraction is reduced. But a much clearer

correlation was obtained when the relative difference in calculated HTC and measured HTC was plotted versus vapor Reynolds number (see Figure 6). This figure shows that overprediction of HTC increased as the vapor Reynolds number decreased below 10,000. Westinghouse considered this result consistent with the basic premise of the droplet contact model. This is because droplet contact is driven by turbulence in the vapor flow, and this should decrease as the vapor Reynolds number decreases. Because WCOBRA/TRAC does not model this decrease, the HTC is overpredicted at low vapor Reynolds numbers. Westinghouse, however, does not consider this a serious deficiency in the code heat transfer models because of the low liquid heat transfer calculated during blowdown as seen in the LOFT comparisons (see Figure a7a and b7a) and prior to quench in the reflood comparison (see Figure 15). Westinghouse also noted in the CER conclusions section (CER Section 3) that the Reynolds number during blowdown is larger than the Reynolds number where overprediction of heat transfer becomes too large.

11.1.3 FLECHT-SEASET Test Analysis

The final tests evaluated in the post-CHF area were FLECHT-SEASET Tests 31504, 31805, and 31701 (reflood rates of 0.97, 0.81, and 6.1 in/s). For Test 31504, Westinghouse evaluated the bundle thermal-hydraulics. The WCOBRA/TRAC analysis of Test 31504 underpredicted the PCT and vapor temperature (see Figures 7a and 7b). Westinghouse attributed this underprediction to the fact that WCOBRA/TRAC underpredicted the heat transfer to the vapor just above the quench front (Figure 13). Westinghouse concluded that the underprediction of the vapor heat transfer was not due to overprediction of the interfacial heat transfer because the vapor velocity comparison in Figure 12 was good. Also, at 10% of the total heat transfer, wall to liquid heat transfer was not an important part of the calculated heat transfer (see CER, page 11). Westinghouse also noted that comparison of predicted and test estimated vapor Reynolds numbers (Figure 16) shows the calculated value was higher, but comparison of the predicted and test estimated Nusselt numbers (Figure 17) shows that the calculated value was lower than that estimated from the test data. In Reference 214, Attachment 1, Westinghouse explained these items (lower predicted heat transfer to the vapor and higher predicted vapor Reynolds number but lower predicted Nusselt number) by noting that the WCOBRA/TRAC heat transfer models to steam are based on

fully developed flow correlations. One example is the Dittus-Boelter correlation.¹⁰² In the test, however, turbulence at the quench front would enhance the test heat transfer at that location. Fully developed flow in the test would not occur for some distance downstream of the mixture level and quench front. Based on the arguments presented by Westinghouse, INEL concluded that physically plausible explanations were provided for the noted differences between the WCOBRA/TRAC results and the test data.

Westinghouse used Tests 31805 and 31701 to investigate the heat transfer/void fraction relationship in the WCOBRA/TRAC comparisons to FLECHT-SEASET tests. First, Test 31805 was considered. Westinghouse noted that simulation of this test had several of the problems identified in other FLECHT-SEASET test comparisons. In particular, the PCT was underpredicted (Figure 19) due to higher predicted HTC's (Figure 20), and this was due to underpredicting the heat transfer to the vapor at the quench front (Figure 21). To evaluate the HTC/void fraction relationship, Westinghouse plotted the cladding temperature versus void fraction and HTC versus void fraction for both the test data and the WCOBRA/TRAC results. The following discussion is for the 6 foot elevation; similar results were found at 10 feet. Evaluating the test data (Figures 23 to 27), Westinghouse pointed out that flow transition from dispersed flow to an inverted annular type flow began at 300 s. The cladding cooldown and HTC increased slightly at that time but the HTC did not indicate a large increase until the rods quenched. Figures 29 and 30 show the same type of comparisons for the WCOBRA/TRAC results. Again, it was found that the cladding cooldown and HTC increased slightly with the transition from dispersed flow to an inverted annular type flow at about 300 s, but the HTC did not indicate a large increase until the rods quenched. Comparison of the calculated and the test estimated void fraction found good agreement (Figure 30) except between 300 to 425 s. The disagreement during this time period is due to fixed hydraulic mesh effects (CER, page 26).

Westinghouse performed a similar evaluation for FLECHT-SEASET Test 31701 (see Figures 37-38 for the test results and Figures 39-40 for the WCOBRA/TRAC results). Results similar to that discussed for Test 31805 were found.

Based on the above HTC versus void fraction evaluation, Westinghouse concluded that WCOBRA/TRAC and the test results indicated similar trends.

11.1.4 G-1 Blowdown Tests

In References 213 and 214, Attachment 1, Westinghouse discussed the compensating error analysis for the G-1 blowdown tests used in the WCOBRA/TRAC code assessment. Westinghouse's analysis showed the code tended to overpredict the vapor temperature resulting in lower calculated heat transfer relative to the test data. However, the rewet temperature was overpredicted, leading to a compensating error in the calculation of the rewet location. The low heat transfer in the film boiling regime compensated for the high rewet temperature leading to an apparently correct rewet location for some tests. In References 213 and 214, Attachment 1, Westinghouse noted this compensating error was addressed by modifying the blowdown cooling HTC uncertainty distribution (by removing the vapor temperature bias in the code/data comparisons) and using a lower bound rewet temperature during HOTSPOT blowdown calculations.

11.1.5 INEL Review

INEL reviewed the information provided by Westinghouse and concluded the results do not indicate evidence of significant compensating errors in WCOBRA/TRAC or problems not addressed by Westinghouse's methodology. For the ORNL tests, superheated steam was measured and calculated. Calculated PCT trends were consistent with the differences between the measured and calculated superheat. For the INEL film boiling tests, WCOBRA/TRAC overpredicted the data, but not to the extent of the TRAC code used in the CSAU study. INEL does not consider this serious for the reasons noted by Westinghouse: (a) low liquid heat transfer calculated during blowdown and prior to quench in reflood and (b) the Reynolds number during blowdown is larger than the Reynolds number where overprediction of heat transfer becomes too large. Also, Westinghouse uses heat transfer multipliers in its uncertainty evaluation to account for differences between measured and calculated heat fluxes, which will correct for this overprediction.

While the Westinghouse analysis indicates there are no major compensating errors in the forced reflood analyses, INEL notes this does not mean the WCOBRA/TRAC analyses of forced reflood tests are without problems. The forced reflood analyses showed that WCOBRA/TRAC tended to overpredict

entrainment in the core, and there was low heat transfer to the vapor just above the quench front (see CER, Section 3, Item 5). This manifested itself in higher heat transfer above the quench front, lower PCTs, earlier turn-around-times, more rapid cooldown, and earlier quench relative to the test data. Because these are the types of effects expected from overpredicting entrainment and low vapor heat transfer at the quench front, the INEL does not consider overpredicting entrainment/low vapor heat transfer in forced reflood tests as compensating errors. However, the problems and their effects need to be addressed, and Westinghouse addressed these areas by ranging the heat flux multiplier in the uncertainty analysis based on the forced reflood tests. Because of the overprediction of heat transfer due to these problems, the average heat transfer multiplier in the uncertainty analysis is less than 1.0. This indicates WCOBRA/TRAC tended to overpredict heat transfer, but use of the multipliers in the uncertainty analysis results in a heat transfer penalty.

Further, during the January 1996 meeting between Westinghouse and the Thermal-Hydraulic Subcommittee of the ACRS, several concerns were raised about the potential for compensating errors in the FLECHT-SEASET Test 31701 analysis, a test with a 6.1 in/s flooding rate. To address these concerns, Westinghouse noted in the February 1996 meeting with the full ACRS committee, that the Test 31701 data was removed from the data base used to develop the reflood heat transfer multipliers. This resulted in a slightly more conservative uncertainty distribution.

Westinghouse adequately dealt with the compensating error identified in the G-1 blowdown tests. In References 213 and 214, Attachment 1, Westinghouse noted this compensating error was addressed by modifying the blowdown cooling HTC uncertainty distribution (to remove the temperature bias in the code/data comparisons) and using a lower bound rewet temperature during HOTSPOT blowdown calculations. The INEL considers this adequate because both modifications dealt with the underlying causes of the compensating errors and resulted in more conservative distributions.

11.2 ECC Bypass/Condensation

As indicated in Table 11.1, Westinghouse used a number of different sources for test data to evaluate ECC bypass and condensation for compensating

errors. Westinghouse's evaluation of WCOBRA/TRAC's ECC bypass calculation is directly related to the CCFL models, and INEL discussed its review of CCFL modeling in Section 12.1 of this report. Therefore, only the condensation models are addressed here.

Westinghouse addressed condensation in the vessel (Volume 1, question 111, References 42 and 45) and in 1-D components (in Reference 11). For the vessel, the code results compared well with the data but there is wide scatter in the data. This is accounted for in the uncertainty analysis (see Section 6 of this report).

The 1-D results (comparisons to the Northwestern tests, Reference 96) showed the interfacial area was overpredicted while the interfacial HTC was underpredicted. This is an example of a compensating error. Westinghouse, however, noted that the overall condensation efficiency in 1-D components is approximately correct as shown in CQD Figures 15-3-48 and 15-3-49 for the full-scale UPTF tests. Because the overall condensation rate is calculated correctly, Westinghouse noted that the compensating error in this case does not compromise the code's ability to predict the overall condensation rate in 1-D components. INEL notes Westinghouse's conclusion is also supported by the fluid temperature comparisons for both UPTF and the Westinghouse/EPRI 1/3rd-scale steam/water mixing tests as discussed in Sections B.2.4 and B.3.1 of this report. Those comparisons show the code adequately calculated the fluid temperature as it exited the simulated cold leg.

Based on ECC bypass/condensation information reviewed, INEL concluded that WCOBRA/TRAC does not have significant compensating errors in the CCFL/condensation models that would compromise the code's ability to realistically calculate LBLOCAs.

11.3 Blowdown/Post-Blowdown Thermal-Hydraulics/Entrainment

To evaluate compensating errors in the blowdown/post-blowdown thermal-hydraulics/entrainment areas, Westinghouse reviewed two LOFT tests, a SCTF test, and a CCTF test. The LOFT tests will be discussed first, followed by the SCTF and CCTF tests. Because of the detailed analyses presented by

Westinghouse, INEL review comments are provided at the end of the discussion for each test facility.

11.3.1 LOFT Analyses - Tests L2-3 and L2-5

To illustrate the compensating error analysis Westinghouse performed for the LOFT test analyses, the discussion of Test L2-3 will be addressed in detail. Similar comparisons for Test L2-5 were made, but those results will only be summarized.

Core thermal-hydraulics were the first area evaluated by Westinghouse. Westinghouse noted that the PCTs for Test L2-3 were predicted well by WCOBRA/TRAC (see Figure a1). Because no incore flow measurements were made in LOFT, only calculated results are available. They show (Figures a2/a3) that the calculated blowdown quench coincides with the return to positive flow at about 5 s. To determine whether the good prediction of core heat transfer is due to compensating errors such as low vapor superheat and low HTC, steam superheat comparisons were made; Figures a4 and a5 compare this parameter at the top and bottom of the core. These comparisons show that both the code and the test data had steam with large superheats exiting the core when the blowdown quench in Figure a1 occurred. After 15 s, the code calculated much higher levels of steam superheat at the top of the core relative to the test data. Westinghouse stated, however, that the steam thermal-couples (T/Cs) are subject to rewet. This is because the T/Cs are located outside the core where some liquid may be present. Also, even if the data measurement is accurate, Figure a4 shows WCOBRA/TRAC conservatively calculated the steam superheat in this test. As will be discussed later, the intact loop flows and the break flows for Test L2-3 were calculated well. When the predicted core flow increased at 5 s, this coincided closely with the time when the broken loop cold leg flow fell below the intact loop cold leg flow allowing a return to positive core flow. When the intact loop cold leg flow decreased at about 10 s, the core flow rate also decreased. Based on the good flow comparisons in the loops and at the break locations, Westinghouse concluded the core flow was also predicted well for this test.

For the system response, Westinghouse compared the system pressure from the test to the code result (Figure a8). WCOBRA/TRAC overpredicted the

pressure early in time and then fell below the measured pressure. Westinghouse noted this was due to underpredicting the hot leg break density, resulting in higher energy and volumetric flow. This reduced the system pressure more rapidly than in the experiment. Figure a9 compares the calculated and measured core level. This comparison shows that WCOBRA/TRAC calculated core recovery later than the test data due to increased ECC bypass (see Figure a27).

Loop behavior was evaluated using fluid flow rates, densities, and velocities in the intact loop hot leg and cold leg and the broken loop hot leg and cold leg. In the intact loop hot leg (Figures a12 to a14), the two flows compared well during blowdown/refill, and the results were consistent. That is, all three parameters compare well. After 40 s, however, the calculated velocity was much larger than the measured velocity (Figure a14). This was the time reflood began in the test, and the measured hot leg density (Figure a13) indicated the presence of entrained liquid in the hot leg. The predicted density, however, did not. The measured velocity is a fluid mixture velocity and the entrainment in the test reduced the measured fluid mixture velocity relative to the prediction. The effect of the accumulator nitrogen was seen starting at 50 s. In the test, the nitrogen injection rapidly reduced the fluid flow through the intact loop. A similar but weaker effect was calculated because Westinghouse's modeling of accumulator nitrogen injection results in the nitrogen entering the system more gradually. This reduces the effects of the insurge of nitrogen.

Intact loop cold leg comparisons are shown in Figures a15 to a20. Because the test spool piece was located upstream of the measurement point, two comparisons for each parameter were provided: one with consistent locations at the measurement point, and one where the predicted value was taken from the injection location. From 0 to 15 s, the fluid mass flow rate, density, and velocity were consistent and agreed well. After 15 s, the calculated density increased because the accumulator came on early due to the more rapid depressurization calculated by WCOBRA/TRAC. After 20 s, the measured density had large variations as the injected water intermittently backed-up through the spool piece. Westinghouse concluded similar effects were not calculated due to the simple drift-flux model used in 1-D components. This simple formulation does not allow WCOBRA/TRAC to model the complex flow

regimes in the intact loop cold leg needed to calculate the backing up of the accumulator water. INEL notes that not calculating this phenomenon does not prevent the code from adequately calculating the LOFT L2-3 system response. At 50 s (see Figures a19/a20), accumulator nitrogen affected both the test and calculated results with the same type of differences as noted for the intact hot leg.

The broken loop hot leg fluid mass flow rate, density, and velocity are shown in Figures a21 to a23. The mass flow compared reasonably well, but the density was underpredicted, and the velocity was overpredicted. Westinghouse noted this is an example of a compensating error. The lower density was due to the rapid depletion of mass at the hot leg nozzle elevation. Figures a24 and a25 show the predicted void fraction at the hot leg nozzle elevation and the elevation just above the upper core plate. More liquid was stored at the bottom of the upper plenum relative to that at the hot leg nozzle elevation. Westinghouse attributed this behavior to the larger upper plenum in LOFT, 6 ft from the core plate to the hot leg elevation, compared to 3 ft for the same distance in a PWR. With a larger upper plenum volume, upper plenum mass storage is more important in LOFT than in a PWR where the smaller upper plenum would promote more entrainment into the hot legs. The difference between the code and the test results was attributed to the inability of the WCOBRA/TRAC nodalization to predict with sufficient accuracy the details of the LOFT upper plenum response (See Reference 214, Attachment 1).

Calculated and measured broken loop cold leg fluid mass flow rate, density, and velocity were compared in Figures a26 to a29. The three parameters compare well, and the results were consistent with each other. The predicted fluid mass flow and density had more ECC bypass than the test data after 25 s. Westinghouse again noted accumulator nitrogen effects in both the test data and the prediction after 50 s. In the test data, accumulator nitrogen increased the fluid velocity, while the weaker nitrogen effect in the calculated results allowed condensation to continue and WCOBRA/TRAC calculated reverse flow at the break.

In evaluating the overall prediction of LOFT Test L2-3, Westinghouse found the intact loop and break flows were predicted well. Therefore, Westinghouse concluded the core flows were also predicted well by WCOBRA/TRAC.

As seen in Figure a1, core heat transfer was calculated well because the predicted PCT compared well with the data. Because both the core flow and the heat transfer were predicted well, Westinghouse concluded there was no evidence of significant compensating errors.

Comparison of the WCOBRA/TRAC analysis of LOFT L2-5 analysis with the test data found the PCT was underpredicted for this test. Westinghouse's evaluation of the predicted results led them to conclude that the PCT underprediction was due to several factors: underpredicting the broken loop cold leg flow (Figure b26) early in time and overpredicting the broken loop cold leg flow later in time. INEL notes that the overprediction of the broken loop hot leg flow early in time (Figure b21) would also impact the early PCT differences found in Figure b1. The early underprediction coupled with a good prediction of the intact loop cold leg flow (Figure b26) allowed the predicted core flow to become positive as seen in Figure b2. This arrested the initial cladding heatup prematurely at 5 s (Figure b1). Overprediction of the broken cold leg flow after 5 s, and a good prediction of intact loop cold leg flow at that time resulted in the core flow becoming negative. This higher calculated break flow also contributed to the cladding temperatures being underpredicted for this test.

INEL Review

Based on the comparisons presented by Westinghouse and reviewed by the INEL, the INEL agrees that the evidence presented supports the conclusion that there are no significant compensating errors in the LOFT Test L2-3 analysis. This is based on the good comparisons of loop and break flows and core heat transfer presented by Westinghouse. INEL also agrees that the L2-5 predicted results are not due to significant compensating errors. Rather, overprediction of core heat transfer resulted from overpredicting the core flow both positive and negative. This is the expected result for these conditions.

11.3.2 SCTF Test 619 Analysis

Figures c1 to c15 show measured and predicted cladding temperatures. The figures show that the modeled rods began to cool almost immediately after

the test started, while the measured data had a 10 s heatup period. Westinghouse concluded this implied early onset of entrainment for the prediction relative to the test. With this exception, the comparisons show the cooldown rate was adequately or conservatively predicted. Vapor temperatures (Figures c16/c17) were also predicted slightly low at the start of the test, consistent with the early entrainment.

Comparison of the calculated and measured void fractions in the core show the code underpredicted the void fraction low in the bundle but overpredicted it high in the bundle (see Figures c18 to c28). These comparisons also show the code calculated sharp changes in void fraction at various times as the quench front moved up the bundle. The test data, however, had an initial drop at the start of the test followed by a gradual transition to lower void fraction. Also, both the test and code results indicate the radial mass distribution was very uniform (Figures c20 and c24).

During a discussion with Westinghouse, INEL noted that the initial drop in void fraction does not seem consistent with the initial cladding heat up and the vapor superheat comparisons caused by delayed entrainment in the test. In Reference 214, Attachment 1, Westinghouse stated the delayed entrainment in the test was supported by the cladding temperature and vapor temperature measurements in the test, but the delayed entrainment was less clear in the void fraction plots (Figures c21 to c24) where there is a drop in void fraction almost immediately in the test data. Westinghouse attributed this difference to the fact that the test void fractions are inferred from differential pressure measurements, which will also pick up pressure drops due to friction from flowing steam.

Comparing cladding temperature to void fraction (Figures c29 (test data) and c30 (WCOBRA/TRAC)), Westinghouse found that changes in void fraction had only a small effect on the cladding cooldown rate until rod quench occurred or was calculated. Based on this, Westinghouse concluded the WCOBRA/TRAC heat transfer model is a relatively weak function of void fraction.

Westinghouse analyzed the liquid mass distribution in the test. The bundle mass comparison found WCOBRA/TRAC underpredicted the bundle mass slightly (Figure c31), indicating higher entrainment consistent with the

FLECHT-SEASET results discussed earlier. Baffle mass and hot leg mass were also underpredicted (Figures c32/c34), but the upper plenum mass was overpredicted (Figure c33). Based on a mass balance analysis, Westinghouse concluded that only the test liquid distribution within the vessel could be considered reliable. An overall test mass balance could not be achieved due to test steam and liquid flow measurement difficulties.

As discussed earlier, Westinghouse found the calculated results indicated early onset of entrainment. This was attributed to differences in the initial water temperature due to differences in the actual and modeled injection locations for the ECC water. The modeled injection location resulted in water with a higher temperature entering the core relative to the test data. A sensitivity run was made where the initial water temperature was reduced to that indicated in test measurements. This resulted in delayed steam generation/entrainment and a short period of heat up being calculated (see Figures c42 to c49 and c5 to c13).

INEL Review

INEL concluded Westinghouse's SCTF analysis does not show any evidence of significant compensating errors. With the exception of the timing of entrainment at the start of the test, void fraction comparisons were in good agreement. Heat transfer was also calculated reasonably well. Differences in vessel liquid distributions were noted, but no evidence of significant compensating errors was indicated in the comparisons.

11.3.3 CCTF Test 62 Analysis

CCTF Test 62 was the final test analyzed for compensating errors. Comparison of predicted and measured cladding temperatures found WCOBRA/TRAC significantly overpredicted the PCT for this test (Figures d3 to d7). Vapor temperature comparisons (d8 and d9) were in good agreement prior to the test T/Cs rewetting.

Comparison of predicted and measured core void fractions indicated the same trends as noted for SCTF:

1. The code results underpredicted the void fraction low in the vessel, and overpredicted the void fraction higher in the vessel (Figures d10 to d15).
2. The test had an initial drop followed by gradual transition to lower void fractions, while the calculated results had a fairly sharp drop to lower void fractions as the quench front moved up the bundle.
3. As the void fraction changes, both the test and calculated cladding cooldown rates indicated little sensitivity to the void fraction changes until rod quenched occurred or was calculated. Westinghouse noted this supports the weak relationship between void fraction and heat transfer in the film boiling regime.

Void fraction in the upper plenum is overpredicted (Figure d16), and the bundle mass is underpredicted (Figure d17) due to excess core entrainment and steam binding.

Test 62 was a gravity reflood test. This means the flooding rate was dependent on downcomer level versus core level and loop pressure drop. Figures d20 and d21 show that good agreement was achieved between the downcomer and core pressure drops. Overall pressure drops in the intact loop and broken loop (Figures d22 and d29) also were in reasonable agreement. Comparisons of the component pressure drops through both loops found some were overpredicted and some underpredicted. This does not necessarily indicate a compensating error because it is not always possible to match exactly a facility nodalization with measurement locations. Also, the areas where pressure drops were underpredicted/overpredicted constitute only a small part of the overall loop pressure drop (for example, see Figure d28).

The intact loop hot leg steam flow was slightly higher as were the steam velocity and density, which indicates consistency in the predicted parameters (Figures d34 to d36). The intact loop hot leg liquid flow was overpredicted (Figure d37) from 100 to 200 s indicating greater entrainment in the calculation. The total intact loop hot leg flow was also overpredicted

(Figure d38) consistent with the overprediction of the steam and liquid flows.

In the intact loop cold leg, both the steam and liquid flows were overpredicted (Figures d39 and d40). However, Westinghouse suspects a measurement problem with the test liquid flow because the measured liquid flow was less than the reported pumped ECC injection flow. In the intact loop, approximately 67% of the hot leg steam flow was condensed by the ECC water in test, and approximately 57% of the steam flow was condensed in the WCOBRA/TRAC calculation. See Figures d34 and d39

For the broken loop hot leg, significant liquid entrainment was calculated prior to 200 s and little was measured (Figure d42). The predicted steam flow was lower prior to 200 s due to greater steam binding in the calculation. Comparison of the broken loop hot leg total flow (Figure d44) with the steam flow in the broken loop cold leg (Figure d45) found all water was vaporized in the steam generator because the two flow rates were the same. This was true for both the test and the calculation.

INEL Review

Westinghouse concluded the following items with which the INEL agrees. The comparisons for CCTF Test 62 indicate consistent calculated results. Higher predicted entrainment led to greater steam binding and less bundle mass relative to the test data. As expected, these resulted in overpredicting the measured cladding temperatures.

This type of result is handled in two ways by Westinghouse. First, it causes a conservative bias in WCOBRA/TRAC plant calculations, and Westinghouse is not taking credit for this conservative bias in the uncertainty evaluation. Second, because the excess entrainment in gravity reflood tests overestimates steam binding, this can mask WCOBRA/TRAC's tendency to overpredict heat transfer due to the higher entrainment, a compensating error (see Westinghouse discussion on compensating errors from the February 1996 full ACRS Committee meeting). Westinghouse accounts for this by not including the gravity reflood data in the heat transfer distributions. Because WCOBRA/TRAC overpredicted PCT in the CCTF gravity reflood simulations, multipliers greater than 1.0

would be calculated for those tests. By excluding that data, the final uncertainty distribution is more conservative.

11.4 Westinghouse Conclusions from the Compensating Error Report

The following is a summary of Westinghouse's conclusions drawn from the compensating error analysis (CER, Section 3, and Reference 214, Attachment 1):

1. Non-equilibrium steam conditions are calculated consistent with conditions measured in a number of experiments. While differences exist between the calculated and measured values, these differences are treated through the heat flux uncertainty used in the overall uncertainty analysis.
2. INEL high pressure film boiling test comparisons showed the predicted heat flux is dominated by forced convection to steam. Droplet contact heat transfer results in overprediction of heat transfer at low Reynolds numbers. However, during blowdown, Reynolds numbers are larger than those where the droplet contact heat transfer becomes too large. Figures a7 and b7 show droplet contact heat transfer during blowdown is small.
3. Comparisons of predicted heat transfer and void fraction for high pressure (INEL tests) and reflood (FLECHT-SEASET and SCTF) tests indicate similar relationships between the calculations and the experiments. Compensating error in the G-1 blowdown test analyses was identified where the rewet temperature is overpredicted but the film boiling heat transfer is underpredicted. This compensating error was accounted for by modifying the blowdown heat transfer uncertainty distribution and using a lower bound rewet temperature in the hot spot cladding temperature calculation.
4. When heat transfer was not predicted well in blowdown integral effects tests, it was due to misprediction of the break flow and resulting core flow, not significant compensating errors in the

heat transfer model. Break flow is one of the key variables ranged in the uncertainty analysis.

5. When heat transfer was not predicted well in reflood tests it was due to excess core entrainment and underprediction of heat transfer to the vapor just above the quench front. These factors combined to produce low vapor temperature, which increased the heat transfer at higher elevations. Excess entrainment was predicted for both forced and gravity reflood tests. Excess entrainment and lower convective heat transfer in forced reflood tests led to higher heat transfer that is accounted for by ranging the heat flux multiplier in the uncertainty analysis. In gravity reflood tests, the higher entrainment also results in lower reflood rates and a conservative bias in the WCOBRA/TRAC simulations.
6. Validation of the CCFL model first without condensation effects, then with condensation effects, demonstrated significant compensating errors do not exist in the prediction of ECC bypass.
7. Detailed analysis of two LOFT tests and CCTF Test 62 indicate the thermal-hydraulic response of the core to loop and break flow is correct and not the result of significant compensating error.

11.5 Summary of INEL Review

Based on review INEL review of the CER, INEL generally agrees with Westinghouse's conclusions because the evidence provided by Westinghouse supports them. The following list provides the references from the CER to support INEL's judgement (the number corresponds to Westinghouse's list in the previous section). Note Westinghouse Item 2 is discussed separately because of additional INEL comments, and the INEL tests noted in Item 3 are also discussed separately.

1. page 4, Table 1; Figure 9; Figures a4/a5; Figures b4/b5; Figure d8.

3. Except for the INEL tests; pages 25-28; Figures 24 to 34 and Figures 37 to 46; page 136; Figures c29/c30.
4. Section III.b, but particularly: pages 97 and 99; Figures b1-b3, b16, b26.
5. The higher entrainment is supported by page 11, page 14, Figures 8a/8b; page 136, page 170, Figure c31. Lower forced convective heat transfer to the vapor just above the quench front is supported by pages 11/12, pages and pages 19-23, Figures 13-16. Westinghouse's response to Volume 2, question 63, Reference 47, also listed both as reasons for underpredicting the PCT in forced reflood experiments.
6. page 62 and Section 12.1 of this report.
7. page 66; Figures a1-a3, a15, a26; pages 97 and 99; Figures b1-b3, b16, b26; pages 190/191; Figures d20-d22, d29, d38, d44.

In discussing Item 2, Westinghouse noted the INEL high pressure film boiling tests showed the predicted heat flux was dominated by forced convection to steam. In Reference 214, Attachment 1, Westinghouse noted this comment was based comparing the TRAC and the WCOBRA/TRAC predicted heat flux. The TRAC predicted heat flux was much higher due to the larger multiplier on the droplet/wall contact heat transfer model. By using the multiplier from the original reference, WCOBRA/TRAC results compared much better to the data, although they were still high. While the INEL does not see this as clearly as Westinghouse does, the INEL does note that the figures referenced by Westinghouse in Item 2, Figures a7 and b7, do show that the liquid HTC is small during blowdown in the LOFT calculations for L2-3 and L2-5. See Figures a6 and b6 for the corresponding vapor HTCs. Also, page 11 and Figure 15 show similar results for a FLECHT-SEASET reflood test.

The information presented by Westinghouse did identify cases where compensating errors were found. These include:

1. Underprediction of interfacial HTC but overpredicting the interfacial area in 1-D components based on the Northwestern tests, Reference 96.
2. Good broken loop hot leg mass flow predictions in LOFT Tests 12-3 and L2-5, but having the fluid velocity overpredicted and the fluid density underpredicted at that location.
3. The WCOBRA/TRAC results of FLECHT-SEASET Test 31701 raised concerns about compensating errors in the analysis.
4. The comparisons for CCTF Test 62 indicate consistent calculated results. Higher predicted entrainment led to greater steam binding and less bundle mass relative to the test data. As expected, these resulted in overpredicting the measured cladding temperatures. However, because the excess entrainment in gravity reflood tests overestimates steam binding, this can mask WCOBRA/TRAC's tendency to overpredict heat transfer due to the higher entrainment, a compensating error.
5. Overpredicting heat transfer in the INEL film boiling tests.
6. Westinghouse identified some compensating error in the G-1 blowdown test analyses where the rewet temperature is overpredicted but the film boiling heat transfer is underpredicted.

Other code problems include:

7. Overpredicting entrainment and underpredicting heat transfer to the vapor just above the quench front in forced reflood tests.

For Item 1, Westinghouse noted in the CER that the overall condensation efficiency in 1-D components was approximately correct as shown in CQD Figures 15-3-48 and 15-3-49 for the full-scale UPTF tests. Because the overall condensation rate was calculated correctly, Westinghouse concluded the compensating error does not compromise the code's ability to predict the

overall condensation rate in 1-D components. INEL notes Westinghouse's conclusion is supported by the fluid temperature comparisons for both UPTF and the Westinghouse/EPRI 1/3rd-scale steam/water mixing tests as discussed in Sections B.2.4 and B.3.1 of this report. Those comparisons showed the code adequately calculated the fluid temperature as it exited the simulated cold leg.

The INEL does not consider Item 2 a serious problem because the LOFT upper plenum is not typical of a PWR, the problem did not cause serious problems in the L2-3 analysis, and, perhaps most importantly, the break flow is a parameter ranged in the uncertainty evaluation.

Westinghouse dealt with Item 3 by removing Test 31701 data from the reflood heat transfer data base used to determine the reflood heat transfer multipliers.

Item 4 was handled in two ways by Westinghouse. First, excess steam binding results in a conservative bias in WCOBRA/TRAC plant calculations, and Westinghouse is not taking credit for this conservative bias in the uncertainty evaluation. For the compensating error, Westinghouse accounts for this by not including the gravity reflood data in the heat transfer distributions. Because WCOBRA/TRAC overpredicted PCT in the CCTF gravity reflood simulations, multipliers greater than 1.0 would be calculated for those tests. By excluding that data, the final uncertainty distribution is more conservative.

For Items 5 and 7, Westinghouse addressed these problems by ranging the heat flux multiplier in the uncertainty analysis based on the forced reflood tests. Because of the overprediction of heat transfer due to these problems, the average heat transfer multiplier in the uncertainty analysis is less than 1.0. This indicates WCOBRA/TRAC tended to overpredict heat transfer, but use of the multipliers in the uncertainty analysis results in an overall heat transfer penalty.

For Item 6, Westinghouse adequately dealt with the compensating error identified in the G-1 blowdown tests. In References 213 and 214, Attachment 1, Westinghouse noted this compensating error was addressed by

modifying the blowdown cooling HTC uncertainty distribution (to remove the temperature bias in the code/data comparisons) and using a lower bound rewet temperature during HOTSPOT blowdown calculations. The INEL considers this adequate because both modifications dealt with the underlying causes of the compensating errors and resulted in more conservative distributions.

Based on the information discussed above, the INEL concluded that WCOBRA/TRAC does not have any serious compensating errors that would compromise WCOBRA/TRAC's ability to perform realistic analyses of LBLOCAs, or Westinghouse has appropriately accounted for the compensating error in the uncertainty methodology.

12. OTHER TECHNICAL ISSUES

During the review, considerable resources were expended on two issues to ensure Westinghouse modeling in WCOBRA/TRAC was adequate in those areas. They are CCFL modeling and accumulator nitrogen modeling. In addition, the Westinghouse approach to modeling T_{MIN} was reviewed. CCFL modeling is important because of the effect it has on the calculation of ECC bypass, and the effect of accumulator nitrogen is important because of the effect it has on the early reflood hydraulics. The T_{MIN} model is important because of its potential to affect the PCT calculation. These three models are discussed in this section with CCFL modeling discussed first followed by accumulator nitrogen modeling and T_{MIN} .

12.1 WCOBRA/TRAC CCFL Modeling Assessment

The proper calculation of CCFL is important to correctly predicting the PCT in a LBLOCA. The main PWR areas of importance are the downcomer annulus for ECC bypass and the upper core plate (UCP) for fall back of liquid carried out of the core. WCOBRA/TRAC does not use CCFL correlations that have been developed; rather it calculates CCFL directly from the basic code equations and constitutive relationships. Westinghouse's response to Volume 1, question 238, Reference 46, discussed calculation of CCFL with WCOBRA/TRAC in detail, and the discussion in that response is the basis for this section. Responses to other questions are referenced as needed to support the review.

Westinghouse noted that correct calculation of CCFL involves plant or experiment nodalization, wall and interfacial drag models and correlations, entrainment models and correlations, and condensation models and correlations. Regarding nodalization, Westinghouse's approach to representing experimental facilities is to use a nodalization as consistent as possible with the PWR nodalization. In Reference 206, Attachment 6, Westinghouse verified this was the case with CCFL experiments used to assess WCOBRA/TRAC. INEL review of the information found that approximately the same size nodes were used in the experiment analyses as in the PWR analyses.

Wall and interfacial drag models are discussed in CQD Section 3 (for interfacial area) and Section 4 (for wall, drag, and entrainment models). As

discussed in Sections A.2 and A.3 of this report, INEL review of the models found them adequate. The effect of condensation is included through the interfacial area and heat transfer discussed in CQD Section 3 (for interfacial area) and Section 5 (for interfacial HTC). As discussed in Section A.5 of this report, INEL review of the interfacial HTC models found them adequate.

To assess WCOBRA/TRAC's ability to calculate CCFL using the above models, Westinghouse performed a number of analyses:

1. Computational experiments in a pipe modeled with a vessel channel model at 1000 psia. See CQD Section 15-1-2, and Volume 3, question 6, Reference 34.
2. Assessment of CCFL at a perforated plate based on experiments at Northwestern University at 1000, 35, and 14.7 psia.²⁰⁸ See CQD Section 15-1-3, and Volume 3, question 6, Reference 34.
3. Create 1/15th and 1/5th scale ECC bypass experiments. See CQD Section 15-5-5 and Volume 3, question 8, Reference 37.
4. Computational experiments linearly expanding the subscale Creare model to full-scale. This was done to evaluate WCOBRA/TRAC calculated CCFL versus J^* scaling (Wallis scaling, Reference 121), K^* scaling (Kutateladze scaling, Reference 122), and UPTF scaling (Reference 123). Based on the analysis in Volume 1, question 238, Reference 46, WCOBRA/TRAC scales according to J^* and UPTF scaling.
5. UPTF full-scale ECC bypass Test 6, Runs 131, 132, 133, 135, and 136. These tests included subcooled liquid injection. See CQD Section 15-1-6; Volume 4, question 2, Reference 21; and Volume 1, question 238, Reference 46.

The INEL reviewed the comparisons between the WCOBRA/TRAC results and the data or correlation provided by Westinghouse in the references cited. For all cases, conservative results were found (such as the UPTF ECC bypass experiments), or there was excellent agreement between the code results and the data or known correlation.

Westinghouse assessed the potential for fallback from the upper plenum to the core at the UCP in its response to Volume 3, question 11, References 20 and 42. That response showed that little fallback is calculated in PWR analyses or in the CCTF Test 62 simulation, and Westinghouse showed that this response is expected because of the high steam flows calculated at the core exit during reflood. This analysis was done for plants without upper plenum injection (UPI).

Based on the review summarized above, INEL concluded WCOBRA/TRAC's models adequately represent CCFL in the downcomer and at the UCP for plants without UPI.

12.2 Modeling the Effects of Accumulator Nitrogen

The Westinghouse WCOBRA/TRAC code includes a methodology that simulates the effects of nitrogen injection following discharge of the liquid from the accumulators. The contention is that the nitrogen injection into the cold legs following discharge of the liquid causes a pressurization of the annulus which has the potential to force large quantities of liquid into the core producing significant reductions in the peak cladding temperature. Review of the available test data shows that UPTF and CCTF attempted to simulate this effect; however, these tests did not quantify the effect on peak cladding temperature. Achilles Test ISP-25 (Reference 76), however, did model nitrogen injection during reflood. In this test, cladding temperature was initially reduced about 90°F due to the increased steam production. However, the increased steam production then forced additional liquid from the core causing an additional heatup of 300°F. Thus, the effects of the nitrogen injection was to initially reduce temperature but subsequently to further degrade core cooling so that the net effect was to increase PCT.

Westinghouse simulates the nitrogen using steam injection while also terminating condensation in the discharge legs and upper annulus. The effects of the nitrogen are expected to degrade condensation; however, the test data in UPTF Test 27 (MPR-1331) and the Achilles Test ISP-25 did not quantify this effect. Furthermore, based on available test data, particularly the Achilles Test ISP-25, there was no large cooling benefit demonstrated following nitrogen injection. In fact, nitrogen injection degraded cooling performance.

The INEL believes that sufficient test data does not exist to demonstrate that significant pressurization develops in the annulus to cause such a rapid increase in core liquid level and abrupt temperature drop as calculated by the WCOBRA/TRAC code near the time of the first reflood PCT. Such effects were not observed to control peak cladding temperature during the LOFT tests. The results of the UPTF Test 27A showed that a surge of water entered the core due to nitrogen discharge. However, this test did not simulate the duration of the core level surge, the long term effects of nitrogen, nor was the effect on core cooling quantified since the increased steam generation that would occur in the core was also not simulated. Dilution of the steam with nitrogen did occur where the mass fraction of steam in the downcomer was reduced to 10% in 0.3 seconds; however, the effect of the dilution on the rate of condensation was also not measured (Reference 105). In the Achilles Test ISP-25, the surge of water into the core momentarily enhanced core cooling but significantly increased steam generation and caused an excess of carryover into the upper plenum producing a net decrease in downcomer/core liquid inventory. Core cooling was degraded for about 50 seconds following nitrogen discharge until the inventory decrease was recovered by accumulation of emergency core coolant. The Achilles test shows a momentary period of core cooling where the cladding temperature was decreased by 90°F but was offset by a subsequent more severely degraded cooling period where the cladding temperatures increased by 300°F.

In the plant simulations, Westinghouse stated that, because WCOBRA/TRAC cannot accommodate non-condensable gases, steam is artificially injected in the annulus while condensation is terminated on the wall surfaces to simulate the pressurization. It is, therefore, not clear how one determines how much steam to inject to model this effect. It is also not clear that condensation is completely terminated everywhere in the annulus. A mixture of steam and nitrogen will degrade condensation; however, based on the mixing and mass fraction of non-condensibles in the steam, condensation could still occur at a lower rate. The effect of the nitrogen on condensation has not been quantified in the experimental data base so this WCOBRA/TRAC assumption is without experimental substantiation.

Given the concerns regarding the nitrogen injection model, the INEL recommended that Westinghouse simulate Achilles Test ISP-25. Westinghouse

used the WCOBRA/TRAC code to model the nitrogen injection as steam, and the code was employed in the same manner as that used in the plant simulations. Results of the evaluation showed that the cladding temperature response was reasonably predicted; however, it is still not clear why the cladding temperature was reasonably predicted while the downcomer level was overpredicted by one to two feet during the initial portion of the test up to the time of peak cladding temperature.

The WCOBRA/TRAC plant calculations reviewed to date show qualitatively the same effects noted in the Achilles test. There is an initial period of improved heat transfer that cools the core. However, long term the simulated nitrogen injection penalizes the vessel mass resulting in an increase in cladding temperature.

Westinghouse performed an analysis to quantify the effects of the nitrogen injection on peak clad temperature. This evaluation resulted in use of the maximum heat transfer coefficient given in Reference 206, Attachment 2, during reflood in the HOTSPOT analyses. Use of this limit to the heat transfer coefficient minimizes the beneficial effects of the nitrogen injection during reflood since the increased heat transfer realized by the additional coolant forced into the core is not credited. Thus, the beneficial effects of the nitrogen injection are minimized. Also, because the HOTSPOT analyses use WCOBRA/TRAC results as boundary conditions, entrainment of annulus water by the nitrogen subsequently increases PCT so that the detrimental effects of nitrogen injection are retained. With beneficial effects minimized (due to the maximum HTC) and detrimental effects retained (due to the reduction in long term vessel mass) in the nitrogen modeling, and given the reasonable Achilles test prediction, this model is considered to be technically justified.

12.3 EVALUATION OF REWET TEMPERATURE

Rewetting or quenching of a hot surface can be defined as the transition from heat transfer that takes place predominantly through a vapor film covering the surface, as in film boiling, to a regime in which the liquid is in direct contact with a large fraction of the wall such as nucleate boiling. Physically, rewetting occurs as the quench front cools the rod surface to the

rewet temperature just downstream of the quench front. Because of the large temperature gradients near the quench front, axial conduction and the enhanced heat transfer that occurs just downstream of the quench front can play an important role in influencing the rewet temperature. Rewet temperature is also dependent on pressure, mass flux, subcooling, cladding material, geometry, and rod surface conditions.²¹⁹ Gap conductance plays an important role as analytical studies have shown that fuel rods with a significant gap resistance rewet faster than rods with little or no gap resistance. This sensitivity is due to the fact that a lesser amount of heat is transferred to the coolant at the quench front when the fuel rod gap conductance decreases. Thus, fuel rods with low gap conductances can produce rewet velocities that are twice those of rods with very high gap resistances.²²⁰ Surface heat flux is, therefore, an important parameter that influences the rewet temperature.

The importance of the rewet temperature on blowdown behavior is that early rewet of the fuel rod can result in non-conservatively removing the stored energy in the rods. As a result, the PCT during reflood will be reduced since any additional energy in the fuel rod at the start of reflood would not have to be removed during this later phase of the transient. Thus, the blowdown rewet model could have an impact on reflood PCT, and errors in the blowdown rewet model could then propagate into the reflood calculated PCT.

Inspection of a cladding temperature plot that approaches the 95th percentile PCT shows that the clad temperature during blowdown never decreases below about 1400°F. As a consequence, the rewet temperature model has no influence on the 95th percentile at the PCT location. Thus, the model shortcomings, particularly the omission of the rod surface effects enumerated above, have no consequence at the limiting PCT location.

However, because of questions on the Westinghouse T_{MIN} model by the ACRS, the method to determine the blowdown T_{MIN} was modified. Also, as mentioned above, an early rewet during blowdown could reduce the PCT during reflood. Westinghouse modified the T_{MIN} model to be the correlation given in Reference 213. The data base supports a T_{MIN} greater than 1000°F. Use of the correlation results in T_{MIN} values that clearly are a lower bound to the blowdown data base. The effect of this modification was to increase PCT. This lower bound value will be applied to HOTSPOT calculations during

blowdown. This lower bound value will ensure that, for transients with hot spot cladding temperatures approaching best estimate values of T_{MIN} , the hot spot will be prevented from rewetting.

The Westinghouse T_{MIN} model, discussed in CQD Section 6-2-6, ignores the importance of surface effects such as heat flux along with the dependence on gap resistance. In WCOBRA/TRAC, the rewet temperature during reflood is predicted using the same correlation as that during blowdown. Regarding the final reflood quench, comparisons of the calculated quench to gravity reflood data demonstrated that a delayed quench of the rod is predicted. The delayed quench during reflood will result in a conservative prediction of the cladding oxidation so that, at the hot spot location, use of this model during reflood tends to maximize the calculated rod and core wide oxidations. However, prior to calculating the PCT, the potential for early rewet below the PCT location could enhance the heat transfer at the hot spot during reflood. The rewet process produces steam and droplets that are entrained up the hot channel enhancing the fluid conditions at the PCT location. This could result in overpredicting the heat transfer up to the time of PCT because of the fluid hydraulics below the PCT location.

In view of the potential for overpredicting the PCT location heat transfer due to the rewet temperature model, the INEL notes the methodology used to determine the multipliers on the reflood HTC's at the PCT location accounts for the effects of local conditions. Should the model produce high heat transfer coefficients at the hot spot due to rewet induced local fluid condition differences, the HTC multiplier will be lower. Thus, the method to generate the heat transfer multiplier will tend to compensate for the error or bias in rewet temperature.

The blowdown T_{MIN} change and the approach for reflood address the INEL concerns identified above on blowdown and reflood rewet temperature so that the model is recommended for approval.

13. COMPLIANCE WITH 10 CFR 50.46 REQUIREMENTS

This section discusses how Westinghouse's methodology meets the requirements of 10 CFR 50.46. This section of the Code of Federal Regulations describes the acceptance criteria for ECCSs for light water reactors.

Part (a) of the regulations states that:

- (1) ECCS performance must be analyzed with an acceptable evaluation model that includes sufficient supporting justification that the analytical techniques used realistically describes the behavior of the reactor system during a LOCA.
- (2) That comparisons to applicable experimental data must be made.
- (3) Uncertainties in the analysis method and inputs must be identified and assessed so that the uncertainties in the calculated results can be estimated.
- (4) The uncertainty must be accounted for when comparing the calculated ECCS performance to the criteria set forth in Paragraph (b) of 10 CFR 50.46 so that there is a high level of probability that the criteria would not be exceeded.

Westinghouse provided the justification of its methodology in the five volume CQD, responses to NRC questions, and special submittals to the NRC. How Westinghouse meets the above requirements is the main topic of this report. CQD Volume 1 described the WCOBRA/TRAC code, and INEL review of that code is summarized in Section 9.1 of this report and discussed in detail in Appendix A of this report. Based on the code review and Westinghouse's comparisons to over 100 tests described in CQD Volumes 2 and 3, INEL concluded that WCOBRA/TRAC realistically describes the behavior of a reactor system during a LBLOCA. INEL review of Westinghouse's code assessment is summarized in Section 4 of this report and discussed in detail in Appendix B of this report. In Volumes 4 and 5 of the CQD and Reference 58, Westinghouse described its methods for determining the uncertainty of the analysis methods and inputs and applying them to the calculated ECCS performance. INEL review of the uncertainty methodology included reviewing all uncertainty

distributions, response surface generation, and their applications to determining the 95th percentile PCT. That review is discussed in Sections 6 and 9.2 of this report. Review of the uncertainty due to reactor input is discussed in Sections 5 and 8 of this report.

Part (b) of the regulations states the five acceptance criteria for the ECCS. The ECCS must ensure:

- (1) The PCT is less than 2200°F.
- (2) The maximum local cladding oxidation does not exceed 17% of the total cladding thickness prior to oxidation.
- (3) The maximum hydrogen generation shall not exceed 1% of the amount that would be generated if all the cladding surrounding the fuel, except that around the plenum volume, were to react.
- (4) Calculated changes in core geometry shall be such that the core remains amenable to cooling.
- (5) After the successful, initial operation of the ECCS, the calculated core temperature shall be maintained at an acceptably low value and decay heat removed for the extended period of time required by the long lived radioactivity in the core.

Westinghouse's realistic LBLOCA methodology meets these criteria as follows:

- (1) Westinghouse's method of determining the 95th percentile PCT is summarized in Section 6 of this report.
- (2) To determine the maximum calculated local oxidation, Westinghouse uses HOTSPOT calculations as discussed in Reference 214, Attachment 12. In this case, the thermal-hydraulic boundary conditions for a WCOBRA/TRAC analysis where the calculated PCT exceeds the 95th percentile PCT are input into HOTSPOT. To account for uncertainties due to turnaround time, cladding

cooldown rate, and quench time, Westinghouse stretches the HOTSPOT transient in time to account for the estimated uncertainties in these areas. The time factor applied stretches the HOTSPOT calculation by approximately 2σ . These HOTSPOT calculations are performed with the burst option off and on (because of the importance of two-side oxidation to the local oxidation calculation) and the larger value selected (Reference 214, Attachment 12). The 95th percentile of the local cladding oxidation results are used to compare to Criterion 2 of 10 CFR 50.46 (see Reference 214, Attachment 12).

- (3) Determination of the maximum core wide hydrogen generation is done using boundary conditions from the same WCOBRA/TRAC analysis that is used for Criterion 2 (Reference 214, Attachment 12). Westinghouse provided additional information on the core wide hydrogen generation calculation in Reference 214, Attachment 12. To account for uncertainties due to turnaround time, cladding cooldown rate, and quench time, Westinghouse stretches the HOTSPOT transient at a 2σ level to account for the estimated uncertainties in these areas. Because the HOTSPOT model is a local model, Westinghouse uses it to estimate the average local oxidation up the rod with the time shift applied. Because not all rods burst, the HOTSPOT model is run with the burst option off for non-burst rods and with the burst option on for burst rods at the burst location (Reference 214, Attachment 12). The peak HOTSPOT average local oxidation result is used with the peak local oxidation from the WCOBRA/TRAC run as a multiplier on the average oxidation of the full HA rod from WCOBRA/TRAC to account for the time shift on the full rod average oxidation. To get the core wide hydrogen generation, Westinghouse assumes the entire core reacts with the adjusted average oxidation of the HA rod, but takes into account power differences based on bounding or actual rod census data.

The multiplier Westinghouse uses is based on the peak local averages from HOTSPOT analyses and the WCOBRA/TRAC HA rod. The average is used for the core wide hydrogen generation criterion because the uncertainties in the full rod average oxidation for

all the rods in the core will tend to cancel due to random local variations. Westinghouse still considers the core wide calculation done at a 95% probability level because: (a) the thermal-hydraulic transient used in the oxidation calculation results in a PCT greater than the 95th percentile PCT and (b) the time shift is done at approximately a 2σ level.

If the above procedure results in a core wide hydrogen generation rate greater than the 1% limit, Westinghouse identified several options available to adjust the core wide oxidation calculation procedure outlined above and reduce the calculated hydrogen generation rate. These options still result in a 95th percentile calculation. See Reference 214, Attachment 12. In Reference 214, List III, Item 5, Westinghouse committed to identifying in the licensing submittal or the engineering report which of the options described in its response to Volume 2, question 62, Reference 214 (Attachment 12) were used in the calculation of cladding core wide oxidation.

- (4) Westinghouse assumes the coolable geometry criterion is met when PCT and oxidation criteria are met.
- (5) Westinghouse meets the long term cooling criterion using methods based on WCAP-8339 and WCAP-8471. These reports were reviewed and approved by the NRC (see Reference 81). They noted that use of the realistic LBLOCA methodology does not affect the methods described in those reports. It is noted however, that Westinghouse's response to Volume 5, question 53, Reference 51 stated that the above WCAP reports were applicable only to current operating plants.

INEL review of the PCT methodology found it adequate to meet NRC requirements of realistic LBLOCA analyses. As stated earlier, Westinghouse's methods for determining the 95th percentile PCT were the subject of the review summarized in this report and discussed in a number of sections.

INEL reviewed the oxidation methodology proposed by Westinghouse to account for uncertainties in the turnaround time, cooldown rate, and quench time. The affect of turnaround time, cooldown rate, and quench time was to shorten the calculated transient relative to the data. The use of a time stretching technique is considered adequate to address these issues because it stretches the time adjusted transient relative to the base transient. Additional conservatism is included with the application of approximately a 2σ time stretch and a thermal-hydraulic transient that results in a PCT greater than the 95th percentile PCT.

For the local oxidation calculation, the 95th percentile cladding oxidation result from a HOTSPOT analysis that includes two-side oxidation is compared to the 17% limit in Criterion 2. INEL considers this adequate because a 95th percentile calculation is compared to the Criterion 2 limit.

For the core wide hydrogen generation criterion, Westinghouse performs the analysis as discussed above. Westinghouse's approach (use of average rather than 95th percentile results) is considered adequate because it is applied to a large population of rods. As Westinghouse noted, in this situation, random variations cancel rather than add. However, Westinghouse still applies a conservative time shift (2σ level) and thermal-hydraulic transient. Because the thermal-hydraulic transient leads to a PCT that is greater than the 95th percentile PCT, Westinghouse always applies a worst case transient that has less than 5% probability of occurring. Based on the information from Westinghouse, INEL considers Westinghouse's approach adequate.

Based on this, INEL concluded that Westinghouse adequately addressed the uncertainties associated with its methodology for meeting Criteria 2 and 3. For Criterion 2, a conservative time shift and thermal-hydraulic transient are used. A 95th percentile calculation is compared to the 17% limit. For Criterion 3, a conservative time shift and thermal-hydraulic transient are also used. Westinghouse noted that use of average values to adjust the full HA rod oxidation to account for the time shift is appropriate because of the large population of rods considered in the whole core criterion.

Regarding the options outlined by Westinghouse in Reference 214, Attachment 12, to adjust the core wide hydrogen generation calculation if the 1% limit is exceeded, the INEL considers the options appropriate. First, none of the options affect the arguments regarding the 95th percentile calculation. That is, a transient with PCT greater than the 95th percentile PCT is always used and the conservative time stretch applied. Second, the options basically involve ways of providing a more accurate estimate of the core wide hydrogen generation rate rather than the bounding type of analysis discussed in the general procedure. Therefore, the INEL recommends the options be found acceptable for use in Westinghouse's realistic methodology. However, when the options are applied, INEL recommends that Westinghouse identify in the plant specific submittal which ones were used.

For the coolable geometry criterion, INEL agrees that meeting Criteria 1 and 2 ensures that a coolable core geometry was maintained. In meeting the PCT criterion, Westinghouse ensures that changes in core geometry due to the LBLOCA transient (for example, cladding swelling and burst and LOCA loads) do not prevent adequate core cooling as evidenced by the highest calculated PCT. This is consistent with 10 CFR 50.46, Appendix K, type of Evaluation Models and use of a realistic LBLOCA methodology for the PCT and oxidation calculation would not change this.

The INEL agrees that long term cooling methods are independent of the methodology used to determine the reactor system response to the initial part of the LBLOCA. Therefore, previously approved long term methods in WCAP-8339 and WCAP-8471 are still applicable. As discussed above, Westinghouse's response to Volume 5, question 53, Reference 51 stated that the above WCAP reports were applicable only to current operating plants. INEL also notes this restricts the review of WCOBRA/TRAC to the initial part of the LBLOCA, and does not make a judgement on the applicability of WCOBRA/TRAC to long term cooling analyses for three- or four-loop plants with cold leg ECC injection.

Based on the above, the INEL concluded that Westinghouse has met Part (a) and has in place methods adequate to show compliance to the five criteria of Part (b) of 10 CFR 50.46. This conclusion holds for the Westinghouse plants addressed in this review: three- and four-loop plants with cold leg injection.

14. CONCLUSIONS

The realistic LBLOCA methodology submittal by Westinghouse was reviewed to determine its compliance with 10 CFR 50.46, NRC guidance in RG 1.157, and the CSAU methodology. Based on the INEL review of the information provided by Westinghouse in WCAP-12945-P, responses to NRC questions, and special submittals, the INEL recommends the Westinghouse realistic methodology be approved subject to certain suggested restrictions. This recommended approval is for LBLOCA analyses in Westinghouse three- and four-loop plants with cold leg ECC injection. The suggested restrictions include:

1. Approval of Westinghouse's methodology depends on the time step sizes used to show small mass and energy errors and PWR time step convergence studies (see Volume 4, question 50, Reference 40). If the time step sizes used in the methodology change, Westinghouse should justify results similar to those identified above are obtained with the new time step scheme.

In addition, the following review limits are noted:

1. Section 13 of this report discussed Westinghouse's methods for meeting the five criteria listed in Part b of 10 CFR 50.46. Westinghouse's response to Volume 5, question 53, Reference 51, noted AP600 long term cooling issues would be addressed separately as part of AP600 licensing. Therefore, this report did not review any information or reach any conclusions relating to AP600 long term cooling. Also, because previously approved methods are used to analyze long term cooling for three- and four-loop plants with cold leg ECC injection, INEL also notes this restricts the review of WCOBRA/TRAC to the initial part of the LBLOCA. No judgement was made on the applicability of WCOBRA/TRAC to long term cooling analyses to three- or four-loop plants with cold leg ECC injection.
2. While some of the review documented in this report applies to the AP600, no conclusions on the implementation of the Westinghouse realistic LBLOCA methodology to the AP600 are possible until the separate AP600 applicability study is completed.

3. Application of the Westinghouse methodology and WCOBRA/TRAC to small-break LOCA was not considered in this review.

During the course of the review Westinghouse agreed/committed to the following items:

1. Based on the NRU results, there is some uncertainty in the transient rod internal pressure (RIP) calculation that will affect the burst temperature criterion in WCOBRA/TRAC analyses. Westinghouse's uncertainty methodology adequately accounts for the uncertainty in transient RIP for local effects. Westinghouse also calculates HA rod burst in the full WCOBRA/TRAC analyses called for in its methodology. If WCOBRA/TRAC calculates a HA rod reflood PCI greater than 1600°F but not rod burst, Westinghouse in Reference 214, List II, Item 2 committed to increasing the initial RIP in the WCOBRA/TRAC HA rod until burst is calculated and choosing the more limiting of the burst and non-burst cases. This will adequately account for transient RIP uncertainties and their effect on rod burst in the WCOBRA/TRAC runs.
2. On CQD page 7-24, Westinghouse stated the fuel pellet thermal expansion model in MATPRO-11, Revision 1, Reference 176, was simplified by omitting the corrections for molten fuel and mixed oxide (Pu). In Reference 214, List II, Item 6, Westinghouse committed to resubmitting the relevant WCOBRA/TRAC models for NRC review if the code will be used to analyze US licensed plants with molten fuel or mixed oxides.
3. As part of the methodology, Westinghouse agreed in Attachment 5, Reference 214, to verify the normality assumption for the initial condition uncertainty distribution on a plant specific basis.
4. In the uncertainty methodology, a number of assumptions for distributions were supported using plant specific data; therefore, in Reference 214, Attachment 5, and Reference 215, Attachments 1 and 2, Westinghouse agreed to verify the following assumptions on a plant specific basis:

- a. Superposition validation data points are normally distributed, with constant variance, around a straight line. The normality must be checked for each phase of the accident for each plant.
 - b. HOTSPOT PCTs are normally distributed. This must be checked at each point where the HOTSPOT PCT is varied in a Monte Carlo sample: the points used to build the response surface for the HOTSPOT standard deviation (σ_{scf}) and the validation points.
 - c. Response surface for σ_{scf} is accurate or conservative. This should be checked by comparing the response surface estimate with the Monte Carlo standard deviation at each validation point. The response surface method should not severely underestimate any standard deviation.
5. The distributions corresponding to WCOBRA/TRAC uncertainty based on experiments ($\sigma_{\text{WC/T}}$) and the uncertainty due to experimental data scatter (σ_{2p}) will be checked for normality if the code is modified or the assessment data base changes. See Reference 214, List III, Item 2.
 6. Based on Reference 214, Attachment 7, the analysis to determine the uncertainty distributions for accumulator and SI temperatures uses plant operating data and/or plant Technical Specifications. Therefore, this analysis must be performed for each plant.
 7. Westinghouse, in Reference 214, List II, Item 8, committed to not changing the value and range of the broken loop cold leg nozzle loss coefficient for plant specific applications. Also, the values developed apply only to LBLOCA and must be justified for other applications.
 8. Westinghouse, in Reference 214, Attachment 9, gave additional explanation on its use of the full Method of Characteristics model for each time step in the code implementation of choked flow. In the above reference, Westinghouse committed to include the information in the CQD.
 9. Westinghouse noted that the choked flow solution is implemented in the pressure solution of the code rather than in the back substitution step

after solving the pressure equation. This results in a smoother pressure and flow response in the code. In Reference 214, Attachment 9, Westinghouse committed to include this information in the CQD.

10. Westinghouse, in Reference 214, List II, Item 10, committed to use the multiplier given in Reference 214, Attachment 4, to account for rod-to-rod radiation effects in the heat transfer multiplier data base.
11. In Reference 214, List III, Item 5, Westinghouse committed to identifying in the licensing submittal or the engineering report which of the options described in its response to Volume 2, question 62, Reference 214 (Attachment 12) were used in the calculation of cladding core wide oxidation if the 1% limit is exceeded.

Other review items include:

1. The INEL notes that the Westinghouse response in Reference 206, Attachment 5, derived the expressions for the shear stress to the wall and to the vapor shown in CQD Eqns. 6-120 and 6-121. Westinghouse concluded that the wall shear stress equation used the incorrect friction factor. To assess the effect, Westinghouse reevaluated FLECHT-SEASET Test 31805 with a corrected version of WCOBRA/TRAC. There was little impact on the PCT, and the results from the corrected code version had slightly later quench times. Westinghouse concluded the effect was small, and the INEL agrees. Therefore, Westinghouse proposed that the error be tracked and corrected when other changes to the code are required.
2. Appendix D of this report gives a detailed review of the WCOBRA/TRAC DFFB model. While a number of concerns were noted in Appendix D, the INEL considered the overall model adequate because of conservatism in the model and the HTC ranging in the uncertainty evaluation. However, because of the potential for changes in one part of the DFFB model to affect the performance of the other parts of the model, the INEL would like to recommend the NRC Staff review the entire DFFB model should one part of the model be changed by Westinghouse in the future.

15. REFERENCES

1. Westinghouse Electric Corporation, Energy Systems Business Unit, Code Qualification Document for Best Estimate LOCA Analysis, Volumes 1 (Rev. 1) to 5, WCAP-12945-P, June 1992 to June 1993.
2. M. J. Thurgood, et al., COBRA/TRAC - A Thermal-Hydraulics Code for Transient Analysis of Nuclear Reactor Vessels and Primary Coolant Systems, Volume 1 to 5, NUREG/CR-3046, PNL-4385, March 1983.
3. F. Orr, USNRC, memo to T. E. Collins, USNRC, "Meeting Summary - Westinghouse Best Estimate LBLOCA Analysis Methodology, January 26/27, 1994," April 13, 1994. (RAIs on Vol 1 to 3)
4. T. E. Collins, USNRC, letter to N. J. Liparulo, Westinghouse, "Request for Additional Information Regarding WCAP-12945-P," June 15, 1994.
5. T. E. Collins, USNRC, letter to N. J. Liparulo, Westinghouse, "Request for Additional Information, Regrading WCAP-12945-P, Enclosure 3," April 21, 1994.
6. F. Orr, USNRC, letter to M. Young, Westinghouse, February 9, 1995.
7. S. M. Bajorek, Westinghouse, letter to C. P. Fineman, INEL, ET-NSASD-MYY-93-70, July 14, 1993 (Submittal A).
8. S. M. Bajorek, Westinghouse, letter to C. P. Fineman, INEL, ET-NSASD-MYY-93-115, December 1, 1993 (Submittal B).
9. S. M. Bajorek, Westinghouse, letter to C. P. Fineman, INEL, ET-NSASD-MYY-94-15, February 21, 1994 (Submittal C).
10. M. Y. Young, Westinghouse, letter to C. P. Fineman, INEL, NTD-NSA-BELOCA-94-022, April 13, 1994 (Submittal D).
11. S. M. Bajorek, Westinghouse, letter to C. P. Fineman, INEL, NTD-NSA-MYY-94-25, May 11, 1994 (Submittal E).
12. S. M. Bajorek, Westinghouse, letter to C. P. Fineman, INEL, NTD-NSA-MYY-94-28, June 7, 1994 (Submittal F).
13. S. M. Bajorek, Westinghouse, letter to C. P. Fineman, INEL, NTD-NSA-MYY-94-31, June 23, 1994 (Submittal G).
14. S. M. Bajorek, Westinghouse, letter to C. P. Fineman, INEL, NTD-NSA-MYY-94-32, June 23, 1994 (Submittal H).
15. M. Y. Young, Westinghouse, letter to C. P. Fineman, INEL, NTD-NSA-MYY-94-35, July 14, 1994 (Submittal I).
16. M. Y. Young, Westinghouse, letter to C. P. Fineman, INEL, NTD-NSA-MYY-94-39, August 3, 1994 (Submittal J).
17. S. M. Bajorek, Westinghouse, letter to C. P. Fineman, INEL, NTD-NSA-MYY-94-46, August 23, 1994 (Submittal K).

18. S. M. Bajorek, Westinghouse, letter to C. P. Fineman, INEL, NTD-NSA-SAI-94-365, September 8, 1994 (Submittal L).
19. M. Y. Young, Westinghouse, letter to C. P. Fineman, INEL, NTD-NSA-MYY-94-48, September 22, 1994 (Submittal M).
20. S. M. Bajorek, Westinghouse, letter to C. P. Fineman, INEL, NTD-NSA-MYY-94-50, October 3, 1994 (Submittal N).
21. S. M. Bajorek, Westinghouse, letter to C. P. Fineman, INEL, NTD-NSA-MYY-94-54, October 17, 1994 (Submittal O).
22. S. M. Bajorek, Westinghouse, letter to C. P. Fineman, INEL, NTD-NSA-MYY-94-55, October 17, 1994 (Submittal P).
23. S. M. Bajorek, Westinghouse, letter to C. P. Fineman, INEL, NTD-NSA-MYY-94-56, October 31, (Submittal Q).
24. S. M. Bajorek, Westinghouse, letter to C. P. Fineman, INEL, NTD-NSA-MYY-94-57, October 31, 1994 (Submittal R).
25. S. M. Bajorek, Westinghouse, letter to C. P. Fineman, INEL, NTD-NSA-MYY-94-58, October 31, 1994 (Submittal S).
26. S. M. Bajorek, Westinghouse, letter to C. P. Fineman, INEL, NTD-NSA-MYY-94-59, October 31, 1994 (Submittal T).
27. S. M. Bajorek, Westinghouse, letter to C. P. Fineman, INEL, NTD-NSA-MYY-94-65, November 11, 1994 (Submittal U).
28. S. M. Bajorek, Westinghouse, letter to C. P. Fineman, INEL, NTD-NSA-MYY-94-67, November 28, 1994 (Submittal V).
29. S. M. Bajorek, Westinghouse, letter to C. P. Fineman, INEL, NTD-NSA-MYY-95-1, January 11, 1995 (Submittal W).
30. S. M. Bajorek, Westinghouse, letter to C. P. Fineman, INEL, NTD-NSA-SAI-95-25, January 16, 1995 (Submittal X).
31. S. M. Bajorek, Westinghouse, letter to C. P. Fineman, INEL, NTD-NSA-MYY-95-5, March 6, 1995 (Submittal Y).
32. S. M. Bajorek, Westinghouse, letter to C. P. Fineman, INEL, NTD-NSA-MYY-95-7, March 16, 1995 (Submittal Z).
33. S. M. Bajorek, Westinghouse, letter to C. P. Fineman, INEL, NTD-NSA-MYY-95-8, March 24, 1995 (Submittal AA).
34. S. M. Bajorek, Westinghouse, letter to C. P. Fineman, INEL, NTD-NSA-MYY-95-9, March 31, 1995 (Submittal BB).
35. S. M. Bajorek, Westinghouse, letter to C. P. Fineman, INEL, NTD-NSA-MYY-95-10, April 7, 1995 (Submittal CC).

36. S. M. Bajorek, Westinghouse, letter to C. P. Fineman, INEL, NTD-NSA-MYY-95-11, April 13, 1995 (Submittal DD).
37. S. M. Bajorek, Westinghouse, letter to C. P. Fineman, INEL, NTD-NSA-MYY-95-12, April 21, 1995 (Submittal EE).
38. S. M. Bajorek, Westinghouse, letter to C. P. Fineman, INEL, NTD-NSA-MYY-95-13, April 28, 1995 (Submittal FF).
39. S. M. Bajorek, Westinghouse, letter to C. P. Fineman, INEL, NTD-NSA-MYY-95-14, May 5, 1995 (Submittal GG).
40. S. M. Bajorek, Westinghouse, letter to C. P. Fineman, INEL, NTD-NSA-MYY-95-15, May 12, 1995 (Submittal HH).
41. S. M. Bajorek, Westinghouse, letter to C. P. Fineman, INEL, NTD-NSA-MYY-95-16, May 19, 1995 (Submittal II).
42. S. M. Bajorek, Westinghouse, letter to C. P. Fineman, INEL, NTD-NSA-MYY-95-17, May 26, 1995 (Submittal JJ).
43. S. M. Bajorek, Westinghouse, letter to C. P. Fineman, INEL, NTD-NSA-MYY-95-19, June 9, 1995 (Submittal KK).
44. S. M. Bajorek, Westinghouse, letter to C. P. Fineman, INEL, NTD-NSA-MYY-95-20, June 15, 1995 (Submittal LL).
45. S. M. Bajorek, Westinghouse, letter to C. P. Fineman, INEL, NTD-NSA-MYY-95-21, June 22, 1995 (Submittal MM).
46. S. M. Bajorek, Westinghouse, letter to C. P. Fineman, INEL, NTD-NSA-MYY-95-22, June 30, 1995 (Submittal OO).
47. S. M. Bajorek, Westinghouse, letter to C. P. Fineman, INEL, NTD-NSA-MYY-95-23, July 7, 1995 (Submittal PP).
48. S. M. Bajorek, Westinghouse, letter to C. P. Fineman, INEL, NTD-NSA-MYY-95-24, July 17, 1995 (Submittal QQ).
49. S. M. Bajorek, Westinghouse, letter to C. P. Fineman, INEL, NTD-NSA-MYY-95-25, August 4, 1995 (Submittal RR).
50. S. M. Bajorek, Westinghouse, letter to C. P. Fineman, INEL, NTD-NSA-MYY-95-26, August 25, 1995 (Submittal SS).
51. S. M. Bajorek, Westinghouse, letter to C. P. Fineman, INEL, NTD-NSA-MYY-95-28, September 22, 1995 (Submittal TT).
52. S. M. Bajorek, Westinghouse, letter to C. P. Fineman, INEL, NTD-NSA-MYY-95-29, November 3, 1995 (Submittal UU).
53. S. M. Bajorek, Westinghouse, letter to C. P. Fineman, INEL, NTD-NSA-MYY-95-30, November 10, 1995 (Submittal VV).

54. N. J. Liparulo, Westinghouse, letter to USNRC Document Control Desk, "Summary of Westinghouse Best-Estimate LOCA Methodology," NTD-NRC-95-4505, July 12, 1995.
55. N. J. Liparulo, Westinghouse, letter to USNRC Document Control Desk, "Presentation Material from WCAP-12945-P Review Status Meeting," NTD-NRC-95-4541, August 29, 1995.
56. N. J. Liparulo, Westinghouse, letter to USNRC Document Control Desk, "Presentation Material from WCAP-12945-P Review Status Meeting," NTD-NRC-95-4560, September 18, 1995.
57. N. J. Liparulo, Westinghouse, letter to USNRC Document Control Desk, "Revised WCAP-12945-P Methodology, Combination of Uncertainties and Compliance with Regulatory Guide 1.157," NTD-NSA-SAI-95-372, September 29, 1995.
58. N. J. Liparulo, Westinghouse, letter to USNRC Document Control Desk, "Revisions to Westinghouse Best-Estimate Uncertainty Methodology," NTD-NSA-SAI-95-391, October 13, 1995.
59. N. J. Liparulo, Westinghouse, letter to USNRC Document Control Desk, "Assessment of Compensating Errors in WCOBRA/TRAC," NTD-NSA-SAI-95-419, November 3, 1995.
60. N. J. Liparulo, Westinghouse, letter to USNRC Document Control Desk, NTD-NSA-SAI-95-420, November 6, 1995.
61. B. Boyack, et al., Quantifying Reactor Safety Margins, NUREG/CR-5249, EGG-2552, December 1989.
62. D. R. Liles, et al., TRAC-PD2, An Advanced Best-Estimate Computer Program for Pressurized Water Reactor Loss-of-Coolant Accident Analysis, NUREG/CR-2054, 1981.
63. USNRC, The Marviken Full Scale Critical Flow Tests, Summary Report, NUREG/CR-2671, May 1982.
64. 2D/3D Program UPTF Experimental Data Report, Test No. 6, Downcomer Countercurrent Flow Test, U9 316/89/2, KWU, 1989.
65. M. Sobajima, et al., Data Report on Large Scale Reflood Test-66, SCTF Test S2-SH1 (Run 604), JAERI-memo 59-282, 1984.
66. A. Ohnuki, et al., Data Report on Large Scale Reflood Test-94, SCTF Test S2-14 (Run 619), JAERI-memo 60-114, 1985a.
67. M. Sobajima, et al., Data Report on Large Scale Reflood Test-99, SCTF Test S2-15 (Run 620), JAERI-memo 60-258, 1985.
68. A. Ohnuki, et al., Data Report on Large Scale Reflood Test-100, SCTF Test S2-16 (Run 621), JAERI-memo 60-259, 1985b.
69. A. Okubo, et al., Data Report on Large Scale Reflood Test-102, SCTF Test S2-18 (Run 623), JAERI-memo 60-268, 1985.

70. T. Okubo, et al., Data Report on Large Scale Reflood Test -- 82 --- CCTF CORE-II TEST C2-4 (RUN 62)---, JAERI-memo 59-540, 1984.
71. T. Iguchi, et al., Data Report on Large Scale Reflood Test -- 83 --- CCTF CORE-II TEST C2-5 (RUN 63)---, JAERI-memo 59-451, 1984.
72. H. Akimoto, et al., Data Report on Large Scale Reflood Test -- 84 --- CCTF CORE-II TEST C2-6 (RUN 64)---, JAERI-memo 59-452, 1984a.
73. H. Akimoto, et al., Data Report on Large Scale Reflood Test -- 86 --- CCTF CORE-II TEST C2-8 (RUN 67)---, JAERI-memo 59-453, 1984b.
74. T. Okubo, et al., Data Report on Large Scale Reflood Test -- 98 --- CCTF CORE-II TEST C2-15 (RUN 75)---, JAERI-memo 60-191, 1985.
75. 2D/3D Program UPTF Experimental Data Report, Test No. 10, Tie Plate Countercurrent Flow Test, U9 316/88/1, KWU, 1988.
76. M. K. Denham and P. Dore, ISP-25, Boundary Conditions and Experimental Procedure for ACHILLES Run A1B105, AEEW, SESD Note 495, September 1988.
77. J. P. Cunningham, et al., ECCS Heat Transfer Experiments with Upper Head Injection, Volume 1: Test Facility, Procedures and Data, WCAP-8400, 1974 (Westinghouse Proprietary).
78. T. S. Andreychek, et al., Blowdown Experiments with Upper Head Injection in G-2 17x17 Rod Array Facility, Volume 1: Test Facility, Procedures and Data, WCAP-8582, 1975 (Westinghouse Proprietary).
79. Westinghouse Electric Corporation, Improved Performance Models for Westinghouse Fuel Rod Design and Safety Evaluations, WCAP-10851-P-A.
80. This reference was deleted in the final TER.
81. D. B. Vassello, USNRC, letter to C. Eicheldinger, Westinghouse, "Topical Report Evaluation for the Westinghouse ECCS Evaluation Model: Supplemental Information," WCAP-8471-P-A, May 30, 1975.
82. Private communication with F. Orr, USNRC, September 27, 1995.
83. American Nuclear Society, "American National Standard for Decay Heat Power in Light Water Reactors," ANSI/ANS-5.1-1979, August 1979.
84. J. V. Cathcart, et al., Zirconium Metal-Water Oxidation Kinetics IV - Reaction Rate Studies, ORNL/NUREG-17, Oak Ridge National Laboratory, 1977.
85. L. Biasi, et al., "Studies on Burnout, Part 3," Energia Nucleare, Volume 14, No. 9, 1967, pp. 530-536.
86. T. A. Bjornard and P. Griffith, "PWR Blowdown Heat Transfer," Thermal and Hydraulic Aspects of Nuclear Reactor Safety, Volume 1: Light Water Reactors, O. C. Jones and S. G. Bankoff, Ed., ASME, New York, 1977, pp. 17-41.

87. J. G. Collier, Convective Boiling and Heat Transfer, McGraw Hill, London, 1972.
88. Compendium of ECCS Research for Realistic LOCA Analysis, NUREG-1230, U.S. Nuclear Regulatory Commission, Office of Nuclear Reactor Research, December 1988.
89. N. Lee, et al., PWR FLECHT-SEASET Unblocked Bundle, Forced and Gravity Reflood Task Data Evaluation and Analysis Report, NUREG/CR-2256, EPRI NP-2013, WCAP-9891, November 1981.
90. PWR FLECHT SEASET 21-Rod Bundle Flow Blockage Task Data and Analysis Report, NUREG/CR-2444, EPRI NP-2014, WCAP-9992, September 1982.
91. E. R. Rosal, et al., FLECHT Low Flooding Rate Cosine Test Series Data Report, WCAP-8651, 1975.
92. E. R. Rosal, et al., FLECHT Low Flooding Rate Skewed Test Series Data Report, WCAP-9108, 1977.
93. D. G. Morris, et al., An Analysis of Transient Film Boiling of High-Pressure Water in a Rod Bundle, NUREG/CR-2469, 1982.
94. C. B. Mullins, et al., Thermal-Hydraulic Test Facility Experimental Data Report for Test 3.03.6AR, NUREG/CR-2525, 1982.
95. R. C. Gottula, et al., Forced Convection, Nonequilibrium, Post-CHF Heat Transfer Experimental Data and Correlation Comparison Report, NUREG/CR-3193, EGG-2245, March 1985.
96. I. S. Lim, et al., Cocurrent Steam/Water Flow in a Horizontal Channel, NUREG/CR-2289, August 1981.
97. G. P. Lilly, et al., Mixing of Emergency Core Cooling Water With Steam, EPRI-294-2, January 1975.
98. P. G. Prassions, et al., Experiment Data Report for LOFT Power Ascension Experiment L2-3, NUREG/CR-0792, 1979.
99. P. D. Bayless and J. M. Divine, Experiment Data Report for LOFT Large-Break Loss-of-Coolant Experiment L2-5, NUREG/CR-2826, 1982.
100. Safety Code Development Group, TRAC-PF1/MOD1: An Advanced Best-Estimate Computer Program for Pressurized Water Reactor Thermal-Hydraulic Analysis, NUREG/CR-3858, LA-10157-MA, July 1986.
101. R. P. Forslund and W. M. Rohsenow, "Dispersed Flow Film Boiling," Journal of Heat Transfer, Volume 90, November 1968, pp. 399-407.
102. F. W. Dittus and L. M. K. Boelter, Heat Transfer in Automobile Radiators of the Tubular Type, University of California Engineering Publications, 1930.
103. This reference was deleted in the final TER.

104. R. A. Shaw, et al., Development of a Phenomena Identification and Ranking Table (PIRT) for Thermal-Hydraulic Phenomena During a PWR Large-Break LOCA, NUREG/CR-5047, EGG-2527, November 1988.
105. P. S. Damere11 and J. W. Simons, Ed., Reactor Safety Issues Resolved by the 2D/3D Program, NUREG/IA-0127, GRS-101, MPR-1346, July 1993.
106. MPR presentation to ACRS Thermal-Hydraulic Subcommittee, June 14, 1990.
107. C. J. Crowley, P. H. Roth, and R. G. Sam, 1/5-Scale Countercurrent Flow Data Presentation and Discussion, NUREG/CR-2106, 1981.
108. L. E. Hochreiter, et al., G-2 17x17 Refill Heat Transfer Test and Analysis, WCAP-8793, 1976 (Westinghouse Proprietary).
109. J. P. Cunningham, et al., G-2 Facility Forced Flooding Tests with a 17x17 Rod Array, Volume 1: Test Facility, Procedures, and Data, WCAP-8551, June 1975 (Westinghouse Proprietary).
110. P. Ihle and K. Rust, FEBA - Flooding Experiments with Blocked Arrays, Data Report 1, Test Series I through IV, KfK, 1984.
111. I. Kataoka and M. Ishii, Mechanistic Modeling and Correlations for Pool Entrainment Phenomenon, NUREG/CR-3304, ANL-83-87, April 1983.
112. M. McCormick-Barger, Experiment Data Report for LOFT Power Ascension Experiment L2-2, NUREG/CR-0492, 1979.
113. J. P. Adams and J. C. Birchley, Quick Look Report on OECD LOFT Experiment LP-LB-1, OECD LOFT-TR-3504.
114. 2D/3D Program UPTF Experimental Data Report, Test No. 25, Downcomer/Cold Leg Steam/Water Interaction Test, E314/90/11, KWU, 1990.
115. 2D/3D Program UPTF Experimental Data Report, Test No. 8, Cold/Hot Leg Flow Pattern Test, U9 316/88/12, KWU, 1988.
116. 2D/3D Program UPTF Experimental Data Report, Test No. 29, Entrainment/Deentrainment Test, E314/90/05, KWU, 1990.
117. G. P. Lilly and L. E. Hochreiter, Mixing of Emergency Core Cooling Water With Steam: 1/3 Scale Test and Summary, EPRI Research Report 294-2, 1975.
118. C. J. Crowley, J. A. Block, and C. N. Cary, Downcomer Effects in a 1/15-Scale PWR Geometry, NUREG-0281, 1977.
119. C. L. Mohr, et al., Prototypic Thermal-Hydraulic Experiment in NRU to Simulate Loss-of-Coolant Accident, NUREG/CR-1882, 1981.
120. C. L. Mohr, et al., LOCA Simulations in the National Research Universal Reactor Program, NUREG/CR-2528, 1983.
121. G. B. Wallis, One-dimensional Two-phase Flow, McGraw-Hill, New York, 1969.

122. S. S. Kutateladze, "Elements of Hydrodynamics of Gas-Liquid Systems," Fluid Mechanics - Soviet Research, Volume 1, 1972, pp. 29-50.
123. H. Glaeser, "Downcomer and Tie Plate Countercurrent Flow in the Upper Plenum Test Facility (UPTF)," Nuclear Engineering and Design, Volume 133, 1992.
124. This reference was deleted in the final TER.
125. W. E. Ford, et al., CSRL-V: Processed ENDF/B-V 227-Neutron-Group and Pointwise Cross-Section Libraries for Criticality Safety, Reactor and Shielding Studies, NUREG/CR-2306, ORNL/CSD/TM-160, June 1982.
126. American Nuclear Society, "Proposed American Nuclear Society Standards - Decay Energy Release Following Shutdown of Uranium-Fueled Thermal Reactors," October 1971.
127. Westinghouse Electric Corporation, VANTAGE+ Fuel Assembly Reference Core Report, Appendix E: ZIRLO High Temperature Oxidation Tests, WCAP-12610-P-A, 1990.
128. Private Communication with D. Hagrman, INEL, (pressure effects), November 29, 1995.
129. J. P. Holman, Heat Transfer, 7th ed., McGraw-Hill, New York, 1990.
130. Y. S. Touloukian, Thermophysical Properties of High Temperature Materials, The Macmillan Co., New York, 1967.
131. Private Communication with D. Hagrman, INEL, (burst models) July 3, 1995.
132. T. M. Anklam, R. J. Miller, and M. D. White, Experimental Investigations of Uncovered-Bundle Heat Transfer and Two-Phase Mixture-Level Swell Under High-Pressure Low Heat-Flux Conditions, NUREG/CR-2456, ORNL-5848, March 1982.
133. G. W. Govier and K. Aziz, The Flow of Complex Mixtures in Pipes, Von Nostrand Reinhold, New York, 1972.
134. J. G. Collier, et al., Two-Phase Pressure Drop and Void Fractions in Tubes, HTFS Design Report No. 15, AERE-R-6454, HTFS-DR-15, 1972.
135. S. Wong and L. E. Hochreiter, Analysis of the FLECHT-SEASET Unblocked Bundle Steam Cooling and Boiloff Tests, NRC/EPRI/Westinghouse-8, 1981.
136. W. H. McAdams, Heat Transmission, McGraw-Hill Co., New York, 1954.
137. I. E. Idel'Chik, Handbook of Hydraulic Resistance, AEC-TR-6630, 1960.
138. D. A. Powers and R. O. Meyer, Cladding Swelling Models for LOCA Analysis, NUREG-0630, April 1980.
139. Private Communication with F. Orr, USNRC, October 2, 1995.

140. A. E. Dukler and Y. Taitel, "A Model for Predicting Flow Regime Transitions in Horizontal and Near Horizontal Gas-Liquid Flow," AICHE Journal, Volume 22, No. 1, January 1977.
141. A. E. Dukler, et al., "Modelling Flow pattern Transitions for Steady Upward Gas-Liquid Flow in Vertical Tubes," AICHE Journal, Volume 26, No. 3, May 1980.
142. M. Ishii, One-Dimensional Drift-Flux Model and Constitutive Equations for Relative Motion Between Phases in Various Two-Phase Flow Regimes, ANL-77-47, 1977.
143. M. Ishii and T. C. Chawla, Local Drag Laws in Dispersed Two-Phase Flow, NUREG/CR-1230, ANL-79-105, 1979.
144. W. H. Henstock and T. J. Hanratty, "The Interfacial Drag and the Height of the Wall Layer in Annular Flows," AICHE Journal, Volume 22, No. 6, November 1976, pp. 990-1000.
145. P. B. Whalley, et al., Experimental Wave and Entrainment Measurements in Vertical Annular Two-Phase Flow, AERE-R7521, 1973.
146. D. F. Tatterson, et al., "Drop Sizes in Annular Gas-Liquid Flows," AICHE Journal, Vol. 23, No. 1, pp. 68-76, 1977.
147. L. B. Cousins, et al., "Liquid Mass Transfer in annular Two-Phase Flow," Symposium on Two-Phase Flow, Volume 2, Exeter, England, Paper C4, 1965, pp. 401-430.
148. P. B. Whalley, "The Calculation of Dryout in a Rod Bundle," International Journal of Multi-phase Flow, Vol. 13, pp. 501-515, 1977.
149. J. C. Dallman and W. L. Kirchner, De-Entrainment Phenomena on Vertical Tubes in Droplet Cross flow, NUREG/CR-1421, LA-8316-MS, April 1980.
150. C. W. Hirt and N. C. Romero, Application of a Drift-Flux Model to Flashing in Straight Pipes, LA-6005-MS, Los Alamos National Laboratory, 1975.
151. N. Zuber and J. A. Findlay, "Average Volumetric Concentration in Two-Phase Flow Systems," Transactions of the ASME, Journal of Heat Transfer, November 1965, pp. 453-468.
152. D. Bharathan, et al., Air Water Countercurrent Annular Flow, EPRI-NP-1165, 1979.
153. G. B. Wallis, "Use of the Reynolds Flux Concept for Analyzing One-Dimensional Two-Phase Flow, Part I, Derivation and Verification of Basic Analytical Techniques," International Journal of Heat and Mass Transfer, Volume II, 1968, pp. 445-458.
154. P. N. Rowe, K. T. Claxton, J. B. Lewis, "Heat and Mass Transfer from a Single Sphere in an Extensive Flowing Fluid," Transactions of the Institute of Chemical Engineers, Volume 43, 1965, T14-T31.

155. G. G. Bruker and E. M. Sparrow, "Direct Contact Condensation of Steam Bubbles in Water at High Pressure," International Journal of Heat and Mass Transfer, Volume 20, 1977, pp. 371-381.
156. J. D. Ford and A. Lekic, "Rate of Growth of Drops During Condensation," International Journal of Heat and Mass Transfer, Volume 16, 1973, pp. 61-64.
157. K. Lee and D. J. Ryley, "The Evaporation of Water Droplets in Superheated Steam," Transactions of the ASME, Journal of Heat Transfer, Volume 90, 1968, pp. 445-451.
158. A. P. Colburn, "A Method of Correlating Forced Convection Heat Transfer Data and a Comparison with Fluid Friction," Transactions of the AIChE, Volume 29, 1933.
159. S. G. Bankoff, et al., Countercurrent Steam Water Flow in a Flat Plate Geometry, NUREG/CR-2783, June 1982.
160. H. J. Kim, S. C. Lee, and S. G. Bankoff, "Heat Transfer and Interfacial Drag in Countercurrent Steam-Water Stratified Flow," International Journal of Multiphase Flow, Volume 11, No. 5, 1985, pp. 593-606.
161. S. Sideman, "Direct Contact Heat Transfer Between Immiscible Liquids," Advances in Chemical Engineering, Volume 6, Academic Press, 1966.
162. H. Asaka, Y. Murao, Y. Kukita, "Assessment of TRAC-PF1 Condensation Heat Transfer Model for Analysis of ECC Water Injection Transients," Journal of Nuclear Science and Technology, Volume 26, Number 11, 1989, pp. 1045-1057.
163. W. M. Kays, Convective Heat and Mass Transfer, McGraw-Hill Book Company, New York, 1966.
164. S. C. Yao, L. E. Hochreiter, and W. J. Leech, "Heat Transfer Augmentation in Rod Bundles Near Grid Spacers," Transactions of the ASME, Journal of Heat Transfer, Volume 104, February 1982, pp. 76-81.
165. L. A. Bromley, "Heat Transfer in Stable Film Boiling," Chemical Engineering Progress, Vol. 46, No. 5, pp. 221-226, 1950.
166. M. L. Pomeranz, "Film Boiling on a Horizontal Tube in Increased Gravity Fields," Journal of Heat Transfer, Volume 86, No. 2, 1964, pp. 213-219.
167. P. J. Berenson, On Transition Boiling From a Horizontal Surface, MIT PhD Thesis, 1960.
168. S. Z. Rouhani and E. Axelsson, "Calculation of Void Volume Fraction in Subcooled and Quality Boiling Regions," Int. J. Heat and Mass Transfer, Vol. 13, 1970.
169. J. H. Kim, "Heat Transfer in Longitudinal Laminar Flow Along Circular Cylinders in Square Array," Heat Transfer Over Rod or Tube Bundles, ASME, 1979.

170. J. C. Chen, "A Correlation for Boiling Heat Transfer to Saturated Fluids in Convective Flow," ASME 63-HT-64, 1963.
171. J. G. Collier, Convective Boiling and Condensation, 2nd Ed., McGraw-Hill Book Co., 1980.
172. S. Levy, "Forced convection subcooled boiling prediction of vapour volumetric fraction," International Journal of Heat and Mass Transfer, Volume 10, 1967, pp. 951-965.
173. Y. Y. Hsu, "Tentative Correlation of Reflood Heat Transfer," 3rd Water Reactor Safety Information Meeting, Germantown MD, 1975.
174. M. E. Ellion, A Study of the Mechanism of Boiling Heat Transfer, Report JPL-MEMO-20-88, California Institute of Technology, 1954.
175. S. C. Cheng, et al., "Transition Boiling in Forced Vertical Flow," NUREG/CR-0357, ANL-78-75, 1978.
176. R. S. Dougall and W. M. Rohsenow, Film Boiling on the Inside of Vertical Tubes with Upward Flow of the Fluid at Low Qualities, MIT Report 9079-76, 1963.
177. K. H. Sun, et al., "Calculations of Combined Radiation and Convection Heat Transfer in Rod Bundles Under Emergency Cooling Conditions," ASME Journal of Heat Transfer, August 1976.
178. S. Yao, L. E. Hochreiter, and C. E. Dodge, "A simple Method for Calculating Radiative Heat Transfer in Rod Bundles with Droplets and Vapor as Absorbing Media," Transactions of the ASME, Journal of Heat Transfer, Volume 101, November 1979, pp. 736-739.
179. M. M. Abu-Romia and C. L. Tien, "Appropriate Mean Absorption Coefficients for Infrared Radiation of Gases," Transactions of the ASME, Journal of Heat Transfer, November 1967, pp. 321-327.
180. W. M. Rohsenow and H. Choi, Heat, Mass, and Momentum Transfer, Prentice-Hall, Englewood Cliffs, New Jersey, 1961.
181. R. E. Henry, "A Correlation for the Minimum Film Boiling Temperature," AICHE Symposium Series, Vol. 138, pp. 81-90, 1974.
182. O. C. Iloeje, et al., "An Investigation of the Collapse and Surface Rewet in Film Boiling in Vertical Flow," J. Heat Transfer, Vol. 97, pp. 166-172, 1975.
183. D. S. Trent and J. R. Welty, A Summary of Numerical Methods for Solving Transient Heat Conduction Problems, Engineering Experimental Station Bulletin No. 49, OSU, Corvallis OR, 1974.
184. C. E. Beyer, et al., GAPCON-THERMAL-2: A Computer Program for Calculating the Thermal Behavior of an Oxide Fuel Rod, BNWL-1898, November 1975.

185. L. J. Siefken, et al., FRAP-T6: A Computer Program for the Transient Analysis of Oxide Fuel Rods, NUREG/CR-2148, EGG-2104, May 1981.
186. D. L. Hagrman, G. A. Reymann, and R. E. Manson, MATPRO-Version 11 (Revision 1), A Handbook of Materials Properties for Use in the Analysis of Light Water Reactor Fuel Rod Behavior, NUREG/CR-0497, Rev. 1, 1980.
187. N. G. McDuffie, "Vortex Free Downflow in Vertical Drains," AICHE Journal, Volume 23, Number 1, January 1977, pp. 37-40.
188. G. K. Batchelor and R. W. O'Brien, "Thermal or electrical conduction through a granular material," Proceeding of the Royal Society of London, Volume 355, No. 1682, July 13, 1977, pp. 313-333.
189. R. G. Deissler and J. S. Boegli, "An Investigation of Effective Thermal Conductivities of Powders in Various Gases," ASME Transactions, October 1958, pp. 1417-1425.
190. N. J. Liparulo, Westinghouse, letter to USNRC Document Control Desk, "Preliminary Responses to Requests for Additional Information Regarding WCAP-12945-P and the Revised Methodology Report," NTD-NSA-SAI-95-445, November 22, 1995.
191. Private communication with D. Hagrman, INEL, December 12-13, 1995.
192. This reference deleted in the final TER.
193. Crane Co. Flow of Fluids through Valves, Fittings, and Pipes, Technical Paper No. 410, 1978.
194. MPR Associates, MPR-1163.
195. Private communication with G. Berna, INEL, December 13, 1995.
196. This reference deleted in the final TER.
197. This reference deleted in the final TER.
198. This reference deleted in the final TER.
199. D. Abdollahian, et al., Critical-Flow Data Review and Analysis, EPRI-NP-2192, January 1982.
200. M. Drucker and V. K. Dhir, Studies of Single- and Two-Phase Heat Transfer in a Blocked Four-Rod Bundle, EPRI-NP-3485, June 1984.
201. This reference deleted in the final TER.
202. J. M. Broughton, PBF LOCA Test Series, Test LOC-3 and LOC-5 Fuel Behavior Report, NUREG/CR-2073, June 1981.
203. N. J. Liparulo, Westinghouse, letter to USNRC Document Control Desk, "Requested Information to Support ACRS Thermal-Hydraulic Subcommittee Meeting on January 18-19, 1996," NTD-NSA-SAI-96-004, January 5, 1996.

204. Westinghouse documentation plan letter, September 18, 1995.
205. N. J. Liparulo, Westinghouse, letter to USNRC Document Control Desk, "Confirmatory Items Related to the Review of WCAP-12945-P," NSA-SAI-96-019, January 24, 1996.
206. N. J. Liparulo, Westinghouse, letter to USNRC Document Control Desk, "Open Issues and Confirmatory Items Related to the Review of WCAP-12945-P," NSA-SAI-96-028, January 26, 1996.
207. M. S. El-Genk, et al., "Experimental Studies of Forced, Combined and Natural Convection of Water in Vertical Nine-Rod Bundles," International Journal of Heat and Mass Transfer, Volume 36, No. 9, 1993, pp. 2359-2374.
208. C. Hsieh, et al., Countercurrent Air/Water and Steam/Water Flow Above a Perforated Plate, NUREG/CR-1808, 1980.
209. G. Yadigaroglu, et al., "Modeling of Reflood," Nucl. Engr. and Design, 145, 1993, pp. 1-35.
210. M. Andreani, et al., Dispersed Flow Film Boiling, NUREG/IA-0042, August 1992.
211. R. Nelson, et al., "A Phenomenological Model of the Thermal Hydraulics of Convective Boiling during Quenching of Hot Rod Bundles Part I: Thermal Hydraulic Model," Nucl. Engr. and Design, 136, 1992, pp. 277-298.
212. M. Renksizbulut, et al., "Experimental Study of Droplet Evaporation in a High Temperature Air Stream," J. of Heat Transfer, 105, 1968, pp. 384-388.
213. N. J. Liparulo, Westinghouse, letter to USNRC Document Control Desk, "Resolution of Issues Related to Review of WCAP-12945-P," NSA-SAI-96-102, March 25, 1996.
214. N. J. Liparulo, Westinghouse, letter to USNRC Document Control Desk, "Docketing of Supplemental Information Related to WCAP-12945-P," NSA-SAI-96-156, April 30, 1996.
215. N. J. Liparulo, Westinghouse, letter to USNRC Document Control Desk, "Docketing of Supplemental Information Related to WCAP-12945-P," NSA-SAI-96-167, May 9, 1996.
216. Code of Federal Regulations, Title 10 - Energy, Part 50 - Domestic Licensing of Production and Utilization Facilities, Section 46 - Acceptance criteria for emergency core cooling systems for light water nuclear power reactors, January 1, 1990.
217. U.S. Nuclear Regulatory Commission, Best-Estimate Calculations of Emergency Core Cooling System Performance, Regulatory Guide 1.157, May 1989.

218. M. Andreani, et al., "Prediction for Dispersed Flow Film Boiling," International Journal of Multiphase Flow, Vol. 20, Suppl., pp. 1-51, 1994.
219. J. J. Carbajo, "A Study of Rewetting Temperature," Nucl. Engr. and Design, Vol. 84, 1985, pp. 21-52.
220. E. Elias and G. Yadigaroglu, "The Reflooding Phase of the LOCA in PWRs. Part II, Rewetting and Liquid Entrainment," Nuclear Safety, Vol. 19, No. 2, March-April 1978, pp. 161-175.
221. F. W. Barclay, et.al., CATHENA MOD-3.2n Theoretical Manual, THB-CD-002, November, 1989.
222. S. Z. Rouhani, et.al., TRAC-BF1/MOD1 Models and Correlations, NUREG/CR-4391, June, 1992
223. The RELAP5 Development Team, RELAP5/MOD3 Code Manual, Models and Correlations, NUREG/CR-5535, August, 1995.

APPENDIX A

WESTINGHOUSE WCOBRA/TRAC MODEL DESCRIPTION AND REVIEW

WESTINGHOUSE WCOBRA/TRAC MODEL DESCRIPTION AND REVIEW

The following sections provide a more detailed description of the WCOBRA/TRAC models and correlations, and the results of the INEL review. The discussion is based on the information in Volume 1 of the CQD, Sections 2 to 9, and Westinghouse responses to questions. During the course of the review, Westinghouse modified the WCOBRA/TRAC code. The code version documented in the CQD was WCOBRA/TRAC, MOD7. Two subsequent code versions were later produced. The first revision focused on improving the entrainment model and produced WCOBRA/TRAC, MOD7A. Appendix A of Reference 58 discussed the changes made to produce WCOBRA/TRAC, MOD7A.Rev.1 by adding additional modeling capability needed for the uncertainty propagation and correcting code errors. WCOBRA/TRAC, MOD7A.Rev.1, is the version documented in this review. Based on INEL review of the changes and Westinghouse discussion of their effects in Appendix A of Reference 58, INEL agrees with Westinghouse's conclusion that the effects of the changes on the experiment simulations are minimal. Therefore, reanalysis with MOD7A.Rev.1 does not appear to be warranted, and the MOD7A experiment simulations apply to MOD7A.Rev.1. Note all references cited in this appendix are listed in the references at the end of the main body of this report, Section 15.

A.1 Conservation Equations - CQD Section 2

A.1.1 Model Description

WCOBRA/TRAC uses a two-fluid, three-field representation of flow in the reactor vessel. The three fields are vapor, continuous liquid, and entrained liquid. Each field uses a three-dimensional set of continuity, momentum, and energy equations with one exception. The continuous and entrained liquid fields use the same energy equation; therefore, the two fields are assumed to be at the same temperature. In the vessel, each phase uses a separate set of conservation equations and constitutive relations. The effect of one phase on another is accounted for by the interaction terms appearing in the governing equations.

Outside the vessel, a one-dimensional representation of primary system components is used. Components such as pipes, pumps, valves, steam

generators, and the pressurizer can be represented with models in WCOBRA/TRAC. The one-dimensional components use a two-phase, five equation, drift-flux model. Two equations are used to represent conservation of mass (mixture and steam mass), two equations used for conservation of energy (mixture and steam energy), and a single equation is used to represent the conservation of momentum. Closure of the field equations requires specifying the interphase relative velocity, fluid properties, interphase mass and heat transfer, and other constitutive relationships.

A.1.2 INEL Review of CQD Section 2

This section is intended to highlight the issues that were of some importance in the review on CQD Section 2. It is not intended to cover all aspects of the review related to Section 2. For further information, the reader should consult the numerous questions related to Section 2 posed by the INEL in the requests for additional information.

The theoretical basis for the code conservation equations of WCOBRA-TRAC is standard. The three-dimensional vessel references the work of Thurgood in the COBRA-TRAC manual, Reference 2.

The one-dimensional network portion of the formulation references Ishii's work, Reference 142.

The formulation of WCOBRA-TRAC was also compared to the CATHENA code,²²¹ the TRAC-BF1 code,²²² and the RELAP5 code.²²³

The basic approach in the reactor vessel is a three field formulation as discussed above. The piping network code is a five-equation drift flux model based on the TRAC-PD2 code. This approach of using a 1-D formulation with a five equation code for the piping systems and the secondary part of the plant is adequate for the LBLOCA since the driving forces are large pressure drops, and the influence of the steam generators is a secondary effect.

The equations are solved for on a staggered grid. By a staggered grid, it is meant that the scalar variables such as pressure, void fraction, and

energies are solved for in control volumes or cells, while the vector quantities such as velocities are solved for on the cell or volume faces.

Due to computer time limitations, Westinghouse uses the subchannel formulation to a great extent instead of the 3-D approach in the vessel. The subchannel approach appears to be a 2-D representation. The subchannel formulation is considered to be adequate, since azimuthal pressure drops during a LBLOCA should be small compared to the axial and radial pressure drops in the vessel. It should also be noted that calculating form loss pressure drops in the 3-D vessel in the azimuthal direction appears to be more of an art than a science, compared to form losses in the axial and radial directions.

As shown in Eqn. 2-57 of the CQD, the formulation numerics are Courant limited, since a semi-implicit approach is used. The semi-implicit approach is quite adequate as long as the time step is kept below the Courant Limit. It should be noted that Westinghouse keeps the time step well below the Courant Limit or even the Courant Limit divided by two, which keeps the formulation stable and accurate (first order for this approach) within the constraints of the formulation.

Upon examination of the equation set, it appears that there is no wall mass generation term. Subcooled boiling takes place at the wall and not at the interface. The INEL believes, however, that this approach is adequate for LBLOCA, since the thermodynamic conditions during the transient quickly approach saturation conditions.

The momentum equations used in the code are standard phasic equations. However, the gravitational head terms in the momentum equations are not linearized with respect to the independent (solution) variables. Such a linearization is expected to increase code stability, and should prevent flow anomalies or unstable flow behavior from occurring at low flow conditions. The exclusion of this linearization is adequate for LBLOCA, since the flow rates are large.

The mixture of averaging and donoring in the discrete equation set is standard for non-equilibrium codes. The implementation of boundary conditions for the vessel and the piping is also standard. Connections between the 1-D loop piping system and the 3-D vessel are performed explicitly with a delta pressure equation (Eqn. 4-257). A loss coefficient is based on UPTF data with the value of K given in Reference 58, Section 3.1.2. This loss coefficient covers LBLOCA conditions because it was determined using UPTF experimental results. The resulting model was then applied to simulations of the LOFT LBLOCA tests with success for both the forward and reverse directions at the vessel connections. Westinghouse, in Reference 214, List II, Item 8, committed to not changing the value and range of the broken loop cold leg nozzle loss coefficient for plant specific applications. Also, the values developed apply only to LBLOCA, and the values developed must be justified for other applications.

It is also noted that a steady state pressure drop relation is used to connect a state of the art multi-dimensional non-equilibrium fluid code such as COBRA to a 1-D five equation non-equilibrium fluid code such as TRAC-PD2. There appears to be very little evidence from the CQD that a true first principles approach on connecting the 1-D mesh to the subchannel mesh was attempted. The explicit numerics of this connection could be a large source of uncertainty with regard to the mathematical stability of this connection in regards to code performance. However, as long as this approach is used with conditions consistent with the LOFT and UPTF data, the use of the input loss coefficients to couple the 1-D and 3-D vessel components is considered adequate.

WCOBRA-TRAC does not utilize the formulation for the viscous shear stress tensor given in Section 2 of the CQD. Standard form losses and Darcy friction are used in the code. It is understood that the viscous shear models are not used since their use would require a fine mesh nodalization, especially near the walls, and would be very CPU time prohibiting for obtaining an answer.

One potential concern that is apparent from Eqn. 2-154 for the 1-D portion of the code is that flux terms containing relative velocity terms use donoring based on relative velocity flow direction. Since relative velocity

is the difference between the gas and fluid velocities, such donoring raises an issue of ambiguity for junction quantities that are derived from donoring based on relative velocity. However, for a LBLOCA, the flows are large, and the relative velocities are small. As a consequence, this approach is adequate for LBLOCA.

The Westinghouse approach of following, as nearly as possible, the nodalization used in comparing to the integral tests is considered an adequate approach.

In summary, the numerics used in WCOBRA-TRAC is semi-implicit and Courant limited. Westinghouse has demonstrated that they stay well below the Courant Limit for LBLOCA. The equation sets are standard and based on accepted formulations by Ishii and others. Westinghouse has done an excellent job in responding to the questions of the reviewers.

Based on the above, Section 2 of the CQD is considered adequate for LBLOCA applications.

A.2 Flow Regimes and Interfacial Area - CQD Section 3

A.2.1 Model Description

In the vessel component, cold and hot wall flow regimes are modeled when appropriate. A cold wall regime is assumed to occur when there are no heated structures in a cell and/or the wall temperature is not above the CHF temperature. The cold wall flow regimes are discussed first followed by the hot wall regimes.

A small bubble flow regime is assumed if the void fraction is less than 0.20. The bubble radius is based on a critical Weber number, and the interfacial area is based on the void fraction and bubble radius. See Section 3-2-2 of the CQD. If the void fraction is between 0.20 and 0.50, a small to large bubble regime (slug flow or bubble/slug flow) is assumed. This is basically an interpolation regime where WCOBRA/TRAC interpolates between the interfacial area assuming all vapor is in small bubbles and all vapor is in large bubbles. In this way, the code accounts for bubble size growth as

void fraction increases and slug flow develops. See Section 3-2-3 of the CQD. A churn-turbulent flow regime is assumed if the void fraction is greater than 0.50. The upper void fraction limit in the churn-turbulent regime is the void fraction at which a stable liquid film is formed. This void fraction is based on a critical void fraction calculated using Eqn. 3-39. The churn-turbulent flow regime is another interpolation regime using the interfacial area of the large bubbles (calculated using the same methods as in small to large bubble regime) and the film/drop flow regime. See Section 3-2-4 of the CQD. Above the critical void fraction, the flow is assumed to be entirely in the film/drop regime. This flow regime has a liquid film on the wall and entrained drops in a vapor core (see Section 3-2-5 of the CQD). It should be noted that limits are applied to bubble and drop sizes to ensure that geometric constraints (like hydraulic diameter for bubbles) are not violated (see Eqn. 3-23) or to ensure drops are not allowed to become too small (see Eqn. 3-45).

The hot wall flow regimes include the inverted annular flow regime. In this regime, the liquid core is assumed to be separated from the hot wall by a vapor film. An inverted liquid slug flow regime is also modeled in which the liquid core of the inverted annular flow regime is assumed to be breaking up into liquid slugs. The logic controlling whether the inverted annular or the inverted slug regime is chosen is whether the liquid is subcooled (inverted annular chosen) or saturated (inverted slug is chosen). See Sections 3-3-2 and 3-3-3 of the CQD. A dispersed droplet flow regime is also modeled and is possible at all void fractions if entrainment mechanisms create the field (CQD Section 3-3-4). If a top quench front forms, WCOBRA/TRAC models two flow regimes, a falling film regime if the void fraction is greater than 0.80 and a top deluge regime if the void fraction drops below 0.80. Details are described in Sections 3-3-5 and 3-3-6 of the CQD.

WCOBRA/TRAC has a separate flow regime map for the one-dimensional components as described in Section 3-4 of the CQD. It is the same as the one-dimensional flow regime map used in TRAC-PD2. The bubbly flow regime is assumed if the void fraction is less than 0.30, the slug flow regime is assumed if the void fraction is between 0.30 and 0.50, the churn flow regime is assumed between void fractions of 0.50 and 0.75, and the annular mist flow regime is assumed if the void fraction is greater than 0.75. If the mass flux

is greater than $2000 \text{ kg/m}^2\text{-s}$, the code logic does not allow the slug flow regime to occur but the flow regime begins to transition to bubbly flow. In addition, the churn flow regime is an interpolation regime between annular mist and either slug or bubbly flow depending on the mass flux. In the one-dimensional components, the flow regime map only influences the flow area for interphase heat transfer. Because of the drift flux model applied in one-dimensional components, correlations are used to describe the relative phase velocities (see Section 4-7 of the CQD).

A.2.2 INEL Review of CQD Section 3

The INEL reviewed CQD Section 3, and that review resulted in a number of questions (see Volume 1, questions 20-47, Attachment 1, Reference 3). During the review process, Westinghouse provided answers to resolve all the items identified by the INEL. For example, in response to Volume 1, question 21b, Reference 15, Westinghouse demonstrated that the flow regime maps used by WCOBRA/TRAC are simpler but adequate to represent the important trends of the more complex flow regime maps proposed by Taitel and Dukler.^{140, 141}

One of the areas discussed in CQD Section 3 is the interfacial areas associated with the various flow regimes. The areas are calculated based on Weber number criteria (see Eqn. 3-15, for example), or the expected flow pattern (see CQD Sections 3-2-3 and 3-2-5). The INEL verified the calculated areas were appropriate for the specified flow regimes or asked Westinghouse to justify the formula used. For example, see Westinghouse's response to Volume 1, question 31, Reference 7, for the film interfacial area. In response to INEL questions, Westinghouse justified the Weber number used to determine bubble size and the basis for minimum drop diameters (see Westinghouse responses to Volume 1, questions, 22, 30, and 42, References 31, 10, and 11).

Based on the review summarized above, the INEL considers the WCOBRA/TRAC flow regime maps and interfacial areas adequate.

A.3 Momentum Transfer Models - CQD Section 4

A.3.1 Model Description

WCOBRA/TRAC momentum transfer models account for momentum transfer between the fluid and the wall, between vapor and continuous liquid, and between vapor and entrained droplets. The vessel wall shear model will be discussed first followed by the vessel form loss, vessel interfacial shear, intercell shear, vessel entrainment/deentrainment, and one-dimensional components.

Separate wall shear models are provided in WCOBRA/TRAC for continuous liquid and vapor. Stresses due to wall friction are not applied to entrained droplets. When the wall is wet, the wall shear is assigned to the continuous liquid, and when the wall is dry (hot wall regime), the wall shear is assigned to the vapor. In two-phase conditions, the two-phase pressure drop model of Wallis, Reference 121, is used. Friction factors vary with Reynolds number with separate formulations for laminar and turbulent flow.

The code allows a form loss to be entered by the code user, and this form loss is divided between the phases as discussed on CQD page 4-5. Input for form losses in both the axial and lateral directions are allowed.

Interfacial shear models use the flow regime maps discussed earlier to calculate interfacial area. The flow regime dependent interfacial drag coefficient is formulated to include a drag coefficient (C_D) or friction factor (f_i), interfacial area, relative phase velocity, and the phasic density. Linear ramps are applied in the small to large bubble regime and the churn turbulent regime (large bubble to film drop). Westinghouse made extensive use of the work by Ishii^{142,143} to determine the drag coefficients. Friction factors for use in the film/drop regime are based on the work of Henstock and Hanratty¹⁴⁴ and Wallis, Reference 121.

WCOBRA/TRAC also calculates an additional interfacial drag force on mesh cell boundaries. The interfaces are detected by differences in void fraction between adjacent cells, and may occur at either the vertical or horizontal cell boundaries. In this model, a constant friction factor is used (see

Eqn. 4-120). Westinghouse noted this model is used to calculate CCFL situations where liquid is flowing down against vapor upflow. To illustrate where this model would be used, Westinghouse discussed its application at the UCP. At this location, there are channels where liquid can pool, such as on the top of the upper core tie plate, and channels representing vapor jets through holes in the UCP. The intercell drag model calculates the vapor jet drag force on the pooled liquid in the adjacent cell.

Entrainment/deentrainment are modeled in WCOBRA/TRAC by the various types of entrainment/deentrainment mechanisms that can occur. The model for entrainment from liquid films includes the effects of droplet breakup from grids and orifices in the calculation of the droplet area. Westinghouse included models for both cocurrent (Whalley, Hewitt, and Hutchinson¹⁴⁵) and countercurrent flow situations (through a critical void fraction model where the critical void fraction represents the maximum possible void fraction for a stable film). The drop size model is based on the work of Tattersson.¹⁴⁶

A separate model is used for entrainment in bottom reflood situations. This model looks at droplet formation resulting from superheated vapor generated by rod quench. The model is based on the work of Kataoka and Ishii, Reference 111, for vapor bubbling through a liquid pool. The droplet size model for bottom reflood is based on the minimum of the hydraulic diameter, a diameter taken from FLECHT data, and a diameter based on a force balance between gravity and interfacial shear. For WCOBRA/TRAC, MOD7A.Rev.1, the minimum droplet diameter allowed at the quench front is given in Reference 27.

Entrainment from top down reflood can occur by two mechanisms. First, is the breakup of pooled liquid as it falls through holes, slots, etc., in vessel hardware into the core. The model adapts the Wallis model, Reference 121, for a single drop falling through an area restriction or orifice. This model generally produces bigger droplets than the second mechanism. The second mechanism is entrainment from falling films at the top quench location when the falling film flow rate exceeds the quench rate. The falling film model assumes all liquid reaching the top quench front location in excess of the vaporization rate at the quench front is entrained. The initial droplet size for the falling film model is determined using a model

based on top spray heat transfer experiments typical of a Boiling Water Reactor. These two models produce droplets of different sizes that WCOBRA/TRAC combines into a single droplet field of average size. Westinghouse noted: (a) the larger droplets from the orifice model dominate, (b) this increases the average drop size, and (c) reduces interfacial heat transfer for top down flooding.

Deentrainment models are provided for film flow, cross flow on upper plenum structures, area changes, and at solid surfaces and liquid pools. The film flow model is based on the work of Cousins¹⁴⁷ and Whalley¹⁴⁸ using a drop concentration gradient diffusion model. Cross flow deentrainment occurs when liquid drops are carried from the core into the vessel upper plenum, and the droplets deentrain on upper plenum structures as they flow to the hot leg nozzles. The work by Dallman and Kirchner¹⁴⁹ was used to determine the deentrainment fraction as a function of the upper plenum design.

The area change deentrainment model is based on a simple flow area ratio. The reduced flow area sweeps the droplets out of the entrained flow field because the drops are assumed to flow normal to the flow area and impact the area reduction.

Finally, deentrainment occurs when entrained liquid flows into a cell with a solid surface at the opposite cell face (for example, flow into a cell with the reactor top head modeled at the opposite cell face) or the cell is in the bubbly flow regime.

The one-dimensional interfacial drag model is based on the Annular Flow Friction Factor model of Hirt and Romero.¹⁵⁰ This work used the single-phase friction factor model of Govier and Aziz, Reference 133, (Eqn. 4-198) and multiplied it by a two-phase multiplier based on the ratio of the liquid velocity and density to the mixture velocity and density (Eqn. 4-203). A homogeneous two-phase friction model is applied (Eqns. 4-207, 4-209, and 4-211) if the void fraction is greater than 0.9995, with linear interpolation between the annular model (used for void fractions below 0.9) and the homogeneous model (used for void fraction greater than 0.9995).

Ishii's, Reference 142, and Zuber/Findlay's¹⁵¹ drift flux models are used to determine the flow regime dependent drift flux velocities. These drift velocities are then used to calculate the relative velocity. As with the vessel component, the one-dimensional components allow for a user input form loss to account for irrecoverable losses.

A.3.2 INEL Review of CQD Section 4

Vessel Models

The INEL reviewed CQD Section 4, and the review resulted in a number of questions (see Volume 1, questions 48-110, Attachment 1, Reference 3). During the review process, Westinghouse provided answers to resolve all the items identified by the INEL. Westinghouse responded to an INEL question to justify the form of the vessel two-phase multipliers used in WCOBRA/TRAC (see response to Volume 1, question 48, Reference 8). In its response, Westinghouse showed the model was a simplified version of the Wallis model (Reference 121, pages 49 and 50) but that it was adequate based on good comparisons to Westinghouse test results discussed in response to Volume 1, question 50, Reference 8. Westinghouse used the same test results in its response to Volume 1, question 50, to justify the use of void fraction to partition the form loss pressure drop.

CQD Section 4-4 discussed the interfacial drag models, and the INEL reviewed them in detail. Most of the WCOBRA/TRAC interfacial drag coefficients were taken from References 142 and 143, which are the work of Ishii and others, for the bubbly to churn turbulent regimes; and friction factors by Wallis, Reference 121, and Henstock and Hanratty, Reference 144, for the film/drop regimes. The use of the drag coefficients/friction factors in WCOBRA/TRAC was reviewed against the original documentation, and Westinghouse was asked to clarify and justify differences or extensions. For example, Volume 1, question 55, Reference 12, asked Westinghouse to justify the use of a drift velocity rather than a terminal velocity in Eqn. 4-52 for a bubble in the distorted particle regime. In its response, Westinghouse noted Eqn. 4-52 was for a multi-particle system and use of the drift velocity was consistent with Ishii and Chawla (Reference 143), page 23.

Another example is the use of Eqn. 4-92 (a friction factor) in a vessel geometry when it was developed from smooth pipe data. In its response to Volume 1, question 68, Reference 37, Westinghouse noted the results from friction factor tests become independent of pipe size for pipe approximately 3 inches in diameter based on Reference 152. They also supplied comparisons to test data to show that the code results for pressure drop and void fraction compared well to test data. Finally, Westinghouse showed that CCFL models developed for simple geometries can be extended to more complex geometries and indicated this supports the extension of friction factor models based on simple geometries to more complex geometries. Based on these arguments, the INEL found the extension of the Wallis model to the vessel adequate.

To justify the use of a single particle C_D in a multiparticle system (Eqn. 4-108), Westinghouse responded in Volume 1, question 73, Reference 8, that the correction factor applied in Ishii and Chawla, Reference 143, is small at conditions expected in a PWR; therefore, the INEL concluded the approximation proposed in the CQD was adequate.

CQD Section 4-5 discussed the vessel intercell drag model used in WCOBRA/TRAC. To verify the adequacy of the model, Westinghouse responded to Volume 1, question 75, Reference 10. They noted the intercell drag model was used in a number of simulations in CQD Section 15-1. INEL review of that section found that simulations that would have used the intercell drag model included a perforated plate, horizontal pipe with several cells vertically, Creare downcomer experiments, and UPTF downcomer bypass experiments. Review of that section and subsequent RAIs showed the WCOBRA/TRAC models calculated CCFL phenomena well or conservatively in the above situations relative to data. Therefore, the INEL found the intercell drag model adequate.

The film entrainment models (discussed in CQD Section 4-6-2) were assessed against UPTF upper plenum entrainment data. This assessment found that the code underpredicted the mass in the upper plenum relative to the test data. Assessment against SCTF and CCTF data found that entrainment from the upper plenum to the hot leg began earlier than the test data. These results indicate the film entrainment model yields conservative results relative to the test data. Therefore, the INEL considers the model adequate for realistic LBLOCA.

The bottom reflood entrainment model was revised during the WCOBRA/TRAC review process. The original version of the model in WCOBRA/TRAC, MOD7, entrained too little liquid in a number of forced reflood tests, resulting in calculated early quench and calculated bundle masses exceeding the test data. The MOD7A version of the code improved the bottom entrainment model resulting in improved bundle mass comparisons and some improvement in quench time comparisons with data (see Reference 27).

Westinghouse's responses to Volume 2, questions 12, 22, 26, 28, 40, and 41, Reference 46, and Volume 2, question 63, Reference 47, showed the MOD7A code version still had difficulty calculating the effects of turnaround times, cooldown rate, and quench times. Similar trends were found with the MOD7 code version. Westinghouse attributed the MOD7A results to overprediction of the entrainment rate and lower heat transfer to the vapor just above the quench front (see Volume 2, question 63). The above areas are of concern because of their potential effects on PCT and rod oxidation. To address these issues, Westinghouse revised its uncertainty methodology to account for these effects. For PCT, Westinghouse addressed these effects by determining heat transfer multipliers based on comparisons to test data that are applied in the uncertainty evaluation. For oxidation, see the methodology discussed in Section 13 of this report. As, discussed in that section, the oxidation methodology adequately accounts for the effects of the above issues on oxidation using a time stretching approach. For the effects of turnaround time on PCT, see also Section B.1 of this report. As discussed in that section, Westinghouse showed that turnaround time was adequately accounted for through the break flow/condensation run matrix. Also, WCOBRA/TRAC tended to overpredict quench time and turnaround time for the gravity reflood tests, which are the tests most representative of the PWR. Based on this, INEL considers the bottom entrainment model adequate for realistic LBLOCA analyses. This is because: (a) the model adequately calculated bundle mass and (b) Westinghouse's methodology adequately accounts for the uncertainties due to the bottom entrainment model.

The code entrainment models for top flooding situations has models for sputtering at the top quench front on the rods and liquid falling through the UCP. Westinghouse discussed the basis for the sputtering front droplet size in response to Volume 1, question 86, Reference 10. The droplet size

generated by the orifice model is limited by a Weber number criterion (see Volume 1, question 87, Reference 8). INEL review of this section found it adequate for LBLOCA in three- and four-loop plants with cold leg injection because the models appear appropriate for the situation and little liquid was found to fall into the core from the upper plenum (see Volume 3, question 11, Reference 42). However, it was concluded additional information was needed for UPI plants.

The entrained droplets are shattered when they impact against a bundle rod spacer grid and WCOBRA/TRAC accounts for this effect. In response to Volume 1, question 92, Reference 45, Westinghouse justified the parameters used in the breakup model (see Eqn. 4-173).

WCOBRA/TRAC allows for the deentrainment of drops due to a variety of mechanisms including contact with the liquid film, cross flow deentrainment on structures, area changes, and flow into liquid pools or onto solid surfaces. The INEL reviewed the models used against the original references or had Westinghouse clarify the basis for the model (see Volume 1, questions 94 to 96, References 33 and 8). INEL found them adequate for LBLOCA because the models were implemented consistent with the original references. Also, the models were used in a wide variety of WCOBRA/TRAC code assessments. For CQD Eqn. 4-186, Whalley (Reference 148) noted that the mass transfer coefficient could be written as a function of the surface tension based on the data presented in the reference. In Reference 214, Attachment 3, Westinghouse noted its research let it to conclude that Eqn. 4-186 was not developed by Whalley but the COBRA/TRAC developers following the suggestion of Whalley. To verify Eqn. 4-186, Westinghouse compared Eqn. 4-186 output to the Whalley data and showed it accurately represented the data.

Based on its review summarized above, the INEL concluded the WCOBRA/TRAC vessel wall and interfacial drag models are adequate.

1-D Component Models

The INEL reviewed the one-dimensional momentum transfer and relative velocity models discussed in CQD Section 4-7. A number of questions arose from this review (Volume 1, questions 97 to 108, Attachment 1, Reference 3),

and Westinghouse adequately responded to these questions. For example, in response to Volume 1, question 47c, Reference 11, Westinghouse noted the one-dimensional, annular flow two-phase friction factor multiplier originated from TRAC-PD2, Reference 62, but was verified by comparison to the HTFS two-phase friction multiplier, Reference 134, in CQD Figures 4-8 to 4-11. INEL review of those figures found the two multipliers gave comparable results over a wide range of conditions.

Another question (Volume 1, question 103, Reference 35) asked Westinghouse to clarify why the CQD formulations for the drift velocities were not consistent with the original Ishii reference (Reference 142). Westinghouse's response showed the apparent differences were only due to the different formulations of the drift velocity used in the CQD and Ishii's report. Finally, the INEL reviewed the WCOBRA/TRAC approach to finding the horizontal drift velocity by taking the minimum of Eqns. 4-222 to 4-224. Westinghouse responded by showing that taking the minimum resulted in choosing the appropriate drift velocity based on pipe size and void fraction (see response to Volume 1, question 106, Reference 7).

As discussed above, a homogeneous two-phase friction model is applied (Eqns. 4-207, 4-209, and 4-211) if the void fraction is greater than 0.9995, with linear interpolation between the annular model (used for void fractions below 0.9) and the homogeneous model (used for void fraction greater than 0.9995). Westinghouse's response to Volume 1, question 100, Reference 11, verified the homogeneous model by comparisons to other models. INEL review of that response found good comparisons between the models.

Therefore, based on the good comparisons to the HTFS correlation for the annular flow two-phase model shown in the CQD, and the good comparisons of the homogeneous model to the other models in Westinghouse's response to Volume 1, question 100, the INEL considers the loop two-phase friction model adequate for LBLOCA analyses.

A.4 Critical Flow Models - CQD Section 4-8

A.4.1 Model Description

WCOBRA/TRAC allows two approaches to calculating critical flow: the TRAC/PD2 approach and the critical flow model package from TRAC-PF1/MOD1.

The TRAC/PD2 approach uses the 6 conservation equations and the constitutive relationships to calculate natural choking. To use this approach, the region where critical flow is expected to occur must be nodalized with cells of very small length.

The TRAC/PF1 critical flow model uses a modified form of the Burnell model for subcooled flow, and the two-phase model was developed using a characteristic analysis approach. The model is void fraction dependent with subcooled, two-phase, and single-phase vapor models. The subcooled and two-phase models are connected by linear interpolation to prevent discontinuity in the calculated critical flow. Westinghouse noted in the CQD that the TRAC/PF1 model is used in PWR LBLOCA analyses because of a reduced bias and uncertainty when compared to the TRAC/PD2 model. The uncertainty analysis performed by Westinghouse on the TRAC/PF1 critical flow model is discussed in Sections 6 and 9.2 of this report.

A.4.2 INEL Review of Critical Flow - Section 4-8

The choked flow models used in WCOBRA/TRAC are standard in terms of using a method of characteristics approach. It is stated in the CQD on page 4-131 that at homogeneous conditions the choked flow model results in the standard HEM model, while if any non-equilibrium is present, the choked flow conditions can deviate appreciably from the HEM model. Based on the standard modeling approach, the Westinghouse model is adequate for LOCA applications.

Westinghouse, in Reference 214, Attachment 9, gave additional explanation on its use of the full Method of Characteristics model for each time step in the code implementation of choked flow. In the above reference, Westinghouse also committed to include the information in the CQD.

Westinghouse noted that the choked flow solution is implemented in the pressure solution of the code rather than in the back substitution step after solving the pressure equation. This approach results in a smoother pressure and flow response in the code. Based on Reference 214, Attachment 9, Westinghouse will document this information in the CQD.

A.5 Interfacial Heat and Mass Transfer Models - CQD Section 5

A.5.1 Model Description

In WCOBRA/TRAC, interfacial heat and mass transfer depends on the interfacial heat transfer coefficient and the interfacial area. The models used for interfacial area are discussed in Section A.2 of this report, while the interfacial heat transfer coefficients are discussed below. Westinghouse combines the two into interfacial heat transfer factors.

The interfacial heat transfer coefficients depend on the flow regime and whether the fluid (vapor, continuous liquid, and entrained droplets) is superheated or subcooled. WCOBRA/TRAC treats the interfacial heat transfer by assuming a saturated interface between the phases with heat transfer to or from the saturated interface.

Westinghouse also noted that metastable states (superheated liquid and subcooled vapor) are inherently unstable and are rarely encountered in LBLOCA analyses. For metastable fluids, Westinghouse's approach in WCOBRA/TRAC was to drive the metastable states to saturation by applying large interfacial heat transfer coefficients. This is true of both the 1-D and vessel models. In its response to Volume 1, question 111, References 42 and 45, Westinghouse noted the HTC's that result for these regimes are designed to cause sufficient vaporization of superheated liquid and condensation of subcooled steam to maintain the phase temperatures near saturation. Westinghouse's response also showed that because of the large HTC's involved a very short time would be required to reduce superheated liquid to a temperature close to saturation. See the Volume 1, question 111 response for details. Based on these considerations, INEL considers the metastable models adequate, and the vessel and 1-D component review that follows focuses on the more important subcooled liquid and superheated vapor regimes.

Presentation of the details of the interfacial heat and mass transfer models are beyond the scope of this report because of the large number of models and correlations involved. Therefore, the reader is referred to Section 5 of the Westinghouse CQD for the details of these models.

A.5.2 INEL Review of CQD Section 5

Vessel Interfacial Heat Transfer Models

The INEL reviewed Section 5 in detail, and the review resulted in a number of questions that Westinghouse responded to during the review process (see Volume 1, questions 111 to 151, Attachment 1, Reference 3). Westinghouse responded adequately to all questions. In most cases, the INEL checked the CQD model description against the original reference cited by Westinghouse and asked them to justify any differences. For example, Volume 1, question 116, Reference 29, asked Westinghouse to clarify differences between CQD Eqns. 5-11 and 5-12 and the original reference from Wallis.¹⁵³ Westinghouse's response adequately described the process by which the CQD equations were derived from the original reference.

In another case, a question (see Volume 1, questions 113a and b, References 33 and 7) asked Westinghouse to justify using a model (Eqn. 5-4) developed for heat transfer from a copper sphere to air for heat transfer from small bubbles to subcooled liquid. The questions also asked Westinghouse to justify the basis for the equation chosen from the original reference¹⁵⁴ because several forms of the equation were available. For use of the model for bubble heat transfer to subcooled liquid, Westinghouse noted the equation was used to simulate a large number of experiments, and it can be applied in PWR calculations because of this extended assessment. That is, Westinghouse extended the range of applicability of the original equation by extending the data base against which the equation was assessed. Regarding the choice of the equation, Westinghouse compared the various forms of the equation from the original reference and several other works. The comparison showed that use of Eqn. 5-4 in the CQD was within the range of Nusselt numbers calculated by the other correlations, and that there was considerable scatter in the data used to develop the correlations. Based on these considerations, the INEL found use of Eqn. 5-4 adequate.

In its response to Volume 1, question 111b (References 42 and 45), Westinghouse provided an extensive review of the interphase heat transfer models and correlations used in the vessel portion as described in CQD Section 5. They noted the interfacial heat transfer models are based on several basic models: (a) conduction within a subcooled liquid drop, (b) forced convection from superheated vapor to a liquid drop, (c) forced convection from a bubble to subcooled liquid, (d) forced convection from superheated vapor to a liquid film, and (e) forced convection from vapor to a subcooled liquid film.

In bubbly flow (small bubble and small to large bubble regimes), when the liquid is subcooled, Westinghouse showed the bubble HTC model in WCOBRA/TRAC (Eqn. 5-4) gives values consistent with those found in another work.¹⁵⁵ To evaluate the effect of the vapor side models, Westinghouse performed sensitivity studies to determine the effect of these models (Eqns. 5-1 (small bubble) and 5-14 (small to large bubble)). These were provided in the response to Volume 1, question 117, Reference 33. In the sensitivity case, the HTC in the small bubble regime was reduced by a large number, and Eqn. 5-14 was replaced with a correlation more representative of the small to large bubble regime but gave HTCs similar to Eqn. 5-14. In this case, changing the interfacial heat transfer from the superheated bubbles resulted in a small PCT change. Thus, the INEL concluded the calculated results are not very sensitive to the models in this area. Therefore, the bubbly models are considered adequate.

For the droplet flow regime on the liquid side, Westinghouse compared the WCOBRA/TRAC values of droplet growth based on Eqn. 5-31 to those measured by Ford.¹⁵⁶ The results, presented in Volume 1, question 123, Reference 11, showed the droplet growth rate was overpredicted early in time but well predicted later in the test. This indicates the condensation model in WCOBRA/TRAC for this regime is giving approximately the correct results. On the vapor side, Westinghouse noted that evaporation of droplets in superheated steam has been the subject of much investigation that supports the model used in WCOBRA/TRAC (Eqn. 5-26). The INEL notes that the original basis for Eqn. 5-26¹⁵⁷ is the one represented in the code, droplet evaporation. Based on the adequate comparison to data for the liquid side HTC and the use of an

appropriate model for the vapor side HTC, the INEL finds the droplet models adequate.

In film flow, both the liquid side and vapor side HTCs are based on the Colburn analogy.¹⁵⁸ On the liquid side, Westinghouse's response to Volume 1, question 121, Reference 33, compared the WCOBRA/TRAC model (Eqn. 5-27) to more recent work (References 159 and 160). The results showed the code model gave HTCs of approximately the same magnitude as the correlations in the references (except for the case using a gas Reynolds number of 50,000 and the equation in NUREG/CR-2783 developed for rough film surfaces). Based on this review and given the scatter in the data for this type of heat transfer, the INEL concluded the film liquid side model was adequate. For the vapor side film model, Westinghouse's response to Volume 1, question 121, Reference 33, showed the WCOBRA/TRAC HTC (Eqn. 5-25) was higher than other models. To evaluate this overprediction, the sensitivity run provided by Westinghouse in its response to Volume 1, question 117, Reference 33, reduced the film HTC from superheated vapor by an appropriate amount. As discussed above, this sensitivity run only showed a small PCT change. Thus, the INEL concluded the calculated results are not very sensitive to the models in this area. Therefore, the vapor side film models are considered adequate.

All condensation models (heat transfer to subcooled liquid) in the vessel are limited by a mass transfer limit (Eqn. 5-12) based on the work of Wallis, Reference 153. This model accounts for the suppression of condensation by non-condensibles. INEL review of the reference found Westinghouse applied the equation as presented by Wallis to develop Eqn. 5-12 as a maximum limit on the interfacial HTC assuming non-condensibles are present. Eqn. 5-12 is used with the regime dependent HTC correlation for subcooled liquid in a minimum function to determine the condensation rate for the regime. For example, see Eqns. 5-13 and 5-37.

Eqn. 5-12 includes a friction factor that Westinghouse assumes to be the constant value given in its response to Volume 1, question 116, Reference 29. The friction factor used is consistent with that found for higher void fraction regimes, but not for lower void fraction regime such as bubbly flow. Westinghouse evaluated the mass transfer limit relative to the small bubble and the small to large bubble regimes in its response to question 116. In

that response, Westinghouse showed that the limit is basically a function of subcooling. In the study, Westinghouse increased the pressure but held the liquid temperature constant, increasing subcooling. As the pressure increased (subcooling increased), the difference between the mass transfer limit and the regime dependent HTC decreased. At the subcooling associated with a pressure of 500 psia in the study, the mass transfer limit HTC was smaller than the regime dependent HTC, and, therefore, would limit the condensation rate. The same effect would be found if the pressure was held constant and the subcooling of the water was increased. This indicates the model is working as desired to limit condensation rates if the code encounters situations where large condensation rates would be achieved. Large condensation rates result in the more rapid accumulation of non-condensibles at the interface, and this can limit condensation heat transfer (see discussion below). This is the effect Westinghouse is trying to model with the mass transfer limit.

As discussed above, application of the friction factor used in the mass transfer limit to low void fraction flow regimes was not directly supported by the value chosen. The mass transfer limit as applied to the bubbly flow regimes, however, does not greatly affect the calculated results. Sensitivity studies for IP2 and VRA provided in response to Volume 1, question 116, Reference 29 showed the effect on the calculated PCT was small when the mass transfer limit was removed from the analyses for the bubbly flow regimes in the vessel (void fractions less than approximately 70% based on the code logic) and 1-D components.

Westinghouse also evaluated the mass transfer limit in the response to Volume 1, question 134, Reference 37. Based on a detailed analysis of the effects of non-condensibles, Westinghouse showed that the higher the condensation rate, the lower the non-condensable gas concentration needed to affect the condensation rate. In its response to Volume 1, question 134, Westinghouse found the mass transfer limit used in WCOBRA/TRAC was approximately equivalent to a non-condensable gas concentration of 0.008 if the interface is smooth and 0.1 if the interface is rough. Based on Figure 134-5 of Volume 1, question 134, these values are consistent with the non-condensable gas present prior to the accumulators emptying and injecting the nitrogen cover gas (note: another model is used to represent condensation suppression due to the injection of the nitrogen cover gas). This implies the

interfacial HTC is limited by Eqn. 5-12 even if only relatively small amounts of non-condensibles are assumed to be present.

Also, Westinghouse will range the vessel condensation rate directly as part of the WCOBRA/TRAC uncertainty analysis. This is discussed further in Section 6 of this report on Westinghouse's propagation of uncertainty analysis.

Based on the above information, the INEL finds the mass transfer limit adequate. The model is an upper bound and will limit the condensation rate if large condensation rates are encountered in a manner consistent with the amount of non-condensable present prior to accumulator nitrogen injection. The model uses a constant friction factor appropriate for high void fractions but was shown not to have a significant effect on PWR analyses in the bubbly regimes. Also, the model uncertainty is ranged in the code uncertainty evaluation.

Under the title of complex flow regimes, Westinghouse investigated those modeled as large liquid drops (the top deluge regime and inverted annular and slug regimes) and the churn-turbulent regime. For the large liquid drop regimes, Westinghouse compared the WCOBRA/TRAC equations with Reference 161. Westinghouse showed the models in WCOBRA/TRAC gave results for drops with internal circulation that increased the HTC in approximately the right amount relative to rigid drop models. On the vapor side, Westinghouse showed the models in the code were used within the range of correlations for drops without internal circulation, and slightly outside the range of correlations for drops with internal circulation based on Reference 161. Based on this, the INEL finds the large drop models adequate.

In the churn-turbulent flow regime, the response to Volume 1, question 111b, Reference 42, focused on condensation heat transfer. In its response, Westinghouse compared the condensation efficiency calculated by WCOBRA/TRAC to that estimated for 1/5th scale Creare tests with low and high ECC injection rates, Reference 107, and UPTF data, Reference 64. The estimates of condensation efficiencies from the tests showed a wide variation, and the WCOBRA/TRAC results fall within the scatter of the data. Also, the condensation model is ranged in the uncertainty evaluation. Based on this,

the INEL considers the liquid side models in the churn-turbulent regime to be adequate. On the vapor side, Westinghouse evaluated the sensitivity of the calculated results in PWR analyses by reducing the film coefficient by an appropriate amount. Based on the response to Volume 1, question 117, Reference 33, the effect was a small PCT change. The drop HTC was not varied in this study; however, the evaporation of drops in superheated vapor is well supported physically and experimentally. The droplet evaporation model in WCOBRA/TRAC, Eqn. 5-26, is based on a correlation developed from experiments on droplet evaporation, Reference 157. Therefore, the INEL considers the churn-turbulent vapor side models adequate.

1-D Interfacial Heat Transfer Models

In 1-D components, the heat transfer to subcooled liquid is based on a constant Stanton number approach (Eqn. 5-122), and the condensation HTC is limited by the same mass transfer limit as the vessel model (Eqn. 5-12) through use of a minimum function (see Eqn. 5-141, for example). In the CQD, Westinghouse stated the Stanton number chosen was based on simulations of CCTF reflood tests.¹⁶² Based on CQD Figure 5-3, the Stanton number chosen will provide a HTC that approximates the lower range of the available correlations.

For WCOBRA/TRAC 1-D components, Westinghouse assumes an interfacial area for subcooled liquid as discussed on page 5-49 of the CQD. In Attachment 1 of Reference 11 Westinghouse showed this approach gives an interfacial area within an order of magnitude of the expected interfacial area based on the calculated flow regimes. The same response showed that WCOBRA/TRAC tended to underpredict the subcooled liquid HTC relative to the results from Northwestern University condensation tests (Reference 96), but the overall condensation rate was calculated relatively well because the interfacial area was overestimated. Although the Northwestern results indicate a compensating error, INEL considers the model adequate for 1-D components because the overall condensation rate is still calculated well as shown in the full-scale UPTF test results discussed below.

Westinghouse also evaluated the condensation mass transfer limit for 1-D models (see its response to Volume 1, question 116, Reference 29). There Westinghouse showed that the limit is basically a function of subcooling as it

was for the vessel models. In the study, Westinghouse increased the pressure but held the liquid temperature constant, increasing subcooling. As the pressure increased (subcooling increased), the difference between the mass transfer limit and Eqn. 5-122 decreased. At the subcooling associated with a pressure of 200 or 500 psia in the study, the mass transfer limit HTC was smaller than the Eqn. 5-122, and, therefore, would limit the condensation rate. The same effect would be found if the pressure was held constant and the subcooling of the water was increased. This indicates the model is working as desired to limit condensation rates if the code encounters a situation where large condensation rates would be achieved, and the accumulation of non-condensibles at the interface could occur as discussed for the vessel model. In Reference 206, Attachment 6, Westinghouse verified the sensitivity study on the effect of the mass transfer limit for the vessel models included the 1-D models. Therefore, a small effect on the calculated PCT for IP2 and VRA was found when the mass transfer limit was removed from the analyses for the vessel and 1-D bubbly flow regimes.

The latest LBLOCA methodology does not include a ranging of the condensation efficiency in 1-D components as is done for the vessel. The INEL considers this adequate based on CQD Figures 15-3-48/49. These figures show the condensation efficiencies calculated for full-scale UPTF Tests 8 and 25 (cold leg steam/water mixing tests) and the corresponding WCOBRA/TRAC calculations. WCOBRA/TRAC does a reasonable job of calculating the condensation efficiencies estimated from the experimental data, and the range of efficiencies in the data is smaller than in the vessel. CQD Section 15-3-3 also showed that WCOBRA/TRAC did an adequate job of calculating the cold leg exit temperatures in both the UPTF tests and Westinghouse/EPRI 1/3rd scale steam/water mixing tests, Reference 97.

Although a compensating error was found, the INEL considers the WCOBRA/TRAC 1-D condensation models adequate. This based on the good overall results for the cold leg in the full-scale UPTF results. Based on the condensation information reviewed, INEL concluded that WCOBRA/TRAC does not have significant compensating errors in the 1-D condensation models that would compromise the code's ability to realistically calculate LBLOCAs.

On the superheated vapor side, Westinghouse uses flow regime specific correlations. Westinghouse information in Attachment 1 of Reference 11 showed the most important superheated vapor heat transfer regime is the annular/mist regime in the hot leg during reflood. In its evaluation, Westinghouse noted WCOBRA/TRAC tended to predict too much entrainment in 1-D components, and the high mixture velocities during this period will result in pure droplet flow. Westinghouse concluded, therefore, that the heat transfer rate from superheated vapor to the liquid would most likely be overpredicted in the hot leg and other 1-D components.

However, further analysis by Westinghouse showed this was not a significant problem with the code. This is because reverse heat transfer from the secondary side of the steam generator (SG) during a LBLOCA vaporizes all droplets and superheats the steam to the secondary side temperature by the time the steam exits the SG tubes. Westinghouse WCOBRA/TRAC analyses of Westinghouse SG tests (Reference 11, Appendix A) and LOFT (see CQD Figure 14-4-41) show the code adequately predicts the steam superheat exiting the SG tubes. Based on these considerations, the INEL finds the WCOBRA/TRAC 1-D component superheated vapor models adequate.

A.6 Wall Heat Transfer Models - CQD Section 6

A.6.1 Model Description

The wall heat transfer models are discussed in CQD Section 6. Separate models are provided for the vessel component and the one-dimensional loop components. The vessel heat transfer models are based on the COBRA-TF program, and the loop models are based on the TRAC/PD2 program.

The vessel heat transfer models follow the standard boiling curve: single-phase liquid, subcooled nucleate boiling, saturated nucleate boiling, transition boiling, inverted annular film boiling, dispersed droplet film boiling, and single-phase vapor. For the vessel, models are supplied to calculate CHF and the minimum film boiling temperature. In the vessel, three HTC's are calculated for each heat transfer regime: wall to vapor, wall to liquid for sensible heat, and wall to liquid for latent heat. In some cases, the HTC is set to zero (for example, the vapor HTC in the single-phase liquid

regime). To account for a variety of fluid conditions, more than one coefficient may be calculated for each heat transfer regime. For example, single-phase vapor heat transfer is based on taking the maximum of a natural convection coefficient, a laminar coefficient, and a turbulent coefficient. In the case of transition boiling, three separate models are also used to determine the heat transfer coefficient. Radiation heat transfer from the wall to the vapor and droplets is calculated by WCOBRA/TRAC and included in the appropriate heat transfer coefficients.

In the vessel dispersed flow film boiling regime, Westinghouse models increased heat transfer due to turbulence from interfacial shear with the droplets and increased turbulence due to fuel bundle grids. WCOBRA/TRAC also accounts for the grid effect in single-phase vapor heat transfer. The increase in heat transfer due to droplet interfacial shear is calculated based on the analogy between wall shear stress and heat transfer described by Kays.¹⁶³ The grid heat transfer enhancement is based on the work of Yao, Hochreiter, and Leech.¹⁶⁴

The loop heat transfer models include: natural and forced convection to single-phase liquid, nucleate boiling, transition boiling, film boiling, convection to single-phase vapor, a two-phase mixture model (used if CHF is not expected), and a separate condensation model. Models are also included to calculate CHF and the minimum film boiling temperature. Where appropriate, the loop models calculate two heat transfer coefficients, wall to vapor and wall to liquid. As with the vessel, the loop models may calculate more than one coefficient for each heat transfer regime.

A.6.2 INEL Review of COD Section 6

The INEL reviewed Section 6 in detail, and the review resulted in a number of questions that Westinghouse responded to during the review process (see Volume 1, questions 152 to 220, Reference 3). Westinghouse responded adequately to all questions.

Vessel Wall Heat Transfer

In most cases, the INEL checked the CQD model description against the original reference cited by Westinghouse and asked them to justify any differences. For example, Volume 1, question 172, Reference 8, asked Westinghouse to clarify differences between CQD Eqns. 6-77, 6-128, and 6-220 and the original reference by Forslund and Roshenow.¹⁰¹ Westinghouse's response showed the difference was due to a parameter change, and the parameter change was properly accounted for when deriving the CQD equations.

Another example is Volume 1, question 186, Reference 11 which asked Westinghouse why the CQD version of the Bromley film boiling correlation was different from a number of different references. Westinghouse's response discussed the differences between the Bromley correlation¹⁶⁵ and several versions of a modified Bromley correlation (for example, see References 166 and 167). The response also provided the correct reference (Reference 166) for the modified Bromley correlation used in WCOBRA/TRAC.

Volume 1, question 158, Reference 36, asked Westinghouse to clarify the use of Reference 168 to justify CQD Eqns. 6-33/34 (used in the nucleate boiling regime) because INEL review of the reference could not find corresponding equations. Westinghouse's response clarified the basis for the CQD equations relative to the original reference. The response showed how the equations in the CQD could be derived from the reference by assuming the single-phase convection to liquid component of subcooled nucleate boiling becomes small relative to the boiling component. To support this assumption, Westinghouse noted that Figure 9 in Reference 17 showed the single-phase convective HTC was 10% or less of the total HTC at wall superheats of approximately 10°F or more. Based on this information, the INEL concluded Westinghouse had adequately clarified the derivation of CQD Eqns. 6-33/34 from Reference 168.

In Reference 17, Westinghouse discussed the vessel wall heat transfer models in detail, including ramps and heat transfer regime transition smoothing techniques. The vessel wall heat transfer map used to select the various heat transfer regimes is shown in CQD Figure 6-3. For the single-phase liquid regime, the HTC is based on the maximum of Eqn. 6-11 (rod bundle

laminar convection based on Reference 169 and Eqn. 6-12 (forced convection from Dittus-Boelter). Westinghouse noted the use of the maximum HTC results in the forced convection correlation being used down to the Reynolds number provided in Reference 17, and this is below the normal laminar/turbulent transition of 2000. However, Figure 7 of Reference 17, showed that between a Reynolds number of 2000 and the WCOBRA/TRAC transition point, the difference between the two HTCs was less than 50%. Given the small range and the 25% uncertainty associated with HTCs, Westinghouse concluded the logic was adequate. The INEL also notes that the single-phase HTC would be applied after the rod quenches and below the quench front; thus the impact of the inaccuracies noted by Westinghouse would not affect PCT or rod oxidation. Therefore, the single-phase liquid model is considered adequate.

Subcooled and saturated nucleate boiling HTCs are calculated with the Chen correlation (Reference 170), although the information in Reference 17 indicated approximations were used for S_{Chen} , F_{Chen} , and ΔP . For the saturated regime, Westinghouse compared the model as implemented in WCOBRA/TRAC with hand calculations based on the Chen model described in Collier, 2nd Edition, Reference 171. See Figure 8, Reference 17. The agreement was good indicating the approximations above are accurate.

To evaluate the subcooled nucleate boiling regime, Westinghouse setup a simple tube model to evaluate the code calculated values for the point on the heated length when fully developed subcooled nucleate boiling begins, and the amount of subcooling present at that location. These were compared to hand calculations based on Eqns. 6.7 to 6.9 in Collier, Reference 171. Westinghouse compared the hand and code calculated values in Reference 17 and found good agreement. Westinghouse concluded the subcooled nucleate boiling model was able to do a reasonable job of calculating the length and remaining subcooling as the transition to saturated nucleate boiling begins. This implies the code models for subcooled boiling calculate the sensible heat transfer to liquid correctly. The Reference 17 information also compared WCOBRA/TRAC results to Figure 6.4 (the Saha and Zuber model) of Collier, Reference 171. Again, good agreement was found. Finally, Westinghouse compared the WCOBRA/TRAC void fraction at which fully developed subcooled nucleate boiling begins to the data of Levy¹⁷² in Collier, Reference 171, Table 6.1 and found the code calculated values were consistent with those

estimated by Levy. Based on the above considerations, the INEL concluded the subcooled and saturated nucleate boiling models are adequate.

The Reference 17 submittal evaluated the transition boiling models in WCOBRA/TRAC in several ways. First, Westinghouse compared HTC's calculated by WCOBRA/TRAC for two FLECHT-SEASET tests (one with a low flooding rate and the other with a high flooding rate) to the Hsu¹⁷³ and Ellion¹⁷⁴ correlations. These correlations were chosen because they were based on data ranges that approximated the two FLECHT-SEASET tests. For the low flooding rate test at low wall superheats (less than 300°F), the Hsu and Ellion correlations both gave higher HTC's than WCOBRA/TRAC. However, for the high flooding rate test at low wall superheats (less than 300°F), the Hsu correlation bounded most but not all of the WCOBRA/TRAC HTC's while the Ellion correlation again gave higher HTC's. At higher wall superheats (greater than 300°F), the WCOBRA/TRAC HTC's and the HTC's from Hsu and Ellion were in good agreement for both tests. Based on this, it appears the WCOBRA/TRAC models give approximately the right shape for the transition boiling curve and HTC's of the right order of magnitude.

To investigate further the effects of ramps and splitting, Westinghouse evaluated specific transition boiling conditions. The effects of subcooling were evaluated by using the Cheng correlation¹⁷⁵ to compare to WCOBRA/TRAC results. Westinghouse noted that transition boiling Model 2 (Eqns. 6-82 to 6-84) is used for low flow, low quality transition boiling. Both the Cheng correlation and WCOBRA/TRAC Model 2 show a HTC increase when the subcooling increases, but the WCOBRA/TRAC calculated increase is less than that calculated by the Cheng correlation. Westinghouse also noted that transition boiling HTC's are difficult to measure and estimate leading to large uncertainties. Therefore, Westinghouse concluded WCOBRA/TRAC does a reasonable job of modeling the increase in HTC with increased subcooling.

The next effect evaluated was high quality. Westinghouse noted that transition boiling Model 1 (Eqns. 6-75 to 6-81) is used for high void transition boiling, and it compared the WCOBRA/TRAC model to several correlations. Based on Figures 19 to 21 in Reference 17, the WCOBRA/TRAC results fall within the ranges of the various correlations.

Based on the above showing that WCOBRA/TRAC gives transition boiling HTC's consistent with other correlations, the INEL concluded the transition boiling models are adequate.

The inverted annular film boiling (IAFB) regime HTC is calculated with a modified Bromley correlation based on Reference 166 (see CQD Eqn. 6-102) and a radiation term to the liquid core, CQD Eqn. 6-104. In this regime, the modified Bromley plus radiation heat flux is split between the continuous liquid, entrained liquid, and the vapor, and Westinghouse verified the sum of the phasic heat transfer HTC's equals that for Eqn. 6-102 plus Eqn. 6-104 (see Volume 1, question 188, Reference 36). In Reference 17, Westinghouse showed that IAFB occurred in the test simulations over a range of conditions very similar to that in PWR analyses. It was also found that the IAFB regime usually does not exist for long time periods in PWR analyses. Based on the above considerations, the INEL considers the IAFB HTC models adequate.

The inverted annular dispersed flow (IADF) regime is a transition regime between IAFB and dispersed flow film boiling (DFFB). It is calculated by interpolating on void fraction the HTC's from IAFB and DFFB. Figure 33 (Reference 17) shows that the liquid HTC for the IADF regime generally bounded above by IAFB liquid HTC's and below by DFFB liquid HTC's. This is expected based on how the IADF HTC is calculated.

The DFFB regime is calculated by superposition of the following effects: forced convection and radiation to steam, radiation to entrained drops, and direct contact drop/wall heat transfer. The INEL notes all these heat transfer mechanisms will be active during DFFB. Westinghouse's analysis of the various components of DFFB heat transfer in Reference 17 showed that the liquid HTC (radiation plus direct contact) is approximately 5% of the vapor HTC at low flooding rates (approximately 0.81 in/s) and even less (approximately 2%) at high flooding rates (8 in/s) (see Figure 36). The DFFB model is discussed more fully in Appendix D of this report. Here it is noted Westinghouse compared the code results to the Dougal-Rohsenow correlation¹⁷⁶ and the Dittus-Boelter correlation (assuming all liquid in the form of vapor) in Figures 34 and 35 of Submittal K. The comparison shows that WCOBRA/TRAC results are generally bounded by the two approaches, but the comparison does not allow more than a reasonableness check on the magnitude of the WCOBRA/TRAC

HTC. To quantify the uncertainty in DFFB HTC, Westinghouse includes ranging of the WCOBRA/TRAC calculated HTC in the uncertainty propagation as discussed below.

The heat transfer enhancement due to steam/droplet turbulence applied in the DFFB was reviewed against the original work, Reference 163. Because INEL review of Reference 163 could not find the supporting information, a question was posed to Westinghouse. Westinghouse's response to Volume 1, question 189a, Reference 12, showed how the CQD equations were developed from Reference 163. Based on the correct use of the original work and the other factors noted in Appendix D, the INEL finds the WCOBRA/TRAC steam/droplet turbulence model adequate. However, INEL asked Westinghouse to clarify the effect of the different f_w on CQD pg 6-47 and Reference 163, Eqn. 7-16. In Reference 206, Attachment 5, Westinghouse noted the difference was due to the example in Reference 163 being for laminar flow while the f_w on CQD page 6-47 was based on turbulent flow. In its response, Westinghouse evaluated the effect of only applying a turbulent equation for f_w and found that is was conservative to do so down to the vapor Reynolds number given in the response. While it may be appropriate to use a laminar correlation below this value, Westinghouse also stated that entrainment at the quench front would not occur at these Reynolds numbers, and the two-phase enhancement model is only applied if droplets are present. Based on this, Westinghouse concluded, and the INEL agrees, that the used of the turbulent expression for all Reynolds numbers is adequate.

The INEL also notes that the Westinghouse response in Reference 206, Attachment 5, derived the expressions for the shear stress to the wall and to the vapor shown in CQD Eqns. 6-120 and 6-121. Westinghouse concluded that the wall shear stress equation used the incorrect friction factor. The effect was to have a larger than appropriate two-phase enhancement factor. The impact was small because WCOBRA/TRAC has an upper limit on the two-phase enhancement factor (see CQD Section 6-2-8). To assess the effect, Westinghouse reevaluated FLECHT-SEASET Test 31805 with a corrected version of WCOBRA/TRAC. There was little impact on the PCT, and the results from the corrected code version had slightly later quench times. Westinghouse concluded the effect was small, and the INEL agrees. Therefore, Westinghouse proposed that the error be tracked and corrected when other changes to the code are required.

The INEL notes that the DFFB regime is very important in LBLOCA analyses because the reflood temperature increase is turned over as a result of DFFB. Thus, PCT is directly related to the HTCs calculated by the DFFB regime. To account for the HTC uncertainty, Westinghouse will range the reflood HTC as part of the WCOBRA/TRAC uncertainty evaluation (see Sections 6 and 9.2 of this report). This ranging will account for the uncertainties in the DFFB HTC calculation. Appendix D of this report gives a detailed review of the WCOBRA/TRAC DFFB model. While a number of concerns were noted in Appendix D, the INEL considered the overall model adequate because of conservatism in the model and the HTC ranging in the uncertainty evaluation. However, because of the potential for changes in one part of the DFFB model to affect the performance of the other parts of the model, the INEL would like to recommend the NRC Staff review the entire DFFB model should one part of the model be changed by Westinghouse in the future.

In the single-phase vapor regime, the HTC to liquid is assumed to be zero. The single-phase vapor regime is calculated by taking the maximum of several correlations as shown in CQD Eqn. 6-7. The turbulent correlation is the maximum of the Wong-Hochreiter and the Dittus-Boelter correlations, with the Wong-Hochreiter correlation usually selected if the Reynolds number is less than the value given in CQD Section 6-2-1. The laminar HTC is based on a Nusselt number given in CQD Eqn. 6-4, which is supported by FLECHT data (see Volume 1, question 151b, Reference 8) and Reference 205, Attachment 5. The code logic uses the Wong-Hochreiter correlation until it is less than the laminar correlation. By equating Eqns. 6-4 and 6-6 and assuming the Prandtl number is 1.0, Westinghouse calculated the Reynolds number where the HTC transition occurs (Volume 1, question 152, Reference 8). The value given in Westinghouse's response to Volume 1, question 152, is less than the normal Reynolds number of 2000 for the completion of the turbulent/laminar transition. It is also less than the RG Section 3.9.3.1 listed value of 2000. In Reference 205, Attachment 5, Westinghouse showed that test data and other correlations support a Nusselt number greater than the WCOBRA/TRAC value in CQD Eqn. 6-4 down to a Reynolds number less than the WCOBRA/TRAC transition point. This resolved INEL questions on WCOBRA/TRAC modeling in this area.

In both the single-phase vapor regime and the single-phase liquid component of DFFB, Westinghouse applies a grid enhancement model. This model

is based on Reference 164. INEL review of the reference found Westinghouse implemented the model in WCOBRA/TRAC as described in the reference; therefore, the model is considered adequate.

In response to Volume 1, question 152, Reference 37, Westinghouse evaluated the vessel heat transfer assessment range of conditions relative to that expected in PWR analyses. On reviewing Table 1 of that response, the INEL found that the Westinghouse heat transfer package assessment covered the appropriate range of conditions except for vapor superheat in DFFB and low vapor Reynolds numbers in single-phase vapor heat transfer. The DFFB vapor superheat entries were experimental maximum/minimum of 400 and 1700°F, and the PWR range was <1800°F. The INEL concluded the experimental maximum was not entered correctly as the maximum vapor superheat for FLECHT-SEASET Test 31805 was shown to be 1800°F in Figure 38, Reference 17. Therefore, the DFFB vapor superheat range was appropriately covered. The vapor Reynolds number entries were experimental minimum/maximum of 3500 and 12,000, and the PWR range was 2500-9500. The INEL again concluded Table 1 was wrong as Table 3 showed a minimum experimental vapor Reynolds number of 2750. However, this is still higher than the PWR range. Therefore, INEL asked Westinghouse to clarify how the experiment range of conditions covers that expected in the PWR. Based on Reference 205, Attachment 5, INEL concluded that Westinghouse has appropriate experimental data for the lower end of the range for single-phase vapor Reynolds number. Therefore, INEL concluded the Westinghouse experimental assessment was appropriate to support application of WCOBRA/TRAC to PWR LBLOCA analyses for three- and four-loop PWRs with cold leg ECC injection.

The vessel radiation model to vapor and entrained droplets is based on the work of Sun, Gonzalez, and Tien.¹⁷⁷ The vapor/droplet absorption coefficients and emissivities are based on References 177, 178, and 179. See Westinghouse response to Volume 1, question 192, Reference 11. Westinghouse also verified the adequacy of the droplet absorption efficiency assumed in WCOBRA/TRAC in its response to Volume 1, question 190, Reference 8. Radiation to an inverted annular liquid column is based on a concentric cylinder model as in Holman, Reference 129. For the inverted annular liquid column model, constant wall and vapor emissivities are used as discussed on CQD page 6-58. Westinghouse provided the basis for these values in its response to Volume 1, question 194, Reference 8. The INEL reviewed the WCOBRA/TRAC radiation model

implementation against the original references and the supporting information provided by Westinghouse and found them consistent; therefore, the radiation model is considered adequate.

1-D Wall Heat Transfer

The 1-D wall heat transfer package is used in the loop components such as the hot and cold legs, pump suction, and SGs. Many of the same correlations used in the vessel model are applied in the 1-D models. See CQD Sections 6-3-1 to 6-3-8. The differences include:

- (a) Using the McAdams, Reference 136, correlation for single-phase liquid natural convection;
- (b) Laminar forced convection to liquid HTC using a Nusselt number of 4.0 based on Roshenow and Choi;¹⁸⁰
- (c) transition boiling HTC to liquid using a wall temperature based interpolation between the heat flux at CHF and the heat flux at the minimum film boiling temperature, T_{MIN} , (see Bjornard and Griffith in Reference 86). The HTC to vapor is based on the 1-D vapor film boiling HTCs (Note: the original coding and CQD discussion showed the 1-D transition boiling model included some double accounting of heat transfer; Westinghouse described the corrections it made to WCOBRA/TRAC in Volume 1, question 206, Reference 30); and
- (d) including the Dougall-Roshenow correlation (Eqn. 6-225), Reference 176; a McAdams natural convection correlation (Eqn. 6-228/9), Reference 136; and a form of the modified Bromley correlation (Eqn. 6-226) (see Bjornard and Griffith in Reference 86) for the vapor HTC in the film boiling regime.

In Reference 29, Westinghouse evaluated the loop wall heat transfer in a PWR analysis. Heat transfer to single-phase vapor and liquid were found to dominate. Westinghouse found the code generally calculated HTCs consistent with standard correlations such as Dittus-Boelter for single-phase vapor

(broken loop hot leg and intact loop SG) or single-phase liquid (intact loop cold legs).

Based on the similarity to the vessel package; the fact that differences are based on well known equations or simplifications considered appropriate for the 1-D models; and the lower importance of wall heat transfer in the 1-D components, the INEL concluded the 1-D wall heat transfer models are adequate.

CHF and T_{MIN} Correlations

The final models to review are the CHF and T_{MIN} models. In both the vessel and 1-D components, CHF is calculated using the Biasi correlation. This is a well-known and widely used CHF correlation, and the INEL considers it adequate. In addition, the vessel model includes the Zuber pool boiling correlation, as modified by Bjornard and Griffith, Reference 86, for low flow situations. Again, this is a well known and widely used CHF correlation, and the INEL considers this model adequate.

The vessel T_{MIN} model is based on the maximum of the homogeneous nucleation model (CQD Eqn. 6-97/98) (see Bjornard and Griffith in Reference 86) and Henry's modification¹⁸¹ of the Berenson correlation (Eqn. 6-99/100). Review of these equations against the original references found them to be correctly implemented in WCOBRA/TRAC. In the vessel, the value of T_{MIN} is also limited to maximum and minimum values given in CQD Eqn. 6-101. Westinghouse's response to Volume 1, question 185, Reference 8, showed these ranges were appropriate based on comparisons to data used in the CSAU report (Reference 61, Appendix N). Uncertainty in T_{MIN} is directly included in the revised uncertainty methodology. Therefore, these models are considered adequate.

The 1-D model for T_{MIN} is the maximum of a homogeneous nucleation model (Eqn. 6-212/213) and the Iloeje model¹⁸² (Eqn. 6-214/215). In the homogeneous nucleation model, the homogeneous nucleation temperature is assumed constant at the critical temperature of water. Based on the Bjornard and Griffith paper in Reference 86, the homogeneous nucleation temperature is an increasing function of pressure as it slowly approaches the critical temperature, varying from 615°F at 100 psia to 705.2°F at the critical pressure. Therefore, the

WCOBRA/TRAC homogeneous nucleation model will give a high estimate of T_{MIN} relative to a more accurate determination of the homogeneous nucleation temperature. However, this is considered adequate by the INEL for use in the 1-D components because an accurate determination of T_{MIN} is not as important in the 1-D components as it is in the vessel. The Iloeje correlation has a mass flux dependence and, to prevent WCOBRA/TRAC from calculating unrealistically high temperatures for T_{MIN} , a 10^5 lbm/ft²-hr upper limit on mass flux is imposed (see Volume 1, question 208, Reference 29). The responses to Volume 1, questions 207 and 208, Reference 29, showed the WCOBRA/TRAC 1-D models gave T_{MIN} results consistent with other code packages and models. Any uncertainties due to these models would be included in the WCOBRA/TRAC uncertainty analysis based on the comparisons to experimental data. Based on the above, the INEL considers the 1-D T_{MIN} models adequate.

A.7 Models for Heated and Unheated Structures - CQD Section 7

A.7.1 Model Description

The vessel model for heated structures allows WCOBRA/TRAC to model nuclear fuel rods, electrical heater rods, and tubes or walls that are expected to exceed the minimum film boiling temperature. An unheated conductor model is used for structures that are not expected to exceed the minimum film boiling temperature. WCOBRA/TRAC uses a finite difference form of the conduction equation based on the approach of Trent and Welty.¹⁸³ This approach allows unequal mesh spacing, temperature-dependent material properties, space dependent material properties, internal resistances (such as gaps), and radial heat generation profiles.

Several special models are included in WCOBRA/TRAC to allow the code to accurately represent a nuclear fuel rod and its response to a LBLOCA. The first is a quench front model. This model includes a fine mesh rezoning technique in the vicinity of the quench front to more accurately calculate heat transfer at the quench front. A two-dimensional heat transfer model is used when the fine mesh rezoning is applied. In this way, the quench front velocity is a function of axial and radial conduction, the boiling curve, and prequench heat transfer. The pellet-cladding gap model is also important to the nuclear fuel rod model. The model accounts for changes in the fuel rod

structure and the fill gas pressure that affect the gap conductance and fuel temperature during a transient. The model is based on the GAPCON¹⁸⁴ and FRAP¹⁸⁵ computer codes.

WCOBRA/TRAC includes models to account for fuel rod deformation: fuel pellet and cladding thermal expansion, cladding elastic deformation, cladding creep deformation, and cladding rupture. For Zircaloy cladding, the cladding rupture temperature correlation of Powers and Meyer, Reference 138, is used. A separate model is employed for Westinghouse's proprietary ZIRLO cladding. The effects of fuel rod deformation are incorporated into the thermal-hydraulic analysis by updating the following items each time step: the pellet-cladding gap, the rod surface area, and the effects of the rod deformation on the core cell continuity and momentum areas.

The fuel pellet and cladding radial and axial expansion models are from MATPRO-11, Version 1.¹⁸⁶ Cladding deformation due to pressure differences across the cladding are based on a thin shell approximation loaded with internal and external forces. The gap gas pressure model is similar to FRAP or GAPCON. If the gap closes, the internal stress comes from the radial displacement of the fuel with the fuel/cladding interface pressure given by Eqn. 7-49. CQD Section 7-4-1 discusses the models for fuel/cladding radial/axial effects due to temperature and pressure. CQD Section 7-4-2 discusses how the gap conductance model is adjusted. CQD Section 7-5 discusses how the effects of swell and rupture are included in the oxidation calculation.

One of the most important models for representing the fuel rod response to a LBLOCA is the cladding reaction model. For Zircaloy cladding, Westinghouse developed the model in WCOBRA/TRAC based on the work of Cathcart and Pawel, Reference 84. Regulatory Guide 1.157 notes this is an acceptable approach. Westinghouse also included in WCOBRA/TRAC a cladding reaction rate model for their proprietary ZIRLO cladding. The cladding reaction model accounts for the reaction of the outer cladding surface and the inner cladding surface if burst occurs. The reaction of both surfaces is assumed not to be steam limited.

A.7.2 INEL Review of CQD Section 7

The INEL reviewed the models for gap conductance/fuel and cladding deformation (other than elastic). That review found them consistent with standard models for these phenomena;¹⁹⁵ therefore, the INEL concluded they were adequate for realistic LBLOCA analyses.

The INEL reviewed the WCOBRA/TRAC cladding elastic deformation model, which is based on a thin shell approximation, and found it consistent with standard models for this phenomenon. The cladding rupture model for Zircaloy-4 (Eqn. 7-66) is taken from Powers and Meyer, Reference 138, and the INEL considers this adequate because it is a widely recognized model for cladding rupture. The cladding rupture model for ZIRLO is shown in CQD Figure 7-20, and Westinghouse noted in Volume 5, question 41, Reference 46, that this is the same model approved by the NRC for 10 CFR 50.46, Appendix K, analyses in WCAP-12610-P-A. The INEL reviewed the CQD figure and found the ZIRLO model adequately represents the data; based on this review and the NRC Appendix K approval, the INEL considers the ZIRLO model adequate.

WCOBRA/TRAC uses the Cathcart-Pawel model (Eqn. 7-74) to calculate the Zircaloy-4 metal-water reaction rate at all temperatures above 1500°F. Westinghouse justified the use of the model below 1900°F by noting the model will overpredict the oxidation rate at the lower temperatures, and the INEL confirmed this by reviewing Reference 84. Based on this argument for temperatures below 1900°F and the RG recommendation for temperatures above 1900°F, the INEL finds the Zircaloy-4 metal-water reaction model adequate. For ZIRLO, Westinghouse proposed a ZIRLO specific model (Eqn. 7-80) developed in Reference 127 to calculate the metal-water reaction rate. In the response to Volume 5, question 41, Reference 46, Westinghouse noted the ZIRLO model for metal-water reaction was not approved by the NRC for 10 CFR 50.46, Appendix K, analyses. Therefore, the INEL reviewed the model in Reference 127 for use in realistic LBLOCA analyses. This review found the ZIRLO model adequately represented the ZIRLO data at temperatures above 2000°F and overpredicted the data below 2000°F. Therefore, the INEL recommends the model be approved for realistic LBLOCA analyses.

On CQD page 7-24, Westinghouse stated the fuel pellet thermal expansion model in MATPRO-11, Revision 1, Reference 176, was simplified by omitting the corrections for molten fuel and mixed oxide (Pu). In Reference 214, List II, Item 6, Westinghouse committed to resubmitting the relevant WCOBRA/TRAC models for NRC review if the code will be used to analyze US licensed plants with molten fuel or mixed oxides.

A.8 Reactor Kinetics and Decay Heat Models - CQD Section 8

A.8.1 Model Description

The reactor kinetics and decay heat models are discussed in Section 8 of the CQD. WCOBRA/TRAC allows either the ANS 1971 (Draft)¹²⁶ or the ANS 1979, Reference 83, models to be used to represent decay heat. For realistic LBLOCA, the ANS 1979 model is used. The calculation of fission heat is based on a point kinetics model and includes feedback from moderator density and fuel temperatures. The contribution to decay heat from actinides is calculated for uranium-239, plutonium-239, and neptunium-239. Finally, the model allows for the direct deposition of energy in the moderator or other structures outside the fuel rod using the Generalized Energy Deposition Model (GEDM). The GEDM is used for fission neutrons, fission gammas, decay gammas, and actinide gammas separately with different redistribution fractions based on the energies of the particles involved. The redistribution kernel is based on higher order neutron and gamma transport calculations for a specific fuel design.

A.8.2 INEL Review of CQD Section 8

The INEL reviewed the point kinetics model implemented in WCOBRA/TRAC and found it consistent with standard models in this area. Comparison of the point kinetics model to the Inhour Equation for step reactivity insertions of $+3.0 \times 10^{-3}$, $+1.5 \times 10^{-3}$, and -3.0×10^{-2} ΔK showed the WCOBRA/TRAC model can accurately reproduce analytic solutions to the Inhour equation. The fission product decay heat model was implemented consistent with standard models, and comparison of the WCOBRA/TRAC model with the ANS 1979 standard showed good agreement (see CQD Table 8-1). INEL review of the actinide decay heat model also found it to be consistent with standard treatment of this heat source.

Therefore, the INEL concluded the reactor kinetics and decay heat models are adequate.

The INEL reviewed the GEDM and considers it a more realistic approach to energy redistribution than that used in other nuclear system codes. Review of the methods for calculating the redistribution kernel parameters found they are adequate based on comparisons of results for a 3x3 fuel assembly array and a 5x5 fuel assembly array. The redistribution fractions used for the particles are also adequate because they are dependent on the energy of the particles, and the values used are reasonable. Overall, the INEL considers the GEDM adequate because it treats neutron and gamma energy redistribution in a rigorous manner based on the energies of each different source.

A.9 One-Dimensional Component Models - CQD Section 9

A.9.1 Model Description

The one-dimensional components in WCOBRA/TRAC provide a means of modeling a number of different loop components. Included are models for pipes, tees, valves, accumulators, pressurizers, steam generators, centrifugal pumps, and problem boundary conditions via breaks and fills. All models are based on TRAC-PD2, and many models are unchanged from their original TRAC-PD2 versions. Section 9 of the CQD presents these models in detail; however, the pump and accumulator models are discussed here because of the special approaches taken with these models.

The pump model calculates the pressure differential across the pump and its velocity as a function of the fluid flow through the pump. Two-phase flow effects can be modeled. The single-phase and two-phase head/flow and torque/flow characteristics of the pumps are provided in homologous curve format. Two-phase head and torque multipliers are used to provide a transition from single-phase to two-phase conditions. Pump speed as a function of time is calculated using Eqn. 9-9.

The accumulator model assumes a nitrogen cover gas over water, and WCOBRA/TRAC assumes the accumulator injection period can be divided into two intervals. Phase A assumes only water is injected, and Phase B assumes a

nitrogen/water mixture and ultimately only nitrogen enters the system. During Phase A, the vapor in the accumulator is assumed to be an ideal gas with nitrogen properties. A sharp interface between the nitrogen and water is maintained by assuming a large relative velocity. As a result only water is discharged during Phase A. As the accumulator discharges, the nitrogen expands, decreasing the component pressure. WCOBRA/TRAC does not have an option to simulate a nitrogen-steam-water mixture. To simulate the nitrogen discharge that occurs in Phase B, the subcooled vapor model in WCOBRA/TRAC is used to provide pressure/flow characteristics similar to nitrogen. To account for the reduced condensation that would occur with nitrogen discharge into the RCS, Westinghouse activates a condensation suppression model in the accumulator and line, the intact cold legs, the upper downcomer region, and the broken cold leg. This model is active as long as the accumulator pressure is significantly higher than the RCS pressure. Details of the model are provided in Section 5-2-11 of the CQD.

A.9.2 INEL Review of CQD Section 9

The WCOBRA/TRAC pump model is of the same type as other pump models where the pump is treated as a momentum source to the fluid. The INEL compared the WCOBRA/TRAC pump model to that described in the COBRA/TRAC manual, and the model is unchanged. Based on CQD Section 16-3, the pump homologous head, torque, and two-phase multiplier curves are based on 1/3-scale pump data. Westinghouse, in its response to Volume 1, question 233, Reference 33, clarified how the two-phase multiplier curves were developed from the single-phase and two-phase homologous data. For example, to determine the two-phase head multipliers, Eqn. 9-7 for the pump head is solved for the multiplier. The pump data is then used to determine the multiplier as a function of void fraction. In this response, Westinghouse noted that CQD Figure 16-3-5 supports the fact that the fully degraded two-phase curve is offset from the single-phase curve by a constant value. Westinghouse used this to extend the fully degraded curve into areas where data is sparse or lacking. Because data is lacking for high void fraction, Westinghouse assumed the head multiplier returns to single-phase values at void fractions greater than 80% using a curve similar to that for void fractions below 20%. Based on the above, the INEL considers the WCOBRA/TRAC model adequate.

As noted above, the accumulator model covers the liquid discharge, transition to two-phase liquid/nitrogen discharge, and nitrogen discharge phases of accumulator injection. The liquid discharge phase and the criterion for transition to two-phase liquid/nitrogen discharge are discussed here. Because of the importance to PWR analyses of the correct modeling of single-phase nitrogen discharge, INEL review of WCOBRA/TRAC's capabilities in these areas are discussed in Section 12.2 of this report.

To verify the liquid discharge phase of accumulator injection, Westinghouse analyzed the IP2 accumulator discharge test. Figure 16-2-3 of the CQD shows WCOBRA/TRAC was able to accurately represent the accumulator tank depressurization during the test. To determine the modeling detail needed in the accumulator discharge line, Westinghouse evaluated two approaches (see CQD Section 16-2-2 and Volume 3, question 33, Reference 20). One approach modeled all piping details and used the WCOBRA/TRAC pipe friction models to calculate the fluid flow. The second assumed a simple, straight pipe with equivalent fluid volume and a fL/D obtained from tests and fluid systems analysis. The results shown in COD Figure 16-2-7 indicate the two approaches were equivalent, but Westinghouse chose to use the second option because it was easier to implement. In its response to Volume 3, question 33, Westinghouse noted that the uncertainty in the accumulator discharge line resistance is estimated, the effect of resistance evaluated in the plant sensitivity studies, and the PCT effects included in the uncertainty evaluation. Based on the above, the INEL concluded the accumulator liquid discharge model is adequate.

In CQD Section 16-2-5, Westinghouse evaluated the critical depth (height above the exit pipe divided by the exit pipe diameter) at which nitrogen would begin to discharge with liquid based on CQD Figure 16-2-8. This figure shows critical depth ratio as a function of the correlating parameter used by Westinghouse. The data show that the critical depth ratio increases if the pipe size is small relative to the reservoir. Based on Volume 3, question 34, Reference 20, Westinghouse chose a critical depth ratio that bounds the values for the smallest pipe data available over the expected range of the Westinghouse correlating parameter. Westinghouse did this because of the small size of the accumulator line relative to the tank.

Another way to determine the critical depth ratio, is to extrapolate the data in CQD Figure 16-2-8. The smallest pipe diameter to reservoir diameter ratio in the figure is larger than the PWR accumulator ratio. If the data available was extrapolated to the PWR pipe to reservoir ratio, the INEL calculated a critical depth ratio and, therefore, a critical depth greater than the Westinghouse values. Based on Westinghouse's response to Volume 3, question 36, Reference 42, this can have a significant effect on the transition volumetric flow (see Figure 36-5).

In Submittal SS, Reference 50, Westinghouse responded by noting the critical depth ratio used in the realistic LBLOCA methodology is based on the assumption that the critical depth ratio approaches a limiting value as the ratio of the drain pipe diameter to vessel diameter approaches zero. This limiting value was the value selected in CQD Section 16-2-5. Work in Reference 187 was discussed to support the asymptotic behavior assumption. INEL reviewed the information in Reference 187 and found it supported Westinghouse's argument. Based on this information, Westinghouse's critical depth ratio is considered adequate.

APPENDIX B

INEL REVIEW OF WESTINGHOUSE WCOBRA/TRAC ASSESSMENT

INEL REVIEW OF WESTINGHOUSE WCOBRA/TRAC ASSESSMENT

This appendix provides an overview of the extensive code assessment work Westinghouse performed on WCOBRA/TRAC. This assessment is required by Part (a) of 10 CFR 50.46, and Westinghouse uses the results in determining an experiment based uncertainty for WCOBRA/TRAC. In Reference 54, Westinghouse compared the highly ranked phenomena in its PIRT to the assessment test matrix. INEL review of the comparison found all the highly ranked phenomena were covered by the test matrix. The separate effects experiments are discussed first followed by the integral experiments and other assessments. Because of the large number of tests analyzed, INEL conclusions are noted at the end of the discussion for each test facility and summarized at the end of this appendix. Note all references cited in this appendix are listed in the references at the end of the main body of this report, Section 15.

B.1 WCOBRA/TRAC Separate Effects Assessment

Westinghouse's separate effects assessment of WCOBRA/TRAC included blowdown, refill, and reflood separate effects experiments. The blowdown and refill experimental facilities include the ORNL THTF, References 93 and 94, and the Westinghouse G-1, Reference 77, and G-2 test facilities. The tests from the G-2 facility included both blowdown, Reference 78, and refill, Reference 108, tests. For reflood, tests from the FLECHT-SEASET, References 89 and 90, FLECHT Low Flooding Rate, Reference 91, and FLECHT Skewed Power Shape, Reference 92, test series were used. Also, reflood tests from the Westinghouse G-2 test facility¹⁰⁹ and the German Flooding Experiments with Blocked Arrays (FEBA) test facility¹¹⁰ were used. Table B.1-1 summarizes Westinghouse's separate effects assessment matrix.

In CQD Volume 2, Tables 11-1-3 and 12-1-3 for blowdown/refill and reflood, respectively, compared the assessment test conditions against those expected in the plants to be analyzed with the realistic methodology. Regarding the reflood assessment matrix, INEL review found it provided adequate coverage of the range of expected reflood conditions.

Table B.1-1 Westinghouse WCOBRA/TRAC Separate Effects Assessment Matrix

<u>Test Facility</u>	<u>Test Number</u>
ORNL THTF	3.07.09B 3.08.6C 3.03.6AR
G-1 Blowdown	148 143 152 153 146 154
G-2 Blowdown	616 652 667 637
G-2 Refill	743 750 760 761 762 767
FLECHT-SEASET	31805 31203 31701 31504 32013
FLECHT Low Flooding Rate	05029 05132 04641
FLECHT Skewed Power Shape	15305 13812 15713 13914 13609
G-2 Reflood	550 562 568
FEBA	223 234 216 229

INEL review of the blowdown/refill assessment found it provided broad coverage of the expected conditions. However, there were some portions of the expected conditions not covered by Westinghouse's assessment. Westinghouse addressed these uncovered areas in their response to Volume 2, question 2, Reference 39, and that response is discussed below.

Regarding pressure during late blowdown, Westinghouse provided the results of G-2 refill Test 764 which covered the appropriate range of pressure conditions for this period. Comparison to the test results showed WCOBRA/TRAC tended to underpredict the heat transfer in this test.

For mass velocity during the early and late blowdown periods, Westinghouse noted the high mass velocities listed in CQD Table 11-1-1 for early blowdown are those typical of steadystate conditions, and the mass velocity in a LBLOCA quickly reduces to that in the ORNL tests within a second or two. For the late blowdown period, Westinghouse noted the code was assessed against G-2 Test 750 with a mass velocity of $9 \text{ lb}_m/\text{s}/\text{ft}^2$. Comparison to the test data and an adiabatic heat up showed WCOBRA/TRAC adequately calculated heat transfer in the low flow conditions.

Regarding the need to cover high subcooling for the early blowdown period, Westinghouse noted the high subcooling listed in CQD Table 11-1-1 is that typical of steadystate conditions, and the subcooling in a LBLOCA quickly reduces to that in the ORNL tests within a second or two. For the low subcooling later in blowdown, Westinghouse discussed the coverage provided by ORNL Tests 3.03.6AR and 3.08.6C. These tests included pressure transients that reduced the pressure, and the subcooling decreased to approximately 9°F .

According to CQD Table 11-1-1, Westinghouse assessment of the peak heat rate did not cover the upper end of heat rates expected in PWR analyses (11-17 kW/ft during early blowdown). Westinghouse's response noted that this value includes all uncertainties, and if the LOFT test uncertainties are included in the highest power LOFT test analyzed (LB-1), then the LOFT peak power is 16.9 kW/ft. Westinghouse also discussed how Figure 33 of the CSAU report (Reference 61) indicated that high linear heat rates do not introduce new phenomena. In Figure 33 of the CSAU report, Westinghouse points out the blowdown PCT is a linear function of the initial power, and that this

relationship is to be expected because the blowdown peak is a function of the initial fuel temperature that varies linearly with linear heat rate.

The final area Westinghouse discussed in its response was core inlet quality. Westinghouse concluded that the more important parameter was core exit quality because the range of core exit quality will determine cladding dryout and vapor superheat. Table 2-1 of Westinghouse's response to Volume 2, question 2, in Reference 39 and Westinghouse's associated discussion regarding the applicability of low flow reflood tests to late blowdown/refill conditions showed the test assessments adequately covered the range of core exit qualities.

Based on the review of the CQD and Westinghouse's response to Volume 2, question 2, Reference 39, the INEL concluded the assessment of blowdown heat transfer adequately covered the appropriate range of conditions.

The following subsections describe the results of the separate effects WCOBRA/TRAC assessment calculations performed by Westinghouse. Because of the extensive nature of the Westinghouse assessment matrix, not all code/test comparisons will be discussed; rather, a summary of the overall code performance will be provided. Details on the separate effects assessment can be found in CQD Volume 2.

B.1.1 ORNL THTF Blowdown Tests

The three ORNL THTF blowdown tests simulated with WCOBRA/TRAC were high pressure (greater than 1849 psia) film boiling tests. The comparisons to test data are found in Figures 11-2-12 to 11-2-22 of CQD Volume 2. Except for Test 3.08.6C, the PCT was reasonably well calculated by WCOBRA/TRAC. In Test 3.08.6C, the PCT was underpredicted by approximately 100°F. In general, WCOBRA/TRAC predicted the correct data trends. For example, when the steam flow was high enough that the cladding temperature decreased downstream of the dryout point, WCOBRA/TRAC calculated the same trend. Similarly, when conditions resulted in the cladding temperature increasing downstream of the dryout point, WCOBRA/TRAC calculated a cladding temperature increase. The code also did a good job of calculating the dryout point in the steadystate test (Test 3.07.9B). The code and data both showed the dryout point at

approximately 62 inches. The transient tests show that the timing/location of dryout as it moved down the bundle was also well predicted. Therefore, Westinghouse concluded, and the INEL agrees, that WCOBRA/TRAC did a reasonable job of calculating the ORNL THTF tests simulated.

B.1.2 G-1 Blowdown Tests

The G-1 tests simulated with WCOBRA/TRAC were run at intermediate pressures (800 psia). Comparison of the WCOBRA/TRAC results to the G-1 blowdown test results shows the code tended to overpredict the cladding temperature and underpredict the heat transfer in the center of the bundle. At the bundle ends, WCOBRA/TRAC calculated a more extensive rewet relative to the test data. See Figures 11-3-7 to 11-3-42 in Volume 2 of the CQD. Westinghouse provided additional figures for G-1 Test 143, the reference test, in its response to Volume 2, question 12, Reference 9. The rewet at the bundle ends appears to be due to the low rod end temperatures that are near the WCOBRA/TRAC T_{MIN} temperature.

Based on the comparisons of calculated and measured results shown in the CQD, INEL concluded WCOBRA/TRAC adequately calculated the G-1 blowdown tests.

B.1.3 G-2 Blowdown Tests

The G-2 tests simulated with WCOBRA/TRAC were also run at intermediate pressures (800 psia). WCOBRA/TRAC comparisons to test data are found in CQD Volume 2, Figures 11-4-8 to 11-4-31. These comparisons show WCOBRA/TRAC tended to compare reasonably well with the experimental data at the bundle ends and overpredict the test data in the middle of the bundle.

Based on the comparisons of calculated and measured results shown in the CQD, INEL concluded WCOBRA/TRAC adequately calculated the G-2 blowdown tests.

B.1.4 G-2 Refill Tests

Low pressure refill tests were also run in the Westinghouse G-2 facility. Comparisons of WCOBRA/TRAC results to test data are found in Figures 11-5-3 to 11-5-39 in CQD Volume 2. In most cases, WCOBRA/TRAC did a

good job of simulating the cladding heat up rate during the tests, and generally WCOBRA/TRAC overpredicted the PCT. In one case, WCOBRA/TRAC underpredicted the PCT by 100°F; however, this test had a maximum, initial cladding temperature of 600°F which is not likely to be encountered in PWR LBLOCA analyses. The code/data comparisons also showed WCOBRA/TRAC results underpredicted the test data at the 118.9 inch elevation in several tests (Tests 760/761/762) even though the initial cladding temperatures were approximately 1000°F. The INEL does not consider this a serious problem because the cladding temperatures are still lower than those associated with PCT calculations, the location was at the end of a rod, and WCOBRA/TRAC tended to overpredict the PCTs in the G-2 refill tests (see CQD Figure 11-5-39).

Based on the comparisons in the CQD, INEL concluded that WCOBRA/TRAC adequately calculated the G-2 refill tests.

B.1.5 Separate Effects Reflood Tests

As discussed previously, Westinghouse used tests from the FLECHT-SEASET, FLECHT Low Flooding Rate, and FLECHT Skewed Power Shape test series, the Westinghouse G-2 test facility, and the German FEBA test facility to perform their separate effects reflood assessment. Although a wide range of tests and test facilities were analyzed, the assessment comparisons showed essentially the same results: adequate prediction of PCT but early cladding temperature turnaround time, overprediction of the cooldown rate, more rapid quench front progression and early quench, underprediction of the bundle steam superheat, and overprediction of the bundle mass relative to the test data. These differences were especially noticeable for tests at low pressure (20 to 40 psia) and long transient times.

Westinghouse determined most of these factors were related to the bottom entrainment model used in WCOBRA/TRAC (see entrainment model discussion in Reference 27). Westinghouse noted the original bottom entrainment model in WCOBRA/TRAC did not calculate enough entrainment relative to more recent models.¹¹¹ Sensitivity studies performed by Westinghouse and reported in Reference 27 showed that modifying the model to calculate more entrainment improved the WCOBRA/TRAC comparisons to bundle mass data considerably but not in the other areas listed above. Increased entrainment improved the bundle

mass comparisons because more liquid was carried out of the bundle. However, the responses to Volume 2, questions 12, 22, 26, 28, 40, and 41, Reference 46, showed that WCOBRA/TRAC, MOD7A, still had difficulty calculating turnaround time, cooldown rate, and quench time accurately relative to the forced reflood test data. The response to Volume 2, question 63, Reference 47, identified the fact that WCOBRA/TRAC tended to overpredict entrainment and underpredict heat transfer to the vapor just above the quench front as the dominate reasons for these calculated results.

For PCT, Westinghouse addressed these effects by determining heat transfer multipliers based on comparisons to test data that are applied in the uncertainty evaluation. Westinghouse addressed these issues for oxidation through the methodology discussed in Section 13 of this report. As discussed in that section, the oxidation methodology adequately accounts for the oxidation uncertainty resulting from the above issues by applying a time shift to the oxidation calculations. In Reference 206, Attachment 6, Westinghouse addressed the effect of underpredicting the turnaround time on PCT. Westinghouse noted that the effect of turnaround time is covered in the methodology through the break flow/condensation run matrix. For the case of VRA given in Reference 206, Westinghouse found reflood turnaround time varied from 69 to 114.5 s and 156 to 249 s for the first and second reflood peaks, respectively. Westinghouse also showed that WCOBRA/TRAC tended to overpredict quench time and turnaround time for the gravity reflood tests, which are the tests most representative of the PWR. Based on the turnaround time variation calculated in the break flow/condensation run matrix and the conservative estimates of quench time and turnaround time for the gravity reflood tests, INEL concluded that Westinghouse adequately addressed the effects of turnaround time on PCT. Therefore, the separate effects reflood test comparisons are considered adequate based on: (a) the INEL review of the comparisons provided and (b) Westinghouse's methodology adequately addressing uncertainty due to turnaround time, cooldown rate, and quench time on PCT and oxidation.

B.2 WCOBRA/TRAC Integral/Large Scale Assessment

The integral/large scale assessment of WCOBRA/TRAC included a number of different test facilities. Westinghouse used tests from the LOFT facility,

References 98, 99, 112, and 113; CCTF, References 70 to 74; SCTF, References 65-69; and UPTF, References 64, 75, and 114-116. The last three facilities were part of the international 2D/3D Test Program of which the NRC was a participant. Table B.2-1 summarizes Westinghouse's integral/large scale assessment matrix.

The following subsections describe the results of the integral/large scale WCOBRA/TRAC assessment calculations performed by Westinghouse. Because of the extensive nature of the Westinghouse assessment matrix, not all code/test comparisons will be discussed; rather, a summary of the overall code performance will be provided. Details on the integral/large scale assessment can be found in CQD Volume 3.

B.2.1 LOFT Assessment

The LOFT facility was the only nuclear powered, integral test facility in the world. LOFT Tests L2-2 and L2-3 were low and intermediate power tests with the reactor coolant pumps (RCPs) left running. Tests L2-5 and LB-1 were intermediate and high power tests where the RCPs were tripped and allowed to coast down. Therefore, the four LOFT tests analyzed provide data to demonstrate WCOBRA/TRAC's ability to predict a number of different variables including: (a) reactor power, (b) ECC bypass, (c) RCP behavior, (d) break flow, (e) nuclear fuel rod cladding temperature, and (f) core and loop flow distribution.

Westinghouse's response to Volume 3, question 1, Reference 42 provided the results of all LOFT assessments redone with the MOD7A version of WCOBRA/TRAC. The PCT comparisons for the tests are shown in Figures a1, b1, c1, and d1 for the four tests. Those comparisons show that WCOBRA/TRAC tended to underpredict the measured LOFT temperatures except for Test L2-3 where the comparison was excellent. The worst underprediction was for Test L2-5 where the test PCT was underpredicted by approximately 175°F. Based on Westinghouse's response to part e of Volume 3, question 1, and Reference 59 on compensating errors, the underprediction of PCT in the LOFT tests was due to the misprediction of break flow and the corresponding effect on core flow and core heat transfer. INEL review of the Test L2-2, L2-5, and LB-1 comparisons found that the hot leg break flow, cold leg break flow, or both was

Table B.2-1 Westinghouse WCOBRA/TRAC Integral/Large Scale Assessment Matrix

<u>Test Facility</u>	<u>Test Number</u>
LOFT	L2-2 L2-3 L2-5 LB-1
CCTF	Run 62 (Test C2-4) Run 63 (Test C2-5) Run 64 (Test C2-6) Run 67 (Test C2-8) Run 75 (Test C2-15)
SCTF	Run 604 (Test S2-SH1) Run 619 (Test S2-14) Run 620 (Test S2-15) Run 621 (Test S2-16) Run 623 (Test S2-18)
UPTF	Test 6, Run 131 Run 132 Run 133 Run 135 Run 136 Test 25, Phase A, Subphases 1a, 1b, and 2-4 Test 8, Phase A Test 10, Phase B, Subphases 1-4 Test 29, Phase B, Subphases 1-6

overpredicted (see Figures a3, c3, c4, d3, and d4), which would affect the core heat transfer. This is also consistent with the underprediction of system pressure in Figures, a2, c2, and d2. The break flow misprediction is discussed in more detail in Section 11 of this report that discusses Westinghouse's work on compensating errors.

Although break flow mispredictions caused the WCOBRA/TRAC calculated PCTs to be lower than the data, the INEL notes the WCOBRA/TRAC uncertainty evaluation directly accounts for the effect of break flow uncertainty on the calculated PCT. Therefore, the Westinghouse LOFT assessments are considered adequate. Also, the detailed analysis of LOFT Tests L2-3 and L2-5 in Section 11 of this report on compensating errors supports the adequacy of the WCOBRA/TRAC LOFT assessments.

B.2.2 CCTF Assessment

CCTF was a large scale test facility designed to study refill/reflood behavior in a four-loop PWR. It was a full height, large diameter facility with a flow area scale factor of 1/21.4. The facility included a 12-foot, electrically heat core and four loops (three intact loops and one broken loop). The tests selected varied the initial power, system pressure, and radial power profile. As shown in Table 14-2-2 of CQD Volume 3, the conditions in the five CCTF tests are representative of those expected in a typical four-loop PWR.

Although Westinghouse reran all the CCTF assessments with the MOD7A code version, only the CCTF Test 62 results were reported in detail (see MOD7A report, Reference 27). The MOD7A results from Reference 27 are discussed here. At elevations above 6 feet, the WCOBRA/TRAC PCT overpredicted the data average, sometimes by several hundred degrees (see Figures 4.4-2 to 4.4-5). The mass comparison in the lower core shows that WCOBRA/TRAC results agreed with the data until approximately 300 s after which it falls below the data (Figure 4.4-9). In the upper core, the bundle mass comparison shows the WCOBRA/TRAC results were always lower than the data (Figure 4.4-10). This would appear to be the cause of the PCT overprediction, less mass in the upper core.

Figures 4.4-14 and 4.4-18 show that WCOBRA/TRAC calculated the mass not found in the upper core was carried into the hot legs and causes increased steam binding relative to the test results. The increased steam binding would slow the WCOBRA/TRAC calculated reflood rate relative to the data causing higher PCTs and later quench times. Review of the MOD7A comparisons found that WCOBRA/TRAC did calculate later quench times relative to the data. Westinghouse discussed the overprediction of liquid flow into the hot legs in detail in its response to Volume 4, question 37, Reference 44.

Westinghouse did provide MOD7A PCT results for the other CCTF tests run in Table 12 of the MOD7A report. Review of those tables found that WCOBRA/TRAC calculated PCTs were generally higher than the measured PCTs for all the other assessments. Table 12 of the MOD7A report also shows that in general WCOBRA/TRAC results showed quenches later than the data.

Additional information is provided in Section 11 of this report discussing Westinghouse's evaluation of compensating errors.

Based on the conservative predictions, the CCTF assessments are considered adequate. Also, the detailed assessment of CCTF Test 62 in Section 11 of this report supports the adequacy of the CCTF analyses.

B.2.3 SCTF Assessment

The SCTF test facility was designed to complement the CCTF test results by providing two-dimensional heat transfer and hydrodynamic data in a PWR core during reflood. The eight bundle design represented a full height, full radial section of a PWR core one bundle wide. Four of the five SCTF tests simulated were forced reflood tests where the accumulator water was injected directly into the facility's lower plenum. The one gravity feed test was Run 604.

Although Westinghouse reran all the SCTF assessments with the MOD7A code version, only the SCTF Test 604 results were reported in detail (see MOD7A report, Reference 27). The MOD7A results from Reference 27 are discussed here. PCT comparisons in Figures 4.3-3 to 4.3-6 show that WCOBRA/TRAC results were mixed with some elevations underpredicted (approximately 6 foot

elevation) and some overpredicted, especially in the upper part of the core. Bundle mass comparisons showed that WCOBRA/TRAC tended to underpredict both the lower and upper core measurements, but the prediction was better in the lower half of the core (Figures 4.3-8 and 4.3-9). Therefore, the overprediction of temperatures in the upper core was due to lower calculated mass in the upper core.

Based on the conservative results, Westinghouse's SCTF assessments are considered adequate. Also, the detailed analysis on SCTF Test 619 in Section 11 of this report on compensating errors supports the adequacy of the SCTF analyses.

B.2.4 UPTF Assessment

The UPTF was designed to provide data on multi-dimensional flow in a PWR. The phenomena studied included:

1. Upper plenum entrainment and deentrainment.
2. Upper core and tie plate cocurrent and countercurrent two-phase flow.
3. Downcomer cocurrent and countercurrent flow.
4. Loop ECC injection condensation and steam/water mixing processes.

The tests simulated with WCOBRA/TRAC were related to Items 1, 3, and 4 above.

The UPTF represented at full-scale the upper plenum region of a German PWR. The facility simulated steam and droplet flow in the core by injecting steam and water into dummy fuel rods. Four loops represented three intact loops and one broken loop.

The upper plenum entrainment/deentrainment tests Westinghouse used to assess WCOBRA/TRAC were UPTF Tests 10B and 29B. For the initial subphase of Test 10B, WCOBRA/TRAC accurately calculated the upper plenum mass (see CQD Figures 15-2-1 and -2). For later three subphases of Test 10B, Westinghouse noted in the CQD that WCOBRA/TRAC overpredicted by a small amount the upper plenum mass. However, Westinghouse considered the WCOBRA/TRAC mass within the data uncertainty.

For Test 29B, the WCOBRA/TRAC results for Subphases 1 to 6 were compared to test data in Westinghouse's response to Volume 3, question 10, Reference 41. In Figures 10d to 10i, it can be seen that WCOBRA/TRAC underpredicted the upper plenum mass storage for these test runs. Summary figures are provided in Figures 10j and 10k. Based on these results, WCOBRA/TRAC underpredicted upper plenum mass storage, implying greater entrainment into the hot legs and SGs. This will cause increased steam binding relative to the measured data, and a conservative bias in WCOBRA/TRAC analyses.

The downcomer ECC bypass experiments analyzed by Westinghouse were Test 6, Runs 131, 132, 133, 135, and 136. As discussed previously, Westinghouse evaluated the WCOBRA/TRAC results relative to test data in its response to Volume 4, question 2, Reference 21. In that response, Westinghouse showed that WCOBRA/TRAC underpredicted ECC penetration (more mass bypassed out the break) and overpredicted ECC penetration time (ECC penetration began later than the data). Again, this introduces a conservative bias into the WCOBRA/TRAC PWR analyses.

Test 25A was run to look at the entrainment calculated from the top of a full downcomer during reflood. Westinghouse's response to Volume 3, question 13, Reference 23, showed that WCOBRA/TRAC adequately calculated the measured entrainment rate for five subphases of this test.

UPTF Test 8, Phase A, was a cold leg steam/water mixing test. Comparison of the measured and predicted cold leg temperatures near the vessel showed adequate agreement (within 10°C, see Westinghouse response to Volume 3, question 21, Reference 20) between the two (see also CQD Figures 14-4-177 and -178 or CQD Figure 15-3-46). Westinghouse also used UPTF Test 25A to look at cold leg steam/water mixing. CQD Figure 15-3-47 compared the measured and predicted cold leg temperatures for this test, and it showed good agreement.

In terms of condensation, Westinghouse calculated the condensation efficiency in the cold leg from the WCOBRA/TRAC results and compared it to that estimated from the test data for Tests 8 and 25. Condensation efficiencies of 80 to 100% were estimated from the test data and 70 to 100% from the WCOBRA/TRAC results (see CQD Figures 15-3-48 and -48). In the CQD,

Westinghouse noted the very high or very low WCOBRA/TRAC condensation efficiencies shown in CQD Figure 15-3-49 were calculated when transient conditions existed at the beginning or end of a simulation or when the steam flow rate was changing; steadystate conditions are those where the points are clustered closely together.

As cold leg void fraction increases and decreases, changes in the condensation rate, relative velocity, vapor velocity, and liquid velocity in the cold leg cause pressure oscillations. These pressure oscillations are observed in the test data and the WCOBRA/TRAC results for both UPTF tests (see CQD Figures 15-3-44 and 15-3-45). The oscillation calculated by WCOBRA/TRAC, however, are three to four times larger than the test data. In the CQD (page 15-3-12), Westinghouse concluded that although WCOBRA/TRAC overpredicts the measured oscillations, they do not impair the code predictive or calculational capability. Based on the comparisons above for temperature and condensation efficiency, the INEL agrees with Westinghouse's conclusion. Based on the above, WCOBRA/TRAC did an adequate job of simulating the UPTF steam/water mixing tests.

Based on the above comparisons, WCOBRA/TRAC did an adequate job of simulating the UPTF tests.

B.3 Other WCOBRA/TRAC Assessments

B.3.1 Westinghouse/EPRI 1/3rd-Scale Steam/Water Mixing Tests

Westinghouse and EPRI performed cold leg steam/water mixing tests in a 1/3rd scale facility, Reference 97. WCOBRA/TRAC assessments using those tests were completed with the original code version, MOD7. Two test series were used to assess WCOBRA/TRAC, an accumulator flow series (No. 6) and an SI only series (No. 5).

One parameter of interest in these tests is the pressure drop induced in the cold leg due to the steam/ECC water interaction. The larger the cold leg pressure drop, the greater the resistance to reflood, and the higher the PCT. Comparisons of WCOBRA/TRAC results to test data in CQD Figures 15-3-12 to -18 for the accumulator tests and Table 1A in Volume 3, question 20, Reference 34,

for the SI tests show the average WCOBRA/TRAC pressure drop generally overpredicted the average measured pressure drop. This implies the WCOBRA/TRAC results are conservative relative to the test data.

Another parameter considered in these tests was the liquid temperature increase as it flowed down the test section. The liquid temperature at the cold leg exit is important because the subcooling present influences whether downcomer boiling is calculated and when it begins. Also, the liquid temperature increases as it condenses steam; therefore, comparison of the calculated and measured liquid temperatures reflects the calculated and measured condensation rates. The comparisons in CQD Figures 15-3-25 to -36 show that, although there are differences in the first part of the test section, by the time the liquid exits the test section, the calculated and measured temperatures compare well. As stated by Westinghouse (CQD page 15-3-6), and the INEL agrees, this indicates that the average condensation rate was calculated reasonably well in these tests.

Pressure oscillations are observed in the test data and the WCOBRA/TRAC results for these steam/water mixing tests (see CQD Figures 15-3-10 (data) and 15-3-1/-7 (WCOBRA/TRAC)). The oscillation calculated by WCOBRA/TRAC, however, are up two times larger than the test data. In the CQD (page 15-3-12), Westinghouse concluded that although WCOBRA/TRAC overpredicts the measured oscillations, they do not impair the code predictive or calculational capability. Based on the comparisons above for pressure drop and temperature, the INEL agrees with Westinghouse's conclusion.

Based on the above comparisons, WCOBRA/TRAC does an adequate job of simulating the Westinghouse/EPRI 1/3rd-scale steam/water mixing tests.

B.3.2 Creare 1/15th and 1/5th Scale ECC Bypass Tests

Westinghouse evaluated WCOBRA/TRAC's ability to calculate ECC bypass in a scaled test facility using 1/15th¹¹⁸ and 1/5th (Reference 107) scale tests performed by Creare. In its response to Volume 3, question 8, Reference 37, Westinghouse provided MOD7A results compared to test data for a variety of injected flow rates. INEL review of the comparisons found excellent agreement between the calculated and measured values for saturated liquid conditions. A

comparison for 70°F subcooled ECC bypass also showed excellent agreement. Based on these comparisons, INEL concluded WCOBRA/TRAC adequately calculated these scaled ECC bypass tests.

B.3.3 NRU Reactor Assessment:

Westinghouse analyzed two NRU tests in the CQD: the tests were Test PTH-110¹¹⁹ and Test MT-3.06.¹²⁰ Westinghouse reanalyzed the NRU tests with the MOD7A version of WCOBRA/TRAC and presented the results in References 23, 34, and 35. The WCOBRA/TRAC, MOD7A, prediction of NRU Test PTH-110 in Westinghouse's response to Volume 3, question 30, Reference 23, (see Figures 30-1 to 30-5) was a significant improvement over the MOD7 version results presented in the CQD (see Figures 16-1-13 to 16-1-18). Westinghouse noted in response to Volume 3, question 30, Reference 23 that in addition to the code version changes, input changes were also made to better reflect the test parameters reported in Reference 119. The comparisons in Volume 3, question 30 show PCT, overall cooldown rate, and quench time comparisons were much better with the revised input and new code version.

For NRU Test MT-3.06, the MOD7A results were presented in response to Volume 3, question 26, Reference 35. The comparisons show that WCOBRA/TRAC underpredicted the PCTs at Level 15 (see Figures 26-1 and 26-2), but it overpredicted the PCTs at Levels 17 and 18 (see Figures 26-3 to 26-5). The underprediction at Level 15 was not as severe as in the CQD analyses (see CQD Figures 16-1-5 and 16-1-6). The difference is due to the greater entrainment calculated with MOD7A (see Volume 3, question 27, Reference 23). This NRU test was run with a variable flooding rate that caused the quench front to stagnate. The quench front in the MOD7A analysis stagnated 12 to 15 inches below that in the CQD analysis. With the lower MOD7A quench front relative to the MOD7 results, higher cladding temperatures resulted.

Westinghouse's response in Volume 3, question 26, compared measured and predicted burst results for Test MR-3.06. Good comparisons were found. In Figure 26-8 Reference 35, however, Westinghouse compared the calculated and measured transient RIP for NRU Test MT-3.06. In the calculation, WCOBRA/TRAC underpredicted the RIP for a period of time due to quenching of the fuel rod at the rod internal plenum location. Later, after the plenum dried out, the

calculated RIP increased, and WCOBRA/TRAC calculated the rod to burst. This implies there is some uncertainty in whether rod burst will be properly calculated.

Westinghouse evaluated this in its response to Volume 3, question 28, Reference 34. Westinghouse noted that in the sensitivity studies for the SQN plant, rod burst was calculated in all cases except when the PCT was below approximately 1625°F. Also, Westinghouse's response to Volume 4, question 40, Reference 53, discussed how the uncertainty in the RIP calculation results in burst temperature variations that are small and within the range of burst temperature variations included in the local effects uncertainty analysis performed with the HOTSPOT code. Therefore, the Westinghouse methodology accounts for the uncertainty in transient RIP for local effects. Westinghouse also calculates HA rod burst in the full WCOBRA/TRAC analyses called for in its methodology. If WCOBRA/TRAC calculates a HA rod reflood PCT greater than 1600°F but not rod burst, Westinghouse in Reference 214, List II, Item 2, committed to increasing the initial RIP in the WCOBRA/TRAC HA rod until burst is calculated and choosing the more limiting of the burst and non-burst cases. This adequately accounts for RIP uncertainties and their effect on rod burst in the full WCOBRA/TRAC runs.

Based on the above discussion, INEL considers the NRU analyses adequately calculated by WCOBRA/TRAC. PCTs were reasonably calculated as were the burst parameters. Based on the NRU results, there is some uncertainty in the transient RIP calculation that will affect the burst temperature criterion; however, the Westinghouse methodology appropriately accounts for this uncertainty as discussed above.

B.4 Summary of INEL Review

This section summarizes the INEL review of the Westinghouse code assessment of the WCOBRA/TRAC code.

B.4.1 Separate Effects Tests

Based on the INEL's review of the separate effects tests discussed in Section B.1 of this report, the following conclusions were reached:

1. Based on the review of the CQD and Westinghouse's response to Volume 2, question 2, Reference 39, the INEL concluded the assessment of blowdown heat transfer adequately covered the appropriate range of conditions. Assessment of reflood heat transfer also covered the appropriate range of conditions.
2. WCOBRA/TRAC did a reasonable job of calculating the ORNL THTF tests simulated.
3. Based on the comparisons of calculated and measured results shown in the CQD, INEL concluded WCOBRA/TRAC adequately calculated the G-1 and G-2 blowdown tests and the G-2 refill tests.
4. WCOBRA/TRAC, MOD7A, had difficulty calculating turnaround time, cooldown rate, and quench time accurately relative to the forced reflood test data. The response to Volume 2, question 63, Reference 47, identified the fact that WCOBRA/TRAC tended to overpredict entrainment and underpredict heat transfer to the vapor just above the quench front as the dominate reasons for these calculated results. For PCT, Westinghouse addressed these effects by determining heat transfer multipliers based on comparisons to test data that are applied in the uncertainty evaluation. Westinghouse addressed these issues for oxidation through the methodology discussed in Section 13 of this report. As discussed in that section, the oxidation methodology adequately accounts for the oxidation uncertainty resulting from the above issues by applying a time shift to the oxidation calculations. In Reference 206, Attachment 6, Westinghouse addressed the effect of underpredicting the turnaround time on PCT. Westinghouse noted that the effect of turnaround time is covered in the methodology through the break flow/condensation run matrix. Westinghouse also showed that WCOBRA/TRAC tended to overpredict quench time and turnaround time for the gravity reflood tests, which are the tests most representative of the PWR. Based on the turnaround time variation calculated in the break flow/condensation run matrix and the conservative estimates of quench time and turnaround time for the gravity reflood tests, INEL concluded that Westinghouse

adequately addressed the effects of turnaround time on PCT. Therefore, the separate effects reflood test comparisons are considered adequate based on: (a) the INEL review of the comparisons provided and (b) Westinghouse's methodology adequately addressing uncertainty due to turnaround time, cooldown rate, and quench time on PCT and oxidation.

B.4.2 Integral Effects Tests

Based on the INEL's review of the integral effects tests discussed in Section B.2 of this report, the following conclusions were reached:

1. Although break flow mispredictions caused the WCOBRA/TRAC calculated PCTs for LOFT to be lower than the data, the INEL notes the WCOBRA/TRAC uncertainty evaluation directly accounts the effect of break flow uncertainty on the calculated PCT. Therefore, the Westinghouse LOFT assessments are considered adequate. Also, the detailed analysis of LOFT Tests L2-3 and L2-5 in Section 11 of this report on compensating errors supports the adequacy of the WCOBRA/TRAC LOFT assessments.
2. Based on the conservative predictions, the CCTF assessments are considered adequate. Also, the assessment of CCTF Test 62 in Section 11 of this report supports the adequacy of the CCTF analyses.
3. Based on the conservative results, Westinghouse's SCTF assessments are considered adequate. Also, the detailed analysis on SCTF Test 619 in Section 11 of this report on compensating errors support the adequacy of the SCTF analyses.
4. Based on the comparisons provided by Westinghouse, WCOBRA/TRAC does an adequate job of simulating the UPTF tests.

B.4.3 Other Assessments

Based on the INEL's review of the other assessments discussed in Section B.3 of this report, the following conclusions were reached:

1. Based on the Westinghouse comparisons, WCOBRA/TRAC does an adequate job of simulating the Westinghouse/EPRI 1/3rd-scale steam/water mixing tests and the Creare scaled ECC bypass tests.
2. Based on the NRU comparisons, INEL considers the NRU tests adequately calculated by WCOBRA/TRAC. PCTs were reasonably calculated as were the burst parameters. Based on the NRU results, there is some uncertainty in the transient RIP calculation that will affect the burst temperature criterion in WCOBRA/TRAC analyses. However, the Westinghouse methodology appropriately accounts for this uncertainty as discussed in Section B.3.3 of this report.

Based on the above results, the INEL concluded WCOBRA/TRAC is adequate to provide realistic analyses of three- and four-loop PWR LBLOCAs.

APPENDIX C

COMPARISON OF WESTINGHOUSE REALISTIC LBLOCA METHODOLOGY
AND
REGULATORY GUIDE 1.157

COMPARISON OF WESTINGHOUSE REALISTIC LBLOCA METHODOLOGY
AND
REGULATORY GUIDE 1.157

A comparison of Westinghouse's methodology to Regulatory Guide (RG) 1.157 is shown in Table C-1. This table compares the RG, Sections 3 and 4, guidance and Westinghouse's realistic model. Notes are located at the end of the table to discuss the basis for INEL findings. Note all references cited in this appendix are listed in the references at the end of the main body of this report, Section 15. Based on information provided by Westinghouse, Westinghouse has met the RG guidance or provided adequate justification for its alternate approach. Therefore, INEL concluded that Westinghouse has adequately met the guidance of RG 1.157.

Table C-1 COMPARISON OF RG 1.157 AND WESTINGHOUSE'S REALISTIC LBLOCA MODEL

RG 1.157 Guidance

3.1 - The initial conditions used in the BE LBLOCA analysis shall be the most limiting over the life of the plant and based on sensitivity studies. Given the assumed initial conditions, relevant factors such as power, peaking factors, and fuel conditions should be calculated in a BE manner. A break spectrum study should be performed, include breaks up to double-ended breaks of the largest pipe in the primary coolant system, be detailed enough to define system response versus break size, and include split breaks with area equal to twice the pipe. Other boundary and initial conditions should be based on plant Technical Specification limits. Consider a single failure when analyzing safety system response and consider the effect of using only onsite or only offsite power.

Westinghouse Realistic Model

Westinghouse performed a sensitivity study to determine the limiting initial conditions for three different plants in CQD Sections 21 and 22. The sensitivity studies showed that BOL core conditions were most limiting. Power, peaking factors, and fuel conditions are calculated in a BE manner (see Note 1). A break spectrum is considered and includes split breaks equal to twice the pipe flow area (see CQD Table 22-6-2 and Note 1) unless the PCT peaked earlier. Some boundary and initial conditions are set at bounding values, and some are set at nominal rather than Technical Specification limits. However, Westinghouse includes the effect of variations in those parameters set at nominal values in a code initial condition bias and uncertainty (CQD Section 26-5). The bias/uncertainty are based on the sensitivity studies in CQD Section 22. The INEL considers this approach consistent with that discussed in RG 4.3.1. Westinghouse accounts for a single failure and offsite/onsite power directly in the analysis by analyzing the worst case. See Note 1.

Table C-1 (continued)

RG 1.157 Guidance

Westinghouse Realistic Model

3.2.1 - The steadystate fuel/cladding gap conductivity should account for fuel burnup, fuel pellet cracking and relocation, cladding creep, and gas mixture conductivity.

Westinghouse closely matches the WCOBRA/TRAC initial fuel temperature to that predicted by a highly detailed fuel rod model used in fuel design. The WCOBRA/TRAC hot rod match with the fuels code is done at the BE level with uncertainties accounted for in the uncertainty propagation. See Note 2.

3.2.2 - Fission heat should be calculated using a BE model for reactivity and reactor kinetics. Temperature and void coefficients should also use BE values. The point kinetics model is acceptable. Control rod insertion may be assumed if expected to occur.

WCOBRA/TRAC incorporates a point kinetics model to evaluate the fission heat (see CQD Section 8-3). See Note 3. The capability of modeling the temperature and void coefficients is included in the code. Plant-specific values are justified with the code application. For the LBLOCA analyses in the CQD, control rod insertion was assumed not to occur because damage to control rod guide tubes could not be precluded.

3.2.3 - Decay heat from actinides, including plutonium, neptunium, and isotopes of uranium, shall be calculated using BE models. The actinide decay heat should be appropriate for the operating history.

Westinghouse's actinide decay heat model accounts for uranium-239 and neptunium-239 (CQD Section 8-4). Plutonium-239 is included in the decay heat model (see CQD Section 8-2). Other plutonium isotopes and other actinides are excluded (see CQD Section 8-9-1). See Note 4.

Table C-1 (continued)

RG 1.157 Guidance

3.2.4 - Fission product decay heat should be calculated in a BE manner. The 1979 ANS decay heat model (Reference 83) is considered acceptable.

3.2.5 - The metal-water reaction rate should be calculated using a BE model. The model should recognize the effects of steam pressure, preoxidation, cladding deformation, and internal oxidation from steam and UO_2 . Data from Cathcart-Pawel, Reference 84, are acceptable for model development for cladding temperatures greater than 1900°F. When cladding rupture occurs, the oxidation will also be calculated for the inside of the cladding in a BE manner.

Westinghouse Realistic Model

WCOBRA/TRAC is capable of using the 1979 ANS decay heat model in the fission product decay calculation, and Westinghouse selects this model for LBLOCA analyses (see CQD Section 8-2). See note 5. The 1971 draft ANS model (Reference 126) is also available.

Westinghouse uses the Cathcart-Pawel metal-water reaction model for temperatures above 1500°F for Zircaloy clad fuel. Note 6 discusses the justification for using the Cathcart-Pawel model below 1900°F. A separate model is available for Westinghouse's proprietary ZIRLO cladding material (see Note 6 for the INEL review). CQD Section 7-5 describes these models. The metal-water reaction model accounts for preoxidation (the initial outer surface oxidation is from the NRC approved PAD code (Volume 1, question 237, Reference 57)) and cladding deformation as recommended by the RG. However, Westinghouse noted that internal oxidation from UO_2 and steam pressure effects are not accounted for by WCOBRA/TRAC (see Note 6). When cladding rupture is calculated, oxidation of the inside of the cladding is calculated.

Table C-1 (continued)

RG 1.157 Guidance

Westinghouse Realistic Model

3.2.6 - Heat transfer from reactor internals should be included in a BE manner.

WCOBRA/TRAC is capable of modeling heat transfer from reactor internals. The model is described in CQD Section 7-2. The INEL considers Westinghouse's approach to calculating reactor internal heat transfer capable of providing a realistic calculation. See Note 7.

3.2.7 - Primary to secondary heat transfer should be accounted for in a BE manner.

WCOBRA/TRAC is capable of modeling primary to secondary heat transfer. The model is described in CQD Section 9-5. The INEL reviewed the SG conduction equation used in WCOBRA/TRAC (Eqn. 7-89) and found it adequate (see Note 8).

Table C-1 (continued)

RG 1.157 Guidance

3.3.1 - The model should calculate cladding swelling from cladding temperature and pressure differences between the inside and outside of the fuel as a function of time in a BE manner. Cladding swell and rupture should be accounted for in gap conductance, cladding oxidation, heat transfer, and fluid flow outside the cladding. Fuel and cladding temperature calculations with time should use gap conductance and other thermal parameters as a function of temperature and time. Calculations of cladding swelling should include: spatially varying cladding temperatures, heating rates, anisotropic material properties, asymmetric cladding deformation, and fuel rod thermal and mechanical parameters.

Westinghouse Realistic Model

Cladding swell and rupture is modeled in WCOBRA/TRAC. The effects of cladding swell and rupture are included in the gap conductance, cladding oxidation, heat transfer surface area, and flow areas. The gap conductance model and the other thermal parameters are a function of temperature and time. The use of multiple axial nodes in the fuel rod allows for axially varying cladding temperatures and heating rates. WCOBRA/TRAC accounts for fuel rod thermal and mechanical parameters through a rod conduction model that has properties of the fuel pellets, gap, and cladding. Fuel and cladding axial and radial thermal expansion are included, and the cladding deformation due to rod/system pressure differences and fuel pellet/cladding contact are also modeled. Anisotropic material properties are not used and asymmetric cladding deformation is not calculated as discussed in Note 9.

Table C-1 (continued)

<u>RG 1.157 Guidance</u>	<u>Westinghouse Realistic Model</u>
<p>3.4.1 - The critical flow model should account for fluid conditions at the break, upstream and downstream pressures, and break geometry. The break flow calculation should be a BE calculation with the break flow uncertainty included in the uncertainty evaluation.</p>	<p>The <u>W</u>COBRA/TRAC critical flow model accounts for break fluid conditions (subcooled, two-phase, and single-phase steam), upstream and cell edge pressures, and break geometry. Guillotine or split breaks and break area variations can be modeled. The break flow was assessed against Marviken tests, and the uncertainty included in the code uncertainty evaluation. See Note 10.</p>
<p>3.4.1.1 - The critical flow models should be checked against an acceptable set of relevant data (covers fluid conditions, geometries, and break types), recognize thermal nonequilibrium conditions when the fluid is subcooled, and provide a transition from nonequilibrium to equilibrium conditions.</p>	<p>The <u>W</u>COBRA/TRAC critical flow model was assessed against Marviken and LOFT data for the appropriate range of fluid conditions and geometries (see Volume 1, question 3a, Reference 44. For break types, see Note 11. Based on Reference 205, Attachment 5, the <u>W</u>COBRA/TRAC model recognizes the effects of nonequilibrium and L/D on critical flow. See Note 11.</p>

Table C-1 (continued)

RG 1.157 Guidance

3.4.2 - ECC bypass during the blowdown phase of a LBLOCA should be calculated in a BE manner based on applicable experimental data. The amount of cooling water stored in the piping or vessel and not expelled should be calculated in a BE manner based on applicable experimental data. The ECCS bypass model should consider the effects of pressure, subcooling, fluid conditions, hot walls, and system geometry.

3.5 - Noding near the break and ECC injection points should be based on sensitivity studies to ensure realistic results.

Westinghouse Realistic Model

WCOBRA/TRAC does not use a special model to calculate ECC bypass; rather, it is calculated from the intercell, interphase, and wall drag interaction. Westinghouse used WCOBRA/TRAC to calculate Creare 1/15th and 1/5th scale bypass tests (References 107 and 118) and UPTF full-scale bypass tests (Reference 64). Those tests varied flow rate, pressure, subcooling, and geometry. The code inputs allow modeling hot walls in the vessel through the use of heat structures and system geometry through node input. The basic equations and constitutive models account for pressure, subcooling, and fluid conditions. Model validation covered the range of conditions expected in PWR analyses (see response to Volume 5, question 45, Reference 25). See Note 12.

In order to use the assessment calculations in the code uncertainty evaluation, the noding near the break and ECC injection points is the same in the assessment models and the PWR models. In this way, modeling uncertainty is included in the code uncertainty. See Note 13.

Table C-1 (continued)

<u>RG 1.157 Guidance</u>	<u>Westinghouse Realistic Model</u>
<p>3.6 - Pressure drops should be calculated using models that include a BE variation of friction factor with Reynolds number and account for two-phase flow effects on friction. The wall friction model should be consistent with that for calculating gravitational and acceleration pressure drops and the same void fraction model used for all three components unless justified.</p>	<p>The model is discussed in the CQD (vessel, Section 4-2; loops, Section 4-7). It accounts for two-phase flow and varies the friction factor with Reynolds number. The uncertainty in the friction pressure drop calculation is included in the uncertainty evaluation. Based on Reference 205, Attachment 5, and the CQD, the code models for wall friction, gravitational, and acceleration pressure drops are consistent, and the code uses the same void fraction for each component. See Note 14.</p>
<p>3.7 - The momentum equation should take into account temporal change of momentum, momentum convection, area change momentum flux, momentum change due to compressibility, pressure loss from wall friction, pressure loss from area change, and gravitational acceleration.</p>	<p>The <u>W</u>COBRA/TRAC momentum equation includes the recommended components of momentum transfer. See Note 15.</p>

Table C-1 (continued)

RG 1.157 Guidance

3.8 - BE CHF correlations developed from appropriate steadystate or transient data are acceptable. Correlations should be used within their range of applicability as specified by the authors. After CHF is predicted, return to nucleate boiling is allowed if local fluid and heat transfer conditions justify it.

3.9 - Post-CHF heat transfer should be calculated with BE models based on applicable steadystate and transient data. The models should account for liquid entrainment, thermal radiation, thermal nonequilibrium, low and high mass flow rates, low and high power densities, and inlet fluid conditions.

Westinghouse Realistic Model

WCOBRA/TRAC uses the Biasi CHF correlation at high mass fluxes and the Zuber correlation as modified by Bjornard and Griffith in pool boiling situations. An annular flow film dryout model is also included. The code calculates return to nucleate boiling if justified by local condition as shown in the LOFT simulations provided in response to Volume 3, question 1, Reference 42. The steam generator component model uses the Biasi CHF correlation. The CHF model data base covers the range of conditions expected in a PWR. See Note 16.

The post-CHF blowdown heat transfer models are described in Sections 6-2-5 through 6-2-9 of the CQD. INEL review of those sections found the WCOBRA/TRAC code models for post-CHF heat transfer accounted for the RG items. See Note 17.

Table C-1 (continued)

RG 1.157 Guidance

3.9.3 - Heat transfer from uncovered rod bundles should account for the effects of radiation and laminar, transition, and turbulent flows. The radiation correlation derived should include a stated procedure to correct for radiation heat transfer and for estimating vapor temperatures. The Hottel procedure in Reference 132 is a satisfactory example.

3.10 - Pump modeling should be based on a BE dynamic model that includes momentum transfer to the fluid with variable pump speed as a function of time. Pump resistance should be justified, and two-phase pump performance should be verified by data comparisons. Pump coastdown following a loss of power should be a BE calculation. A locked pump rotor need not be assumed unless calculated to occur.

Westinghouse Realistic Model

The single-phase vapor model accounts for transition between laminar and turbulent flows. A vapor and entrained drop radiation model is included in WCOBRA/TRAC. Based on Reference 205, Attachment 5, the INEL believes that the WCOBRA/TRAC models are adequate to meet the RG recommendations or Westinghouse adequately justified its alternate model. See Note 18.

The pump model accounts for momentum transfer to the fluid and pump speed varies with time. See Eqns. 9-1, 9-2, and 9-9. Empirically determined single- and two-phase homologous curves are input. These curves allow the calculation of pump resistance as a function of volumetric flow and pump speed for single- and two-phase flow. WCOBRA/TRAC has the capability to calculate pump coastdown following a loss of power (see Eqn. 9-9). See Note 19.

RG 1.157 Guidance

Westinghouse Realistic Model

3.11 - The flow through the hot region shall be calculated as a function of time, and the hot region shall not be greater than one fuel bundle. Core flow in the hot region should include cross flow and flow blockage. The numerical scheme should ensure unrealistic oscillations do not result.

WCOBRA/TRAC is capable of modeling a single hot assembly and including the effects of cross flow. WCOBRA/TRAC calculates the core flow as a function of time. The cladding swell and rupture model accounts for these effects on core flow area. Westinghouse applies numerical damping, convergence criteria, time step controls, and modeling technology to ensure unrealistic flow oscillations do not occur. See response to Volume 5, question 48, Reference 22. See Note 20.

3.12.1 - BE containment pressures should be used and include the effects of containment heat sinks and all pressure reduction systems assumed to be available.

Westinghouse's realistic methodology will use previously approved containment pressure models. These models will be used with WCOBRA/TRAC mass and energy release rates. See Note 21.

3.12.2 - Refill and reflood rates should use BE models. The model should be able to: (1) take into consideration the thermal-hydraulic characteristics of the core, ECCS, and the primary and secondary systems and (2) calculate a two-phase level in the core.

WCOBRA/TRAC has the capability of modeling the thermal-hydraulic characteristics of the core, ECCS, and the primary and secondary systems. The code can calculate a two-phase core level (this is discussed in more detail under RG 3.12.2.1).

Table C-1 (continued)

RG 1.157 Guidance

3.12.2.1 - The level swell model should be checked against an acceptable set of relative data and include the effects of depressurization, boiloff, power level, fluid conditions, and system geometry. The pumps should be assumed to operate in the expected manner. The fluid leaving the core should be calculated in a BE manner and include the effects of cross flow and core fluid distribution. Unique ECCSs should be accounted for. The effects of accumulator nitrogen discharge after draining accumulator water should be included in the calculation.

Westinghouse Realistic Model

The WCOBRA/TRAC two-phase core level model was assessed against a wide range of FLECHT (low flooding rate, Reference 91, and top skewed, Reference 92) and FLECHT-SEASET, (References 89 and 90) test data. The effect of pumps on or off is analyzed and the worst case chosen. Westinghouse showed the entrainment model used to calculate carryover is capable of calculating experimental data adequately (see response to Volume 3, question 19, Reference 50). Cross flow is calculated between core channels (for example, see CQD Figure 20-2-6, Section 3: Core). The core fluid distribution is calculated axially (see Volume 4, question 37, Reference 44) and radially between the core channels. WCOBRA/TRAC is capable of accounting for unique ECCS such as downcomer injection. WCOBRA/TRAC includes models to account for accumulator nitrogen (see Section 12.2 of this report). See Note 22.

Table C-1 (continued)

RG 1.157 Guidance

Westinghouse Realistic Model

3.12.3 - Interaction between steam and the ECC water shall be taken into account in a BE manner.

WCOBRA/TRAC includes a two-fluid, non-equilibrium model that directly calculates steam/ECC water interaction. This model was shown to adequately represent the phenomena in CQD Section 15-3. See Note 23.

3.12.4 - Refill and reflood heat transfer should be based on BE calculations of flow through the core, accounting for unique ECCS. The calculations should account for flow blockage due to cladding swell or rupture. Heat transfer calculations based on two-phase core conditions during refill should be justified by comparison to experimental data.

WCOBRA/TRAC calculates the core flow directly from the basic equations, and it is capable of accounting for unique ECCS. The code accounts for flow blockage due to cladding swelling and rupture. Westinghouse calculates core heat transfer during refill based on WCOBRA/TRAC calculated conditions including two-phase conditions. Comparisons to G-2 refill tests, Reference 108, justified this approach. See Note 24.

Table C-1 (continued)

RG 1.157 Guidance

Westinghouse Realistic Model

4.1 - The calculational uncertainty should include the uncertainty from individual code models, experimental data, boundary and initial conditions, fuel behavior, and simplifying assumptions and approximations. The calculational uncertainty should be determined to the 95% probability level when comparing the calculated results to the requirements of 10 CFR 50.46

Westinghouse determined the code bias and uncertainty for the code models, power distribution, break flow paths, initial conditions, and simplifying assumptions. The bias and uncertainty for simplifying assumptions in code models are part of the code bias and uncertainty based on test data comparisons. Other simplifying assumptions are those due to model input choices. Westinghouse accounts for these using scoping studies to select conservative input (see response to Volume 5, question 51, Reference 40. These biases and uncertainties are used in a Monte Carlo simulation to determine the 95th percentile PCT for comparison to 10 CFR 50.46 requirements. See Note 25.

Table C-1 (continued)

<u>RG 1.157 Guidance</u>	<u>Westinghouse Realistic Model</u>
<p>4.2 - The code uncertainty should be determined by direct comparison between calculated results and experimental data from integral and separated effects experiments at different scales. The comparisons should account for measurement limitations and calibration errors. The codes predictive ability will need to be evaluated for several key parameters and over several time intervals. Justification for the uncertainty treatment should be provided. Effects of scale on the calculated results should be assessed.</p>	<p>Westinghouse determined the <u>WCOBRA/TRAC</u> uncertainty by direct comparison to both integral and separate effects experiments. Uncertainty due to measurement effects are accounted for in the uncertainty evaluation. Westinghouse evaluated several thermal-hydraulic parameters in addition to PCT to ensure the absence of significant compensating errors (see Note 26). Westinghouse calculated separate biases and uncertainties for the blowdown and first and second reflood PCTs. Westinghouse justified the biases and uncertainties applied in CQD Sections 19, 26, and 27 and Reference 58. Westinghouse found the code did not have a scale bias. See Note 27.</p>
<p>4.3.1 - Uncertainty due to boundary and initial conditions and equipment performance should be accounted for in the uncertainty evaluation. The parameters considered may be limited by setting their values to conservative limits.</p>	<p>The uncertainty due to boundary and initial conditions is accounted for by Westinghouse's methodology. In some cases, a nominal value is used (if the parameter is tightly controlled) and bounding assumptions are also applied; in other cases, the boundary and initial condition uncertainty is directly included in the uncertainty analysis. See CQD Sections 25 and 26-5 and Reference 58, Section 4.3.1. See Note 28.</p>

Table C-1 (continued)

RG 1.157 Guidance

4.3.2 - The uncertainty associated with fuel behavior cannot be determined from integral experiments that use electrically heated rods. Uncertainties to be quantified and included in the overall code uncertainty are those from fuel conductivity, gap width and conductivity, and peaking factors.

Westinghouse Realistic Model

Westinghouse directly accounts for peaking factor uncertainty in the uncertainty analysis (see CQD Section 26) using a power distribution response surface and Monte Carlo simulation (MCS). Based on its revised methodology, fuel conductivity and gap width/conductivity uncertainties are accounted for by matching the WCOBRA/TRAC initial fuel temperature to that from a detailed fuel rod model at the BE level and then varying the fuel conductivity and gap conductivity in the HOTSPOT model. See Note 29.

Table C-1 (continued)

<u>RG 1.157 Guidance</u>	<u>Westinghouse Realistic Model</u>
<p>4.3.3 - Other factors include those not evaluated by the comparisons to integral effects tests. For example, the decay heat calculation and the cladding metal-water reaction model cannot be evaluated from tests that use electrically heated rods. Another area is the use of break discharge coefficients. Quantify the uncertainty from models that have not been evaluated by comparison to integral effects tests and include it in the overall code uncertainty.</p>	<p>Uncertainties due to the decay heat calculation and the cladding metal-water reaction rate are included (see Section 3.1.3, Reference 58). The uncertainty due to use of break discharge coefficients is accounted for in the global model response surface and MCS. See Reference 58, Section 4.4.2. In its response to Volume 4, question 55, Reference 16, Westinghouse noted that CQD Section 17 reviewed the code assessment matrix/results. That section showed the code had no deficiencies that would significantly impact the PWR PCT calculation, and the assessment covered the main processes important to PCT calculations. See Note 30.</p>

Table C-1 (continued)

<u>RG 1.157 Guidance</u>	<u>Westinghouse Realistic Model</u>
<p>4.4 - The methods used to determine the overall calculational uncertainty at the 95% probability level should be provided and justified. Justification should be provided for the assumed parameter distributions and ranges considered. Evaluation at the 95% probability level is needed only for the worst case break. Justification must be provided to demonstrate the overall uncertainty for the worst case break bounds the uncertainty for all other breaks in the break spectrum. If it can be shown that meeting the temperature criterion at the 95% probability level ensures with an equal or greater probability that the other 10 CFR 10.46 criteria will not be exceeded, then explicit consideration of the probability of exceeding the other criteria may not be required.</p>	<p>Westinghouse discussed and justified the uncertainty approach in CQD Sections 26 and 27 and Reference 58. Westinghouse justified the assumed parameter distributions and ranges in Reference 58. Westinghouse, in Volume 5, question 53, Reference 51, clarified its position on the uncertainty on the worst break and other 10 CFR 50.46 criteria. See Note 31.</p>
<p>4.5 This section noted that the CSAU methodology (Reference 61) represents an approach developed by the NRC to evaluate overall PCT uncertainty.</p>	<p>Section 2 of this report compared the Westinghouse and CSAU methodologies and concluded the Westinghouse methodology met the intent of the CSAU approach.</p>

Notes to Table C-1:

1. The INEL reviewed the results of Westinghouse's initial condition sensitivity studies in CQD Section 22. As indicated by Westinghouse, the results showed BOL was most limiting.

Based on CQD Section 25, Westinghouse assumes the core power in the WCOBRA/TRAC runs is the maximum licensed core power without uncertainties. The INEL considers this appropriate because it is the maximum power at which the plant is allowed to operate and will result in the highest PCT. Uncertainties in core power are accounted for in the uncertainty evaluation through the power distribution uncertainty.

While most nuclear power plants operate in baseload mode with low peaking factors, transient operation is possible, and the Technical Specifications allow a wide range of peaking factors to account for plant transients. Westinghouse accounts for this peaking factor variation by developing a power distribution response surface. This response surface is based on WCOBRA/TRAC runs that vary the peaking factor and power distribution. For example, the F_0 is varied as discussed in Section 4.4.1.1 of Reference 58 and shown in Table 4.4.1-1. The response surface is then used in the Monte Carlo simulation to account for power distribution effects on the 95th percentile PCT. The base PCT in the Monte Carlo simulation uses a power distribution with F_0 given in Reference 58, Table 4.4.1-1, power shape 10. The $F_{\Delta H}$ values used in the run matrix are also discussed in Section 4.4.1.1 of Reference 58 and shown in Table 4.4.1-1. Transient F_0 uncertainty is accounted for as discussed in Section 9.2 of this report. Measurement uncertainties are accounted for during the Monte Carlo analysis by sampling the uncertainty distribution also discussed in Section 9.2 of this report. The INEL considers this adequate because the base PCT is the result of medium to high peaking factors, measurement uncertainties are accounted for, the F_0 uncertainty distribution covers the calculated range, and the uncertainty analysis will overestimate the possibility of high peaking factors in the 95th percentile PCT evaluation.

For fuel conditions, see Note 2 for initial stored energy and Notes 4 and 5 for decay heat.

The break spectrum results for three plants reported in CQD Section 22-6 were reviewed and Westinghouse included guillotine breaks of the recommended size. The split break spectrum also included breaks of the recommended size except for one plant that had the peak split break PCT at a break area equal to the cold leg area. In this case, the split break spectrum was not extended to 2 times the cold leg area. The Westinghouse uncertainty methodology accounts for guillotine and split breaks separately.

The single failure Westinghouse assumes is the loss of a train of pumped ECC for the calculation of the primary system response but loss of only a low head pump for the containment pressure calculation to minimize containment pressure. The INEL considers this adequate to account for single failure effects because it is a conservative approach to both ECC flow to the primary system and the containment pressure.

2. The initial stored energy is based on the NRC approved PAD code, Reference 79. Westinghouse stated the code includes the effects of high-temperature cladding creep, gas mixture conductivity, fuel burnup, fuel pellet cracking and relocation, and operating temperature creep. To ensure the stored energy in WCOBRA/TRAC matches that calculated with PAD, Westinghouse adjusts the initial gap size to match the best-estimate fuel average temperature to within +5°F at the peak power location for all rods modeled. Uncertainties in fuel stored energy are accounted for in the HOTSPOT model through variations in the gap conductance and the fuel conductivity. Based on the use of a best estimate plus uncertainties approach for the initial stored energy from a model that is NRC approved, the INEL considers Westinghouse's model adequate.
3. The INEL reviewed the reactor kinetic models and found them consistent with standard practice. In addition, Westinghouse validated the point kinetics model. In CQD table 8-15, Westinghouse compared the WCOBRA/TRAC point kinetics model response (reactivity insertion and asymptotic period) to step reactivity insertions of +0.003, +0.0015, and -0.030

delta-K in the absence of external feedback methods to those calculated analytically by the Inhour equation. The comparison shows very good agreement between the two. Therefore, based on the INEL review and the good agreement between the code and the analytical solutions, the INEL considers the WCOBRA/TRAC point kinetics model adequate for realistic LBLOCA calculations.

4. INEL review of the actinide decay heat model found it consistent with standard practice. Decay heat model parameters are based on the 1979 ANS Standard (decay heat constants, see CQD page 8-16). In Reference 214, List I, Westinghouse indicated the value of R used in CQD Eqns. 8-14/15 (and Eqn. 14/15 from the 1979 ANS Decay Heat Standard) is based on ENDF-B/V data.¹²⁵ The INEL considers these two sources adequate to support the BE nature of the actinide decay heat model.

The actinide decay heat model only includes neptunium-239 and uranium-239. Westinghouse included the plutonium-239 decay heat in the fission product decay heat calculation. It clarified its reasons for not modeling other actinides in response to Volume 1, question 231, Reference 29. Based on the information from Westinghouse in that response, the INEL concluded that Westinghouse had adequately justified the WCOBRA/TRAC actinide decay heat model.

Westinghouse discussed the actinide decay heat modeling assumptions in Attachment 2, Reference 57. The modeling of actinide decay heat for the HR and HA rod is different from the average and low power rods. For the HR and HA rod, actinide decay heat is chosen based on a burnup that maximizes the actinide decay heat contribution to the calculated PCT.

For the average and low power rods, Westinghouse noted that the actinide decay heat was based on the facility operating history. This is accomplished by using a burnup of 10,000 MWD/MTU which provides a slightly conservative combination of heat sources (decay heat and stored energy) for these rods. This burnup is conservative as discussed in Reference 57, Attachment 2, and Reference 55. In Reference 55, Westinghouse also noted that no credit is taken in the decay heat calculation for prior shutdowns of previously burned assemblies (for

example, prior refueling outages). Credit for these outages would reduce the decay heat from those assemblies in their second or third fuel cycle.

Based on these considerations, the INEL concluded that Westinghouse has adequately justified the time-in-life used for the actinide decay heat model.

5. INEL review of the fission product decay heat model found it consistent with standard practice.

Westinghouse compared the fission product decay heat model output from the WCOBRA/TRAC model to that based on the ANS 1979 Standard in CQD Table 8-2. Based on the excellent agreement between the two shown in the table, the INEL considers the WCOBRA/TRAC fission product decay heat model to adequately represent the ANS 1979 standard.

6. As discussed in the table, the WCOBRA/TRAC models vary from the RG in several areas. First, WCOBRA/TRAC uses the Cathcart-Pawel model below 1900°F. Westinghouse justified this by noting the model overpredicted the original data base below 1900°F (see response to Volume 1, question 225, Reference 8). Westinghouse supported this by noting the discussion in Reference 84 on page 67 and the comparison in Figure 30 of the reference. INEL review of Reference 84 found the information Westinghouse indicated supported the assertions made by Westinghouse. Also, in Reference 84, INEL found the authors noted that oxidation is not describable by parabolic kinetics models below 1742°F and that extrapolation of high temperature rate constant data below 1832°F will result in overprediction of oxide layer growth and total oxygen consumption. See page 118, Reference 84 (Cathcart/Pawel). This is consistent with the Westinghouse information. Given that the WCOBRA/TRAC model differs from the RG in a conservative direction, the INEL considers use of the Cathcart-Pawel model below 1900°F adequate.

To support the ZIRLO metal-water reaction rate model, Westinghouse provided information for a ZIRLO specific model developed in Reference 127. In the response to Volume 5, question 41, Reference 46, Westinghouse noted the ZIRLO model for metal-water reaction was not

approved by the NRC for 10 CFR 50.46, Appendix K, analyses. Therefore, the INEL reviewed the model in Reference 127 for use in realistic LBLOCA analyses. This review found the ZIRLO model adequately represented the ZIRLO data at temperatures above 2000°F and overpredicted the data below 2000°F. Therefore, the INEL recommends the model be approved for realistic LBLOCA analyses.

Two other areas where the WCOBRA/TRAC models differ from the RG are the lack of modeling a steam pressure effect and internal oxidation from UO_2 . The INEL considers this adequate because the oxidation model is not steam limited when applied to either cladding surface. This more than compensates for the not modeling these effects (Reference 128). Also, as noted by Westinghouse in Reference 57 the system rapidly depressurizes in a LBLOCA minimizing any steam pressure effects.

7. Westinghouse includes a conduction model to represent reactor internal heat transfer. The INEL reviewed the model in CQD Section 7-2 and found Westinghouse used a standard approach to solving the heat conduction problem. The WCOBRA/TRAC equations were compared to the conduction solutions provided in Holman,¹²⁹ and found to be consistent. The vessel models allow for modeling a wall (flat plate) or hollow and solid cylinders. No specific conservatisms in the conduction model were noted by Westinghouse or found by the INEL review.

Material properties in the vessel are supplied by the user (see CQD Section 10-5-1). Westinghouse noted that standard references such as Touloukian¹³⁰ or material properties from the material vendor are used.

Based on these considerations, the INEL considers WCOBRA/TRAC capable of providing a realistic calculation of reactor internal heat transfer. Questions on the material properties used or the actual use of the model would require an evaluation of a plant specific submittal.

8. The INEL reviewed the steam generator heat transfer model described in CQD Section 9-5. That section referenced CQD Section 7-7 as providing the conduction model for the steam generator tubes. The INEL reviewed Section 7-7, and the SG conduction equation used in WCOBRA/TRAC is found

in Eqn. 7-89. In Reference 206, Attachment 6, Westinghouse compared the results of the as coded CQD Eqn. 7-89 to an analytical solution for a 1-D pipe. INEL found a good comparison between the WCOBRA/TRAC output and the analytical solution. Based on this, INEL considers the WCOBRA/TRAC 1-D conduction equation for the steam generator adequate for realistic LBLOCA analyses.

9. The WCOBRA/TRAC cladding swell and rupture model is described in CQD Sections 7-4-1 and 7-4-2. The models and INEL review are discussed in Section A.7 of this report. Review of the model found that the WCOBRA/TRAC models included most of the RG recommended items except for anisotropic material properties and asymmetric cladding deformation. The INEL considers this adequate because the uncertainties associated with the use of averaged strain data overwhelms these omissions. The scatter in the burst strain relative to an average strain model is illustrated in CQD Figures 7-18 (Zircaloy) and 7-20 (Westinghouse ZIRLO cladding).¹³¹ The INEL also notes that the burst strain uncertainty is accounted for directly in Westinghouse's uncertainty propagation.
10. The critical flow model for realistic LBLOCA analyses is discussed in CQD Section 4-8-2. The INEL reviewed the WCOBRA/TRAC critical flow model and found that it included the RG recommended items: fluid conditions at the break are accounted for by using the appropriate model based on void fraction (see CQD page 4-127), upstream and downstream pressures are accounted for by assuming equilibrium conditions at the break plane (CQD page 4-127) and stagnation conditions at the cell center based on the cell center conditions (CQD Eqns. 4-260 and 4-263, for example), and geometry effects (L/D) through CQD Eqn. 4-259 and following discussion.

The INEL review also considered the comparisons to Marviken test data Westinghouse provided in CQD Section 16-4. The Westinghouse analysis discussed in Section 16-4 showed that the model calculated the Marviken data to within the range shown by the code/data comparisons in CQD Figure 16-4-36 for L/D ratios given in CQD Table 16-4-2. Because of the importance of the break flow on the calculated PCT, Westinghouse included the break flow as part of the model uncertainty evaluation. This was incorporated through a response surface to account for break flow effects

on PCT that was developed based on the thermal-hydraulic run matrix (a series of WCOBRA/TRAC runs) where the C_D was varied as shown in Table 4.4.2-1, Reference 58. Based on Reference 58, this range covers 100% of the data (see Figure 3.1.1-8, Reference 58). Also, Westinghouse samples the full range of C_D s found in the Marviken comparisons in the uncertainty analysis and includes an extrapolation error for C_D s outside the response surface range. Based on this, the INEL considers the WCOBRA/TRAC critical flow model adequate to meet RG Section 3.4.1.

11. The Westinghouse methodology accounts for break type, split or guillotine. The PCT from a cold leg guillotine break with medium to high peaking factors and moderate power shape skewing is calculated with WCOBRA/TRAC. A Monte Carlo simulation to account for uncertainties due to peaking factors and power shape, initial conditions, models, and local HR effects is used to determine the 95th percentile PCT for the guillotine break. The basis for INEL finding this approach adequate is discussed in the main body of this report.

Westinghouse calculates the limiting cold leg split break through direct WCOBRA/TRAC runs. The limiting split PCT is then used as the basis for a separate Monte Carlo simulation to account for uncertainties due to power shape, initial conditions, and local HR effects. Westinghouse successfully supported using the power shape and initial conditions uncertainties based on the guillotine break (see Reference 58). The code model uncertainty is not used in the split break Monte Carlo because of the choice of the limiting split break. Finally, local HR rod effects are calculated directly for the limiting split break via a HOTSPOT calculation. The INEL found this adequate because the split break is accounted for in Westinghouse's analysis and the information provided by Westinghouse supports its approach. See also Section 9.3 of this report.

Based on Reference 205, Attachment 5, the critical flow model accounts for nonequilibrium and L/D effects. When the L/D is less than 1.5 for the cell connected to the break, conditions as discussed in Reference 205, Attachment 5, are allowed. When the L/D for the cell connected to the break is greater than 1.5, the code assumes stagnation conditions based on equilibrium. If nonequilibrium conditions are

calculated, equivalent equilibrium conditions are obtained and used in the model. In Reference 205, Westinghouse noted this approach was consistent with Reference 199. INEL reviewed the reference and found it supported the Westinghouse approach. Therefore, INEL concluded that the WCOBRA/TRAC critical flow model adequately meets the RG guidance.

12. ECC bypass is calculated by the interaction of the interphase drag, wall friction, and condensation models. Westinghouse discussed the bypass model in its response to Volume 4, question 2, Reference 42. The information provided there showed the bypass model overpredicted the bypass in the UPTF bypass tests, Test 6, Run Nos. 131, 132, 133, 135, and 136. Westinghouse calculated vessel fill ratios (calculated result over measured result), and these showed the WCOBRA/TRAC model overpredicted the amount of bypass because the vessel fill ratios were all less than one. This indicates the WCOBRA/TRAC models tend to be conservative rather than a BE representation of ECC bypass. Westinghouse calculated a plant specific estimate of the conservatism from the extra bypass for the VRA model in its response. The estimate showed the PCT was approximately 55°F higher due to the increased bypass and the longer refill period. The INEL also notes that Westinghouse does not take direct credit for the ECC bypass conservatism in the uncertainty analysis. That is, Westinghouse does not include a direct, negative bias in the Monte Carlo simulation for the ECC bypass conservatism.

Westinghouse also evaluated the model against Creare 1/15th and 1/5th scale test data in CQD Section 15-1-5 and provided additional details in its response to Volume 3, question 8, Reference 37. The comparisons between test data and WCOBRA/TRAC results provided in its response to Volume 3, question 8, showed the code did a good job of representing the Creare data.

Based on the above, the INEL finds that the Westinghouse model for ECC bypass is conservative and such conservatism is allowed by the RG.

13. In general, the INEL agrees with Westinghouse's approach regarding the need to keep nodalization consistent between the test simulations used to determine the code uncertainty and the plants. By keeping the

nodalizations consistent, Westinghouse is using the approach that best allows the code uncertainty to be applied to plant analyses without additional uncertainty questions needing to be addressed due to nodalization differences.

This being said, the INEL also notes the following items:

- (1) The Westinghouse uncertainty analysis does include a nodalization uncertainty (see CQD Section 19-6).
- (2) Westinghouse did a nodalization study (see Volume 4, question 17, Reference 21) where the number of nodes in the in cold leg models for UPTF (Test 8) and the Westinghouse Steam Water Mixing Tests (Test 629) was reduced by a factor of about 1.4 to make the node lengths consistent with the plant models. The results showed the calculated liquid temperatures at the end of the pipe for the two nodalizations were essentially the same.
- (3) For critical flow, Westinghouse did a nodalization study based on the Marviken test analyses in CQD Section 16-4. Two Marviken tests were analyzed with two and four nodes in the test nozzle. CQD Figures 16-4-28/29 show little change in the flow rate was calculated due to this change.

Therefore, Items 2 and 3 above support the adequacy of the plant nodalizations.

14. The INEL reviewed CQD Sections 4-2 and 4-7.

Vessel Model

As noted in the table, both two-phase conditions and friction factor variation with Reynolds number are accounted for in this model. For laminar flow, the standard friction factor model is used, and for turbulent flow, a fit to the Moody friction factor model is used (see CQD Eqns. 4-5a,b and the response to Volume 1, questions 49/52, Reference 7). In the vessel, the two-phase wall pressure drop model is based on that

developed by Wallis (Reference 121), which is considered adequate because it is a widely accepted model.

WCOBRA/TRAC allows form losses to be input and partitions the form loss by α weighting. This is adequate based on the fact that the phases flow together and mix together as they flow through an orifice, for example. Around a bend or elbow this assumption may not accurately reflect the flow structure, but overall, the assumption does not seem unreasonable. Also, orifice type test data provided by Westinghouse showed good comparisons between test and code calculations for pressure drop (see Westinghouse's response to Volume 1, question 50, Reference 8).

The wall friction, however, is not α weighted. The code determines whether the wall is in a cold or hot condition. If cold, the code applies the wall drag to the liquid only, and the wall drag is applied to the vapor only if the wall is hot. This seems like an adequate approach for the fluid-wall interaction.

Loop Model

The loop friction model also varies the friction factor based on the Reynolds number (Eqns. 4-198, 4-207), and it includes a two-phase multiplier (Eqns. 4-203, 4-209). The two-phase friction factor model is based on a simplification of the Colebrook equation (according to Reference 133, the WCOBRA/TRAC model varies up to 4% from the Colebrook equation). Comparison of the WCOBRA/TRAC two-phase multipliers with the HTFS¹³⁴ multiplier showed good agreement over a wide range of conditions (see CQD Figures 4-8 to 4-11). A homogeneous two-phase friction model is applied (Eqns. 4-207, 4-209, and 4-211) if the void fraction is greater than 0.9995. Westinghouse's response to Volume 1, question 100, Reference 11 verified the homogeneous model by comparing to other models. Linear interpolation between the annular model (used for void fractions below 0.9) and the homogeneous model (used for void fraction greater than 0.9995) connects the two models. Therefore, based on the good comparisons to the HTFS correlation for the two-phase model shown in the CQD, and the good comparisons of the homogeneous model to the other

mode, in Westinghouse's response to Volume 1, question 100, the INEL considers the loop two-phase friction model adequate for LBLOCA analyses.

MODEL CONSISTENCY

Based on Reference 205, Attachment 5, and CQD, the basic variables in the WCOBRA/TRAC friction models are phasic density and velocity and void fraction. The code calculates these parameters directly from the conservation equations and uses them consistently for each term of the friction model. The code uses the same void fraction for each component. For example the same phasic velocity and void fraction are used in CQD Eqns. 2-45 and 4-3. Therefore, INEL considers the approach in WCOBRA/TRAC to be consistent with RG 1.157 guidance in this area.

For range of applicability, see Section 10.2 of this report.

15. The INEL reviewed the equations as documented in the CQD. The momentum equations contain the RG recommended items. The review also found the equations consistent with standard practice. Therefore, they are adequate for realistic LBLOCA analyses.
16. The Biasi and Zuber (and its modifications) CHF correlations are widely used in reactor analysis codes to calculate CHF; therefore, the INEL considers them adequate for LBLOCA analyses. Collier (Reference 87) noted the Biasi correlation correlated 85% of the data base (over 4500 data points) within $\pm 10\%$. The code applies the Biasi correlation above $30 \text{ g/cm}^2\text{-s}$ with a linear interpolation to the Zuber correlation at flows below $30 \text{ g/cm}^2\text{-s}$ (see CQD Eqn. 6-68). Collier gives the lower bound of the Biasi correlation data base as $10 \text{ g/cm}^2\text{-s}$ which indicates WCOBRA/TRAC uses the Biasi correlation within the data base flow range except for part of the interpolation regime (between 10 and $0 \text{ g/cm}^2\text{-s}$) until the Zuber correlation is used alone at zero flow. This extension is considered appropriate to allow for a smooth transition between the Biasi and Zuber correlations. The Zuber correlation is only applied at low flows as conditions approach pool boiling (less than $30 \text{ g/cm}^2\text{-s}$) and is used alone at zero flow. The other data base ranges for diameter, length, flow, quality, and pressure for the Biasi correlation given in

Collier indicate the Biasi correlation covers the range of conditions expected in a PWR. Based on the above review, the INEL considers the WCOBRA/TRAC CHF model to have met the RG and finds it adequate for LBLOCA analyses.

17. The post-CHF models in CQD Sections 6-2-5 through 6-2-8, account for the RG recommended items:
 1. Liquid entrainment: See Eqns. 6-75, 6-85, 6-112, and 6-118. In Reference 205, Attachment 5, Westinghouse discussed how transition boiling model 2 meets this RG item because an entrainment term is not directly included in this model (see CQD Eqn. 6-82). Westinghouse noted that entrainment effects would be accounted for indirectly through the F_{wet} term used in CQD Eqn. 6-83 and defined in CQD Eqn. Eqn. 6-84. Model 2 is a simple model that uses F_{wet} to interpolate between heat flux at the CHF point and the T_{MIN} point. Westinghouse also noted that CQD Eqn. 6-89 shows that WCOBRA/TRAC takes the maximum of transition boiling Model 1, which includes entrainment effects directly, and Model 2. In Submittal K, Attachment 1, Reference 17, Westinghouse noted that Model 2 tends to be used a lower void fractions and Model 1 tends to be used at higher void fractions. INEL notes the higher void fractions is where the effects of entrainment would be more important. Based on this, the INEL considers the transition boiling models to be consistent with the RG recommendations.
 2. Thermal radiation: See Eqns. 6-75, 6-82, 6-85, 6-111, 6-112, and 6-118.
 3. Thermal nonequilibrium: WCOBRA/TRAC calculates separate heat transfer to the liquid and vapor fields which can be at different temperatures that are calculated locally.
 4. Low and high mass flow rates: Forced convection to vapor accounts for a locally calculated mass flux in Eqns. 6-75, 6-82, 6-85, 6-111, and 6-118.

5. Low and high power densities: These are accounted for through the effect on the local HTC of the local fluid conditions. The local fluid conditions reflect the effects of high and low power densities upstream of a given location. Also, the local high or low power density will be reflected in the local wall temperature. Further, Westinghouse noted in Reference 205, Attachment 5, that the code assessment matrix included tests for a range of linear heat rates and axial power variations. Therefore, uncertainty in this parameter is included in the HTC multipliers used in the uncertainty evaluation discussed in Section 6 of this report.
6. Subcooled and saturated inlet fluid conditions: WCOBRA/TRAC calculates subcooled or saturated inlet fluid conditions based on the heat transfer to the ECC upstream of the core inlet. These fluid conditions pass into the core, and local heat transfer to the phases determines how subcooling is lost or saturated fluid becomes superheated. See also Item 3 above.
18. The single-phase vapor model is based on the Dittus-Boelter (Reference 102) and Wong-Hochreiter¹⁰⁵ correlations for turbulent flow and a Nusselt number given in CQD Eqn. 6-4 for laminar flow. The laminar flow Nusselt number is based on References 89 and 205, Attachment 5. For Reynolds numbers less than 2000, the McAdams correlation¹³⁶ is also evaluated.

Transition between turbulent and laminar flow is allowed by choosing the maximum heat transfer coefficient from amongst the four correlations. Attachment 1, Reference 17, was a study of the vessel heat transfer package. The evaluation in that submittal gave the Reynolds number for turbulent/laminar flow transition (see Figure 44) in the heat transfer model. This showed the WCOBRA/TRAC model extrapolated the turbulent correlations into the transition and upper laminar regions. The WCOBRA/TRAC transition value is also lower than the transition at a Reynolds number of 2000 recommended in the RG.

In Reference 205, Attachment 5, Westinghouse indicated that:

- (a) Its review of the literature found the RG recommended transition from turbulent to laminar conditions at a Reynolds number of 2000 is better explained by a range of Reynolds numbers. For example, Holman (Reference 129) was cited to support a transition range of 2000 to 4000. Westinghouse noted the data base for the Wong-Hochreiter correlation covered Reynolds numbers down to 2500, which is well within the transition region cited by Holman. If this transition data is extrapolated, Nusselt numbers greater than the $\bar{N}_{COBRA/TRAC}$ value in CQD Eqn. 6-4 are found at Reynolds numbers below the $\bar{N}_{COBRA/TRAC}$ transition point. The extrapolated values are also higher than the 7.86 found by Kim (Reference 169) and in agreement with Kays (Reference 163) for flow through a staggered array.
- (b) Test data analysis for FLECHT-SEASET Test 32013 supports a Nusselt number greater than the $\bar{N}_{COBRA/TRAC}$ value at a Reynolds number lower than the $\bar{N}_{COBRA/TRAC}$ transition point.
- (c) Westinghouse compared test data at low Reynolds numbers (1000 to 2000) to the $\bar{N}_{COBRA/TRAC}$ laminar Nusselt number multiplied by:
(1) the maximum $\bar{N}_{COBRA/TRAC}$ two-phase enhancement factor discussed in CQD Section 6-2-8 (to account for possible trace droplets in the data used in the comparison) and (2) a factor to account for possible drop contact heat transfer. This comparison showed that the resulting Nusselt number still was a lower bound to most of the measured test data shown in Figure C, Attachment 5, Reference 205.
- (d) Finally, Westinghouse compared the $\bar{N}_{COBRA/TRAC}$ model to a single-phase correlation developed in Reference 207. The comparison showed that the $\bar{N}_{COBRA/TRAC}$ model underpredicted the correlation to a Reynolds number less than the $\bar{N}_{COBRA/TRAC}$ laminar/turbulent transition point. That is, the correlation gave Nusselt numbers greater than the CQD Eqn. 6-4 value to this Reynolds number.

Therefore, Westinghouse concluded its review supported the WCOBRA/TRAC models in the transition region.

Based on the above, INEL considers the Westinghouse information sufficient to justify its alternate approach in the area of laminar/turbulent transition and its choice of Nusselt number for laminar flow. Also, INEL review of Reference 200 found that it discussed a laminar/turbulent transition between Reynolds numbers of 1160 and 1610 based on the test results reported, and this supports the Westinghouse review. Therefore, the WCOBRA/TRAC model is considered adequate.

A radiation model is included to account for radiation from the rods to the steam and entrained drops. Vapor temperature is calculated directly from the WCOBRA/TRAC vapor energy equation.

The RG discussed a Hottel procedure (Reference 132) to correct for radiation heat transfer in a single-phase vapor heat transfer model based on test data. A review of the WCOBRA/TRAC models found that only the Wong-Hochreiter model was based on data where there was the potential for radiation heat transfer. In Reference 206, Attachment 6, Westinghouse stated the test data used to develop the Wong-Hochreiter model was limited to wall temperatures less than 400°F. In that situation, radiation heat transfer was not important.

Based on information provided by Westinghouse, INEL believes Westinghouse showed the WCOBRA/TRAC models are consistent with the RG recommendations for radiation heat transfer.

For the vessel and loop post-CHF models, Westinghouse showed in response to Volume 1, question 213, Reference 29 for the loop and Volume 2, question 2, Reference 39 for the vessel that the blowdown assessment range for single-phase vapor heat transfer covered the appropriate PWR range of conditions. For reflood, see Section 10.2 of this report.

19. The INEL reviewed the pump model for WCOBRA/TRAC described in CQD Section 9-4. The momentum transfer from the pump to the fluid is treated as a momentum source term (Eqns. 9-1/9-2), and pump speed as a function

of time is calculated (Eqn. 9-9). The pump head and torque models are based on empirical homologous curves derived from a scaled pump with similar specific speed. The homologous curves determine the pump resistance based on volumetric flow and pump speed in both single- and two-phase flow. This model is basically an empirical model and is considered consistent with other pump models based on a homologous curve approach. Therefore, it is considered to have met the RG and adequate for LBLOCA analyses.

Westinghouse showed in the response to Volume 5, question 47, Reference 48, that a locked rotor need not be considered. The response noted the broken loop pump speed increased to less than X% of nominal in the three plants analyzed in the CQD, and pump flywheel integrity was assured up to a pump speed of Y% of nominal, where $X < Y$. (Note the values for X, Y, and Z (used below) are given in the Volume 5, question 47 response, and Westinghouse considers them proprietary information.) If flywheel integrity is maintained, a locked rotor will not occur. The value of Y% was achieved, however, by assuming a minimum ultimate tensile strength for the flywheel material, but without the 30% derating of the tensile strength noted in the ASME code. If the 30% tensile strength derating is included, flywheel integrity is only assured up to Z% of nominal speed, where $X > Z$. The NRC Staff found this approach acceptable, and closed the issue. Subsequent INEL discussion with the NRC Staff found that the 30% derating in the ASME code did not apply to the pump concerns addressed here. Therefore, the INEL agrees with the NRC closure of this item.

20. The INEL reviewed the CQD to determine:

- (a) The plant models in CQD Section 20 included a hot assembly and the code calculates the core flow as a function of time.
- (b) The models included cross flow between the hot assembly and surrounding assemblies. All the different core regions are connected by crossflow junctions. The INEL reviewed Westinghouse's approach to calculating crossflow loss coefficients in its response

to Volume 4, question 65, Reference 16. The approach was found adequate because it was based on Idel'Chik.¹³⁷

- (c) The effects of cladding swell and rupture are accounted for in the core hydraulic calculations. The methods used are described in CQD Section 7-4-2. The INEL reviewed those methods and found they account for the flow blockage by adjusting the flow areas of the continuity cells each time step to reflect the deformed cladding. Momentum cell flow areas are also updated each time step using the average outer rod diameter from the continuity cells above and below the momentum cell center. If burst is calculated for the HA rod this is accounted for using the method of Powers and Meyer.¹³⁸ The burst strain is converted to a flow area reduction factor and applied to the continuity cell containing the HA rod burst elevation. Momentum cell flow area is also adjusted using a elevation weighting approach (see Eqn. 7-72).
- (d) Westinghouse stated they applied numerical damping, convergence criteria, time step controls, and modeling technology to ensure unrealistic flow oscillations do not occur. See response to Volume 5, question 48, Reference 22. The INEL considers these to be standard numerical analysis techniques to ensure unrealistic results do not occur and, therefore, adequate in this situation.

Based on the above, the INEL considers Westinghouse's approach to RG 3.11 adequate to meet the RG and for LBLOCA analyses.

21. As noted in the table, Westinghouse will use previously approved containment pressure models with WCOBRA/TRAC mass and energy release rates. This is adequate to meet the RG as it should give a bounding approach to the containment pressure calculation for LBLOCA analysis.
22. RG 1.157, Section 3.12.2.1, discussed the phenomenon of level swell. Westinghouse noted in response to Volume 5, question 49, Reference 44, that level swell is more important for small-break LOCAs while the phenomena of importance to LBLOCAs are entrainment and carryover. NUREG-1230, Reference 88, Tables 5-1 and 5-2, was cited to support this

distinction. Therefore, Westinghouse focused on entrainment/carryover rather than level swell. The INEL agrees with this distinction as it is consistent with our understanding of the important LBLOCA phenomena, and it is consistent with the Westinghouse PIRT. Reflood assessments for the core and upper plenum were carried out in UPTF, CCTF, SCTF, and FLECHT facilities. Various core radial and axial power distributions and various bundle geometries (15x15 and 17x17) were simulated in these facilities. Volume 3, question 19, Reference 50, and Volume 4, question 37, Reference 44, discussed entrainment/carryover and axial void distributions due to two-phase mixtures in the core.

The INEL considers the effects of depressurization, boil-off, power level, fluid conditions, and system geometry accounted for in WCOBRA/TRAC due to the basic models in the code and the constitutive models. For example, the code calculates separate liquid and vapor temperatures, depressurization will result in vaporization of fluid at pressures consistent with the local liquid temperature, different power levels will result in different heat transfer conditions to the core fluid, and boil-off will occur as core heat transfer causes fluid to be saturated and boil. System geometry effects are accounted for by nodalization and code model input (for example, cell lengths and hydraulic diameters).

Based on these considerations, the INEL considers the two-phase core model and the carryover/entrainment models adequate to meet the RG and for realistic LBLOCA analyses.

23. The steam/water mixing test results in CQD Section 15-3 were reviewed. The results there showed that the WCOBRA/TRAC results overpredicted the measured pressure drop in the cold leg. Overprediction of the pressure drop is conservative. Also, the temperature of the fluid exiting the cold leg was adequately calculated. Therefore, the INEL considers the WCOBRA/TRAC results bounding and adequate to meet the RG and for realistic LBLOCA analyses. In addition, Westinghouse ranges a condensation multiplier directly in the uncertainty evaluation. The range of the multiplier is based on comparisons to UPTF test data. See Sections 6 and 9.2 of this report.

24. Comparisons of WCOBRA/TRAC results to G-2 refill test data show the code adequately calculated the test data. See CQD Sections 11-5 and 13-3-3. In general, WCOBRA/TRAC tended to overpredict the refill test PCT (see CQD Figure 11-5-39). These results indicate the code tends to provide a conservative estimate of heat transfer during refill. Based on this conservative trend, the INEL considers the two-phase, refill models adequate to meet the RG and for realistic LBLOCA.
25. In Reference 58, Westinghouse evaluated the sources of uncertainty in its LBLOCA methodology. Sources of uncertainty included the code uncertainty (including experimental uncertainty and simplifying assumptions (Volume 5, question 51, Reference 40)). Other sources of uncertainty included, for example, code models, initial and boundary conditions, fuel behavior, decay heat, cladding oxidation, and break flow.

Westinghouse does use simplifying assumptions to make the calculation of the overall uncertainty more practical. To support the assumptions used, Westinghouse provided the results of sensitivity studies (see Section 5.1.3 of Reference 58, for example). Also, Westinghouse modified its methodology in Reference 205, Attachment 2, to verify the superposition assumptions. Validation runs are made using WCOBRA/TRAC-HOTSPOT, and those results are compared to the results obtained from the superposition methods. The differences are used to develop a correction that is applied in the Monte Carlo simulation. Thus, if the assumptions in the superposition model are bad, and it performs poorly, the validation step will account for the poor performance. Because of the validation step, the INEL considers the simplifying assumptions in Westinghouse's methodology adequately justified.

26. In Reference 59, Westinghouse evaluated a number of post-CHF heat transfer, downcomer bypass, and blowdown/post-blowdown thermal-hydraulics/entrainment tests for compensating errors. INEL evaluation of the CER is found in Section 11 of this report. In summary, the INEL concluded that WCOBRA/TRAC does not have any serious compensating errors that would compromise WCOBRA/TRAC's ability to perform realistic analyses of LBLOCAs, or Westinghouse has appropriately accounted for the compensating error in the uncertainty methodology.

27. In Section 18 of the CQD, Westinghouse evaluated the effects of scale on the WCOBRA/TRAC uncertainty evaluation. They noted the NRC CSAU analysis (Reference 61) determined there were no scale effects for data on blowdown phenomena. Although the CSAU analysis raised concerns about the effects of scale on data for reflood phenomena, no apparent scale effect for reflood was found. Westinghouse noted that because WCOBRA/TRAC was assessed against this data, there should be no scale effect for the code predictions for reflood. The INEL notes these tests were run at facilities covering a wide range of scales. The CQD also noted that WCOBRA/TRAC was assessed against full-scale UPTF data in the areas of ECCS bypass, hot leg entrainment, and vessel plenum behavior. Other large scale tests include Marviken Critical Flow tests, accumulator tests at a plant, CCTF, SCTF, and G-1 and G-2 test facilities. Given the range of scales considered by Westinghouse, the INEL agrees that scaling concerns were adequately addressed by Westinghouse's code assessment process. Further information is found in Section 7 of this report.
28. The INEL reviewed Westinghouse's method of accounting for boundary and initial conditions uncertainty. Nominal values are used if the parameter is tightly controlled, or the sensitivity studies showed parameter variation had little effect on the PCT. An example is the pressurizer level, which is tightly controlled. In some cases, the uncertainty was covered by assuming a bounding value that was often based on Technical Specification limits. The use of the minimum SI flow is an example of this type of bounding approach. In other cases, the PCT variation due to a parameter change was determined from the plant sensitivity studies discussed in CQD Section 22. This variation was used to determine the plant specific uncertainty to the allowed or expected variation in the parameter. Then, the uncertainty was included in the uncertainty analysis through the initial condition uncertainty (CQD Section 26-5). The effects of accumulator temperature, pressure, and volume are examples of this type of approach. Based on this review, the INEL considers Westinghouse to have met the RG recommendations to include boundary and initial conditions uncertainty in the uncertainty analysis. Further information is found in Section 8 of this report.

29. Westinghouse includes the peaking factor uncertainty directly in the uncertainty analysis by a response surface. The INEL reviewed this approach and asked Westinghouse to justify the run matrix used to develop the power shape response surface. Westinghouse's response (see Volume 5, question 8, Reference 38) showed the run matrix adequately accounted for power shape effects on the calculated PCT. Information from Westinghouse in Reference 190 adequately addressed INEL concerns on the response surface generation from the run matrix data. Westinghouse's revised methodology (Reference 58) directly accounts for fuel conductivity and gap conductance/width uncertainties through a Monte Carlo analysis that varies the fuel conductivity and gap conductivity in the HOTSPOT model (see Section 9.4 of this report). Based on the review discussed in Section 9.4 of this report, the INEL concluded the Westinghouse HOTSPOT approach was adequate to meet the RG in this area.
30. The decay heat uncertainty is accounted for through the power shape response surface (see Volumes 5, question 7, Reference 38). INEL review found that: (a) the uncertainty is based on the ANS 1979 decay heat standard and a conservative estimate of that uncertainty (see Figure 3.1.3-6, Reference 58) and (b) Westinghouse's approach adequate to include the decay heat uncertainty in the overall results (see Section 9.2 of this report). The cladding metal-water reaction rate uncertainty is accounted by using a BE reaction rate on the HR and then accounting for the uncertainty in the HOTSPOT model. The INEL considers this adequate to meet the RG in these areas.

The INEL reviewed the code model response surface that includes the break flow uncertainty using information provided by Westinghouse in Reference 58. Westinghouse's information showed how the response surface run matrix was based on WCOBRA/TRAC runs where the break flow multiplier was varied to capture 100% of the data in the break flow distribution (based on comparisons to Marviken test data). Westinghouse also demonstrated how the response surface would be modified if analyses results showed higher PCTs as the discharge coefficient increased or decreased. Based on this information, the INEL found Westinghouse's approach to critical flow uncertainty adequate to meet the RG.

The INEL reviewed CQD Section 17 and Westinghouse's PIRT (Volume 1, question 2, Reference 37). Based on that review and the review to a large number of RAIs, the INEL concluded that WCOBRA/TRAC has no deficiencies that would preclude using WCOBRA/TRAC for realistic LBLOCA PWR PCT calculations, and the assessment covered the main processes important to PCT calculations.

31. In its response to Volume 5, question 53, Reference 51, Westinghouse clarified the bases for its conclusions that a break in the cold leg (DEG or split) is the worst case break. For hot leg and pump suction breaks, positive effects include: the break location prevents core flow reversal or delays it, all accumulators are functional, ECC bypass is eliminated or reduced, and a larger downcomer head is maintained. Westinghouse supported these arguments with reference to the results of a pump suction break analysis for IP2 reported in CQD Section 22-2. In that study, the blowdown and reflood PCTs were 600°F and 700°F lower, respectively, than the base case DEG cold leg break. Given the size of these reductions, Westinghouse concluded there was sufficient margin for the other break locations that even if the code uncertainty was larger for the other break locations, the cold leg break location would still be limiting.

The INEL agrees with Westinghouse assessment. Lower PCTs for the other break locations is consistent with past LBLOCA analysis experience for the reasons noted above. Also, the question of larger WCOBRA/TRAC uncertainty for other break locations was discussed with the NRC Staff. The NRC Staff concluded that Westinghouse had shown there was sufficient margin to cover possible increases in uncertainty for the cold leg versus other break locations,¹³⁹ and the INEL agrees with that assessment.

The response to Volume 5, question 53, also addressed how the non-PCT criteria of 10 CFR 50.46 would be met. The only criteria were an uncertainty would affect the calculated results are, Criterion 2, maximum local oxidation, and Criterion 3, maximum core wide hydrogen generation. (Note: For Criteria 4 and 5, Westinghouse uses the same methods as for 10 CFR 50.46, Appendix K, analyses.) For Criteria 2 and 3, see Section 13 of this report.

APPENDIX D

EVALUATION
OF THE
WCOBRA/TRAC DISPERSED FLOW FILM BOILING HEAT TRANSFER MODEL

EVALUATION
OF THE
WCOBRA/TRAC DISPERSED FLOW FILM BOILING HEAT TRANSFER MODEL

Note that the references cited in the following discussion are found in Section 15 of this report.

Accurate prediction of the post-critical heat flux heat transfer in a nuclear steam supply system during reflood of the core is essential to quantify the safety margins following a design basis large-break loss-of-coolant accident (LOCA). Following a design basis large-break LOCA, the peak cladding temperature typically occurs during reflood of the core, so the heat transfer process which ultimately cools the hottest fuel is characterized by a highly dispersed flow consisting of liquid drops distributed in a superheated steam environment. Thus, to permit accurate quantification of the safety margin, accurate prediction of the cooling capability in the upper portion of a nuclear core during dispersed flow film boiling (DFFB) is required. Given the importance of the cooling effects during dispersed flow, a review of the methods in the WCOBRA/TRAC (WCT) code follows since this model is integral to the calculated peak clad temperature (PCT) achieved during the reflooding of a pressurized water reactor (PWR).

A general description of the reflood process is presented followed by a discussion of the methods employed in the WCT code to model dispersed flow heat transfer. Key phenomena needed to accurately predict dispersed flow heat transfer are enumerated, along with comments on the WCT methodology.

D.1 Reflood Behavior

At the initiation of reflood of the core, subcooled liquid enters a steam filled, hot, core. As more emergency core cooling water enters the core at the bottom, complex heat transfer and multi-dimensional two-phase flow phenomena develop. During reflood, the core experiences forced convection heat transfer to subcooled liquid at the bottom, then, when the liquid saturates nucleate boiling develops followed by transition boiling, film boiling, DFFB, and finally forced convection to steam at the very top. The steam generated in the liquid expands the steam-liquid mixture region into the

core. If the liquid contacts the cladding and the cladding temperature is above the rewet temperature, sputtering occurs producing a population of droplets above the quench front. The breakup of waves on the liquid-steam interface during annular and inverted annular flow along with the release of large bubbles from the mixture surface are the major source of these droplets, and it is noted that the particular flow regimes where the drops are produced dictate the initial size of the droplets. The steam, disengaging the two-phase surface, accelerates up the core, entraining liquid droplets and carrying them upward. Sometimes the steam disengaging the two-phase surface does so in bursts of bubbles that lead to bursts of entrained liquid droplets, which can cause variations in droplet sizes leaving the quench front. Once the reflood has progressed sufficiently, eventually there will be enough entrained droplets to cool the upper portions of the core terminating the heatup of the fuel rods. Dispersed flow heat transfer clearly plays a key role in determining the reflood PCT following a large break LOCA.

D.2 WCOBRA/TRAC DFFB Model

Since DFFB heat transfer is the dominant heat transfer mechanism controlling peak clad temperature, it is important to understand the details of the dispersed flow heat transfer methodology in WCT.

The WCT DFFB heat transfer model consists of four parts. They are:

- 1) convective heat transfer from the wall to the vapor,
- 2) radiative heat transfer from the wall to the vapor,
- 3) radiative heat transfer from the wall to the droplets, and
- 4) droplet-wall direct contact heat transfer.

Interfacial heat transfer between the drops and the steam is also an important contribution to the heat transfer processes during dispersed flow and will be discussed later. Radiation between the drops and steam is not modeled.

It should be noted that the WCT methodology does not model rod-to-rod radiation during DFFB and the convection to steam heat transfer regimes. This can be a serious limitation since the data base used to quantify the dispersed flow heat transfer model includes rod-to-rod radiation effects. The implication of the lack of a rod-to-rod radiation model on the prediction of the total heat transfer rate during dispersed flow will also be discussed later. The details of dispersed flow heat transfer will be discussed first.

In computing the DFFB heat transfer, the individual heat flux components, including the radiation and convection contributions discussed above, are modeled separately. While this is the standard modeling approach, the difficulty that arises is that the adequacy of the modeling of the individual contributions comprising dispersed flow heat transfer cannot be verified independently. Moreover, the modeling of DFFB consists of a highly coupled thermal and hydrodynamic problem, where the modeler must develop accurate thermal-hydraulic models in order to achieve good heat transfer predictions. Many times the heat transfer modeling is over-adjusted to overcome deficiencies in the hydrodynamic models. Best estimate methodologies should attempt to incorporate the best thermal and hydrodynamic models.

The most significant challenge in predicting dispersed flow heat transfer is the calculation of the steam superheat. Once the steam superheat is known, the computation of the fuel rod heat flux becomes straightforward. The superheat of the vapor must be obtained from a heat balance involving heat transfer from the superheated vapor to the droplets. The interfacial heat transfer is, therefore, a major controlling factor where the interfacial area is also needed. As a consequence, the distribution in interfacial area and relative velocity between the droplets and the vapor, which controls the interfacial heat transfer mechanism, must also be known. This interfacial area depends not only on void fraction distribution, but also on the spectrum of droplet diameters, so that droplet hydrodynamics is also of key importance.

As mentioned above, the vapor superheat is the most significant challenge to successfully modeling dispersed flow heat transfer. To accomplish this, the droplet distribution and droplet diameters are needed. The radial distribution of droplets along with the radial temperature profile are also important.²⁰⁹ Even though the WCT code is three-dimensional in the vessel

component, where cross flow through the core is accommodated, the information on the distribution of variables in the direction normal to the main flow is lost since the intensive quantities have to be represented by values that result from averaging over cross sections that are orders of magnitude larger than the area of the subchannel enclosed between four rods. Thus, with respect to heat transfer in the mist flow regimes, the information concerning velocity, temperature, and droplet concentration is often not always captured in the multi-dimensional codes.²¹⁰ Furthermore, droplet concentration and the distribution of sizes are strongly dependent on previous history and on the generation mechanisms.

The WCT code basically ignores the flow regime relationship to the droplet production and uses an average local droplet diameter obtained from the local Weber number. As with most all other codes, the WCT code methodology incorrectly assumes that this mean diameter provides an adequate representation of the droplet population. Modeling all the relevant phenomena and representation of the entire spectrum of droplet diameters by a single average droplet diameter satisfying all averaging requirements is not rigorously possible and is a major shortcoming of all safety analysis codes, including the WCT code.

Droplet size, as mentioned earlier, is also history dependent. That is, the flow regimes dictate the size of droplets produced at their birth sites. During reflood, the liquid core during the inverted annular flow regime can contain surface waves from which liquid drops are stripped. Ligaments of liquid can form and with increased agitation can breakup into large slugs and eventually drops with sizes that differ from those produced by the stripping of the drops at the liquid surface. Steam can also disengage from the mixture region in the vicinity of the quench front in bursts producing a spectrum of drop sizes with a non-uniform axial concentration. Experimental data further shows that at short distances from the generation point, drops of very different size attain the same velocity, further illustrating the limitations of the Weber number criterion for drop size computations. Use of this aerodynamic stability criterion can also lead to physical inconsistencies further away from the droplet generation site.

The WCT code uses a model that computes entrainment based on the critical velocity to lift a droplet. The Weber number is then used to produce an average drop size for this entrained liquid. This model suffers from the limitation that it does not consider the details of the particular flow regimes under which the drops are produced. Beyond the point of droplet production, the axial evolution of the drop diameter is determined using an interfacial area transport equation in the WCT code. Important phenomena such as evaporation and the breakup at grids is considered in determining further changes in drop size in the WCT code.

The WCT model for DFFB includes the radiation and convection components enumerated above. Having discussed some of the important effects influencing DFFB, each of the models in the WCT are discussed next.

D.2.1 Wall-to-Vapor Heat Transfer

The heat transfer to single phase vapor is computed in the WCT code as the maximum coefficient from laminar flow assuming the Nusselt number given in CQD Eqn. 6-4, from Dittus-Boelter for turbulent flow, from the Wong-Hochreiter correlation, and from McAdams correlation for turbulent natural convection. These correlations are standard for heat transfer to single phase vapor.

This forced convection model also includes a two-phase enhancement factor that improves the wall-to-steam heat transfer when liquid drops are present, and was inferred from the FLECHT data. The enhancement factor on the heat transfer is based on the work of Kays (Reference 163). CQD Figure 6-11 compares the Westinghouse model to the data. The large scatter in the data, however, clearly indicates that the correct parameters that control this phenomenon have yet to be identified. Westinghouse's justification of the model is weak because of the large data scatter.

Furthermore, Westinghouse performed a FLECHT sensitivity study where the drop size was increased by a factor of 1.36. The resulting vapor temperature increased; however, the clad temperature remained the same. Westinghouse indicated the larger drop size produced an increase in wall heat transfer because of the relative velocity parameter included in the model. This does not appear to be consistent with experiment (discussed below) and can be

attributed to the fact that all phenomena needed to properly characterize the effects of drop sizes on wall heat transfer to single phase vapor have not been identified (Reference 210). Experimental data for coarse drop sizes (that is, drop diameters > 0.0015 ft.) show that as the drop diameter increases, the heat transfer enhancement decreases. For the large drop sizes, a drop free region near the wall exists with the dispersed phase flowing in the central region. Only, the smaller drops tend to impact the walls. This experimental observation explains the reason for the absence of appreciable enhancement in heat transfer coefficient which has been reported for large drops.

While these concerns are noted, INEL concluded the uncertainty evaluation accounts for the potential overprediction of heat transfer due to this model through the multipliers that are developed based on code/data comparisons. If the model results in overpredicting the HTC relative to test data, the multiplier Westinghouse applies will account for this effect. Also, the maximum two-phase enhancement multiplier applied in WCOBRA/TRAC (see CQD Section 6-2-8) will prevent severe overprediction of the heat transfer enhancement.

D.2.2 Radiation to Drops and Vapor

The WCT code uses the network method to compute the radiation to drops and the vapor. This model assumes an optically thin medium for the radiation heat transfer so that any portion of the fluid exchanges radiant heat directly with the boundary surfaces. This model provides an adequate response for radiation to the mixture for the optical thicknesses encountered during reflooding following a large-break LOCA.

D.2.3 Droplet-Wall Contact Heat Transfer

The direct contact heat transfer where drops contact the wall is based on the Forslund-Rohsenow model (Reference 101). This model is questionable since it was originally developed to account for an additional heat transfer mechanism at low quality and high mass flux that occur near the quench front. Even more questionable is the use of the Forslund-Rohsenow model in conjunction with the Bromley correlation which was originally done in the TRAC

code. The Forslund-Rohsenow model was intended to represent the total heat flux to the liquid; however, Westinghouse corrected this oversight which is quite common in safety codes.

The Forslund-Rohsenow droplet-wall contact model, developed from DFFB of nitrogen in small diameter tubes, is applied to rod arrays where the probability of the drops impinging the rods is less, since drops, unlike that of the test conditions, can flow around rods without impingement. The model is also applied throughout the entire dispersed flow regime. This droplet-wall contact effect begins at the inverted annular regime and increases through to the agitated inverted annular regime, where the effect is at a maximum due to either high turbulence or some possible liquid-wall contact. Downstream of the agitated region, this droplet-wall contact effect decreases and becomes negligible once the highly dispersed flow region develops.²¹¹ The WCT code simulates the direct wall contact effects throughout the entire dispersed flow region. Sensitivity studies performed by Westinghouse show that the Forslund-Rohsenow model can represent 5 to 10% of the total heat transfer during DFFB in the WCT code. As evidenced by the code's overprediction of entrainment for the FLECHT tests, the void fraction dependence of this model would also produce an additional enhancement in the direct wall contact contribution, further driving up the heat transfer rate during dispersed flow under these conditions. Errors in the entrainment then can propagate into the heat transfer model through the application of the Forslund-Rohsenow model, which tends to reduce the clad temperature. Sensitivity studies by Westinghouse on nodalization also show that the entrainment rate in the WCT code is very sensitive to the node size. Thus, no attempt can be made to investigate additional nodal detail because, with more nodes, the smaller node size reduces the steam production in the volume which significantly reduces the entrainment. The limitation in the entrainment model restricts the nodalization to approximately 14 axial volumes, and, with this nodalization, the entrainment model produces severe discontinuities or step changes in the heat transfer coefficient as the entrainment level passes through each axial volume.

As mentioned above, experimental data demonstrates that the coarse or larger drops tend to flow in the central regions between the rods while only the smaller drops can impinge the walls. Since the Forslund-Rohsenow model

does not distinguish between drop sizes, the void fraction dependence of this model can produce an enhancement of the wall heat transfer during dispersed flow, which may not be justified. However, while this concern is noted, INEL concluded the Westinghouse uncertainty evaluation accounts for the potential overprediction of heat transfer due to this model by the multipliers that are developed based on code comparisons to test data. If the model results in overpredicting the HTC relative to test data, the multiplier Westinghouse applies will account for this effect.

D.2.4 Interfacial Heat Transfer

The interfacial heat transfer model for vapor droplet heat transfer is based on the original work of Lee and Ryley (Reference 157). This correlation is based on a very low range of vapor superheats so its use in high vapor temperature environments is questionable. It also tends to predict higher heat transfer rates than other correlations such as the model developed by Renksizbulut and Yuen.²¹² Also, the droplet diameters do not cover the full range of droplet sizes that are expected to be encountered during large-break LOCA reflood. Moreover, when questioned, Westinghouse performed some calculations showing the effect of drop size on the clad temperature response for FLECHT-SEASET Test 31203. The sensitivity to other tests was not provided. Increasing the drop size by a factor of 1.36 produced about a 75°F increase in steam temperature, but had a negligible effect on the peak clad temperature. While the larger drop can increase turbulence in the steam, which is included in the WCT wall heat transfer model, the overall effect on peak clad temperature may be reduced or masked due to the potential for the interfacial heat transfer rate to overpredict the vapor-to-droplet heat transfer. The larger drop size did delay the turn-around time and improved the clad temperature response, moving the prediction more closer to the data. This suggests that even a larger drop size of 0.007 ft. (which is representative of the upper range in drop sizes for this test) would be more appropriate. Westinghouse contends that the range of drop sizes used in the sensitivity study are more representative of the FLECHT data. However, because of the inaccuracies in using a single droplet diameter to represent the entire population, use of the larger drop is considered an improvement simply because it moves the clad temperature profile toward the data. Use of the larger drop size can be justified, particularly since the code operates at

the minimum drop size allowed by the Weber number, and a single drop size offers a crude approximation, at best, during this heat transfer regime.

The WCT comparisons with FLECHT show a general underprediction of the steam superheat. This may be due in part to the improper heat transfer partitioning between the vapor and liquid above the quench front, and the deficiencies noted above in the overall dispersed flow heat transfer model. While this concern is noted, INEL concluded the Westinghouse uncertainty evaluation accounts for the potential overprediction of heat transfer due to this model by the multipliers that are developed based on code comparisons to test data. By using the overall HTC to develop the multipliers, the effects of local condition differences are included. Thus, if the model results in overpredicting the HTC relative to test data, the multiplier Westinghouse applies will account for this effect.

D.3 Omission of a Rod-to-Rod Radiation Model

Westinghouse has chosen not to include rod-to-rod radiation as part of their fuel rod heat transfer model. This has implications regarding the correctness of their calculated multipliers on the heat transfer coefficient used during reflood since the multipliers are based on comparisons with the FLECHT data base, which includes rod-to-rod radiation. The INEL questioned the need to quantify this radiation contribution since the computation of multipliers for the reflood convection heat transfer coefficient using the FLECHT total heat transfer data is incorrect due to the fact that the FLECHT data includes rod-to-rod and rod-to-thimble thermal radiation effects. As such, rod-to-rod radiation should be subtracted from the FLECHT total heat transfer rate prior to a comparison with the WCOBRA/TRAC calculated convective heat transfer coefficients. Comparisons of the code predictions to the corrected FLECHT heat transfer coefficient may then result in a lower multiplier on the convective component, since the WCOBRA/TRAC code consistently overpredicts the convective heat transfer rate from the hot rod during dispersed flow heat transfer.

Removal of the rod-to-rod radiation component from the data will tend to increase the penalty on reflood heat transfer resulting in higher calculated peak clad temperatures when the WCOBRA/TRAC realistic methodology is employed

in plant calculations. Without subtracting thermal radiation from the total heat transfer coefficient from the FLECHT data, Westinghouse is, in effect, adjusting their convective reflood heat transfer model to accommodate thermal rod-to-rod radiation behavior. Thus, an effect which is highly non-linear or proportional to temperature, T^4 , is imbedded in the convective coefficient which is linear in T .

Based on the INEL concerns regarding rod-to-rod radiation, Westinghouse reviewed the FLECHT data and computed the convective heat transfer coefficients at the time of PCT for several FLECHT low flooding rate experiments. Based on the Westinghouse evaluation, the total convective heat transfer coefficient multiplier given in Reference 214, Attachment 4, was computed to remove rod-to-rod radiation effects from the total heat transfer coefficient at the plane of interest in the bundle. The multiplier is based on a comparison of the bundle wide average planar convective heat transfer coefficient at the time of the PCT, with that of the total convective heat transfer coefficient experienced by each of the rods at this elevation, for several FLECHT tests.

The multiplier was based on limited bundle data. That is, there was insufficient bundle thermocouple data to analyze the radiation contribution for all rods at a given elevation. INEL calculations show that depending on the proximity of the rod of interest to thimbles, the equivalent rod-to-rod radiation heat transfer coefficient can be as high as 30% of the total heat rate. As such, the limited data makes it impossible to perform a more thorough analysis. A more complete data set is expected to show that the average rod-to-rod radiation heat transfer coefficient is closer to 10-15% of the total heat transfer.

While the above concerns are noted, INEL found the overall Westinghouse methodology treats DFFB heat transfer conservatively. The heat transfer coefficient in HOTSPOT is limited to the mean value during dispersed flow, only the negative aspects of nitrogen injection or entrainment of fluid from the annulus are included in the model, the entrainment model enhances steam binding effects, high heat transfer coefficients are removed from the data base, only data on low reflood rates are used to develop the reflood heat transfer coefficient multipliers, and a lower limit on the rewet temperature

is used during blowdown. Moreover, qualitatively, the thimble density in a plant assembly is higher than that for the FLECHT tests, so some rods in the plant assembly will tend to have a higher rod-to-rod radiation contribution.

Based on the above, the rod-to-rod radiation heat transfer multiplier computed by Westinghouse is considered adequate. This multiplier will be applied to the HOTSPOT analysis to remove rod-to-rod radiation effects from the hot rod calculation in the WCOBRA/TRAC methodology. This multiplier will be applied to all hot rod calculations regardless of location. With the inclusion of this penalty in the HOTSPOT analysis, the HOTSPOT model is considered a conservative treatment of the hot rod peak clad temperature.

D.4 INEL Conclusions

While the INEL cited a number of concerns regarding the dispersed flow heat transfer model in the WCOBRA/TRAC code, the overall model is recommended for acceptance. This is because the deficiencies in the ability of the model to predict the data base are rectified using multipliers on the hot spot heat transfer coefficient. An evaluation of the calculated heat transfer coefficients with the data results in a reflood heat transfer coefficient distribution with a median multiplier given in Reference 206, Attachment 3. An additional multiplier given in Reference 214, Attachment 4, is used to further adjust the calculated heat transfer coefficient to account for the omission of rod-to-rod radiation. The combination of these two penalties results in a median multiplier less than 0.90 on the hot spot heat transfer coefficient to remove bundle rod-to-rod thermal radiation effects and to adjust the calculated heat transfer coefficient with low reflood rate based heat transfer coefficients. The acceptability of this reflood model is further supported by the fact that the reflood heat transfer multiplier distribution was based on low flooding rate experimental data. Therefore, in the plant applications, where the reflood rates will tend to be higher, the model is considered a conservative representation of expected plant behavior.

Lastly, it should be mentioned that there is no known mechanistic model that includes an accurate description of all of the thermal and hydrodynamic processes characterizing DFFB heat transfer. Thus, while Westinghouse could improve their modeling in this area²¹⁸ (that is, this model

is not considered state-of-the-art), there many unanswered questions that limit the means to assess each of the individual contributions affecting DFFB heat transfer. Advancements in the state-of-the art regarding DFFB experimentation have been limited since multi-fluid, multi-dimensional models were first introduced some 10 to 15 years ago. Also, the experimental data is insufficient to provide the thorough understanding needed to allow one to utilize the full capabilities of multi-fluid, multi-dimensional codes.

BIBLIOGRAPHIC DATA SHEET

(See instructions on the reverse.)

INEL-95/0603

2. TITLE AND SUBTITLE

TECHNICAL EVALUATION REPORT, WESTINGHOUSE CODE
QUALIFICATION DOCUMENT FOR BEST ESTIMATE LOSS OF
COOLANT ANALYSIS, WCAP-12945-P

3. DATE REPORT PUBLISHED

MONTH YEAR
MAY 1996

4. FIN OR GRANT NUMBER

L1696

5. AUTHOR(S)

C. P. FINEMAN
C. L. ATWOOD
D. S. LUCAS
L. W. WARD

6. TYPE OF REPORT

Technical Evaluation
Report

7. PERIOD COVERED (Include Dates)

8. PERFORMING ORGANIZATION - NAME AND ADDRESS (If NRC, provide Division, Office or Region, U.S. Nuclear Regulatory Commission, and mailing address; if contractor, provide name and mailing address.)

IDAHO NATIONAL ENGINEERING LABORATORY
LOCKHEED IDAHO TECHNOLOGIES COMPANY
P.O. BOX 1625
IDAHO FALLS, ID 83415

9. SPONSORING ORGANIZATION - NAME AND ADDRESS (If NRC, type "Same as above"; if contractor, provide NRC Division, Office or Region, U.S. Nuclear Regulatory Commission, and mailing address.)

U.S. NUCLEAR REGULATORY COMMISSION
OFFICE OF NUCLEAR REACTOR REGULATION
WASHINGTON, DC 20555

10. SUPPLEMENTARY NOTES

11. ABSTRACT (200 words or less)

The Idaho National Engineering Laboratory (INEL) reviewed the five volume topical report Code Qualification Document for Best Estimate Loss of Coolant Accident Analysis, WCAP-12945-P. The review evaluated Westinghouse's realistic methodology for large-break loss-of-coolant accident (LBLOCA) analysis to determine the performance of emergency core cooling systems (ECCS) following a LBLOCA. The methodology will be applied to Westinghouse three- and four-loop pressurized water reactors (PWRs) with cold leg injection. Because of the realistic approach to determining the performance of the ECCS, the INEL evaluated conformance of the methodology described in WCAP-12945-P to Nuclear Regulatory Commission requirements in 10CFR50.46, guidance in Regulatory Guide 1.157 (RG 1.157) and the Code Scaling, Applicability, and Uncertainty (CSAU) Methodology. Based on the INEL review of the information provided by Westinghouse in WCAP-12945-P, responses to NRC questions, and special submittals, the INEL recommends the Westinghouse realistic methodology be approved subject to certain suggested restrictions. This recommended approval is for Westinghouse three- and four-loop plants with cold leg ECC injection.

12. KEY WORDS/DESCRIPTORS (List words or phrases that will assist researchers in locating the report.)

13. AVAILABILITY STATEMENT

Unlimited

14. SECURITY CLASSIFICATION

(This Page)

Unclassified

(This Report)

Unclassified

15. NUMBER OF PAGES

16. PRICE